The University of Hull

# The Generation of an Immunosuppressive Microenvironment by Soluble Factors in Head and Neck Squamous Cell Carcinoma

Thesis submitted for the degree of PhD by

Elizabeth Rose Roberts

BSc (Hons), Newcastle University

MRes, Newcastle University

January 2018

## Abstract

Tumour infiltrating lymphocytes (TIL) in head neck squamous cell carcinoma (HNSCC) are enriched in Treg, a finding confirmed in the current study, which is thought to be a contributing factor to immunosuppression and tumour evasion. Soluble factors released by malignant HNSCC cells may contribute to the enrichment of Treg by inducing differentiation from naïve T cells and their migration to the tumour.

Using multi-colour flow cytometry, increases in $CD4^+CD25^{hi}$, $CD4^+CD25^+CD39^+$, $CD4^+CD25^+CD26^-$ and $CD4^+CD25^+FoxP3^+$ Treg phenotypes were observed in TIL from HNSCC compared to PBMC. Following culture of $CD4^+CD25^-$ T cells with conditioned medium (CM) collected from dispersed tumour samples, there was an increase in CD39 expression but not FoxP3 compared to control cultures that were cultured in complete growth medium. Furthermore these cells were unable to suppress the proliferation of $CD4^+CD25^-$ T cells in CFSE assays. Soluble factors in CM from UMSCC cell lines and tumour-derived fibroblasts were unable to induce the expression of any Treg markers following culture with $CD4^+CD25^-$ T cells. Culture with CM also had no effect on T cell apoptosis, with no significant increase in $PI^-AnexinV^+$ of CaspACE-binding in T cells cultured with CM compared to controls.

The expression of the chemokine receptors, CXCR3, CCR4, CCR5 and CCR6 was analysed on T cell populations from HNSCC PBMC and TIL and healthy control PBMC using five-colour flow cytometry. Increased proportions of $CXCR3^+$ and $CCR5^+$ T cells were observed in HNSCC TIL compared to HNSCC PBMC but were no different between the patient and healthy control PBMC. CCR4 and CCR6 were expressed on a higher proportion of Treg from HNSCC PBMC compared to healthy controls but no difference was observed on CTL. In TIL the percentage expression of CCR4 and CCR6 were no different in that of HNSCC patient PBMC. Despite these observed differences in receptor expression, soluble factors in tumour dispersed CM was unable to induce T cell chemotaxis. Overall, although limited effects were observed from soluble factors in tumour CM, the different expression of chemokine receptors suggests there may be a role for soluble factors in Treg recruitment. However whether this is responsible for Treg accumulation or general to all T cells is unclear.

# Table of Contents

## List of Figures

## List of Tables

## Abbreviations

| | |
|---|---|
| AgPC | Antigen presenting cell |
| APC | Allophycocyanin |
| BSA | Bovine serum albumin |
| CAF | Cancer associated fibroblasts |
| CD | Cluster of differentiation |
| CFSE | Carboxyfluorescein succinimidyl ester |
| CIN | Cervical intraepithelial neoplasia |
| $CO_2$ | Carbon dioxide |
| CTL | Cytotoxic T lymphocyte |
| CTLA-4 | Cytotoxic T lymphocyte antigen -4 |
| Cy5.5 | Cyanine dye 5.5 |
| DC | Dendritic cell |
| DMEM | Dulbecco's modified eagle medium |
| DMSO | Dimethyl sulphoxide |
| DNA | Deoxyribonucleic acid |
| EDTA | Ethylenediaminetetraacetic acid |
| EGF | Epidermal growth factor |
| ELISA | Enzyme-linked immunosorbance assay |
| ESCC | Oesophageal squamous cell carcinoma |
| FACS | Fluorescence activated cell sorting |
| FAF | Fibrosis associated fibroblasts |
| FasL | Fas ligand |
| FGF | Fibroblast growth factor |
| FITC | Fluorescein isothiocyanate |
| FSC | Forward scatter |
| GITR | Glucocorticoid-induced TNFR-related protein |
| GVHD | Graft versus host disease |
| HCV | Hepatitis C viruc |
| HGF | Hepatocyte growth factor |
| HIV | Human immunodeficiency virus |
| HNSCC | Head and neck squamous cell carcinoma |
| HPV | Human papilloma virus |

| | |
|---|---|
| ICAM-1 | Intracellular adhesion molecule (ICAM)-1 |
| IFN-γ | Interferon gamma |
| IL | Interleukin |
| IPEX | Immunodysregulation polyendocrinopathy enteropathy X-linked disease |
| JAM-A | Junctional adhesion molecule-A |
| LBRC | Lateral border recycling compartment |
| LFA-4 | Lymphocyte function-associated antigen-4 |
| LN | Lymph node |
| LSM | Lymphocyte separation medium |
| MHC | Major histocompatibility complex |
| MSC | Multipotent stromal cells |
| MTS | 3-(4,5-dimethylthiazol-2-yl)-5-(3-carboxymethoxyphenyl)-2-(4sulphophenyl)-2H-tetrazolium, inner salt |
| NAF | Normal activated fibroblasts |
| NK | Natural killer |
| NPC | Nasopharyngeal carcinoma |
| NSCLC | Non-small cell lung carcinoma |
| OSCC | Oral squamous cell carcinoma |
| OPSCC | Oropharyngeal SCC |
| PBMC | Peripheral blood mononuclear cells |
| PBS | Phosphate buffered saline |
| PD-1 | Programmed cell -1 |
| PD-L1 | Programmed cell death -ligand 1 |
| PE | R-phycoerythrin |
| PECAM-1 | Platelet/endothelial cell adhesion molecule-1 |
| PI | Propidium iodide |
| PS | Phosphatidylserine |
| PSGL-1 | P-selectin glycoprotein ligand-1 |
| RCC | Renal cell carcinoma |
| SD | Standard deviation |
| SDF-1 | Stromal derived factor -1 |
| SEM | Standard error of the mean |
| SMA | Smooth muscle actinin |

| | |
|---|---|
| SSC | Side scatter |
| S1P | Sphingosine-1 phosphate |
| TAM | Tumour-associated macrophage |
| TEM | Trans-endothelial migration |
| TCR | T cell receptor |
| TGF-β | Transforming growth factor-beta |
| Th | T helper |
| TIL | Tumour infiltrating lymphocytes |
| TNF-α | Tumour necrosis factor-alpha |
| TRAIL | TNF-related apoptosis-inducing ligand |
| Treg | T regulatory lymphocyte |
| TSDR | Treg specific demethylated region |
| UMSCC | University of Michigan squamous cell carcinoma |
| VCAM-1 | Vascular cell adhesion molecule-1 |
| VLA-4 | Very late antigen-4 |

## Thesis Associated Presentations

Roberts E., Green V.L., Stafford N.D., Greenman J. The influence of soluble factors from the head and neck squamous cell carcinoma tumour microenvironment on regulatory T cell induction and PBMC viability. Poster session presented at: NCRI Cancer Conference 2016 November 6th-9th; Liverpool, UK.

Roberts E., Green V.L., Stafford N.D., Greenman J. The effect of the tumour microenvironment (TME) on the generation of suppressive iTreg cells in head and neck squamous cell carcinoma (HNSCC). Poster session presented at: British Association of Head and Neck Oncologists Annual Scientific meeting 2016 May 13th; London, UK.

Roberts E., Green V.L., Stafford N.D., Greenman J. The role of soluble factors released by head and neck squamous cell carcinoma (HNSCC) in the generation and of suppressive Treg cells. Poster session presented at: EMBO Tumour Microenvironment and Signalling Symposium 2016 April 3rd-6th; Heidelberg, Germany.

## Acknowledgements

First and foremost I would like to thank my supervisors Vicky Green and John Greenman for all their guidance and support over the last four years, and especially for the hours they have spent reviewing this thesis and their continued encouragement throughout. I would like to acknowledge Thomas Carey for kindly providing the UMSCC cell lines used in this study, and the surgeons and registrars at the ENT Department at Castle Hill Hospital and the Oral Maxillofacial Department at Hull Royal Infirmary for providing us with the tumour biopsy samples, particularly Professor Nick Stafford and Mr Stephen Crank. I would also like to thank Beryl Brignall for providing the funding for this project.

I would like to say a huge thank you to Ruth Bower, James Williamson, Jo Smith, Ramsah Cheah, Andrew Riley, Simon Fraser, Alison Bentley, Holly Wilkinson, Mat Hardman and all my colleagues at Daisy, for not just the help and advice but also the cake and the company. Finally, I will be forever grateful to my mum, dad, Al and James, who have always encouraged and supported me every step of the way, including but not limited to late night IT support.

## Authors Declarations

I confirm that this work is original and that if any passage(s) or diagram(s) have been copied from academic papers, books, the internet or any other sources these are clearly identified by the use of quotation marks and the reference(s) is fully cited. I confirm that any patient information obtained to produce this piece of work has been appropriately anonymised.

# Chapter 1 Introduction

Cancer patients are often immunosuppressed (von Bernstorff *et al.*, 2001; Duray *et al.*, 2010; Yaguchi & Kawakami, 2016) and this has been recognised as an important factor for tumour growth and progression. Studies have reported that alterations in levels of immune cells and cytokines influence prognosis, and can impact on the effectiveness of treatments (Balermpas *et al.*, 2014a). A better understanding of the intricacies of the immune system in cancer may allow the development of novel therapies, improved prognostic abilities and targeted treatment regimens.

## 1.1 Head and neck squamous cell carcinoma

The majority (>95%; Sanderson & Ironside, 2002) of head and neck cancer originates in squamous epithelial cells that line the upper aerodigestive tract (Figure 1.1). Head and neck squamous cell carcinoma (HNSCC) is the sixth most common cancer worldwide (Torre *et al.*, 2015), affecting the oral and nasal cavities, oropharynx, hypopharynx, nasopharynx and larynx. Despite better understanding of the disease causes and improvements to patient care, the 5-year survival has remained low, at around 40-50% (Leemans *et al.*, 2011). This is likely due to both the inter- and intra-tumour heterogeneity within these cancers, which have proved a major obstacle in the development of effective treatments.

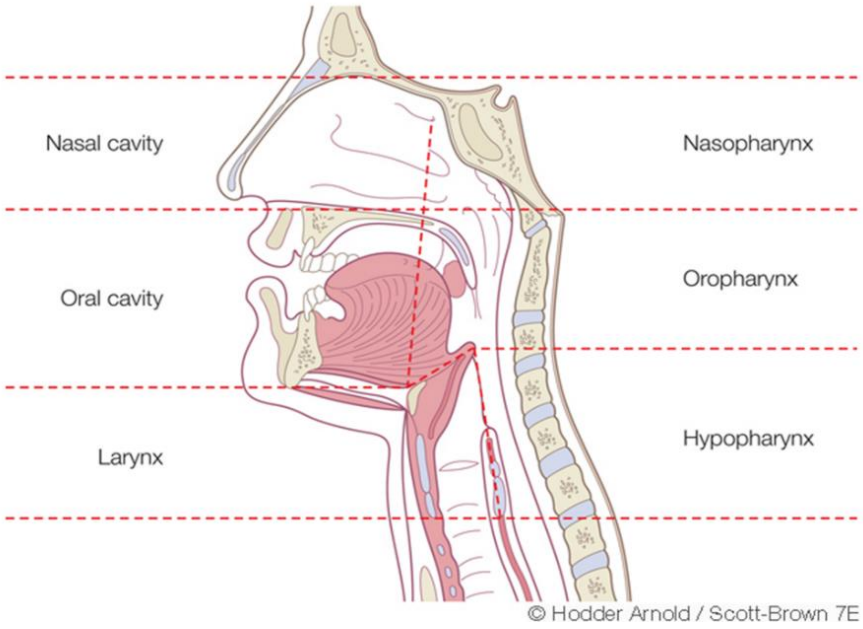


**Figure 1.1: The cross section of the head and neck regions implicated in HNSCC**
Taken from (Gleeson, 2008).

### 1.1.1 **Aetiology**

As with all cancers, HNSCC is fundamentally a genetic disease and carcinogens that increase the rate of accumulation of genetic aberrations increase the risk of its development. The major contributing risk factors in HNSCC are smoking, heavy alcohol consumption and contraction of the sexually transmitted human papilloma virus (HPV).

#### 1.1.1.1 *Smoking*

The link between smoking and cancer is now well established, with tobacco use recognised as being implicated in cancers of the lung, oesophagus, stomach, liver, pancreas, cervix, bladder, head and neck and leukaemia (Danaei *et al.*, 2005). A pooled analysis from 17 case-control studies across Europe and America, including data from over 11,000 HNSCC patients and 16,000 controls, found an increased risk from smoking in all HNSCC cancer subsites (overall odds ratio [OR] of 2.37; Table 1.1). However the larynx was found to be particularly susceptible to smoking induced cancer (OR of 6.76) (Hashibe *et al.*, 2009). Furthermore, this risk is increased with smoking frequency, duration and number of cigarettes smoked (Hashibe *et al.*, 2007; Hashibe *et al.*, 2009). Studies have found that of the over 6000 chemicals in tobacco smoke, more than 60 are known carcinogens (Hoffmann *et al.*, 2001; Talhout *et al.*, 2011). Despite this, not all smokers will develop cancer. There are genetic factors that affect the variation in susceptibility between individuals, particularly in genes encoding metabolising enzymes (Sato *et al.*, 2000; Ruwali *et al.*, 2009; Maurya *et al.*, 2014). In addition, smoking has also been shown to effect the success of treatment, with patients who continue to smoke during radiation therapy having a poorer rate of response and higher mortality rate (Browman *et al.*, 1993; Hoff *et al.*, 2012).

**Table 1.1: Odds ratios for alcohol consumption and tobacco use on developing head and neck cancer**

| | Odds ratio (OR; 95% CI) | | | |
|---|---|---|---|---|
| | Head and neck cancer overall | By subsite | | |
| | | Oral cavity | Pharynx | Larynx |
| Alcohol alone | 1.06 (0.88-1.28) | 0.79 (0.60-1.04) | 1.28 (0.91-1.80) | 1.21 (0.77-1.92) |
| Tobacco alone | 2.37 (1.66-3.39) | 1.74 (1.10-2.76) | 1.91 (1.39-2.62) | 6.76 (4.58-9.96) |
| Tobacco and alcohol | 5.73 (3.62-9.06) | 4.78 (2.59-8.81) | 5.42 (3.21-9.16) | 14.22 (8.26-24.46) |

The odds ratios (95% confidence intervals; CI) associated with alcohol consumption, tobacco use, or combined alcohol consumption and tobaccos use, in head and neck cancer overall and by subsite, adapted from Hashibe *et al*. 2009.

#### 1.1.1.2 *Alcohol consumpation*

As with smoking, heavy alcohol consumption has been associated with a number of different cancers. The risk of drinking on developing head and neck cancer increases in a dose dependent manner (Pelucchi *et al.*, 2006; Hashibe *et al.*, 2007). Hashibi *et al*. (2006), determined the risk of drinking more than three drinks a day increased to 1.93 compared to 1.03 in those who consumed 1-2 drinks a day. These differences were particularly notable in cancers of the larynx and pharynx, were the risk more than doubled between drinking 1-2 drinks a day (1.2 and 1.26 for laryngeal and pharyngeal cancers respectively) and more than three drinks a day (3.16 and 2.94). The carcinogenic component associated with alcohol is acetaldehyde, an intermediate formed in the breakdown of alcohol to acetate (Seitz & Stickel, 2007). This conversion is carried out by the enzymes alcohol dehydrogenase and acetaldehyde dehydrogenase (Figure 1.2). Increased alcohol consumption, increased alcohol dehydrogenase activity or decreased acetaldehyde dehydrogenase activity facilitate the accumulation of acetaldehyde and increase the risk of developing cancer. In terms of HNSCC, the carcinogenic effect of alcohol is primarily due to its nature as an organic solvent, facilitating the entry of other carcinogens into cells. It is due to this characteristic that smoking and alcohol have a synergistic effect on HNSCC development, together accounting for up to 75% of all cases, though the contribution varies depending on the sub site affected (Table 1.1; Blot *et al.*, 1988; Hashibe *et al.*, 2009).

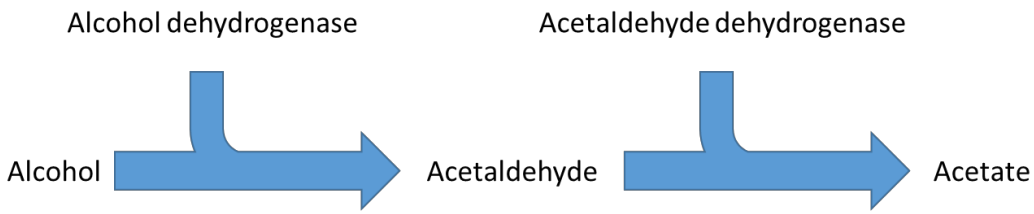


**Figure 1.2: The breakdown of alcohol to acetate, by alcohol dehydrogenase and acetaldehyde dehydrogenase, forming the carcinogenic intermediate acetaldehyde**

#### 1.1.1.3 *Diet*

Diet may also influence the risk of developing HNSCC, with numerous studies supporting an inverse correlation with intake of fruits and vegetables (Boeing *et al.*, 2006; Bravi *et al.*, 2012; Chuang *et al.*, 2012). However, data has been inconsistent and not all studies have observed this association (Peters *et al.*, 2008). Conversely, increased intake of red and processed meats, have been shown in the majority of cases to correlate positively with HNSCC risk (Levi *et al.*, 1998; Bravi *et al.*, 2012; Chuang *et al.*, 2012). The variability of the effect of diet on HNSCC development in the literature, particularly between results in Asian and Western populations, is speculated to be due to the general dietary differences between these populations. For example, in a study by Chuang *et al.* (2012), which included data from 22 case-control studies carried out in Europe, the US, Latin America and Japan, a positive association was observed overall between red meat intake and HNSCC risk, however a negative correlation was observed in the Japanese population. In this study the authors speculated this difference was due to the much lower consumption of red meat and higher consumption of fruit and vegetables in the Japanese population than in Europe and the US (Chuang *et al.*, 2012). Furthermore, smoking and alcohol consumption can be confounding factors in these studies, as generally smokers have a poorer diet, including greater levels of alcohol and fewer fruit and vegetables, than non-smokers (Dyer *et al.*, 2003). The most commonly observed trend, suggesting a diet high in fruit and vegetable and low in red meat correlates with a decreased HNSCC risk is consistent with observations from other forms of cancer, including colorectal, pancreatic, oesophageal and lung cancers (La Vecchia *et al.*, 1999; Marmot *et al.*, 2007).

The influence of environmental factors, such as diet, on HNSCC risk may differ depending on the underlying aetiology and their interaction with other environmental or genetic factors. For example, the positive association between fruit and vegetable intake and lower HNSCC

risk, is particularly strong for those who also smoke and drink high levels of alcohol (Chuang *et al.*, 2012). Furthermore, a study analysing whether the presence of HPV influences the effect of fruit consumption on HNSCC risk, observed a positive correlation in patients with the virus, compared with a negative correlation in those without (Meyer *et al.*, 2008).

#### 1.1.1.4 *Human papillomavirus*

Infectious agents are thought to contribute to more than 15% of worldwide cancers (Kuper, 2000). HPV is the major attributing cause of cervical cancer. Of the over 100 known types of HPV, 15 are found to be present in more than 95% of cervical cancers (Bosch *et al.*, 2002). These are considered to be high risk types, the most common of which, HPV 16 and 18, account for about 60% of cases. HPV 16 is also the most highly associated with HNSCC, and is particularly prevalent in cases of oropharyngeal cancer (D'Souza *et al.*, 2007). In cervical cancer the progression from HPV infection to malignancy can take years and is preceded by cervical intraepithelial neoplasia (CIN); the abnormal growth of squamous cells of the cervix (Snijders *et al.*, 2006). CIN does not always progress to cancer and is often eliminated by the host's immune system (Trimble *et al.*, 2005). However, the implementation of screening programmes to detect for these potentially precancerous cells has led to a significant decrease in incidence of cervical cancer (Peto *et al.*, 2004; Bray *et al.*, 2005). Results from studies estimating the prevalence of cervical HPV infection in women are highly variable, with estimates as high as 90% (Revzina & DiClemente, 2005); what is clear however is that the majority of women that are infected with HPV do not develop cervical cancer. Although there is a reasonable understanding of the molecular processes involved in the progression of infection to cervical cancer (Figure 1.3; Doorbar, 2006; Narisawa-Saito & Kiyono, 2007), what drives HPV infection to malignancy in some cases and not others is not understood.

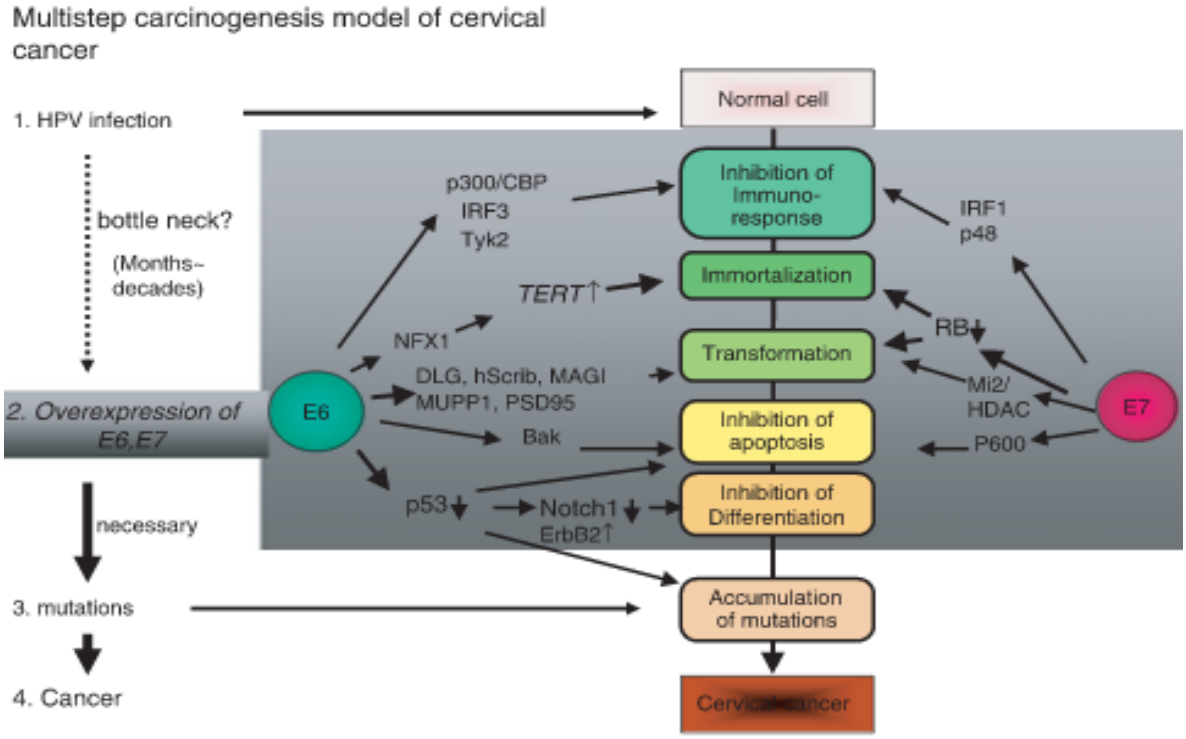


**Figure 1.3: Multistep carcinogenesis model of cervical cancer**
Taken from Narisawa-Saito and Kiyono (2007)

The early HPV viral proteins E6 and E7 are essential for transforming benign keratinocytes to cancerous cells in culture (Munger *et al.*, 1989). It is thought that the major cancer-causing interactions of the E6 and E7 proteins are with the tumour suppressor p53 and retinoblastoma protein (Rb) respectively (Figure 1.3; Narisawa-Saito & Kiyono, 2007). Of HNSCC, it is primarily oropharyngeal SCC (OPSCC) that are $HPV^+$. The profile of these $HPV^+$ tumours seems to differ quite dramatically to those that are $HPV^-$; tending to have fewer genetic alterations $HPV^+$ tumours have been associated with a better patient prognosis (Fakhry *et al.*, 2008; Westra, 2009). Exactly why this is the case is not understood, however it is apparent that $HPV^+$ tumours constitute a distinct subgroup with a specific molecular pathogenesis (Dok & Nuyts, 2016).

### 1.1.2 Genetic aberrations associated with susceptibility

There is evidence that there is a genetically inherited component to HNSCC, influencing carcinogen susceptibility, as the risk of cancer goes up 1.7 fold in patients with a first-degree family history of HNSCC and increases the combined risk from alcohol and cigarette use from 3.34 to 7.21 (Negri *et al.*, 2009). Genetic polymorphisms have been identified in genes involved in DNA repair, the cell cycle and metabolising enzymes that are strongly implicated in both disease susceptibility and outcome of treatment (Hopkins *et al.*, 2008). Genetic variations in xenobiotic-metabolising enzymes, responsible for the activation or deactivation of carcinogenic substances, can affect their functionality and therefore could influence an individual's susceptibility to a particular carcinogen (Ho *et al.*, 2007). Polymorphisms in the cytochrome p450 family of activating enzymes, particularly *CYP1A1*, have been associated with a slight increased susceptibility to tobacco related cancers, including head and neck cancer. Deficiency of the enzyme aldehyde dehydrogenase (ALDH)-2, due to a polymorphism in *ALDH2,* frequently observed in the Asian population, has also been associated with a high risk of alcohol associated oropharyngeal cancer (Yokoyama *et al.*, 1998).

The implications of many other somatic mutations are well established in cancer development, with the loss or gain of function of their resultant proteins frequently observed across a number of different cancer types. Of particular interest are genes known to be involved in growth signalling pathways, evasion of apoptosis, angiogenesis, and tumour metastasis, all of which are pathways frequently altered in cancer (Singh, 2008).

#### 1.1.2.1 *Mutations in components involved in the cell cycle and apoptotic pathways*

The faulty regulation of the cell cycle is central to the transformation of healthy cells to their neoplastic counterparts. In normal cell growth, cells respond to signals telling them when to enter the cell cycle and begin the process of mitotic division. This process is tightly controlled and includes checkpoints that can induce DNA repair or apoptosis if a cell becomes damaged or mutated (Lukas *et al.*, 2004; Figure 1.4). In carcinogenesis, these processes are disrupted by mutations that activate the proliferative response, generally by deactivating tumour suppressors that restrict the cell cycle or by upregulating oncogenes that activate the cell cycle, and prevent initiation of the apoptotic pathway. Some of these genes are master regulators, aberrant expression of which affects a range of downstream targets and so can disrupt more than one of these pathways.

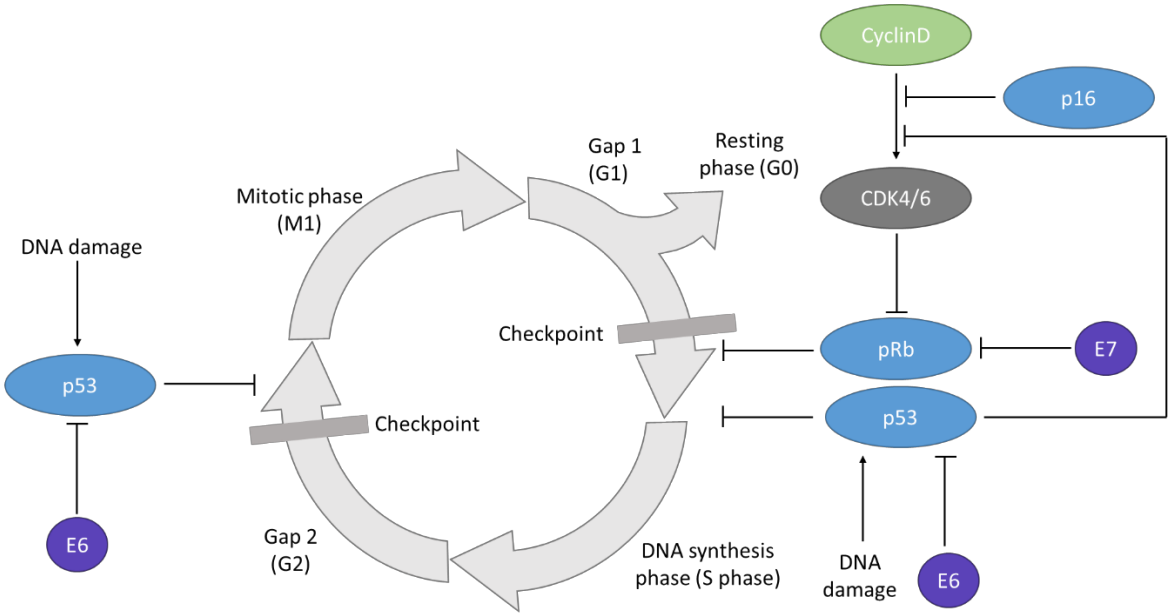


**Figure 1.4: An overview of the role of the p53 and RB pathways in regulating the cell cycle, with focus on the proteins that are often mutated in HNSCC**
Following the damage or mutation of DNA, p53 accumulates and activates the expression of downstream genes that results in cell cycle arrest at G1 or G2 phase checkpoints. The protein pRb binds to and inhibits the transcription factors that are responsible for activating the transcription of genes that regulate the move from G1 phase to S phase of the cell cycle. Throughout the cell cycle, cyclins are up and downregulated to tightly control the activation of cyclin-dependent kinases (CDK). The accumulation of cyclinD activates CDK4 and CDK6, which in turn phosphorylates pRb, leading to its inactivation. Inactivation of pRb leaves transcription factors free to initiate the transition to S phase. The over expression (green) or loss/deactivation (blue) of certain proteins involved in the cell cycle pathway by genetic or epigenetic mutations, or by the viral proteins (E6 and E7; purple) are frequent events in HNSCC.

A key protein frequently inactivated in cancer is the tumour suppressor p53, encoded by *TP53*. The p53 protein, regulates the cell cycle, inducing cell cycle arrest and if necessary apoptosis of damaged cells. In normal healthy cells, p53 is quickly degraded and levels are low, however it accumulates in response to DNA damage or stress caused by external stimuli (Sakaguchi *et al.*, 1998). In these cases, it inhibits the transition between the G1/S phases and the G2/M phases of the cell cycle by activating a number of downstream genes (Levine, 1997). Mutations in *TP53* are found in more than half of HNSCC patients, and are particularly prevalent in $HPV^-$ tumours, were they correlate with poor prognosis (Poeta *et al.*, 2007; Leemans *et al.*, 2011). In $HPV^+$ tumours, there are fewer *TP53* mutations; in these cases the HPV E6 protein is thought to contribute to the inactivation of wild type p53 (Poeta *et al.*, 2007).

Another tumour suppressor frequently found to be affected in HNSCC is the retinoblastoma protein (pRb; Rothenberg & Ellisen, 2012). pRb regulates the transition of the cell cycle from G1 to S phase, by inhibiting transcription of the necessary proteins (Dyson, 1998). It

is often inactivated in tumour cells, either directly by mutations in *RB* or binding of the HPV E7 protein, or indirectly by mutations in the genes of upstream proteins (Nevins, 2001). In HNSCC mutations in *RB* tend to be relatively rare and pathogenesis is more frequently a result of the aberrant expression of other proteins in this pathway (Alvi *et al.*, 2002). Cyclin D is one such protein, which is frequently upregulated in (~30%) HNSCC tumours and correlates with poor prognosis (Namazie *et al.*, 2002). This is primarily due to amplification of 11q3 chromosomal region, where the *CCND1* (CCND1) oncogene gene is located, which has been observed in more than 80% of $HPV^-$ HNSCC tumours. Upon forming a complex with the cyclin dependent kinases (CDK)-4 or -6, cyclin D binds to pRb, and pRb is phosphorylated causing its inactivation (Kato *et al.*, 1993). Inactivation of the protein p16 is another common event in HNSCC, usually due to homozygous deletion or methylation of its gene, *CDKN2A* (Shintani *et al.*, 2001). Loss of the 9p21 chromosome region on which *CDKN2A* resides is one of the most common genetic alterations in $HPV^-$ HNSCC (Smeets *et al.*, 2006). The p16 protein inhibits cyclin D activity and prevents Rb phosphorylation, preventing cells from transitioning to S phase. The loss of p16 in HNSCC is associated with a worse prognosis (Namazie *et al.*, 2002; Weinberger *et al.*, 2004).

Overexpression of the epidermal growth factor receptor (EGFR) is the most common event in HNSCC, observed in up to 95% of cases (Grandis & Tweardy, 1993). EGFR is a transmembrane protein involved in initiating the cell cycle, promoting cell growth and survival. Binding of its ligand EGF to EGFR initiates signals in the cell via a number of pathways including the Ras-MAPK and PI3K-PTEN-AKT pathways (Chong & Janne, 2013). Mutations to the *EGFR* oncogene and in genes for the downstream proteins that lead to increased activity of these pathways have been shown in HNSCC (Rothenberg & Ellisen, 2012). Despite the prevalence of EGFR upregulation in HNSCC, and its correlation with poor prognosis, it has had limited success as a target for therapy and is limited in terms of an overall predictive marker (section 1.1.5.1).

In addition to the pro-apoptotic p53, other apoptosis regulating proteins dysregulated in cancer include the anti-apoptotic Bcl-2 family. Bcl-2 and Bcl-XL are upregulated in HNSCC and impede the efficacy of chemotherapy by preventing cancer cells from entering the apoptotic pathway, normally induced following DNA damage (Trask *et al.*, 2002). Targeting these proteins at the protein or mRNA level has been shown to induce apoptosis of HNSCC cells and sensitise them to apoptosis by chemotherapy reagents (Sharma *et al.*, 2005; Li *et*

*al.*, 2007), but nothing has as yet been translated into the clinic. With a better understanding of the aetiology and molecular biology behind HNSCC, it may be possible in the future to predict those most at risk and take steps to prevent its development. The influence of increased knowledge of the causative factors in cancer development can already be observed by the changes in incidence rates.

### 1.1.3 Incidence

The last few decades have seen an increase in the overall incidence of HNSCC. However, the incidences of the different HNSCC sub sites vary considerably (Louie *et al.*, 2015). In Western Europe, a decreased incidence has been observed in cases of HNSCC originating in the hypopharynx and larynx, sites most strongly associated with tobacco use, while cases of oropharyngeal cancer have seen an increase (Figure 1.5; Pelucchi *et al.*, 2006; Sturgis & Cinciripini, 2007; Jemal, 2011; Louie *et al.*, 2015). Although historically the typical HNSCC patient is male, over the age of 60 with a history of smoking, the increase in oropharyngeal tumours are typically found in younger patients. For instance the incidence of cancer of the tonsil and base of tongue in the US increased by 4% and 2% respectively, between 1973 and 2001 (Shiboski *et al.*, 2005). This shift is thought to be attributable to the escalation in incidence of HPV-associated HNSCC, to which the oropharynx is particularly susceptible (Herrero *et al.*, 2003; D'Souza *et al.*, 2007; Sturgis & Cinciripini, 2007).

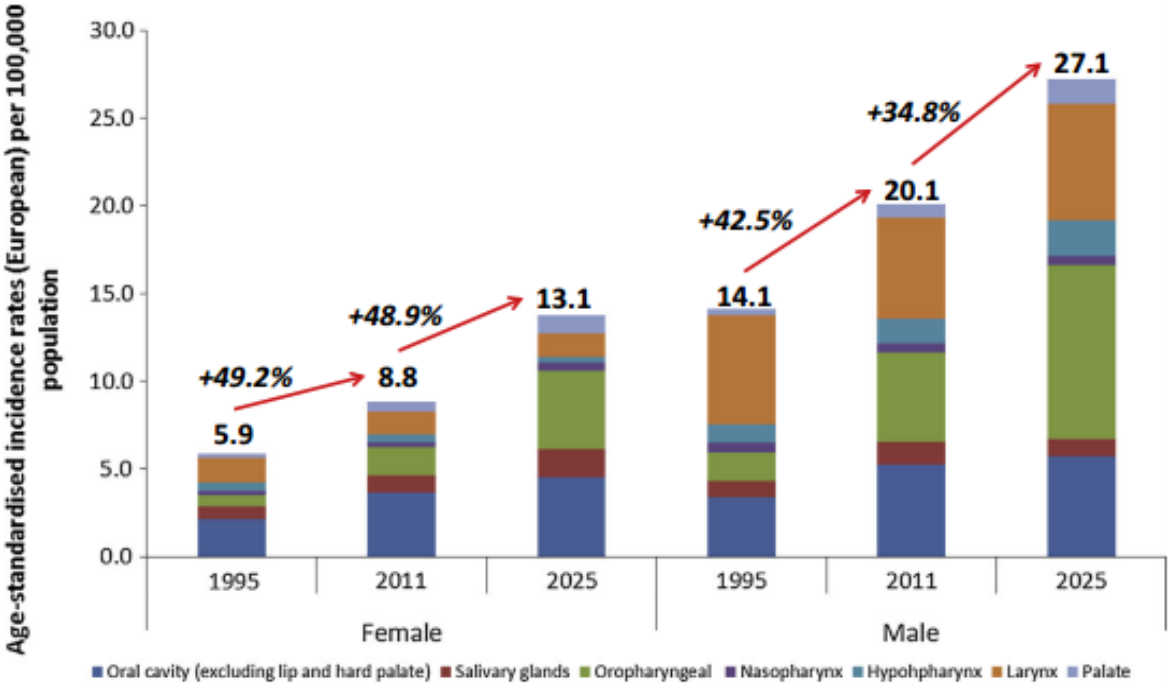


**Figure 1.5: "Distribution of head and neck cancers by anatomic site in 1995, 2011 and projected in 2025."** Taken from Louie *et al.* (2015).

Given the increased frequency in HPV driven tumours, and the differences in treatment outcome of these tumours, it is likely HPV status will play a routine role in instructing patient treatment strategies in the future. Although it has been proposed that treatment should be de-escalated in patients with HPV associated tumours, the best method to diagnose and treat these tumours is still under investigation (Morbini & Benazzo, 2016).

### 1.1.4 TNM staging

At present, treatment of HNSCC is primarily determined according to the stage of the cancer, which is classified by the TNM system (Lydiatt *et al.*, 2017). The first universal edition of the TNM classification of malignant tumours was put together in the 1960s and has continued to be revised over the last few decades by the International Union Against Cancer (UICC) and the American Joint Committee on Cancer (AJCC). The exact definitions of the stages vary between different anatomical sites, but are based on the size and spread of the tumour (Table 1.2). The T stage, relates to the size and invasiveness of the primary tumour, the N stage to the involvement of regional lymph nodes and the M stage to whether there are any distant metastases. Most recent revisions also take into account HPV status and the

presence of extra-nodal extension (ENE), defined as the extension of the metastatic carcinoma through the lymph node capsule and into the surrounding connective tissue (Lydiatt *et al.*, 2017). Accurate standardised TNM staging is important for clinicians to assess treatment options and predict patient prognosis and for researchers to track the changes in tumour biology throughout its progression.

**Table 1.2: AJCC staging of non-HPV associated (p16-negative) oropharyngeal tumours**

| **T Stage** | |
|---|---|
| Tx | Primary tumour cannot be assessed |
| Tis | Carcinoma *In Situ* |
| T1 | Tumour 2 cm or less in greatest dimension |
| T2 | Tumour larger than 2 cm but not larger than 4 cm in greatest dimension |
| T3 | Tumour larger than 4 cm in greatest dimension or extension to lingual surface of epiglottis |
| T4a | Moderately advanced local disease; tumour invades the larynx, extrinsic muscle of tongue, medial pterygoid, hard palate, or mandible |
| T4b | Very advanced local disease; tumour invades lateral pterygoid muscle, pterygoid plates, lateral nasopharynx, or skull base or encases carotid artery |
| **N stage** | |
| Nx | Regional lymph nodes cannot be assessed |
| N0 | No regional lymph node metastasis |
| N1 | Metastasis in a single ipsilateral lymph node, 3 cm or smaller in greatest dimension and ENE-negative |
| N2a | Metastasis in a single ipsilateral lymph node larger than 3 cm but not larger than 6 cm in greatest dimension and ENE-negative |
| N2b | Metastasis in multiple ipsilateral lymph nodes, none larger than 6 cm in greatest dimension and ENE-negative |
| N2c | Metastasis in bilateral or contralateral lymph nodes, none larger than 6 cm in greatest dimension and ENE-negative |
| N3a | Metastasis in a lymph node larger than 6 cm in greatest dimension and ENE-negative |
| N3b | Metastasis in any node(s) and clinically overt ENE-positive |
| **M stage** | |
| Mx | Distant metastasis cannot be assessed |
| M0 | No distant metastasis |
| M1 | Distant metastasis |

Adapted from Lydiatt *et al.*, 2017.

### 1.1.5 **Current Treatment**

If detected early HNSCC tends to have a favourable prognosis, however often patients present with advanced disease (O'Hara & Bradley, 2002); the cancer already having spread to the lymph nodes in the neck. In such cases it is not uncommon for patients to be diagnosed

with metastatic occult primary HNSCC, where the primary tumour site is never identified. More than 90% of these occult metastatic tumours are $HPV^+$ (Motz *et al.*, 2016). The choice of treatment for HNSCC patients is based on clinical staging, which takes into account primary tumour size, lymph node involvement, metastases, and HPV status, as well as general patient health.

In the UK, current treatment of early-stage HNSCC is usually surgical removal of the tumour or radiotherapy (Argiris *et al.*, 2008; NICE, 2016). In many cases the outcome following either treatment is similar and normally the decision of which option to take is based upon where the tumour is located. Although surgery may be preferable, as it avoids the negative toxic effects associated with radiation, a balance is sought between complete removal of the tumour and organ preservation. HNSCC can be associated with significant morbidity and maintaining quality of life following treatment is a high priority. At present it cannot be predicted which tumours will react favourably to which treatment, and this remains an active area of research.

In later stage locally-advanced disease, a mixture of surgery, radiation and chemotherapy is usually prescribed. In these cases chemoradiotherapy (CRT) has provided a step forward in patient treatment, proving to be more beneficial than either chemotherapy or radiotherapy alone. In a meta-analysis concomitant CRT was shown to increase overall survival of HNSCC patients by 6.5% at 5 years compared to radiation alone (33.7% vs 27.2%; Pignon *et al.*, 2009). It can be used as a definitive therapy, prior to, or after surgery (Seiwert *et al.*, 2007b; 2007a).

#### 1.1.5.1 *Targeted therapies*

Significant advancements in treatment types, such as better tools for more precise surgery and delivery of radiotherapy, along with the development of integrative treatment strategies has reduced the morbidity and mortality associated with HNSCC (Bernier & Bentzen, 2003). Recently increased understanding of the molecular mechanisms behind cancer development has led to the introduction of targeted therapies. Perhaps one of the most successful examples to date, is imatinib, which revolutionised the treatment of chronic myeloid leukaemia (CML) (Hehlmann *et al.*, 2005). Imatinib, a tyrosine kinase inhibitor, works by targeting Abelson kinase (ABL), which is constitutively expressed in CML, due to chromosomal rearrangement. The ability to specifically target cancerous cells is a step forward from

conventional chemotherapy, which targets dividing cells indiscriminately; hence the associated side effects, including hair loss and immune suppression. These therapies can be used in combination with drugs targeting other pathways or alongside chemotherapy or radiotherapy and, it is hoped, will not have the toxic side effects associated with traditional cancer treatments.

The EGFR inhibitor cetuximab is currently a targeted treatment option for HNSCC. EGFR is involved in a multitude of pathways (Section 1.1.2.1), and overexpressed in up to 95% of HNSCC tumours (Grandis & Tweardy, 1993), however it is unknown exactly what its role is in terms of HNSCC. Originally cetuximab, a monoclonal antibody which binds to EGFR, was approved for the treatment of colorectal cancer (CRC) expressing the wild type *KRAS* oncogene (Lievre *et al.*, 2006). Despite the increase in response rate in a subset of HNSCC patients when cetuximab is given alongside radiotherapy, there have been difficulties in identifying the patients that will best respond to this targeted therapy (Mehra *et al.*, 2008).

Despite advances in HNSCC treatments, the 5-year survival rate remains at less than 50% (Leemans *et al.*, 2011), highlighting the need for improved understanding of the complex network of interactions at play in HNSCC. The heterogeneous nature of tumours and differences in soluble factors and cells constituting their surrounding microenvironment are often impeding factors when it comes to their effective treatment.

### 1.1.6 **The tumour microenvironment**

In solid tumours, malignant cells make up just one part of a unique tumour microenvironment (TME; Figure 1.6). Consisting of extracellular matrix, fibroblasts, vascular endothelial cells and immune cells. The components of the TME determine the ability of a tumour to grow and eventually metastasise as well as influence how a tumour responds to specific treatment regimens (Hanahan & Weinberg, 2011). Moreover, by releasing soluble factors such as cytokines and chemokines into this environment, tumours themselves are able to influence neighbouring cells, and promote an environment beneficial for their own progression. Consequently, as well as directly targeting the tumour cells, manipulation of the components of the tumour stroma is also being investigated as an avenue for future therapy.

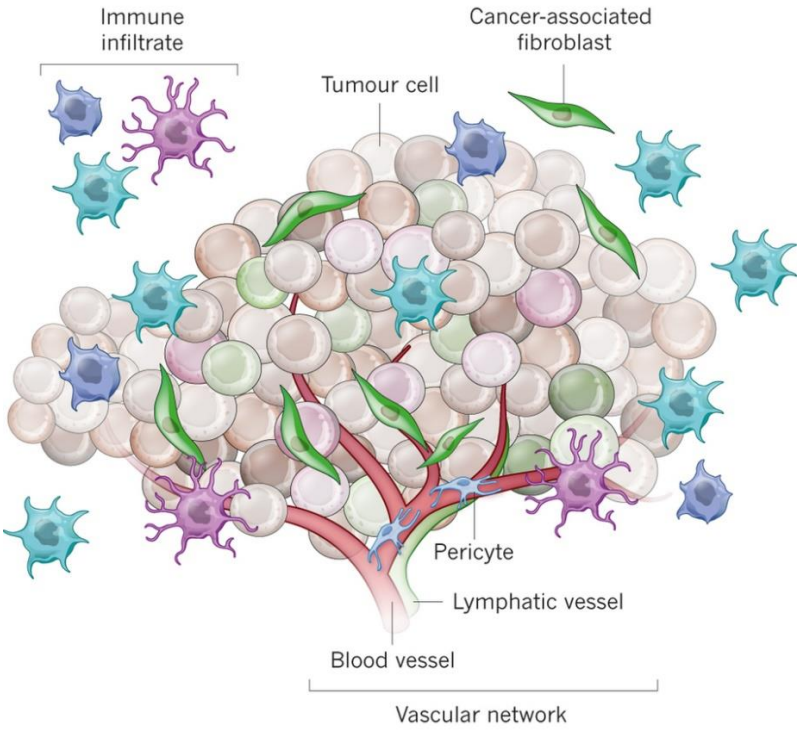


**Figure 1.6: Illustration of the tumour microenvironment**
In addition to malignant tumour cells, a large proportion of the mass of a solid tumour is comprised of stromal cells, including cancer-associated fibroblasts, infiltrating immune cells and vascular endothelium. Taken from (Junttila and de Sauvage 2013).

#### 1.1.6.1 *Cancer associated fibroblasts*

Cancer associated fibroblasts (CAFs) are the major component of the tumour stroma. CAF in the TME are a heterogeneous population. Most commonly described CAF are phenotypically similar to myofibroblasts; activated fibroblasts involved in inflammation and wound healing (Otranto *et al.*, 2012). However, unlike the normal activated fibroblast (NAF) present in wounds, CAF have enhanced proliferative properties and differ in terms of their morphology and secretome compared to NAF (Kalluri, 2016). In this respect parallels have been drawn between CAF and the fibrosis-associated fibroblasts (FAF) observed in dysregulated wound healing (Kalluri, 2016). In fibrosis, myofibroblasts become over active (FAF) and do not deactivate after the wound has closed. In addition to the highly proliferative, myofibroblast-like CAF, other distinct subsets exist, including a senescent population of CAF that promote tumourigenesis by the secretion of soluble factors (Orimo & Weinberg, 2007).

CAF release high levels of factors implicated in promoting tumour growth, such as transforming growth factor (TGF)-β, stromal derived factor (SDF)-1, epidermal growth factor (EGF), fibroblast growth factor (FGF)-2 and hepatocyte growth factor (HGF; Bhowmick *et al.*, 2004). They contribute toward tumour progression and metastasis by increasing proliferation of cancer cells, inhibiting their apoptosis, stimulating angiogenesis and enhancing tumour cell migration (Shiga *et al.*, 2015). There is evidence that they may also contribute to drug resistance by modulating the sensitivity of tumour cells to therapeutic agents (Li *et al.*, 2015b).

The origin of CAF are not fully understood, however there is evidence that they can be converted from normal fibroblasts in the TME or can be derived from epithelial- and endothelial-mesenchymal transition (EMT or EndoMT), from the cells of nearby adipose tissue or from mesenchymal stem cells (MSC; Shiga *et al.*, 2015). These differing origins are likely to contribute toward the phenotypic and functional heterogeneity observed in CAF (Orimo & Weinberg, 2007).

HNSCC CAF have been shown to enhance the proliferation of oral squamous cell carcinoma (OSCC) cells, compared with NAF, by the secretion of high levels of keratinocyte growth factor (KGF; Lin *et al.*, 2011). Galectin-1 released by HNSCC CAFs has also been shown to play a role in the increased migration of OSCC cells *in vitro*, via CCL2 induction (Wu *et al.*, 2011). Increased TGF-β expression has been observed in HNSCC CAF, compared with NAF (Rosenthal *et al.*, 2004; Takahashi *et al.*, 2015). Furthermore, it has been suggested that characteristics of the HNSCC stroma may be a better predictor of prognosis than those of tumour cells; for example high stromal smooth muscle actin (SMA) expression was found to be the strongest predictor of prognosis in a study assessing the relationship between disease mortality and a variety of clinical, pathological, and molecular characteristics of OSCC, including tumour stage, level of tumour invasion, presence of metastasis, level of immune infiltrate and EGFR expression, (Marsh *et al.*, 2011). They may also influence how a tumour responds to therapy. The co-culture of HNSCC cell lines with HNSCC CAF or with HNSCC CAF conditioned medium, prevented the inhibition of cell growth by cetuximab, suggesting soluble factors released by CAF may contribute to cetuximab resistance (Johansson *et al.*, 2012).

The TME is a dynamic environment in which the constituent cells adapt to increased survival pressure caused by changes to their local microenvironment, such as hypoxia. Both CAF and tumour cells are known to have an altered metabolic response and interact in a metabolic symbiosis that favours tumour growth (Liu *et al.*, 2016). Cancer cells stimulate CAF to undergo glycolysis, leading to the production of energy rich nutrients that fuel their further growth (Martinez-Outschoorn *et al.*, 2011).

In addition to CAF, another major constituent of the tumour stroma that has garnered much interest over recent years, are the tumour infiltrating immune cells. As with CAF, these cells are markedly different compared to those found in-healthy control tissue and consist of a wide variety of interacting cell types, the balance of which is probably a determining factor towards tumour survival or elimination.

## 1.2 The immune system

The human immune system is made up of a number of highly specialised cells, functioning together to defend the body against pathogens. Changes in the balance of these cell populations or their inactivation can lead to a compromised immune system and autoimmunity (Wing & Sakaguchi, 2010). It is the job of these cells to distinguish foreign, potential disease causing material from healthy self-cells and send out appropriate signals to initiate processes for their disposal. The variety of pathogenic agents the immune system has to recognise, from bacteria and viruses, to the hosts own damaged cells, has driven the adaptation of a highly complex system, able to up and down regulate its response according to the immediate needs.

### 1.2.1 Tumour-immune system interaction

The process of immunosurveillance, was proposed in the 1950s as a major barrier to the development of cancerous cells into tumours (Burnet, 1957). The surface expression of tumour-associated antigens enables immune cells to distinguish tumour cells from those of healthy tissue, and elicit an immune response (Coulie *et al.*, 2014). In some cases tumour evasion is thought to be due to inefficient recognition of cancerous cells, by the downregulation of the antigen processing or presenting machinery (section 1.2.2.3) and antigen loss (Garrido *et al.*, 1997; Johnsen *et al.*, 1998). However, tumours are often enriched in activated immune cells, suggesting that in these cases an immune response is stimulated by the presence of these malignant cells (Koch *et al.*, 2006). Furthermore, studies

in melanoma and ovarian, breast, prostate, renal cell, oesophageal, colorectal and head and neck cancers found that the presence of tumour infiltrating lymphocytes (TIL) was an indicator of a positive prognosis (Vesalainen *et al.*, 1994; Halpern & Schuchter, 1997; Marrogi *et al.*, 1997; Naito *et al.*, 1998; Nakano *et al.*, 2001; Schumacher *et al.*, 2001; Zhang *et al.*, 2003; Balermpas *et al.*, 2014a). Despite this, the immune cells present are unable to eradicate tumours *in situ*. Further investigation has proven the TME to be highly immunosuppressive, with factors released by tumour cells themselves contributing to evasion of the immune system by disabling the effects of cytotoxic immune cells.

### 1.2.2 **T lymphocytes**

T lymphocytes are a type of white blood cell, involved in mediating adaptive immunity, which mature in the thymus. They express the surface marker CD3 and can be further subdivided into populations of specialised cell types with distinct roles in the coordination of an effective immune response. These subsets can be recognised based on the expression of distinct surface proteins.

#### 1.2.2.1 *T helper and cytotoxic T cells*

The T cell population is primarily made up of T helper (Th) cells and cytotoxic T cells, which express the surface markers CD4 and CD8, respectively. However, other subpopulations of T cells such as natural killer (NKT) T cells, a highly specialised cell type with roles in both the adaptive and innate immunity (Lang, 2009), also make up a small percentage of $CD3^+$ lymphocytes (<10%; Koreck *et al.*, 2002). Th cells and cytotoxic T lymphocytes (CTL) are found in the peripheral blood at an approximate 2:1 ratio. While Th cells are responsible for the activation of a variety of other immune cells, including B cells, other T cells and macrophages, CTL directly target and eliminate infected, cancerous or damaged cells (Andersen *et al.*, 2006). T helper cells can be further categorised into Th1, Th2, Th17, Th22, Th9, T follicular helper cells (Tfh) and T regulatory cells (Treg), which secrete distinct repertoires of proteins, corresponding to their different roles (Protti *et al.*, 2014). Th1 cells tend to be pro-inflammatory, mainly involved in targeting intracellular parasites and viruses and mediating the activation of cell destruction and phagocytosis. Th2 elicit responses against extracellular organisms and are associated with both inflammation and immune suppression. A skew toward a Th2 response is responsible for asthma and allergies where Th2 cells orchestrate an inflammatory response by stimulating B cell differentiation and the activation and recruitment of eosinophils (Cousins, 2017). They can

also release factors regarded as anti-inflammatory, such as IL10, and dampen down the Th1 response by release of IL4 (Kidd, 2003). Th17 cells are a highly plastic cell type that are mainly associated with protection against fungal and bacterial pathogens at the mucosal membranes of the small intestine, respiratory tract and skin (Muranski & Restifo, 2013). Th17 cells are overactive in various autoimmune diseases and contribute to the development of graft versus host disease (GVHD; (Muranski & Restifo, 2013; Tabarkiewicz *et al.*, 2015). Treg are a suppressive population of cells, involved in immune regulation by inhibiting other types of immune cells (Section 1.2.2.4). The roles of Th1, Th2, Th17 and Treg in cancer have been widely studied, whilst relatively little is known of the relevance of Th9, Th22 and Tfh in this context (Protti *et al.*, 2014).

All T cells are initially released from the thymus into the periphery in a naïve state. Naïve T cells are inactive cells that have yet to come into contact with the specific antigen that will cause their activation to a T effector. Once activated, the differentiation of naïve $CD4^+$ T cells in to different Th effector cells is regulated by cytokine signalling (Section 1.2.7).

#### 1.2.2.2 *αβ/γδ T cells and V(D)J somatic recombination*

All T cells express T cell receptors (TCR) on their surface, which recognise specific antigens and mediate their activation to an effector state. These TCR are heterodimers, the majority of which, consist of an alpha and a beta protein chain (αβ T cells). These highly variable chains account for the ability of T cells to recognise a variety of different antigens. A smaller population of T cells (<5% of peripheral T cells) exist whose TCR consist of beta and gamma chains (γδ T cells; Kabelitz *et al.*, 2007). Members of this unconventional T cell subset are not reliant on MHC restricted activation (described in Section 1.2.2.4) and do not express the conventional Th and CTL markers CD4 and CD8 (Wu *et al.*, 2014). γδ T cells are activated in response to a diverse type of antigens, including MHC and non-MHC surface proteins, soluble proteins, small peptides, phosphoantigens and lipids, and therefore rely on different mechanisms of activation (Born *et al.*, 2013). They are most commonly found in mucosal tissue and skin where they protect against pathogens by the release of cytokines, promoting Th effector differentiation, and can also act as antigen presenting cells (Wu *et al.*, 2009). Each TCR protein chain consists of a constant (C) region, variable (V) region, joining (J) region and, in the case of β and δ chains, a diversity region (D; Figure 1.7). In the thymus, gene segments encoding the V, D and J regions undergo random recombination, resulting in a range of diverse amino acid sequences that can recognise a large repertoire of antigens.

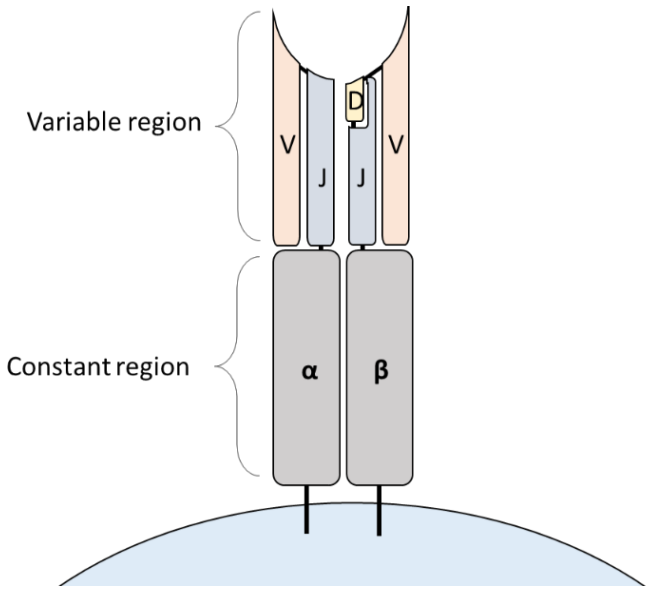


**Figure 1.7: αβ T cell receptor**

#### 1.2.2.3 *MHC restricted T cell activation*

In the periphery T cells circulate throughout the blood and lymphatic systems, in an inactive or resting state. Upon recognition of a specific pathogenic antigen, T cells are activated, inducing their differentiation and/or proliferation. In order for T cells to recognise their specific antigens the latter must be bound to major histocompatibility complex (MHC) molecules (Figure 1.8), a caveat termed MHC antigen restriction that introduces a significant level of control to T cell activation (Wu *et al.*, 2002). T cell activation usually takes place in secondary lymphoid organs but can also take place at other peripheral sites including tumours (Thompson *et al.*, 2010). T cells bind to MHC via their TCR receptors and the co-receptors CD4 and CD8. Th cells bind to peptides expressed on MHC class II found principally on antigen presenting cells (AgPC). AgPC are able to internalise foreign antigenic peptides, where they are processed and presented on an MHC class II molecule at the cell surface. MHC class I molecules are found on all nucleated cells and normally display antigens derived from intracellular proteins to CTL. An additional mechanism, termed cross presentation, enables AgPC to process and present extracellular proteins on MHC I molecules to CTL (Rock & Shen, 2005). Cross presentation is an important mechanism in cancer, were the tumour antigen is not present in AgPC.

In addition to the TCR signal, a secondary co-stimulatory signal is required, usually via the CD28 receptor, which recognises the ligands CD80 and CD86, expressed on AgPC (Wu *et*

*al.*, 2002). Following activation various other co-stimulatory receptors are upregulated on the T cell surface which on interaction with their ligands, provide the survival signals required for an efficient T cell response (Chen & Flies, 2013).

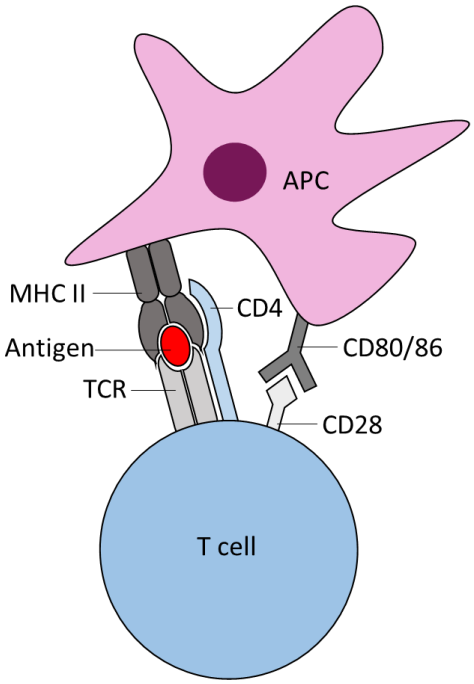


**Figure 1.8: The activation of CD4⁺ T cells by antigen presenting cells**
The two signal model for CD4⁺ T cell activation, an antigen recognised by their specific T cell receptor (TCR) must be presented on an AgPC via an MHC molecule.

On the surface of cancerous cells, MHC class I present tumour antigens, which upon recognition by the corresponding TCR elicit a cytotoxic response from CTL. The mechanism of MHC and antigen processing is often found to be faulty in tumour cells, leading to the downregulation of tumour antigens and impairing their recognition by immune cells (Leone *et al.*, 2013).

#### 1.2.2.4 *Thymic selection*

T cells mature from thymocytes, following both positive and negative selection processes in the thymus (Figure 1.9; Takaba & Takayanagi, 2017). Initially, on entering the thymus these cells are double negative, i.e. lack both CD4 and CD8 surface receptors. Following TCR somatic recombination, thymocytes express CD4 and CD8, which are required to stabilise the interaction between TCR receptors and MHC II and MHC I molecules respectively. Cells with TCRs that successfully bind to MHC molecules on the thymic epithelial cells are

positively selected; it is this stage that determines commitment to CD4 or CD8 lineage (Germain, 2002). Any cells that are unable to bind, undergo apoptosis. Negative selection then takes place, were apoptosis is induced in cells with too high an affinity to MHC. When effective this process ensures cells leaving the thymus are single positive (i.e. express one of either CD4 or CD8) and self-tolerant. This stringent selection ensures that the final pool of mature T cells that are released into the periphery display both MHC antigen restriction and self-tolerance. Surgical removal of the thymus from mice or its failure to form properly in development, as in *nude* mice, leads to immunodeficiency (Kojima & Prehn, 1981; Wang *et al.*, 1998). In humans the immunodeficiency observed in sufferers of DiGeorge syndrome is the result of underdevelopment or absence of the thymus (Wilson *et al.*, 1993; Davies *et al.*, 2017).

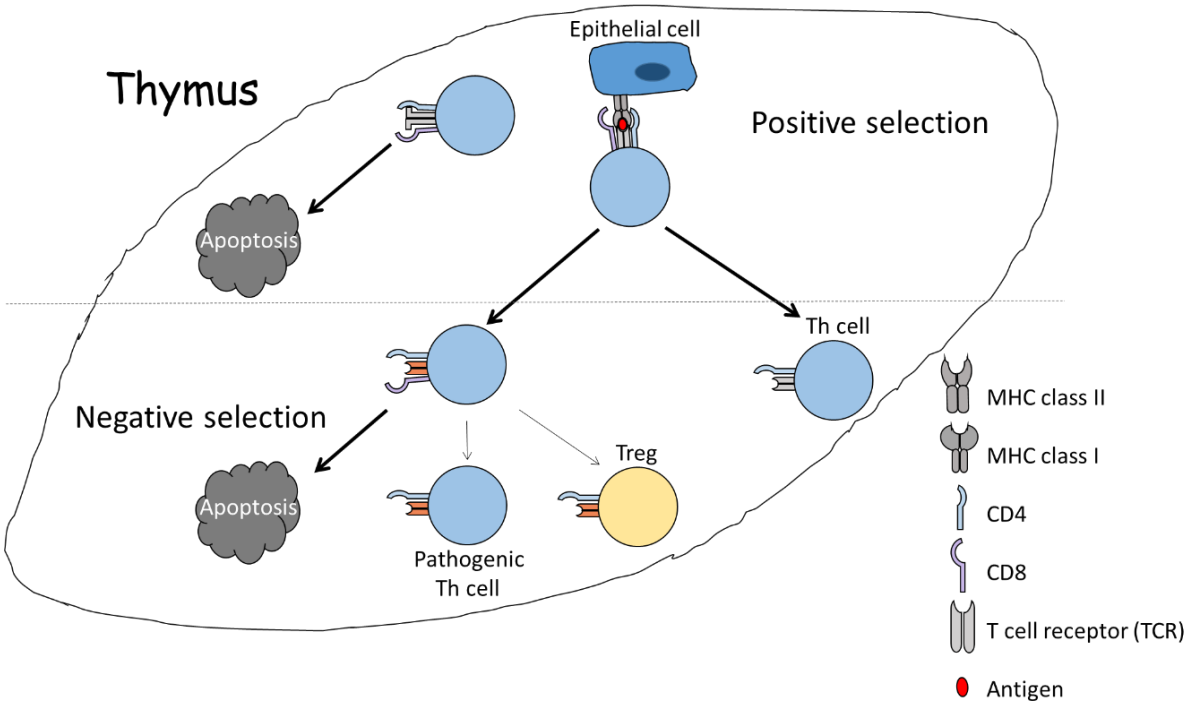


**Figure 1.9: Positive and negative selection of T cells in the thymus**
Thymocytes develop into mature T lymphocytes in the thymus. Cells with TCRs that successfully bind to MHC molecules on the thymic epithelial cells are positively selected, while those unable to bind undergo apoptosis. Cells with too high an affinity to MHC (orange TCRs) then go through negative selection. When effective (bold arrows) cells leaving the thymus are single positive and self-tolerant. Some self-reactive T cells that avoid negative selection may become suppressive Treg, however others may enter the periphery as pathogenic T cells.

#### 1.2.2.5 *T regulatory cells*

Despite the thymic selection process some self-reactive T cells end up in the periphery where, if activated, they can become pathogenic (Itoh *et al.*, 1999). Fortunately, mechanisms exist to keep these cells in check; one such mechanism involves a subset of $CD4^+$ T cells called T regulatory cells (Treg). Treg act as suppressor cells, mediating the effects of other immune cells.

The presence of a cell population able to modulate T cell function had long been speculated as a method of self-tolerance. This theory was supported by numerous studies that noted the loss of a sub population of T cells in mice as being responsible for the resulting autoimmune diseases (Sakaguchi *et al.*, 1985; Powrie & Mason, 1990; Smith *et al.*, 1991). Identifying these cells proved more challenging however, but the suppressive action was later attributed to a subgroup of $CD4^+$ T cells that expressed the alpha chain of the interleukin-2 (IL2) cell surface receptor CD25 (Sakaguchi *et al.*, 1995; Asano *et al.*, 1996). Making up 5-10% of $CD4^+$ T cells in humans and mice, removal of these cells leads to the expansion of auto reactive T cells and the development of an autoimmune phenotype (Asano *et al.*, 1996). Other T cells do exist that are also thought to have suppressor activities, including a subset of $CD8^+$ T cells (Cosmi *et al.*, 2003; Wei *et al.*, 2005). However, the $CD4^+CD25^{+/high}$ population is the most extensively studied, due to it being the most common, and is what is classically referred to as a Treg. In addition to the suppression of auto-reactive T cells, Treg are also involved in modulating the immune response to infectious agents and inhibiting the inflammatory response (Wan & Flavell, 2008).

A further breakthrough in the study of Treg came in the identification of the transcription factor Forkhead Box P3 (FoxP3) as a specific marker, necessary for mouse Treg development (Fontenot *et al.*, 2003; Hori *et al.*, 2003; Khattri *et al.*, 2003). A mutation in this gene was found to be the causative factor for the X-linked multi-systemic autoimmune disease seen in scurfy mice (Brunkow *et al.*, 2001), and in human immunodysregulation polyendocrinopathy enteropathy X-linked disease (IPEX; OMIM: #304790; Bennett *et al.*, 2001; Wildin *et al.*, 2002). In both cases, a lack of functional FoxP3 allows autoreactive T cells to go unchecked and the resulting autoimmune diseases are usually fatal in infancy (Wildin *et al.*, 2002). Genetic ablation of *Foxp3* in mice prevents Treg development and leads to a severe autoimmune phenotype, similar to that of scurfy mice (Kim *et al.*, 2007). It has also been shown that forced expression of FoxP3 increases Treg number and is

sufficient to induce a regulatory function in both $CD4^+CD25^-$ and $CD8^+$ murine T cells *in vitro* (Khattri *et al.*, 2003). Moreover, ectopic *Foxp3* expression in naïve $CD4^+$ cells could successfully rescue the disease phenotype of inflammatory bowel disease (IBD) and autoimmune gastritis mouse models *in vivo* (Hori *et al.*, 2003), further highlighting the importance of this gene in the control of Treg development and securing its status as a master regulator. The role of FoxP3 in human T cells however has proved to be more elusive. In contrast to observations from murine studies, expression of FoxP3 is not sufficient to induce suppressive activity (Allan *et al.*, 2007; Tran *et al.*, 2007). It is clear that FoxP3 has an important role in the formation of human Treg, and elucidating this role remains an important obstacle to overcome in order to gain a better understanding of the development and maintenance of this cell population.

Treg, as is the case with other T cells, recognise a wide range of antigens. However, the TCR repertoire in Treg only partially overlaps that of conventional T helper cells, with the Treg population containing a greater number of cells reactive to self-antigens (Hsieh *et al.*, 2006; Pacholczyk & Kern, 2008). It is thought to be these characteristics that allow Treg to protect against autoimmunity, in addition to modulating the response to infectious agents.

Treg appear in the periphery of normal healthy mice three days from birth (Asano *et al.*, 1996). Thymectomy prior to this time leads to the development of autoimmune diseases, as any pathogenic self-reactive T cells that escaped deletion in the thymus will not be suppressed (Kojima *et al.*, 1976; Taguchi *et al.*, 1980; Kojima & Prehn, 1981; Tung *et al.*, 1987). Although historically Treg were thought to solely originate in the thymus, increasing evidence has been found supporting the existence of distinct subpopulations of Treg, broadly split according to their origin, into those that are thymically derived (natural Treg) and others which are induced from $CD4^+$ naïve T cells in the periphery (induced Treg). Although there are some phenotypic and functional variations between the subsets, the full nature of these variations is not yet fully understood. Moreover, attempts to further elucidate these differences are complicated by a lack of distinction between the two groups, which have no specific biological markers; each will be discussed in turn.

#### 1.2.2.6 *Natural and induced T regulatory cells*

Natural Treg (nTreg) are those $CD4^+CD25^{hi}FoxP3^+$ Treg derived in the thymus. They are a polyclonal population, able to recognise a diverse range of antigens, and are estimated to

make up 1-2% of $CD4^+$ T cells in the periphery (Baecher-Allan *et al.*, 2001). Induced or adaptive Treg (iTreg) are generated from naïve T cells in the periphery following antigen activation and their differentiation is mediated by soluble factors, such as the cytokines TGF-β and IL10 (Figure 1.10). The exact contribution of these cells to the overall pool of Treg in a healthy individual is not clear, with studies suggesting it could be anywhere between 4 and 30% (Lathrop *et al.*, 2008; Thornton *et al.*, 2010). Knowledge of these cells has been gained from mouse models and the work carried out from cells induced *in vitro*, as studies using Treg directly isolated from humans will consist of a mix of both n and iTreg. Consequently, these cells are less well defined than nTreg, and there is inconsistency in the literature regarding their characterisation.

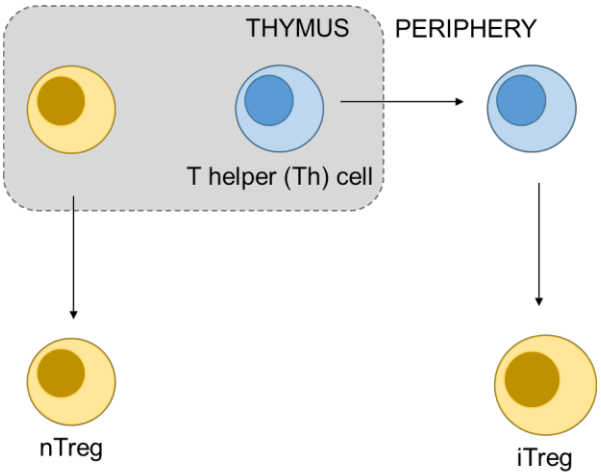


**Figure 1.10: Treg develop in the thymus (nTreg), or are induced from naïve T cells in the periphery at secondary lymphoid organs or other tissue (iTreg)**
Once in the periphery nTreg require activation via their TCR to become functionally suppressive. TCR activation is also necessary for iTreg induction, therefore activation is an essential part for both nTreg and iTreg functionality.

As understanding of Treg has increased, in order to clearly distinguish the cell types being discussed and eliminate any ambiguity between studies, suggestions have been made to update the terminology used to describe these cells (Shevach & Thornton, 2014). In this case nTreg should be referred to as thymically derived (t)Treg and the induced Treg separated to distinguish *in vitro* induced Treg (iTreg) and those induced *in vivo* in the periphery (pTreg). Throughout the current study, all Treg induction experiments were carried out *in vitro* to model the peripheral induction that takes place in cancer patients and were thus called iTreg. Furthermore, any analysis measuring induced Treg in patients was carried out based on

findings from human iTreg or the various pTreg subsets (Tr1, Th3), in which case these are referred to specifically.

#### 1.2.2.7 *Induced T regulatory cell subtypes*

The induction of Treg, requires antigen stimulation and the presence of certain cytokines (Hoffmann *et al.*, 2004; Bergmann *et al.*, 2007). Subgroups have been defined according to their cytokine expression profiles and factors required for their differentiation and development (Wan & Flavell, 2006). For example Th3 cells, involved in oral tolerance, are induced by the differentiation factor IL4 and have high TGF-β secretion (Weiner, 1997; Inobe *et al.*, 1998). T regulatory 1 (Tr1) cells have been found to be induced *in vivo* in the periphery in mice and *in vitro* from both mouse and human cells, in the presence of IL10, and characteristically express high levels of IL10, and TGF-β and little or no IL2 and IL4 (Groux *et al.*, 1997; Bergmann *et al.*, 2007; Haringer *et al.*, 2009). Originally associated with the suppression of inflammatory responses in the intestine (Read *et al.*, 2000), Tr1 cells have been identified in human peripheral blood and are also prevalent in the HNSCC TME (Bergmann *et al.*, 2007; Haringer *et al.*, 2009).

In addition to the cytokines released by and utilised in the induction of different subsets of iTreg, such as Tr1 cells, there are also some phenotypic distinctions (Table 1.3). However, other iTreg are phenotypically similar to nTreg, or their surface markers are not well defined (e.g. Th3), making the task of distinguishing between various subsets challenging. Studying nTreg and iTreg separately and assessing how they contribute in different immune settings is therefore problematic. Although candidate markers have been proposed to distinguish nTreg and iTreg their specificity and thus ability to effectively differentiate the two subsets is contentious.

**Table 1.3: Phenotypes associated with human CD4$^+$ regulatory T cells (Treg) and the expression of these markers on other conventional T helper cells**

| | nTreg | iTreg | | Other CD4$^+$ Th subsets | References |
|---|---|---|---|---|---|
| | | FoxP3$^+$iTreg | Tr1 | | |
| **CD25** | +/high | + | - | Activated Th cells | (Allan *et al.*, 2007; Schuler *et al.*, 2014) |
| **CD26** | -/low | -/low | -/low | Conventional Th cells | (Salgado *et al.*, 2012) |
| **CD39** | + | + | + | Some memory T cells | (Mandapathil *et al.*, 2009; Schuler *et al.*, 2014; Mascanfroni *et al.*, 2015; Fang *et al.*, 2016) |
| **CD73** | +*/- | + | + | Subset of conventional Th cells | (Mandapathil *et al.*, 2009; Mandapathil *et al.*, 2010a) |
| **CD127** | -/low | -/low | -/low | Resting Th cells | (Liu *et al.*, 2006; Alves *et al.*, 2008; Costa *et al.*, 2015) |
| **CTLA4 (CD152)** | + | + | + | Activated Th cells | (Read *et al.*, 2000; Takahashi *et al.*, 2000; Bacchetta *et al.*, 2002) |
| **FoxP3*** | + | + | - | Activated Th cells | (Allan *et al.*, 2007; Zeng *et al.*, 2015) |
| **GITR** | + | + | + | Activated Th cells | (McHugh *et al.*, 2002; Ronchetti *et al.*, 2015) |
| **Helios*** | + | +/- | Unknown | Activated T cells | (Thornton *et al.*, 2010; Kim *et al.*, 2012) |
| **LAP/GARP** | - | +/- | Unknown | - | (Battaglia & Roncarolo, 2009; Tran *et al.*, 2009; Wang *et al.*, 2009b) |
| **Nrp1 (CD304)** | +/- | +/- | | Activated T cells | (Battaglia *et al.*, 2008; Milpied *et al.*, 2009) |

*Intracellular markers

### 1.2.2.8 *Identifying T regulatory cells*

CD25 and FoxP3 are commonly used as markers for Treg in both humans and mice. However, both are also expressed on human activated T cells (Allan *et al.*, 2007). To distinguish Treg from these activated T cells, Treg are often defined based upon their expression of a high level of CD25. However, defining the cut-off point for a "high" CD25 expression is subjective and can lead to variation between studies. Commonly the level is set according to CD25 expression on $CD4^-$ lymphocytes, so that any cells exceeding the level of CD25 expression on the $CD4^-$ cells are defined as having $CD25^{hi}$ expression (Figure 1.11a; Lundgren *et al.*, 2005). A study by Stauss *et al.* (2007b) used a mean fluorescent intensity (MFI) exceeding 120 to define $CD25^{hi}$ expression, based on their findings that $CD4^+CD25^+$ cells below this cut off failed to suppress other T effector cell populations (Figure 1.11b). Contour or density plots can also be used to aid in gating $CD25^{hi}$ cells, for example Finney *et al.* (2010) only included cells with CD25 expression above the 90% contour level of the $CD4^+$ cells (Figure 1.11c). A limitation with these methods is that some Treg will express an intermediate level of CD25 similar to that in the $CD4^-$ population, thus may not be included in the $CD25^{hi}$ gate. When identifying Treg for use in functional assays there is therefore a balance between identifying as many Treg as possible, whilst maintaining a pure population.

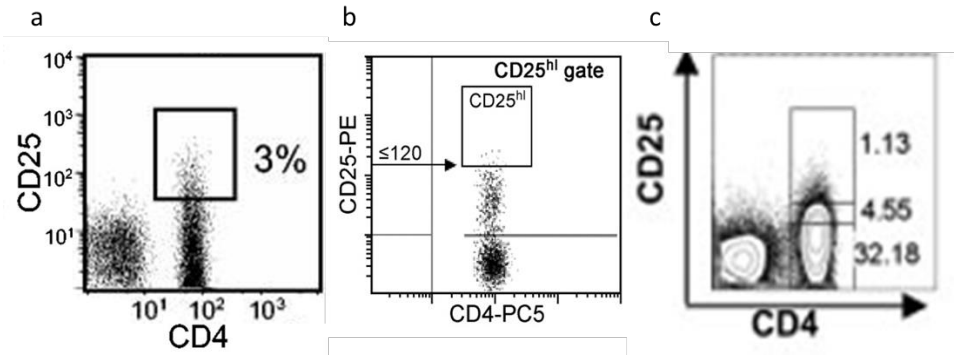


**Figure 1.11: Commonly used methods for defining $CD25^{hi}$ lymphocytes**
Scatter graphs and contour plots taken from three different studies showing the expression of CD4 and CD25 on healthy control PBMC (Lundgren *et al.*, 2005; Strauss *et al.*, 2007b; Finney *et al.*, 2010). $CD25^{hi}$ lymphocytes were defined as cells with (a) CD25 expression exceeding that of $CD4^-$ lymphocytes, (b) CD25 expression with an MFI greater than 120 or (c) CD25 expression above the 90% contour level on $CD4^+$ cells. $CD25^{hi}$ expression varied in the three studies; 3% of $CD4^+$ lymphocytes, 0.5% of $CD4^+CD25^+$ lymphocytes and 1.13% of $CD4^+$ lymphocytes, respectively.

Upon activation *in vitro* human T effector cells have been shown to transiently up regulate FoxP3 (Gavin *et al.*, 2006; Allan *et al.*, 2007; Tran *et al.*, 2007). Although many studies have shown that no regulatory action is conferred by the induction of FoxP3 expression (Allan *et al.*, 2007; Tran *et al.*, 2007), others have observed a corresponding gain in suppressive activity *in vitro* (Pillai *et al.*, 2007). However, where this was the case, over time these cells lost their suppressive capabilities with the corresponding down regulation of Foxp3, reverting back to conventional effector T cells. This transient expression could prove problematic when looking to induce and isolate Treg for clinical therapy. It is unknown whether the phenotypic plasticity that has been observed in many of these studies is a characteristic of all $FoxP3^+$ T cells or limited to a subset, and if the latter what proportion this is of the overall Treg population. It is clear that caution must be taken in interpreting FoxP3 expression alone as an indicator of stable Treg, and that it is useful to look for expression of other markers, in addition to $CD25^{high}$ and FoxP3, concomitantly. Furthermore, given that FoxP3 is localised in the nucleus, requiring cells to be permeabilised prior to staining, it cannot be used for the identification of Treg for subsequent functional studies.

Although FoxP3 itself may not be a definitive Treg marker, it contains an intronic CpG rich Treg specific demethylated region (TSDR) that distinguishes stable FoxP3-expressing Treg from activated T cells (Baron *et al.*, 2007). Demethylation of the TSDR, also known as conserved non-coding DNA sequence 2 (CNS2), correlates with the stability of FoxP3 expression, and high levels of demethylation may distinguish nTreg from iTreg (Lin *et al.*, 2013). Epigenetic regulation of additional conserved non-coding DNA sequences (CNS) in the FoxP3 gene has been shown to be important in both nTreg and iTreg generation and maintenance. *In vivo* KO of these regions in mice induced differing effects on the peripheral Treg pool (Zheng *et al.*, 2010). Knockout of the CNS3 region led to a five-fold decrease in the proportion of $FoxP3^+$ thymocytes, but made no difference to the level of FoxP3 expression in the individual $FoxP3^+$ cells. This suggests CNS3 is important in the initial generation of nTreg and iTreg. These differences were less marked in the periphery of these mice, and in heterozygous KO, suggesting the reduction in Treg generation could be compensated for by increased Treg expansion. Although CNS1 KO had no effect on thymic Treg generation, it did impede iTreg induction both *in vitro* and in the periphery. CNS2 KO led to a reduction in the proportion of FoxP3 expression in the spleen and lymph nodes, but not in the thymus. Furthermore, in contrast to wild type cells CNS2 KO cells lost FoxP3

expression following *in vitro* culture and adoptive transfer to T cell deficient recipients. Therefore, suggesting a role for CNS2 in FoxP3 stability and Treg maintenance.

Tr1 cells express neither CD25 or FoxP3 (Zeng *et al.*, 2015), and it maybe that other subsets of human iTreg may also lack these classical Treg markers, making the search for alternatives imperative.

Other commonly used markers for the identification of Treg exist (Table 1.3), including the cell surface receptors cytotoxic T-Lymphocyte Associated Protein 4 (CTLA-4; Read *et al.*, 2000; Takahashi *et al.*, 2000) and glucocorticoid-induced tumour necrosis factor receptor-related protein (GITR; McHugh *et al.*, 2002). However, neither of these markers are expressed by all Treg and are limited to certain subsets. Treg can also be negatively selected according to the absence of CD26 and CD127 (Liu *et al.*, 2006; Salgado *et al.*, 2012). Expression of the surface receptor CD127 was found to be reciprocal to that of FoxP3 in $CD4^+$ human Treg (Liu *et al.*, 2006) making it a useful alternative for the selection of Treg for functional studies, however it is also down regulated on TCR activated T cells (Alves *et al.*, 2008). The lack of expression of CD26 has been suggested as a better option for use in Treg selection as it is not down regulated on activation, so its expression remains high in activated conventional $CD4^+$ T cells. Therefore, CD26 is able to distinguish naïve and activated T cells from Treg (Salgado *et al.*, 2012). However, CD26 is weakly expressed on a small number (~15%) of Treg (Mandapathil *et al.*, 2012).

Due to the upregulation of many of the proposed Treg markers in activated T cells (McHugh *et al.*, 2002), an alternative method used to define Treg is by testing the cells for their ability to suppress conventional T cell function. These experiments however require a high yield of cells, which are not always readily available. Phenotypic identification using a combination of known markers remains to be the best method to determine the presence of Treg.

It has been proposed that the Helios molecule, may be able to distinguish nTreg from iTreg of mice and humans (Thornton *et al.*, 2010; Kim *et al.*, 2012). Helios is a lymphopoietic transcription factor thought to play a role in activating IL2 production in Treg (Baine *et al.*, 2013). Thornton *et al.* (2010), found that Helios was present in approximately 70% of human and murine peripheral Treg but not in iTreg induced *in vitro* or *in vivo*. Additionally, Treg expressing effector cytokines usually associated with iTreg were found predominantly to be $Helios^-$ and those expressing Helios were observed to have typically higher CpG

demethylation in the FoxP3 TSDR than those that did not, further supporting the notion that Helios$^+$ Treg are thymically derived (Kim *et al.*, 2012). However this viewpoint has proved controversial and other studies have recorded conflicting results (Akimova *et al.*, 2011; Himmel *et al.*, 2013). Analysis of human cord blood, found that some FoxP3$^+$ Treg (<10%) did not express Helios (Ayyoub *et al.*, 2013; MacDonald *et al.*, 2013), perhaps indicative that some Helios$^-$ Treg can also be thymically derived. Studies by Akimova *et al.* (2011) and Himmel *et al* (2013) found that Helios was not restricted to Treg and that nTreg also contain Helios$^-$ cells. The dynamic nature of circulating lymphocytes can make it difficult to accurately characterise some of these cells and has hindered attempts to find distinct markers. Whether or not Helios accurately distinguishes thymically-derived Treg from those induced in the periphery, it appears to define a distinct Treg subtype and is another marker that may be useful for identifying Treg.

Other features also exist that are thought to be specific to certain subsets of Treg, such as expression of the LAP/GARP complex and neuropilin-1. Glycoprotein A repetitions predominant (GARP) is a membrane bound protein that was recently discovered to bind latent TGFβ, via its constituent latency-associated peptide (LAP), and facilitate its surface expression. LAP and GARP are expressed on activated human Treg with a potent suppressor function but are absent on the majority of both FoxP3$^+$ and FoxP3$^-$ activated non-Treg (Tran *et al.*, 2009; Wang *et al.*, 2009b). It is these properties that may make this subset of markers of particular promise for future immunotherapy. Tran *et al* were able to make use of the highly specific expression of LAP alongside that of IL1 receptors to develop a protocol for purifying Treg from expanded T cell cultures (Tran *et al.*, 2009).

A lot of the research on Treg has been carried out on mice. The difficulties in translating results from murine studies to applications in human medicine, is highlighted by the expression profile of neuropilin-1 (Nrp1). Studies in mice have found that Nrp1 is present on Treg but not on activated T cells (Bruder *et al.*, 2004; Yadav *et al.*, 2012). Furthermore, it has been proposed as a surface marker for murine nTreg (Weiss *et al.*, 2012; Yadav *et al.*, 2012), but not iTreg. Contrastingly, in humans Nrp1 is expressed on a small subset of Treg found in secondary lymphatic tissue but is absent from peripheral blood isolated Treg (Battaglia *et al.*, 2008; Milpied *et al.*, 2009). This Nrp1$^+$ Treg subset has been noted to be particularly prevalent in cancer patients. Its function is thought to involve enhancement of the interaction between Treg and dendritic cells during antigen recognition and there is

evidence that it may be important in mediating tumour infiltration of Treg (Chaudhary *et al.*, 2014). Furthermore, T cell specific ablation of Nrp1 in mice significantly reduced Treg numbers at the tumour site and hindered tumour growth (Hansen *et al.*, 2012). Hence, the further characterisation of $Nrp1^+$ Treg may have prognostic and therapeutic value.

Expression of the ectonucleotidases CD39 and CD73 has been associated with a subset of Treg (Borsellino *et al.*, 2007; Whiteside *et al.*, 2012). The $CD4^+CD39^+$ has been observed to largely correspond with the $CD4^+FoxP3^+$ Treg population, with more than 90% of $FoxP3^+$ human peripheral Treg expressing CD39 (Mandapathil *et al.*, 2009). In contrast, CD73 is found to be more widely expressed on $CD4^+$ Th cells (Mandapathil *et al.*, 2009). Whilst in mice CD39 and CD73 are co-expressed on the surface of Treg, in humans CD73 is expressed internally in $CD39^+$ nTreg, and only transiently on the surface of $CD39^+$ iTreg (Whiteside *et al.*, 2012).

The absence of a definitive Treg marker has meant that the way Treg are defined and analysed varies considerably between studies, making direct comparisons difficult. For example, an increase in Treg cells determined by an increase in a particular marker, such as FoxP3 may not correspond with an increase in another marker, such as CD39. In addition, different methods of induction may well lead to differences in iTreg phenotype. For example, iTreg generated following polyclonal T cell activation by anti-CD3/CD28 were observed to be less suppressive than those activated with antigen presented by AgPC (Zhao *et al.*, 2014). Despite the lack of consensus on how to best define Treg, the markers that have been associated with these cells (Table 1.3) have helped to shed some light on the mechanisms employed for their regulatory function.

#### 1.2.2.9 *Functional mechanisms of T regulatory cells*

The mechanisms by which Treg are able to exert their suppressive function are yet to be fully established. However, there is evidence from *in vitro* studies and the expression of certain functional markers, including CD25, CTLA-4 and CD39, that they act through numerous mechanisms. This is not surprising given the variety of cell types they are able to influence (Figure 1.12).

*In vitro*, Treg are naturally anergic cells with a potent suppressive function; only a small number are needed to suppress a much larger population of conventional T effector cells (Vercoulen *et al.*, 2009; Candia *et al.*, 2017). Although they require activation via their TCR

in order for suppression to be triggered, once active they are able to suppress in a non-specific manner, preventing the activation and proliferation of both $CD4^+$ and $CD8^+$ lymphocytes irrespective of their TCR specificity (Takahashi *et al.*, 1998; Thornton & Shevach, 1998), as well as suppressing monocytes, dendritic cells (Grossman *et al.*, 2004), natural killer (NK) cells (Smyth *et al.*, 2006) and B cells (Zhao *et al.*, 2006). Treg also require significantly lower doses of antigen (10 to 100 times) for their activation compared to conventional T cells (Takahashi *et al.*, 1998).

*In vivo,* Treg mechanism of action is harder to measure, but also requires TCR stimulation. Again, once Treg are activated, their specificity becomes redundant; however it is worth noting that the transfer of Treg specific for the relevant tissue associated antigens results in more effective organ specific autoimmune disease prevention than transfer of polyclonal Treg (Tang *et al.*, 2004). This suggests that antigen specificity may be important for directing migration, or that Treg may require continuous re-stimulation to maintain effective suppression. Historically, the majority of experiments looking at Treg function are carried out using murine or *in vitro* models, inferences made from these are limited by the previously stated discrepancies between mouse and human Treg phenotypes and because *in vitro* systems do not fully recapitulate the complexity of systems *in vivo*.

#### 1.2.2.9.1 Cell-contact dependent suppression

The importance of cell-cell contact for Treg suppression differs between studies. Some *in vitro* experiments led to the hypothesis that direct cell-cell contact was a requirement for Treg to exert their suppressive function, as when separated by a semi permeable membrane they were unable to prevent proliferation of activated effector T cells (Takahashi *et al.*, 2000). Additionally, in the same study, supernatant collected from cultured Treg was unable to prevent proliferation of conventional T cells.

Treg are known to interfere with the interaction between AgPC, such as DC, and conventional T cells, preventing naïve T cell activation and their differentiation to T effector cells (Figure 1.12). High CTLA-4 expression on the surface of Treg exerts a suppressive action by binding CD80 and CD86 on DC, inducing downregulation of these molecules (Wing *et al.*, 2008). CD80 and CD86 are required for the costimulatory signalling necessary for T cell activation. Thus CTLA-4 mediated downregulation of these receptors prevents the activation of other naïve T cells. The binding of CTLA-4 to DC also induces the secretion

of the immunomodulatory enzyme indolamine 2,3-dioxygenase (IDO), which leads to production of immunosuppressive kynurenine (Grohmann *et al.*, 2002). Another receptor that is highly expressed on Treg is lymphocyte activation gene-3 (LAG-3), which binds to MHC II (Huang *et al.*, 2004). On binding, LAG-3 induces inhibitory signals that suppress DC activation and maturation (Liang *et al.*, 2008).

Another cell-contact dependent mechanism Treg employ for immune suppression is by cytolysis of target cells. Both nTreg and iTreg have been shown to utilise this pathway and can use it to directly target a range of immune cells (Grossman *et al.*, 2004; Gondek *et al.*, 2005; Zhao *et al.*, 2006; Cao *et al.*, 2007). Human Treg have been shown to release the cytolytic proteases granzyme A and B as well as the pore forming molecule perforin, which mediates granzyme entry to target cells (Grossman *et al.*, 2004; Zhao *et al.*, 2006). Once in the cell the granzymes induce programmed cell death via caspase independent or dependent pathways, respectively (Lieberman, 2010). There is evidence from mouse studies that Treg can also implement granzyme mediated suppression that is perforin independent (Gondek *et al.*, 2005).

#### 1.2.2.9.2 Cytokine mediated suppression

It is universally recognised that cytokines play an important role in T cell growth and function as well as the maintenance and induction of the various subpopulations (Section 1.3.1). Treg suppression may also be mediated by cytokines, with the secretion of high levels of immunosuppressive IL10 and TGF-β by Treg particularly well documented, and more recently IL35 (Section 1.3.1). Although blockade of these cytokines does not prevent Treg mediated suppression *in vitro*, there is evidence that they are involved in T cell suppression *in vivo (*Asseman *et al., 1999;* Read *et al., 2000)*. It is also possible that cytokines contribute to suppression by increasing the sensitivity of other T cells to suppressive factors or by the further induction, or expansion of Treg, rather than acting directly in suppression.

IL2 is important for the maintenance and expansion of conventional T cells and Treg both *in vitro* and *in* vivo in the periphery (Takahashi et al., 1998; Thornton & Shevach, 1998; Bayer et al., 2005), and is thought to play a role in preventing apoptosis of these cells following TCR stimulation (Refaeli *et al.*, 1998). High CD25 expression on Treg may act as an IL2 sink, binding to IL2 in the surrounding environment and depriving other conventional T cells of the IL2 required for their activation and expansion (Pandiyan *et al.*, 2007).

#### 1.2.2.9.3 Other mechanisms of suppression

CD39 and CD73 are ectonucleotidases found on Treg that work together to degrade ATP to adenosine, a known immunosuppressant (Deaglio *et al.*, 2007). This process is highly important in the regulation of the inflammatory response, where the accumulation of ATP provides pro-inflammatory signals to immune cells. CD39 and CD73 break the ATP down to AMP and then to adenosine, supporting immunosuppression (Antonioli *et al.*, 2013). Adenosine signalling takes place via four G-coupled protein receptors, however the receptor predominantly expressed on immune cells is the A2A adenosine receptor (A2AR; Fredholm *et al.*, 1994). Adenosine induces a shift in the cytokine expression profile released by mature DC, particularly a reduction in IL12 and IFN-γ and increase in IL10 production, which favours differentiation of Th2 cells (Panther *et al.*, 2003). The release of adenosine by Treg has also been shown to induce DC migration, leading to the formation of DC-Treg clusters and preventing activation of effector T cells (Ring *et al.*, 2015). In lymphocytes, the stimulation of A2AR impedes TCR signalling, leading to decreased IL2 production and decreased CD25 expression, as well as decreased production of IFN-γ and IL4 (Csoka *et al.*, 2008), leading to an overall reduction in T cell proliferation and differentiation. Furthermore, stimulation of A2AR in mice led to enhanced TGF-β production and induction of $FoxP3^+$ iTreg (Zarek *et al.*, 2008).

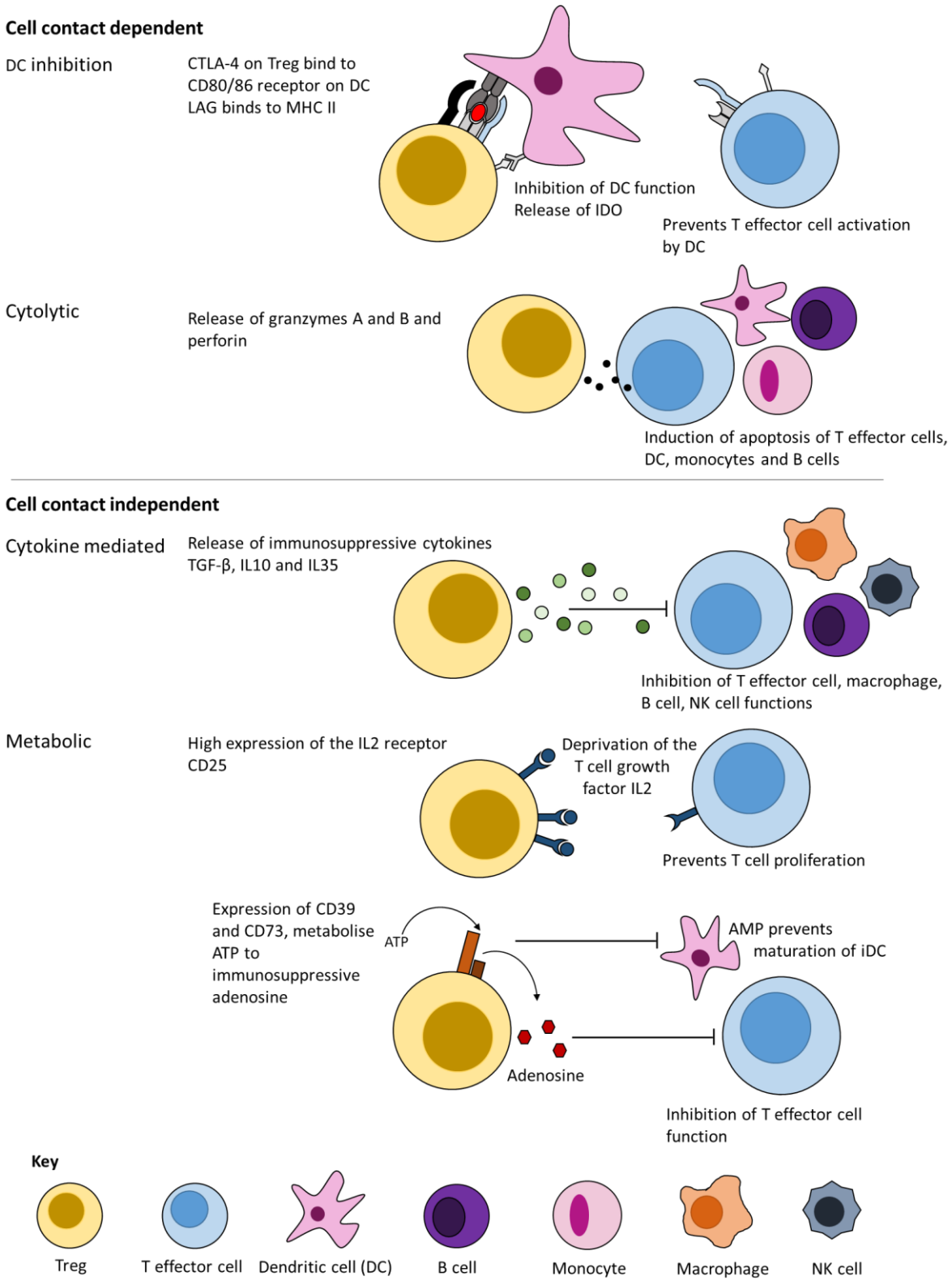


**Figure 1.12: The mechanisms of suppression employed by Treg**

Treg use cell-cell contact dependent and independent mechanisms for immunosuppression. Cell contact dependent mechanisms can directly target T cells by granzyme mediated cytolysis (either perforin dependent or independent), or indirectly by inhibition of AgPC. Non-contact dependent mechanisms include the release of immunosuppressive cytokines, or deprivation of the growth factor IL2 and the metabolism of ATP to adenosine by the receptors CD39 and CD73. Adapted from Liberal *et al*. (2015).

It is likely that suppression relies on a variety of different mechanisms, which may vary between subsets, and correspond with the differences in marker expression. Human Treg studies have looked at Treg as a mixed population or at iTreg induced *in vitro*, as at present it is not possible to distinguish between subsets. The prominent mechanism of suppression may therefore vary depending on the setting. One such setting, where establishing the role of Treg is particularly important is in cancer. HNSCC in particular has been found to contain notably high levels of infiltrating Treg (Mandal *et al.*, 2016).

### 1.2.3 T regulatory cells in cancer

Cancer patients, including those with HNSCC, are often immunosuppressed and are reported to have increased levels of Treg both in the periphery and in the tumour microenvironment (Woo *et al.*, 2001; Liyanage *et al.*, 2002; Ichihara *et al.*, 2003; Miller *et al.*, 2006; Strauss *et al.*, 2007a; Strauss *et al.*, 2007b; Chi *et al.*, 2010). *In vitro* studies have shown that soluble factors released by human tumours can attract existing Treg and induce iTreg from naïve T cells (Zou, 2005). The original speculation was that an accumulation of these cells in the TME would promote tumorigenesis, by suppressing the immune system, and would therefore correlate with poor patient prognosis. For many solid tumour types, including ovarian, breast, hepatocellular and non-small cells lung carcinomas (NSCLC), this seems to be the case. However, whether or not Treg are always beneficial to tumour development is a matter of debate, and is probably dependent on spatiotemporal factors. For example, an increase in infiltrating Treg in the tumours of colorectal cancer (CRC) patients was seen to correlate with a positive prognosis (Salama *et al.*, 2009; Hanke *et al.*, 2015). This is speculated to be due to the role of Treg in preventing inflammation (Erdman & Poutahidis, 2010), a process with clear links to tumour formation and growth. In murine studies, the adoptive transfer of Treg can suppress the progression of bacterially induced-colon cancer (Erdman *et al.*, 2003; Maloy *et al.*, 2003). It therefore, may be that Treg can have both beneficial and detrimental effects depending on the type of cancer, its aetiology and the stage of development of the tumour.

It may also be the case that the localisation of Treg rather than the number of Treg present in a tumour, may be the more important prognostic factor (Mizukami *et al.*, 2008b). Gastric cancer patients whose Treg were mostly dispersed throughout the central tumour compartment had a worse prognosis than those whose Treg were mainly located in peri-tumoural regions (Mizukami *et al.*, 2008b).

The association between increased intratumoral Treg in HNSCC and patient prognosis is uncertain, with some studies observing a positive correlation (Badoual *et al.*, 2006; Badoual *et al.*, 2013; Bron *et al.*, 2013; Lukesova *et al.*, 2014), while others note a negative (Sun *et al.*, 2012) or no correlation (Pretscher *et al.*, 2009; Balermpas *et al.*, 2014a). This could be reflecting the differences between the HNSCC cohorts used in the studies. Levels of Treg in the periphery of HNSCC patients have been shown to increase with cancer progression (Drennan *et al.*, 2013; Sun *et al.*, 2014; Sun *et al.*, 2015) and a population of activated Treg was found to be negatively correlated with prognosis. In laryngeal squamous cell carcinoma (LSCC) patients, there was an increase in the proportion of Treg with an activated phenotype ($CD4^+CD45^-FoxP3^+$) during disease progression, while resting Treg decreased ($CD4^+CD45^+FoxP3^+$), presumably by conversion to an active state (Sun *et al.*, 2015). Further understanding and identifying different subtypes of Treg will be key to unravelling the part Treg play in cancer. It is likely that changes in the overall number of Treg in cancer is only part of the story, and alterations to Treg function are also important. For example, Treg from HNSCC patients have been shown to be more potent suppressors than those of healthy controls (Drennan *et al.*, 2013).

Although the prognostic significance of Treg in cancers is not always clear, there is evidence that inhibiting the immunosuppressive cells in the tumour environment in conjunction with stimulating tumour immunity may lead to effective cancer treatment (Curiel, 2007). The presence of high levels of Treg following vaccination can impede efficacy, and reducing numbers of peripheral Treg has shown some promise in improving patient outcome (van der Burg *et al.*, 2016). Furthermore, although studies in mice have noted that the depletion of Treg breaks tumour tolerance and encourages a rejection response, it also led to the development of severe autoimmune diseases (Onizuka *et al.*, 1999; Shimizu *et al.*, 1999). Therefore, a careful balance must also be sought between improving the local tumour immune response and maintaining peripheral immune regulation. Establishing the contribution of the different Treg subsets to the total tumour infiltrating Treg population and whether their roles differ, will be essential for the development of future therapies.

Rather than the number of Treg or their function alone, it could be the balance between different cell populations that is the more telling indicator of prognosis. For example, a high ratio of CD8:Treg has been correlated with improved overall survival (Shang *et al.*, 2015). Furthermore, T effectors recovered from HNSCC TIL are often compromised; with defects

in signalling and function (Reichert *et al.*, 1998). This adds a further level of complexity when drawing conclusions relating to the presence of certain T cell populations.

### 1.2.4 Cytotoxic T cells in head and neck cancer

Unlike Th cells, CTL are able to directly target and lyse tumour cells. MHC class I molecules that are involved in initiating their activation are found on all nucleated cells. One of the most common mechanisms of action of CTLs is via the delivery of granzymes and perforin to the surface of target cells (Cullen *et al.*, 2010). In addition CTLs express FasL and can induce cell death by the Fas/FasL pathway (Rouvier *et al.*, 1993). It is well established that increased levels of tumour infiltrating CTL are beneficial for cancer patients, with the outcome for HNSCC patients with high levels of CTL infiltration being more favourable (Nasman *et al.*, 2012; Nordfors *et al.*, 2013; Balermpas *et al.*, 2014a). However, often CTLs in the TME have impaired function, exhibiting an exhausted phenotype (Zarour, 2016), or are suppressed due to the presence of other factors, such as Treg

### 1.2.5 Th1/Th2 cells in head and neck cancer

There has been no prognostic benefit observed from increased tumour infiltrating $CD4^+$ cells in HNSCC (Nordfors *et al.*, 2013; Balermpas *et al.*, 2014a). This is likely because they represent a mixed population of cell types (Figure 1.13), with diverse and sometimes opposing, roles in immune modulation. Th1 cells activate CTL and other immune cells, orchestrating the destruction of malignant cells. In contrast Th2 cells are traditionally viewed as being pro-tumourigenic, inhibiting the induction of cell mediated immunity (Ellyard *et al.*, 2007). The skew toward a tumour promoting Th2 phenotype in HNSCC is supported by the observed increase in the Th2- associated cytokines, IL10 and IL6, and the reduced Th1-associated IL12 in the plasma of HNSCC patients with advanced disease (Sparano *et al.*, 2004).

### 1.2.6 Th17 in head and neck cancer

Th17 cells represent a highly plastic cell population. There is much contradiction around their association with prognosis for cancer patients (Ye *et al.*, 2013). In the HNSCC patient periphery, Th17 were observed to be enhanced compared to levels in healthy controls. Furthermore, tumour supernatants collected from HNSCC cell lines were able to facilitate Th17 recruitment and promote their induction *in vitro* (Kesselring *et al.*, 2010).

Contrastingly, Th17 cells in the peripheral blood of patients with malignant salivary gland tumours, was lower than in that of patients with benign tumours, while healthy controls had the highest levels of circulating Th17 cells (Haghshenas *et al.*, 2015). Th17 can mediate both pro- and anti-tumorigenic effects, including promoting angiogenesis, activating CTLs and recruiting Th1 cells (Ye *et al.*, 2013), however it is unclear whether these cells favour or impede tumour growth overall. Furthermore, Th17 cells are considered an unstable T cell population that can transdifferentiate into Treg and Th1 cells under certain conditions (Geginat *et al.*, 2016; Liu *et al.*, 2017).

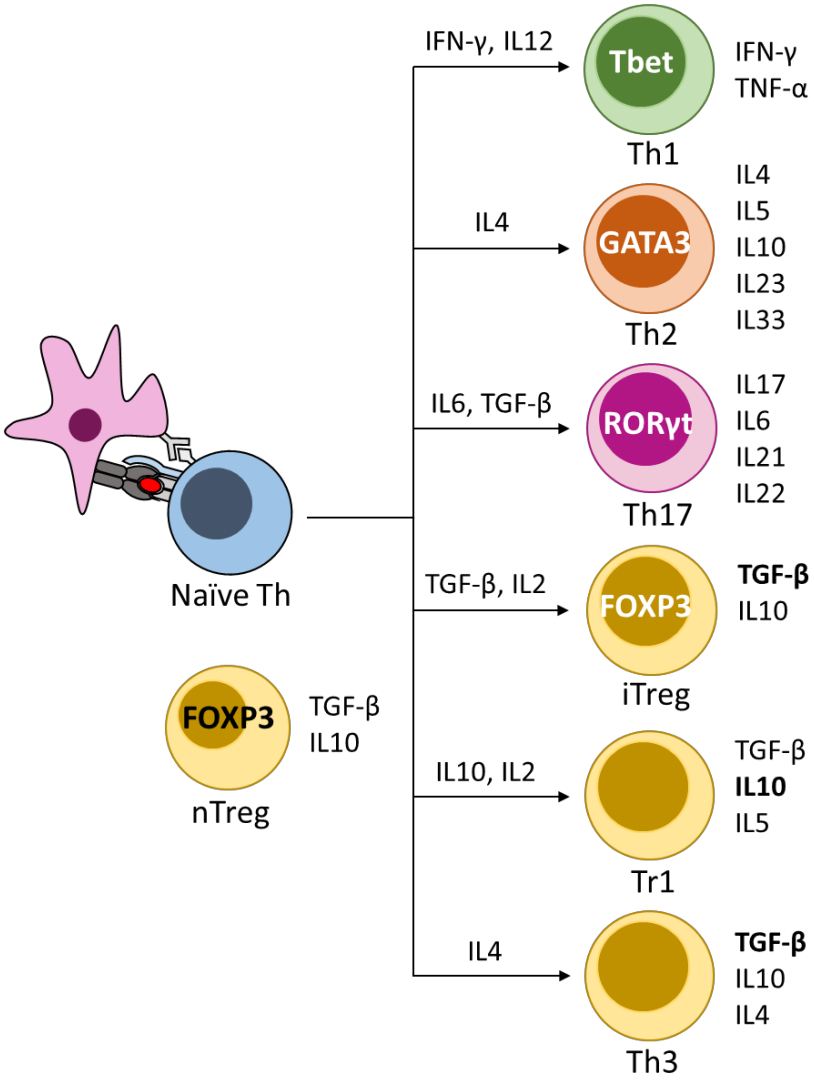


**Figure 1.13: T cell differentiation is mediated by cytokines**
Cytokines mediate the differentiation of naïve T cells into their effector subsets, following activation. The commitment to each lineage is orchestrated by different transcription factors. Each T effector cell subset released a distinct repertoire of cytokines. The cytokines primarily responsible for suppression in the different Treg subsets are highlighted in bold. Adaoted from (Zhou *et al.*, 2009), Bassett, (2010) and (Wu *et al.*, 2014).

### 1.2.7 **CD4⁺ plasticity**

Cytokines can also mediate the differentiation of $CD4^+$ T cells, following their activation and can induce reprogramming into other Th subsets (Luckheeram *et al.*, 2012). Th1 and Th2 differentiation are reliant on interferon-γ (IFN-γ) and IL12 and on IL4, respectively (Kidd, 2003), while TGF-β can drive the differentiation of both $FoxP3^+$ iTreg and Th17 (Kimura & Kishimoto, 2010). However, these cells can also be derived independently of TGF-β, with Tr1 cells developing in the presence of IL10 and Th17 by IL1β and IL23 (Roncarolo *et al.*, 2006; Ghoreschi *et al.*, 2010). Furthermore, various *in vitro* and *in vivo* murine models have demonstrated that Th17 can convert to Treg and *vice versa*, under particular conditions (Xu *et al.*, 2007; Gagliani *et al.*, 2015), and that similarly both Treg and Th17 can be converted to Th1-like cells (Kleinewietfeld & Hafler, 2013). Although Th17 and Treg have been observed to be particularly plastic, there is increasing evidence that this capability may be common to other Th effector subsets, hence these subsets may not represent terminally differentiated cells, as was once thought (Luckheeram *et al.*, 2012).

### 1.2.8 **Other immune cells in head and neck cancer**

Although T cells remain one of the most extensively studied of the tumour infiltrating immune cell populations, there are numerous studies documenting the influence of tumour cells on the activation and function of other immune cells. Interactions between these cell populations are likely to be what determines the overall success of a tumour to progress. Levels of NK cells, another cell of lymphoid lineage, are reduced in the periphery of HNSCC patients compared with healthy controls and functionally suppressed in the TME (Accomando *et al.*, 2012; Bottcher *et al.*, 2013). NK cells are highly important in immune surveillance and can directly target and lyse malignant cells. There is evidence that both Treg and some tumour cells can directly suppress the function of NK cells (Ghiringhelli *et al.*, 2005; Vitale *et al.*, 2014). Increased NK infiltration into the tumour is associated with a better prognosis in HNSCC patients (Mandal *et al.*, 2016)

Another important immune cell population prevalent in the TME are macrophages, phagocytic white blood cells that are activated in response to infection. Classically, they are described to be polarised toward a classical (M1) or alternative (M2) phenotype upon activation, which mirrors that of lymphocytes (Gordon, 2003). However, it is likely that a spectrum of intermediate phenotypes exists between these two subsets (Xue *et al.*, 2014).

Pro-inflammatory M1 macrophages promote Th1 cell differentiation, while M2 cells are associated with Th2 lymphocytes and an anti-inflammatory response. In the TME, tumour associated macrophages (TAMs) can differentiate from circulating monocytes or nearby resident tissue macrophages (Yang & Zhang, 2017). In the HNSCC microenvironment, TAMs are generally skewed toward the M2 phenotype, which have been associated with late stage disease and poor prognosis (Mori *et al.*, 2011; Fujii *et al.*, 2012; Balermpas *et al.*, 2014b). Furthermore, M2 macrophages release soluble factors that promote immunosuppression, for instance by the induction of Treg (Schmidt *et al.*, 2016b).

In addition to Treg and M2 macrophages, myeloid-derived suppressor cells (MDSC) are another cell type that contribute to the immune suppression observed in the TME. MDSCs are a heterogeneous population of pro-tumourigenic immature myeloid cells. They have been associated with Treg induction, and the inhibition of effector T cell function by impaired TCR activation and migration (Filipazzi *et al.*, 2012). Despite the composition of immune cells in the TME being relatively well documented, it remains unclear as to how tumours manipulate this balance and the role each of these cells plays in immune evasion, tumour invasion and metastasis.

## 1.3 Immune cell regulation in the tumour microenvironment

The tumour microenvironment is highly enriched in immune cells, particularly relevant to this are a group of signalling proteins called cytokines that play an extensive role in orchestrating the immune response. In addition, to their roles in cell differentiation (Section 1.2.7) they can also act as growth factors and are involved in cell migration. In many cases these molecules are highly pleiotropic, and their effects are determined by the presence or absence of other factors in the surrounding environment. Alterations to this complex network can lead to the enrichment of certain immune cell populations and the inhibition of others, promoting an immune suppressive environment that supports the growth and spread of cancer and impedes cancer therapies. One such example is the increase in the proportion of suppressive Treg observed in many solid tumours (Section 1.2.3). Suggested mechanisms for this Treg enrichment are by the increased proliferation of nTreg, induction of iTreg from $CD4^{+}CD25^{-}$ or naïve precursors (Section 1.2.2.4.6), increased apoptosis of other T effector cells, or by the increased recruitment or retention of Treg at the tumour site; all processes influenced by soluble factors present in the tumour milieu (Figure 1.14).

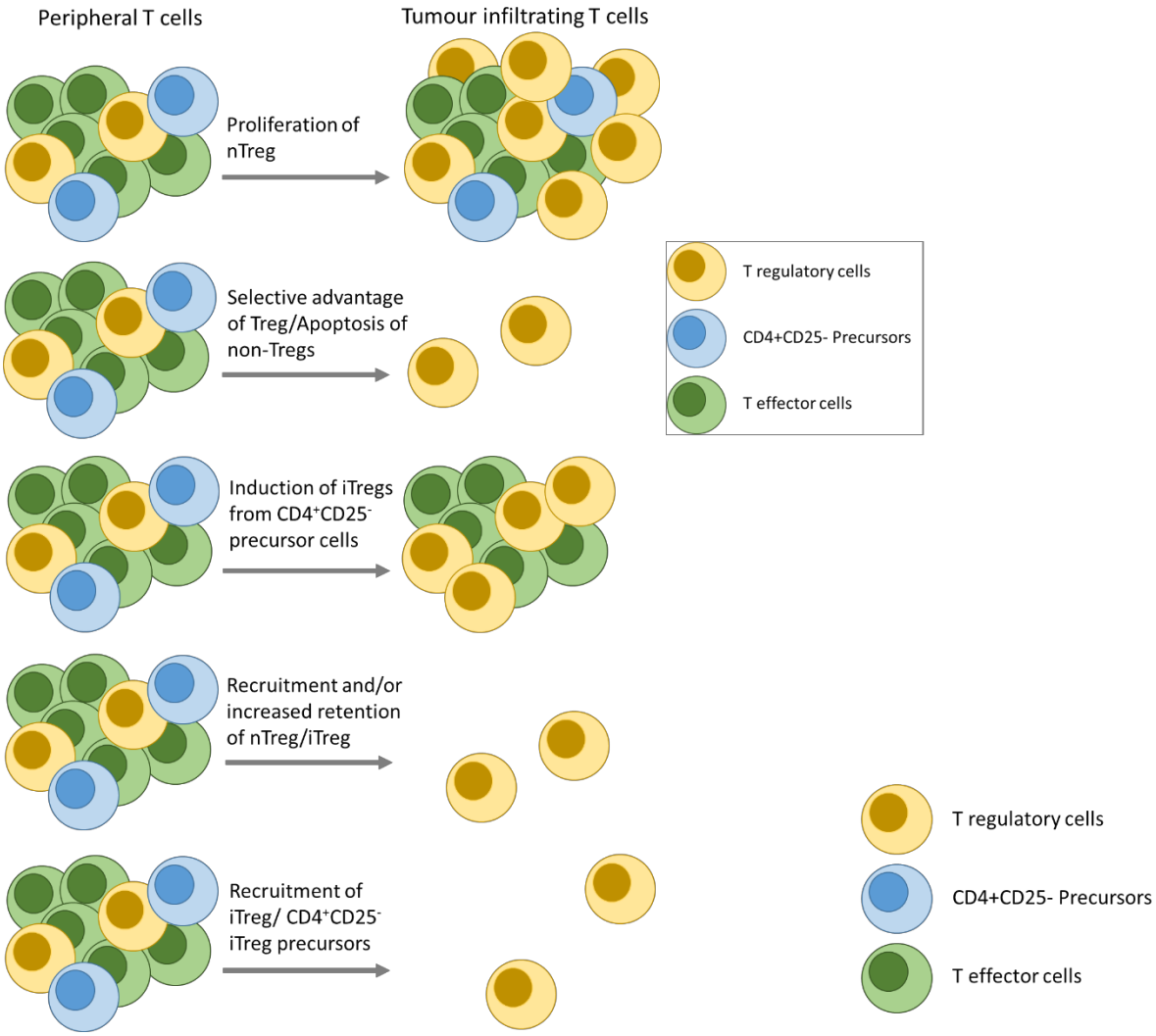


**Figure 1.14: Mechanisms of Treg enrichment in the TME**
The proportion of Treg in tumours has been observed to be significantly higher than that observed in the periphery. Accumulation of these cells could be by an increase in nTreg proliferation at the tumour site, the targeted apoptosis of other T effector cells, iTreg induction or preferential recruitment and/or retention of Treg at the tumour site.

### 1.3.1 Soluble factors and immunosuppression

Parallels between the immune environment present in many solid tumours and that induced in an inflammatory response have been proposed, with cytokine profiles common to both. The link between inflammation and cancer has long been appreciated, with chronic inflammation a known risk factor for carcinogenesis (Coussens & Werb, 2002). This inflammation is usually a secondary response to persistent infection, such as the response to HPV in HNSCC and cervical cancer (Section 1.1.1.4), or to faulty immune regulation, such as inflammatory bowel disease (IBD)-associated colon cancers. In addition to promoting

DNA damage by the release of reactive oxygen and nitrogen species, chronic inflammation can lead to immunosuppression (Wang & DuBois, 2015). A twelve chemokine gene expression signature associated with a T cell inflamed phenotype was identified in melanoma (Messina *et al.*, 2012). In a study looking at the expression of these twelve chemokines, this signature was observed in up to 50% of the 100 HNSCC cases investigated, and was particularly prevalent in $HPV^+$ tumours (75% compared with 23% in $HPV^-$; Saloura *et al.*, 2014).

Cytokines upregulated in inflammatory environments, including TNF-α, IL6, IFN-γ and TGF-β, mediate the activation, differentiation, proliferation, apoptosis and recruitment of immune cells (Figure 1.15; Yoshimura, 2006; Duray *et al.*, 2010). However, some have opposing effects on different cells or in different circumstances, making picking apart this complex network of proteins difficult.

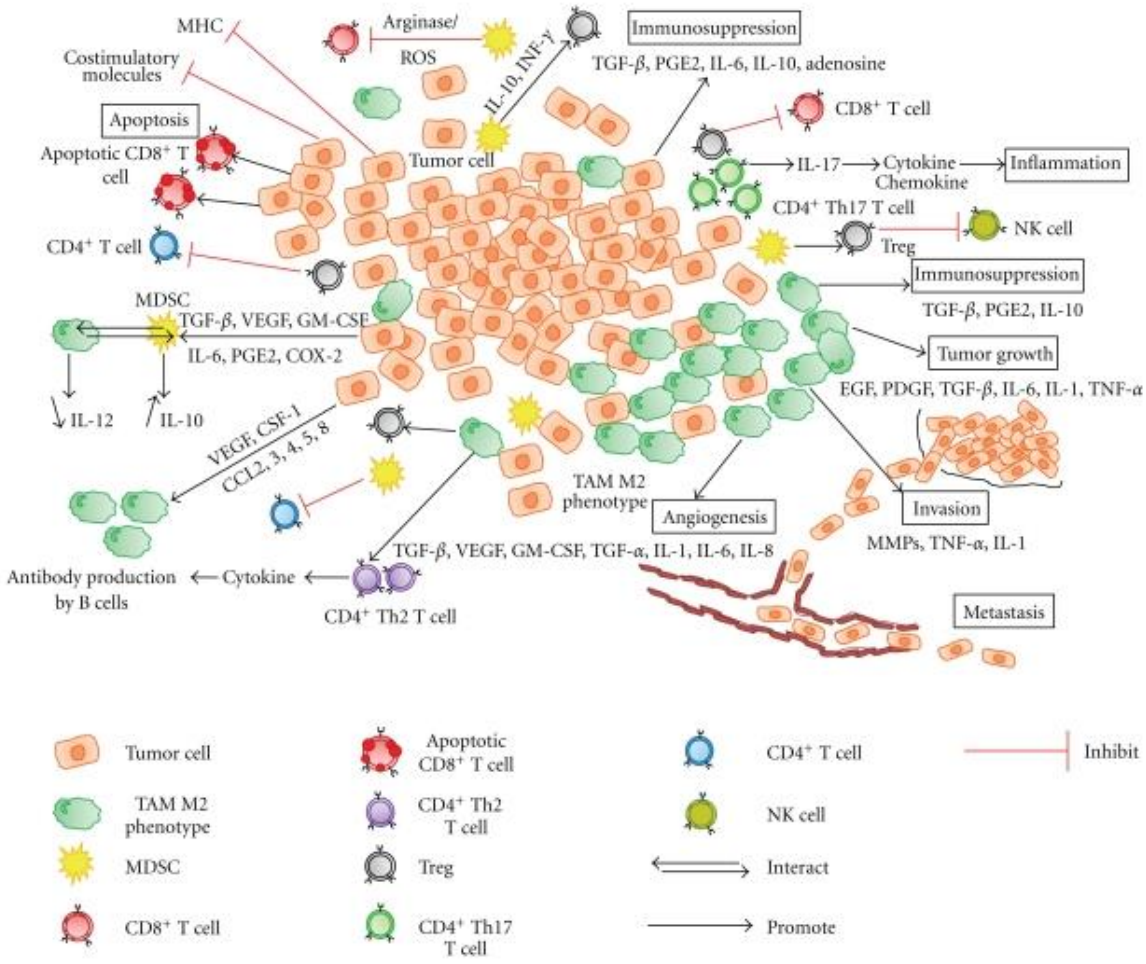


**Figure 1.15: The complex regulation of immune suppression in the tumour microenvironment by cytokines**
Taken from (Duray *et al.*, 2010)

### 1.3.1.1 *TGF-β and its role in immune regulation in the tumour microenvironment*

Transforming growth factor-beta (TGF-β) is a pleiotropic, ubiquitously expressed cytokine, which virtually all cell types can secrete and are responsive to. Three isoforms are expressed in mammals, TGF-β1, TGF-β2 and TGF-β3 (Piek *et al.*, 1999). TGF-β1, being the first identified and most commonly upregulated in cancer is also the most extensively studied and much of the discussed research is based on this isoform. Though present in all normal tissues at a basal level, high levels are found in areas of tissue injury, where it is released by platelets and lymphocytes in order to curtail cell proliferation and inflammation and induce tissue repair (Roberts *et al.*, 1986; Barrientos *et al.*, 2008; Bierie & Moses, 2010).

TGF-β is an important tumour suppressor, with malfunctions in TGF-β signalling leading to tumorigenesis (Massague *et al.*, 2000). Paradoxically, it also plays an important role in the

progression and metastasis of tumours (Drabsch & ten Dijke, 2012). The dichotomous role of TGF-β in cancer is generally thought to be suppressive in early stage tumours, initiating growth arrest, while in later stages it promotes epithelial to mesenchymal transition (EMT), an important prelude to metastasis. As cells become cancerous, they can become unresponsive to TGF-β in the environment, for example through the loss of TGFBR1/2 or a downstream signalling component (Levy & Hill, 2006).

Until more recently when looking at the effect of TGF-β in cancer, it was primarily the effect on the tumour epithelial cells that was considered. However as *in vivo* results did not always reflect what was seen in single cell-type *in vitro* models, sometimes giving counter-intuitive responses, there has been increased interest in the effects of TGF-β on the different aspects of the TME, and the diversity of cell types this encompasses.

In the immune context, TGF-β is generally considered to be tumour promoting, contributing to immune evasion by promoting immunosuppression. Among its immunosuppressive effects are, the induction of Treg, the recruitment of MSDCs and macrophages, the promotion of M2 polarisation of macrophages and the suppression of CTLs, NK cells and DC cells (Flavell *et al.*, 2010). Contrastingly, TGF-β can also have pro-inflammatory effects, by mediating differentiation of Th17 cells and in some situations promoting CTL activation, and has been noted to play a major role in chronic inflammation (Sanjabi *et al.*, 2009).

In HNSCC, TGF-β expression is upregulated in tumours and adjacent tissue compared to oropharyngeal tissue from healthy controls (Lu *et al.*, 2004b). In general, TGF-β upregulation in tumours is associated, with increased inflammation, angiogenesis and metastasis and an overall worse prognosis (Lu *et al.*, 2004b; Levy & Hill, 2006).

#### 1.3.1.2 *Immune cell regulation by IL10 in the tumour microenvironment*

IL10 is another immunosuppressive cytokine, with a diverse range of effects; its receptor being widely expressed on haematopoietic cells (Couper *et al.*, 2008). IL10 inhibits Th1 activation by inhibiting MHC class II expression and expansion and promotes polarisation of M2 macrophages and induction of Treg (Maggi, 2010; Hsu *et al.*, 2015; Makita *et al.*, 2015). However, it may also have immune stimulatory properties and has been observed to increase CTL activation and proliferation in some settings (Nizzoli *et al.*, 2016). The main sources of IL10 in the TME are Treg, Th2 cells and M2 macrophages (Curry *et al.*, 2014).

High levels of IL10 secretion is a characteristic feature of Tr1 cells and can help in the identification of this subset (Haringer *et al.*, 2009).

IL10 concentration had been reported to be on average, nearly five times higher in the plasma of HNSCC patients compared with healthy controls (Lathers & Young, 2004). Furthermore, IL10 is increased in the plasma of patients with late (T3/4) stage tumours and tumours with nodal involvement compared with early (T1/T2) tumours or tumours with no nodal involvement, respectively (Sparano *et al.*, 2004). In a study of laryngeal SCC, although only ten of the 50 patient serum samples contained detectable levels of IL10, patients with late stage tumours had more detectable levels of IL10 than those with early stage tumours (Gunaydin *et al.*, 2012).

### 1.3.2 **Programmed cell death and immune regulation**

Another way of regulating immune cells is by the induction of programmed cell death – apoptosis. Apoptosis is a form of highly regulated programmed cell death that can be initiated in response to a variety of internal and external stimuli, and is imperative for embryonic development and maintaining homeostasis (Kerr *et al.*, 1972). In contrast to necrosis, which was traditionally considered to be an unregulated form of death caused by external trauma, apoptosis follows strict mechanisms to ensure cells are disposed of cleanly (Figure 1.16). Rather than rupturing and releasing their contents into their surroundings, apoptotic cells form small membrane-bound apoptotic bodies which are then phagocytosed by other cells (Saraste & Pulkki, 2000). This avoids causing an inflammatory reaction, which can have detrimental effects on neighbouring cells, and allows for the recycling of cellular components.

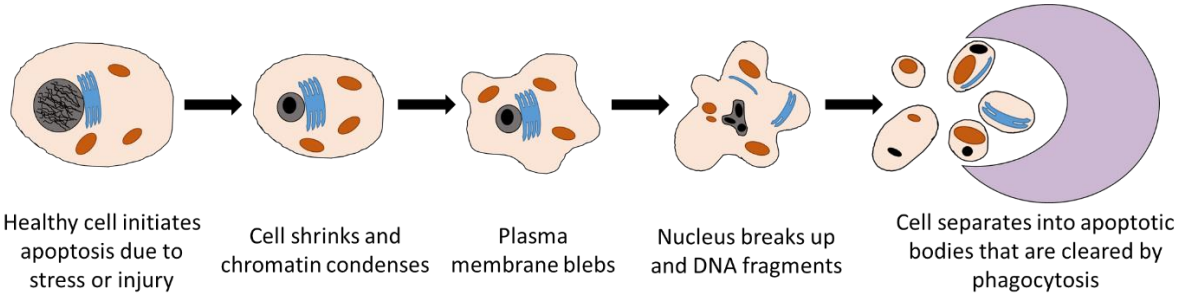


**Figure 1.16: Apoptosis is a form of programmed cell death, sometimes referred to as 'cell suicide'**
As a result of cell injury or stress apoptosis may be initiated; and the cell begins down an irreversible pathway. The cell shrinks, proteins are activated to break down its components, and the chromatin in its nucleus condenses. The membrane then starts to bleb as its cytoskeleton begins to collapse. Enzymes break up the nucleus and DNA becomes fragmented, while other cellular components remain relatively intact. The cell separates into small apoptotic bodies containing organelles and parts of the nucleus. Proteins released by the cell and changes to the plasma membrane during this process attract phagocytes, which clear the apoptotic bodies by phagocytosis.

#### 1.3.2.1 *Pathways involved in apoptosis*

Apoptosis can be triggered by either an intrinsic or extrinsic signalling pathway (Elmore, 2007). The intrinsic pathway is initiated from within a cell and is activated by abnormalities such as DNA damage and viral infection. The deletion of autoreactive T cells in the thymus by apoptosis works via the intrinsic signalling pathway (Williams *et al.*, 1998). In these cases, mitochondrial membrane permeabilisation is induced allowing pro-apoptotic factors, including cytochrome c, to be released from the mitochondrial intermembrane space into the cytosol. External cues can initiate extrinsic cell signalling via receptors, such as Fas (Locksley *et al.*, 2001), which in turn leads to the formation of a death-inducing signal complex (DISC), or can indirectly induce apoptosis by causing damage to the cell that initiates the intrinsic pathway. Both the intrinsic and extrinsic pathways eventually converge initiating a caspase cascade (Section 1.3.2.2).

#### 1.3.2.2 *Caspase cascade*

Caspases are cysteine proteases that are initially released as inactive zymogens (procaspases; Figure 1.17). Upon proteolytic cleavage the initiator caspases (caspase-2, -8, -9 and -10) become enzymatically active and in turn cleave the executioner caspases (caspase-3, -6 and -7; Logue & Martin, 2008). Executioner caspases act on a broad range of downstream proteins that carry out the various morphological and biochemical requirements for apoptosis. Initiator caspases 8 and 10 are cleaved by DISC via the external signalling pathway (Walczak & Sprick, 2001). The activation of caspase 9, is mediated by a complex

of cytochrome c and apoptotic protease activating factor (APAF)-1, known as an apoptosome (Li *et al.*, 1997; Srinivasula *et al.*, 1998).

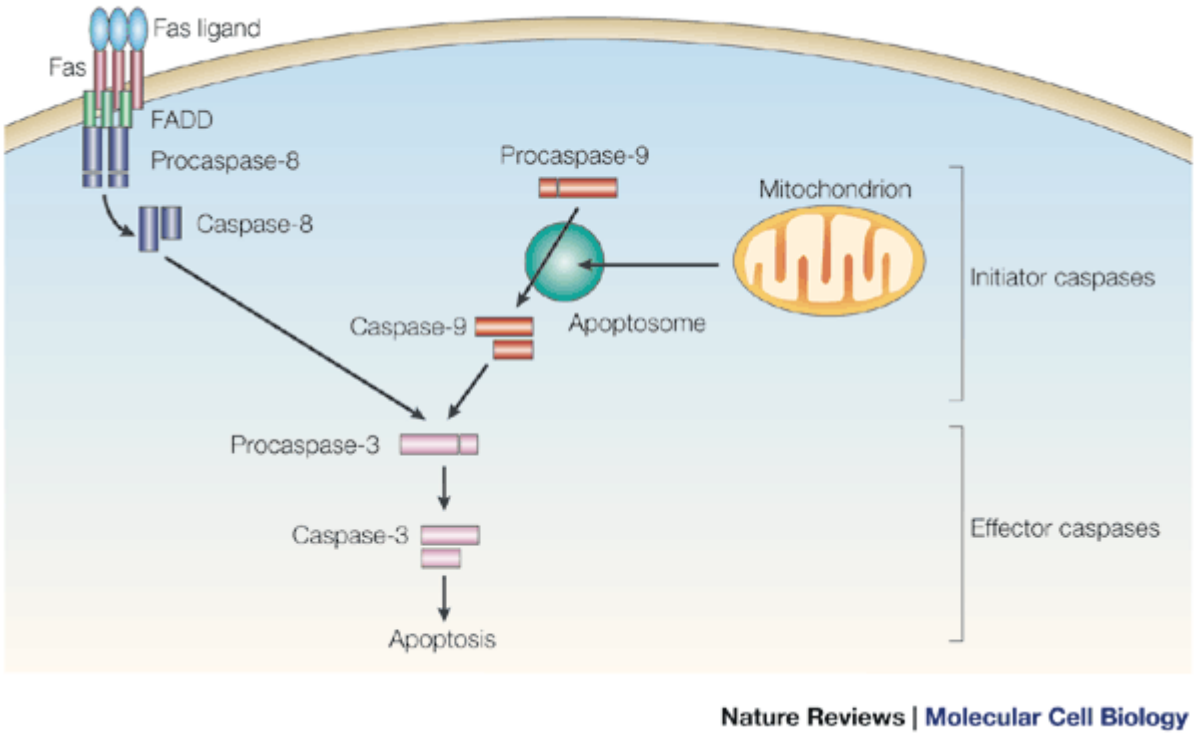


**Figure 1.17: Activation of the caspase cascade**
Taken from (Holcik & Korneluk, 2001). Fas ligand binds to the death receptor Fas, a member of the TNF-α family of receptors. Fas-associated protein with death domain (FADD), in turn can then bind to Fas, resulting in the recruitment of procaspase 8 to form a death-inducing signal complex (DISC). DISC cleaves procaspase 8 to its active form. In the intrinsic pathway, proteins are released by the mitochondria and form an apoptosome, which cleaves caspase 9. These initiator caspases then activate the downstream executioner caspases, such as caspase 3.

### 1.3.2.3 *Apoptosis in cancer*

In carcinogenesis, malignant cells circumvent apoptosis (Hanahan & Weinberg, 2000; 2011). Many of the well-established cancer-related genes have been found to play a role in disrupting the apoptotic pathway (section 1.1.2) and defects in apoptotic machinery can promote tumour development in mice (Lowe & Lin, 2000). This gives cancer cells a survival advantage over their healthy counterparts, as they are able to survive in environments that would usually trigger their death. Furthermore, this reduced apoptotic potential facilitates metastasis. In this case, a lack of external survival cues, in the form of cell-cell and cell-matrix interactions, does not elicit the normal response of apoptosis. This enables the

malignant cells to travel through the blood stream to other areas of the body and establish secondary tumours. Most chemotherapies work by inducing apoptosis, for example by causing damage to DNA in cells. It is likely that their limited effect in some instances is in part due to the mechanisms of apoptosis already being faulty in cancer cells. Agents that inhibit anti apoptotic molecules (eg, Bcl-2) or promote apoptotic factors could sensitise cancer cells to apoptosis (Schmitt & Lowe, 1999). In addition to the defects in their own apoptotic machinery (Section 1.1.2.1), tumour cells can induce apoptosis in immune cells to increase their survival advantage.

#### 1.3.2.4 *Immune cell regulation in the tumour microenvironment by induction of apoptosis*

Apoptosis is imperative for maintaining cell populations at the necessary levels throughout the body, including cells of the immune system. Following the accumulation of immune cells during inflammation, apoptosis is a normal physiological response to prevent deleterious effects to healthy tissue and re-establish homeostasis (Giovannetti *et al.*, 2008). Upon T cell activation, programmed death receptor-1 (PD-1) and Fas, a member of the TNF receptor family, are up-regulated on their surface (Ju *et al.*, 1995; Keir *et al.*, 2008). Stimulation of these receptors by the associated ligand leads to deactivation and/or apoptosis of immune cells. This provides a means of modulating the immune system both at sites of inflammation and during activation at secondary lymph nodes.

The PD-1/PD-L1 axis has shown success as a target for cancer therapy (section 1.4). PD-L1 inhibits T cell function by promoting anergy and can induce T cell apoptosis upon binding with the PD-1 receptor (Dong *et al.*, 2002). PD-L1 has also been shown to enhance the TGF-β mediated induction of iTreg and increase their efficacy, further contributing to the suppressive nature of the TME (Francisco *et al.*, 2009). PD-L1 is upregulated on tumour cells themselves as well as on tumour infiltrating immune cells, including DC and macrophages (Zou & Chen, 2008). In a meta-analysis comparing the gene expression of PD-1 and PD-L1 in HNSCC from 18 studies, increased levels were observed in HNSCC tissue compared to healthy tissue (Yu *et al.*, 2015). Histological analysis showed that the PD-1 was predominantly expressed on the tumour associated immune cells, while the majority of PD-L1 was expressed on the surface and in the cytoplasm of the tumour cells.

Fas and its ligand FasL are membrane bound proteins, however both can also exist in soluble forms (sFas and sFasL) in the TME and in serum (Tanaka *et al.*, 1996; Gastman *et al.*, 1999).

Binding of Fas to its ligand induces apoptosis of the recipient cell. Membrane-bound FasL (mFasL) is cleaved by metalloproteinases (MMPs) to its soluble form (Tanaka *et al.*, 1996), however the efficacy of sFasL to induce apoptosis is thought to be greatly reduced compared with mFasL (Tanaka *et al.*, 1998). The two forms of FasL have been suggested to have opposing roles in the TME; the binding of sFasL to Fas may protect against the effects of mFasL (Hohlbaum *et al.*, 2000). Other TNF family members, such as TNF-α and TNF-α related apoptosis-induced ligand (TRAIL), are also important regulators of apoptosis. TRAIL and FasL double knockout mice have a more severe lymphoproliferative disease than those deficient in FasL only (Sedger *et al.*, 2010), suggesting a role for TRAIL in the regulation of the immune response. Its immunomodulatory effects appear to be in part due to its role in mediating T cell apoptosis (Janssen *et al.*, 2005). However, stimulation of the TRAIL receptor does not always lead to cell death, and can instead exert regulatory effects by deactivation of T cells, preventing their proliferation (Lehnert *et al.*, 2014). As with PD-L1, expression of FasL and other TNF receptor ligands is another pathway tumours exploit for their survival.

If Treg, conventional Th cells and CTL differ in their susceptibility to apoptosis in the TME this could lead to changes in the balance between these cell types, potentially tipping it in favour of immune suppression. Another mechanism tumours may use to create a favourable immune environment is by the preferential recruitment of certain immune cell types.

### 1.3.3 Cell trafficking in the tumour microenvironment

Migratory factors secreted by cells in the TME can influence the components of the immune filtrate. Chemokines are a family of cytokines responsible for the homing and retention of immune cells. They are recognised by chemokine receptors expressed on leucocytes and are released by a variety of cell types, including tumour cells, CAF and leucocytes themselves (Chow & Luster, 2014). Target cells migrate along the chemokine concentration gradient to the site of chemokine release (Figure 1.18; Balkwill, 2004). To date there have been twenty chemokine receptors identified to recognise more than forty chemokines (Pease & Williams, 2006). The ability of these receptors to recognise more than one chemokine is termed chemokine redundancy and is a confounding factor when investigating chemokine/receptor interactions.

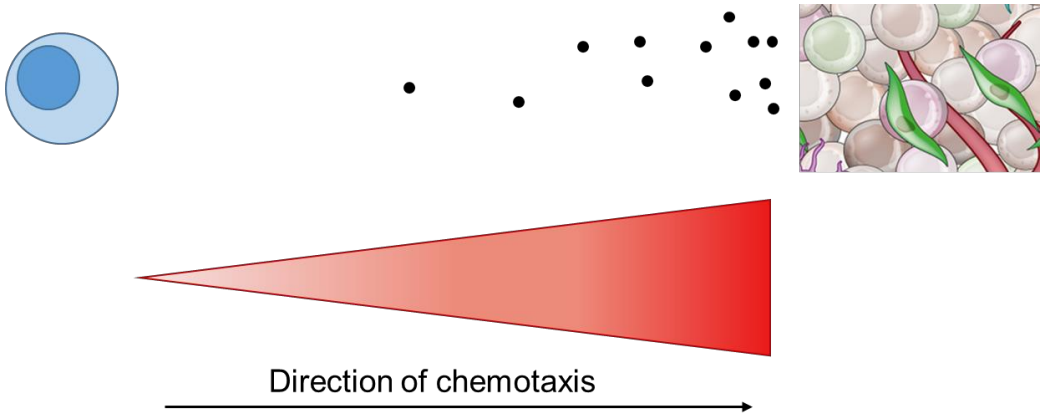


**Figure 1.18: Release of chemokines by cells in the TME results in a chemokine gradient**

Chemokines are categorised according to the position of their first two cysteine residues at their N terminus (Zlotnik & Yoshie, 2000). The CC family of chemokines contain adjacent cysteines, CXC and $CX_3C$ chemokines are separated by one and three amino acids respectively, and XC chemokines have just one cysteine at their N terminus. Different types of immune cells express different chemokine receptors and thus chemokines are able to shape the local immune environment.

Receptor expression can also differ between different types of T cells, and can change with activation status. For example, CCR7, involved in T cell migration into secondary lymphoid organs, is downregulated on activated T cells and is often used to distinguish naïve or resting T cells from activated effector T cells (Forster *et al.*, 1999; Sallusto *et al.*, 1999). Though some receptors are primarily associated with certain immune cell types, their expression is not always exclusive to these cells. CXCR5, the receptor for CXCL13, is expressed on the majority of B cells were it is involved in the homing of these cells to lymphoid follicles. However it is also found on T follicular helper cells (Tfh), a subset of memory T cells that make up approximately 13-15% of $CD4^+$ T cells in blood (Breitfeld *et al.*, 2000). Tfh cells play a role in the development and maturation of B cells.

Chemokines can be loosely grouped according to two main functions; homeostasis and inflammation (Table 1.4). Homeostatic chemokines are constitutively expressed in organs or tissue, facilitating tissue-specific homing and entry and exit from the tissue (Zlotnik & Yoshie, 2012). For example, CCL19 and CCL21 are expressed in secondary lymphoid

tissue, where they mediate the migration of CCR7 expressing immune cells (Forster *et al.*, 2008). In contrast, inflammatory chemokines are released in response to infection and tissue injury (Moser & Willimann, 2004). They fine-tune the accumulation of the different cell types necessary in response to the situation. There is some overlap between homeostatic and inflammatory chemokines (CCL17, 20, 22).

**Table 1.4: Some of the different roles of homeostatic and inflammatory chemokines**

| Cell type | Role |
|---|---|
| **Homeostatic** | |
| CXCL12 | Haematopoiesis and emryogenesis (Ara *et al.*, 2003; Nassari *et al.*, 2017) |
| CXCL13 | Homing of B cells and Tfh cell to lymph node and splenic follicles (Ansel *et al.*, 2000; Breitfeld *et al.*, 2000) |
| CXCL14 | Haematopoiesis and emryogenesis (Nassari *et al.*, 2017) |
| CCL19, CCL21 | Homing of naive T cells and dendritic cells to the lymph node (Forster *et al.*, 2008) |
| CCL25 | Homing and development of immature T cells to thymus (Campbell & Butcher, 2002) |
| **Inflammatory** | |
| CXCL1, CXCL2, CXCL8 | Protection against bacterial infection, acute inflammation (Russo *et al.*, 2014) |
| CXCL9, CXCL10, CXCL11 | Protection against pathogens at mucosal surfaces (Mikhak *et al.*, 2006) |
| CCL2 | Atherosclerosis, asthma, allergic inflammation (Turner *et al.*, 2014) |
| CCL3, CCL4 | Rheumatoid arthritis synovitis acute inflammation (Iwamoto *et al.*, 2008) |
| CCL5 | Allergic inflammation (John *et al.*, 2003) |
| CCL17, CCL27 | Homing of T cells to skin (Riis *et al.*, 2011) |
| CCL25 | Homing of T cells to mucosal epithelia of the intestine for protection against pathogens (Campbell & Butcher, 2002) |

#### 1.3.3.1 *Leucocyte trans-endothelial migration and T cell circulation*

During an immune response, for entry into a site of inflammation, circulating leucocytes must first exit the bloodstream by trans-endothelial migration (TEM). TEM is a multi-step process, involving first the tethering of leucocytes to the vascular endothelial wall followed by their rolling along the endothelium (Muller, 2016). The cells must then adhere to the

endothelium before entering the final phase of TEM and migrating through the endothelial wall to the adjacent tissue.

The initial tethering of immune cells is mediated by selectins, glycosylated transmembrane proteins that interact with numerous ligands, including P-selectin glycoprotein ligand-1 (PSGL-1); Moore, 1998). E-selectin and P-selectin are upregulated on endothelial cells (and in the case of P-selectin also platelets) in response to inflammation and injury, a process mediated by the cytokines TNF-α and IL1 (Wyble *et al.*, 1997). While P-selectin is constitutively expressed in endothelial cells, where it is stored in vesicles for quick delivery to the cell surface when required, E-selectin is only transcribed in response to cytokine signalling at the time of inflammation (Lowenstein *et al.*, 2005). P-selectin surface expression can therefore occur within minutes of cytokine stimulation, while E-selectin expression occurs within two hours (Lowenstein *et al.*, 2005; Murphy, 2017). E-selectin and P-selectin mediate the initial capture and tethering of leucocytes to the endothelium by binding to ligands, such as PSGL-1, on the leucocyte surface (Somers *et al.*, 2000). The high association (on-) and dissociation (off-) rates of the interactions between selectins and their ligands results in the rolling of the cells along the endothelium (Chang *et al.*, 2000). L-selectin (CD62L) expressed on leucocytes also contributes toward tethering and rolling by binding PSGL-1 on endothelial cells (Spertini *et al.*, 1996). In addition, it can facilitate secondary leucocyte tethering by leucocyte-leucocyte interactions (Alon *et al.*, 1996).

The presence of membrane-bound chemokines at the endothelial surface causes upregulation of integrins on leucocytes and their activation to a high affinity state (Tanaka, 2000). Integrins are involved in the adhesion of leucocytes to the endothelium causing the arrest of leucocyte rolling. They bind to intracellular adhesion molecule (ICAM)-1 and vascular cell adhesion molecule (VCAM)-1, which accumulate at the endothelial cell surface (Barreiro *et al.*, 2002). ICAM-1 is expressed constitutively on endothelial cells and is upregulated in response to inflammatory cytokines, while VCAM-1 is only expressed following cytokine stimulation (Schleimer *et al.*, 1992; Lawson & Wolf, 2009). The integrins primarily responsible for leucocyte arrest are lymphocyte function-associated antigen (LFA)-1 and very late antigen (VLA)-4 which bind ICAM-1 and VCAM-1, respectively.

Upon adhering to the vascular endothelial surface, the final stage of TEM is the movement of cells through the endothelial barrier. This can either be via the paracellular route, between

endothelial cell junctions, of the transcellular route, passing directly through the endothelial cells (Turowski *et al.*, 2008; Muller, 2011). In the paracellular route, adhesion molecules at endothelial junctions that bind ligands found on leucocytes, such as platelet/endothelial cell adhesion molecule (PECAM)-1, junctional adhesion molecule (JAM)-A,-B, -C ICAM-1 and -2, are thought to guide paracellular migration of leucocytes, while the phosphorylation of VE-cadherin leads to destabilisation of the junction (Turowski *et al.*, 2008). Similar adhesion molecule expression has been observed in transcellular migration (Muller, 2011). In both cases adhesion molecules PECAM-1 and JAM are delivered to the site of leucocyte adhesion by endosomal trafficking by the lateral border recycling compartment (LBRC) (Mamdouh *et al.*, 2003). In most cases the LBRC migrates toward the leucocyte at the endothelial cell border, enlarging the junction and bringing with it additional adhesion molecules (Muller, 2011). However, in some cases the LBRC meets the leucocyte at the cells surface and as it fuses with the plasma membrane acts as a pore lined with adhesion molecules allowing the leucocyte to pass directly through the cell (Mamdouh *et al.*, 2009).

The TEM of different immune cell types is under tight regulation. The differential expression of adhesion molecules and chemokines on the endothelium ensures only leucocytes expressing particular integrins and chemokine receptors migrate out of the bloodstream and into the inflamed tissue.

Naïve, effector and memory T cells express different repertoires of chemokine receptors, reflecting their different roles and requirements (Griffith *et al.*, 2014). Memory cells are mainly localised in tissue, whereas naïve T cells circulate in the periphery through the secondary lymphoid organs (Berard & Tough, 2002). Peripheral lymphoid tissue is the major site of T cell activation; the highly organised architecture at these sites facilitates naïve T cell scanning of AgPC (Masopust & Schenkel, 2013). This increases the opportunity for T cells to come into contact with their cognate antigen. As with the migration of cells from the blood stream into peripheral tissue during inflammation, the entry into and exit out of secondary lymphoid organs requires TEM, and is therefore mediated by chemokines and adhesion molecules. For TEM of naïve T lymphocytes into the lymph node (LN) from high endothelial venules (HEV), L-selectin (CD62L) on the T cell surface, mediates T cell rolling along the endothelial surface by binding transmembrane glycoproteins (Galkina *et al.*, 2007). LFA-1 on T cells is activated by the interaction of CCR7 on the T cell with CCL21 bound to the surface of HEV (Bao *et al.*, 2010). LFA-1 then binds to ICAM-1 and T cells migrate

into the LN by TEM (Evans *et al.*, 2009). Stromal cells in the T zone of the LN induce recruitment of T cells by release of CCL21 and CCL19 (Chang & Turley, 2015). T cells scan the DC in the LN for their cognate antigen, and if it is not present exit via the cortical sinuses (Kaiser *et al.*, 2005). The sphingosine-1 phosphate (S1P) receptor, expressed on naïve T cells mediates this migration back into the circulation (Cyster & Schwab, 2012).

S1P is found in the lymph and blood, and its presence causes the desensitisation of S1P receptors on T cells (Garris *et al.*, 2014). Therefore, following initial entry into the LN, cells are relatively unresponsive to S1P. The lack of S1P in the T cell zone of the LN ensures sensitivity to S1P is restored over time and T cells migrate out into the S1P enriched regions of the lymph and blood (Baeyens *et al.*, 2015). Furthermore, S1P is downregulated on T cells upon recognition of their cognate antigen (Lu *et al.*, 2004a; Shiow *et al.*, 2006). This ensures the cells are retained in the LN long enough to scan the numerous DC and establish suitable binding to cause their activation. Once cells are sufficiently primed they downregulate CCR7 and L-selectin and upregulate S1P and tissue homing chemokines so they can migrate out of the lymph node to the site of inflammation (Klinger *et al.*, 2009; Benechet *et al.*, 2016). The upregulation of specific homing chemokines can be determined by the lymph node it is activated in, for instance cells activated in gastrointestinal- associated draining LN upregulate CCR9, which is involved in homing to the intestinal mucosa (Johansson-Lindbom & Agace, 2007). Following resolution of the immune reaction, a small proportion of cells become memory T cells, a subset of cells that can rapidly respond to immune assault. Some of these memory T cells, stay in the tissue as resident memory T cells and others circulate back through the periphery, including T central memory cells, a subset which express CCR7 and can re-enter the LN (Roberts *et al.*, 2005).

In addition to their role in chemotaxis, chemokines can also affect cell function, activation and retention. In the case of the receptor CCR7, its two ligands p lay different roles in the regulation of T cell migration. CCL21 mediates chemotaxis and CCL19 desensitises/internalises CCR7 once in the secondary lymphoid tissue allowing cells to recirculate back through the periphery (Zlotnik & Yoshie, 2012).

As with other cytokines, expression profiles of chemokines and their receptors have been found to be altered in the tumour microenvironment and periphery of cancer patients, where

they not only play a role in immune cell recruitment but also in tumour invasion, metastasis and angiogenesis.

#### 1.3.3.2 *Chemokines and tumours*

Chemokine receptors have been found on the surface of numerous solid tumours (Vela *et al.*, 2015). In HNSCC, much of the current research has focussed on receptor expression on tumour cells themselves, and resulting metastasis, rather than on the secretion of chemokines by the tumour and the effect on leucocyte recruitment and tumour immune evasion. In relation to cancer, the two major chemokine/receptor interactions discussed in the literature are CXCL12 and its receptor CXCR4, and CCL19 and its receptor CCR7. The CXCL12/CXCR4 pathway is known to promote increased tumour cell motility, leading to metastasis. Multiple studies have observed an increase of both CXCR4 and CXCL12 in HNSCC tumours, using both IHC and mRNA quantification (Albert *et al.*, 2013). They are found at increased levels in late stage tumours, and correlate with increased risk of lymph node and distant metastases and poor survival in HNSCC. CCR7 has also been observed to be upregulated in HNSCC tumours and correlates with increased lymph node metastasis (Ueda *et al.*, 2010). Chemokines and their relation to immune cell migration in HNSCC is less well defined.

#### 1.3.3.3 *Immune cell regulation by chemokines in the tumour microenvironment*

Many tumour cells are known to secrete chemokines, some of which have been associated with Treg migration. For example, CCL22, a ligand of the CCR4 receptor highly expressed on Treg, is secreted by ovarian cancer cells (Curiel *et al.*, 2004; Kimpfler *et al.*, 2009). Stromal cells, including immune cells themselves also release chemokines (Chow & Luster, 2014). For example, CTL in melanoma are thought to be the source of the increased levels of CCL2 (a Treg chemoattractant), rather than the tumour cells themselves (Spranger *et al.*, 2013). The receptor CCR5 has recently been found to be upregulated on the Treg of the tumour infiltrating lymphocytes (TIL) from colorectal cancer patients compared to healthy tissue, and there is evidence that knocking out this receptor may slow cancer progression in mice (Ward *et al.*, 2015). This is of particular interest as an antagonist for the human CCR5 receptor already exists and has been found safe for the treatment of patients with HIV. A better understanding of the chemokines and cytokines in the tumour microenvironment will help shed light on how the suppressive Treg cells become enriched in TIL.

### 1.3.4 T cell regulation using checkpoint inhibitors for cancer immunotherapy

Promoting the T cell response to tumours by targeting immune checkpoints has already been shown to be a successful strategy in some cancer patients. In particular inhibitory molecules blocking the CTLA-4 and PD-1/PD-L1 pathways have been approved for the treatment of metastatic melanoma, NSCLC, RCC and HNSCC (Brahmer *et al.*, 2015; Motzer *et al.*, 2015; Weber *et al.*, 2015; Ferris *et al.*, 2016; Bauman *et al.*, 2017). These mechanisms are imperative in regulating the normal physiological immune response, aiding in the restoration and maintenance of homeostasis. However, in tumours they contribute to immune evasion. Removal of these inhibitory signals allows effector immune cells within the TME to establish an effective anti-tumour response, and promotes tumour rejection.

CTLA-4 is expressed exclusively on T cells, were it competes with the T cell costimulatory CD28 molecule for binding to CD80/86 on AgPC. It inhibits T cell activation directly by stimulating inhibitory signals and indirectly by cleaving CD80/86 from AgPC, preventing CD28 binding (Qureshi *et al.*, 2011). CTLA-4 is upregulated on activated T cells and expressed constitutively on Treg, were it plays a role in their immunosuppressive function (Section 1.2.2.9.1). Blockade of CTLA-4 promotes T cell activation, and in addition hampers Treg-mediated immunosuppression; both factors that contribute to an overall enhancement in the immune response (Wing *et al.*, 2008; Peggs *et al.*, 2009). In mice, blockade of CTLA-4 leads to tumour regression in immunogenic tumours, however it is unable to elicit a response in non-immunogenic tumours (Leach *et al.*, 1996; van Elsas *et al.*, 1999). In subsequent human trails of advanced melanoma, CTLA-4 blockade by ipilimumab led to increased long term survival of patients (18% at 2 years compared to 5% with a gp100 peptide vaccine; Hodi *et al.*, 2010).

The PD-1/PD-L1 axis is another immune checkpoint that has been successfully targeted for cancer treatment. PD-L1 is constitutively expressed on DC and macrophages and upregulated on T cells following their activation (Zou & Chen, 2008). It is absent or low from healthy tissue but highly expressed in many different tumour types, including more than 85% of HNSCC (Muller *et al.*, 2017; Pai *et al.*, 2017), were it induces T cell dysregulation and contributes toward immune escape. Its receptor, PD-1, is more widely expressed than CTLA-4; in addition to activated cells it is also present on B cells and NK cells (Thibult *et al.*, 2013; Della Chiesa *et al.*, 2016). While CTLA-4 acts to inhibit the activation signal at the time of TCR stimulation, PD-L1 dampens the effector function of

activated T cells within tumour tissue. Blocking the PD-1/PD-L1 pathways can prevent the induction of effector T cells anergy and inhibit Treg function and induction.

Other inhibitory molecules targeting physiological immunoregulatory mechanisms are under investigation. For example, LAG-3 is highly expressed on Treg, where it has a functional role in immunosuppression (section 1.3.4). LAG-3 upregulation on $CD4^+$ Th cells increases their susceptibility to Treg mediated suppression (Durham *et al.*, 2014). LAG-3 is also upregulated on CTL following activation and this has an inhibitory effect on CTL effector function independent of Treg (Grosso *et al.*, 2007). LAG-3-KO in mice or blockade with a LAG-3 antibody has been shown to enhance the number and effector function of CTL and Th cells. While KO of Lag3 alone in mice had little effect on tumour regression, double KO Lag3-/- PD1-/- mice or treatment with antibodies for both PD-1 and LAG-3 had a synergistic effect on tumour clearance and survival (Woo *et al.*, 2012). There are currently four LAG-3 inhibitory molecules under investigation in Phase I and II clinical trials for the treatment of various solid tumours, including melanoma, RCC, NSCLC, breast cancer, pancreatic cancer and lung cancer (Andrews *et al.*, 2017).

Stimulation of the A2AR receptor on T cells is another such mechanism that can potentially be targeted for cancer therapy. In the TME levels of adenosine are often high, due to hypoxic conditions, high cell turnover and enhanced expression of the ectonucleotidases CD39 and CD73, which can contribute toward immunosuppression. In A2AR KO mice, tumours grow more slowly and respond better to treatments with cancer vaccines and PD-1 blockade than wild type mice (Waickman *et al.*, 2012). Targets of A2AR are in the early stage of clinical trials for the treatment of solid tumours but have been approved for the treatment of Parkinson's disease, where they were found to be well-tolerated (Pinna, 2014; Vijayan *et al.*, 2017). An alternative route for the inhibition of the immunosuppressive effects of adenosine are to target the CD39/CD73 ectonucleotidases (Vijayan *et al.*, 2017).

As immunotherapies develop there is an increased requirement for biomarkers to identify which patients will respond to which therapies. Even in responsive tumour types, the majority of patients will not benefit from treatment. Observed responses to the PD-1 inhibitor Nivolumab in melanoma patients and NSCLC patients are 40% and 19% respectively (Borghaei *et al.*, 2015; Robert *et al.*, 2015). The high rate of somatic mutations in melanoma and NSCLC is speculated to contribute toward the success of checkpoint

blockade in treating these tumours, due to the corresponding increase in tumour-associated antigens (Lawrence *et al.*, 2013; Rizvi *et al.*, 2015; Van Allen *et al.*, 2015). This is support by observations in melanoma and NSCLC, where tumours with a high mutational load were observed to respond better to CTLA-4 treatment and to PD-1 blockade, respectively (Rizvi *et al.*, 2015; Van Allen *et al.*, 2015). This trend is also likely true for other tumour types. A study investigating the correlation of tumour mutational burden with response to PD-1/PD-L1 immunotherapy in 1,638 patients with 21 different tumour types found the outcome was better when tumours had a high tumour mutational burden (progression free survival of 12.8 months *vs.* 3.3 months (Goodman *et al.*, 2017).

## 1.4 Study aims and rationale

Avoiding immune destruction is one of the hallmarks of cancer (Hanahan & Weinberg, 2011). The elevated level of suppressive Treg in HNSCC tissue compared to in the patient periphery potentially contributes toward this immune evasion. As with all immune regulation, soluble factors play an imperative role in tightly regulating this process. Many studies have looked at the role of individual factors or combinations of a few factors, either *in vitro* or *in vivo* using mouse gene knockout or overexpression models. However, in reality, the interaction of the tumour with the immune system is much more complex, and these models can fail to recapitulate the intricate interactions occurring in the TME. This may explain why some *in vitro* findings have not translated into success *in vivo*.

Although, an increasing number of cytokines, chemokines and growth factors released by tumours have been implicated in Treg expansion, induction and recruitment, their role in the context of the TME is unclear. For example, often cytokines have multiple, seemingly paradoxical roles, that vary depending on the presence of other factors. Previous work carried out in the group has shown that conditioned medium collected from *in vitro* cultures of HNSCC and stromal cells, contains a diverse range of cytokines and chemokines that can directly influence proliferation and function of T cells (Smith, 2016). Both similarities and considerable differences were also noted between the factors excreted by the different components of the TME.

In this respect, the current study has looked at the whole secretome of the HNSCC tissue and stromal components. Using CM collected from dissociated HNSCC patient tumour biopsies, HNSCC cell lines and HNSCC tumour-derived fibroblasts, this study will assess the ability

of the soluble factors, released by these specific components, to enrich the Treg population in the HNSCC microenvironment. Specifically, by the induction of the suppressive Treg from sorted $CD4^{+}CD25^{-}$ T cell populations as well as by inducing T cell apoptosis and the preferential recruitment of Treg. Throughout this study, samples were collected from newly presenting HNSCC patients with no previous history of cancer, who had not undergone any previous cancer treatment. The study also primarily uses PBMC from healthy individuals as targets for the soluble factors, to circumvent the fact that tumour derived PBMC may already have been influenced by the tumour. An improved understanding of how Treg come to be enriched in the TME; the contribution of the different potential mechanisms and the soluble factors involved could lead to new avenues to explore for immunotherapy in the future.

# Chapter 2 Materials and Methods

## 2.1 General Cell Culture

All cell culture techniques were carried out in a class II laminar flow hood and all surfaces and bottles swabbed with 70% ethanol to ensure maintenance of sterile conditions.

## 2.2 HNSCC cell lines

Laryngeal and oropharyngeal cell lines were provided by Dr Thomas Carey, University of Michigan, USA (UMSCC; Table 2.1). Monolayer cultures were maintained in approximately 10 ml of Dulbecco's Modified Eagle's Medium (DMEM; Lonza, Castleford, UK) supplemented with foetal bovine serum (FBS; 10% final concentration, Biosera, East Sussex, UK), penicillin/streptomycin (0.1 U/ml and 0.1 mg/ml respectively; Lonza), non-essential amino acids (0.1 mM; Lonza) and L-glutamine (2mM; Lonza) in 75 $cm^2$ flasks (Sarstedt, Leicester, UK). Cells were incubated at 37$^oC$ and 5% $CO_2$ in a humidified atmosphere until they reached 80% confluence, after which time they were passaged by trypsinisation (section 2.2.2). Cell lines were frequently tested for *Mycoplasma* (section 2.2.1.1).

**Table 2.1: University of Michigan Squamous Cell Carcinoma Cell Lines (UMSCC) used in the study (Brenner *et al.*, 2010)**

| UMSCC cell line | Age | Gender | Location (and associated HNSCC subsite) of origin | Location of tumour | TNM Stage |
|---|---|---|---|---|---|
| 4 | 47 | Female | Tonsillar pillar (Oropharynx) | Base of tongue | T3N2aM0 |
| 11a | 65 | Male | Epiglottis (Larynx) | Epiglottis | T2N2aM0 |
| 11b | 65 | Male | Supraglottic (Larynx) | Supraglottic | T2N2aM0 |
| 12 | 71 | Male | Larynx | Larynx | T2N1aM0 |
| 14a | 58 | Female | Floor of mouth (Oral) | Floor of mouth | T1N0Mo |
| 47 | 53 | Male | Lateral tongue (Oral) | Lateral tongue | T3N0M0 |
| 81b | 53 | Male | Tonsil (Oropharynx) | Tonsillar pillar | T2N0M0 |

#### 2.2.1.1 *Mycoplasma*

Cell lines were tested for the presence of *Mycoplasma* using a *Mycoplasma* testing ELISA kit, according to the manufacturer's instructions. Cells infected with *Mycoplasma* were discarded and replaced with a fresh batch.

### 2.2.2 Trypsinisation of adherent cell lines

To maintain cells in a proliferative state for experimentation, the cells were passaged upon reaching 80% confluence. To detach the monolayer from the bottom of the flask, medium was removed and the monolayer washed with phosphate buffered saline (PBS; Oxoid™, Thermo Fisher Scientific) before the addition of (1 ml/25 $cm^2$ flask and 3 ml/75 $cm^2$ flask) trypsin/ethylenediaminetetraacetic acid (EDTA; 0.05%/0.02% in PBS; Lonza). The cells were incubated at 37ºC for up to 10 minutes in the trypsin/EDTA and then agitated to encourage the displacement of any remaining adherent cells. Complete medium was added to the flask to inhibit the trypsin/EDTA and the cell suspension was centrifuged at 400 x *g* for 3 minutes to pellet the cells. The cells were either counted (section 2.2.4) and adjusted to an appropriate concentration for further experiments, aliquoted for cryostorage (section 00) or sub-cultured at a 1:3 dilution for further growth.

### 2.2.3 Jurkat cells

Non-adherent Jurkat cell (ECACC) cultures were maintained in approximately 10 ml of X-Vivo 20 Medium (Lonza) supplemented with 10% FBS and penicillin/streptomycin (0.1 U/ml and 0.1 mg/ml) in 75 $cm^2$ flasks and incubated at 37ºC and 5% $CO_2$ in a humidified atmosphere. Once the cells had reached a sufficient density, they were sub-cultured at a 1:4 dilution.

### 2.2.4 Cell counting with trypan blue exclusion

Cell pellets were resuspended in a known volume of PBS, and 10 µl of the cell suspension was added to an equal volume of 0.4% trypan blue (Sigma, Dorset, UK). The cells were loaded on to a haemocytometer and the cells in the central chamber grid were counted under a light microscope (Figure 2.1). Numbers of viable and non-viable cells were recorded, so percentage viability could be determined. During all experiments, only the total number of viable cells was used. An average was taken from counts in two chambers and the number of cells was calculated using the formula in Figure 2.1.

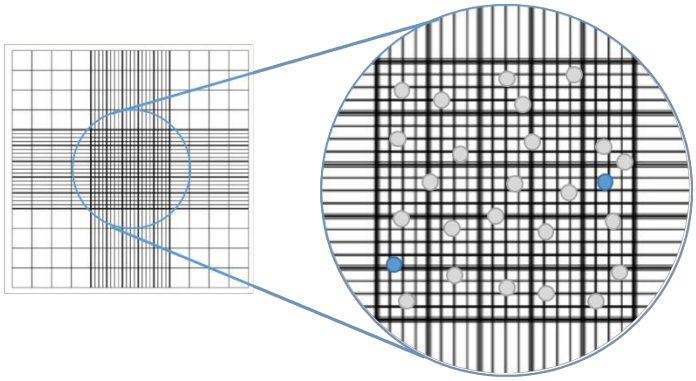


Total cell number = Mean number of cells in two chambers x dilution factor (=2) x volume of cell suspension x $10^4$

**Figure 2.1: Counting cells using a haemocytometer**
The compromised membranes of non-viable cells allow trypan blue to pass through, so the cells appear blue when viewed under the microscope. Two counts were taken from the central chamber of the haemocytometer, a mean number of viable cells was determined from these counts, multiplied by the dilution factor of 2, the volume of cell suspension and x$10^4$.

### 2.2.5 Cryogenic storage of cell lines

To maintain sufficient stocks of cell lines for future experiments, cells were cryopreserved and stored in liquid nitrogen. Adherent cells were removed from 75 $cm^2$ flasks using trypsin/EDTA as described in section 2.2.2. These cells were then resuspended in 3 ml of medium containing 10% dimethyl sulphoxide (DMSO; Sigma) and aliqouted into 1 ml aliquots in cryovials. Cells were cooled at a rate of 1°C/minute in a cryofreezing vessel, containing isopropanol, overnight by placement in a -80°C freezer, before being transferred for long term storage into liquid nitrogen.

### 2.2.6 Collection of cell line supernatant as conditioned medium

For the collection of conditioned medium (CM), UMSCC cells (Table 2.) were seeded at 1 x $10^6$ cells/well in a 6 well plate (Sarstedt) in 1 ml of complete medium. Culture supernatant was collected after 1, 2 and 3 days, centrifuged at 400 x *g* for 3 minutes to pellet cell debris and the resulting CM was aliquoted and stored at -80°C for future use.

## 2.3 Head and neck squamous cell carcinoma patients and healthy controls

Venous blood and tumour biopsy samples were collected from newly presenting HNSCC patients attending the ENT Department at Castle Hill Hospital and the Oral Maxillofacial Department at Hull Royal Infirmary, Hull and East Yorkshire Hospital NHS Trust, for resection surgery to remove either the primary tumour mass or the metastatic nodes. Healthy control blood was obtained from the National Blood and Transplant Service or from healthy volunteers. All biological samples were collected following obtaining written informed consent, under ethical approval from the Hull and Humber Research Ethics committee (10-H1304-7) and Hull & East Yorkshire NHS Trust (R0988), and were processed immediately upon arrival in a Class II laminar flow biological safety hood.

### 2.3.1 Isolation of PBMC from whole blood

For the isolation of PBMC from the peripheral blood of patients or healthy individuals, venous blood was drawn into a sodium heparin coated (200 IU/ml of blood final concentration) syringe or (17 IU of heparin/ml of blood) Vacutainers® (BD Biosciences, Oxford, UK). The blood was diluted in an equal volume of PBS before being layered (1:1) onto lymphocyte separation medium 1077 (LSM; PAA, Yeovil, UK) for density gradient centrifugation at 400 x *g* for 30 minutes with the centrifuge brake being off. The resulting "buffy coat" layer containing lymphocytes (Figure 2.2) was transferred into a tube containing an equal volume of PBS and centrifuged at 300 x *g* for 10 minutes to wash the cells. The cell pellet was resuspended in PBS, combined with cells from other tubes and centrifuged again at 300 x *g*. The viability of the PBMC was assessed using trypan blue exclusion (section 2.2.4) and the cells were either used straight away or cryopreserved by pelleting and resuspending in 1 ml aliquots of FBS containing 10% DMSO, before cooling in a cryofreezing vessel overnight and transfer to liquid nitrogen for long term storage (Section 2.1.5).

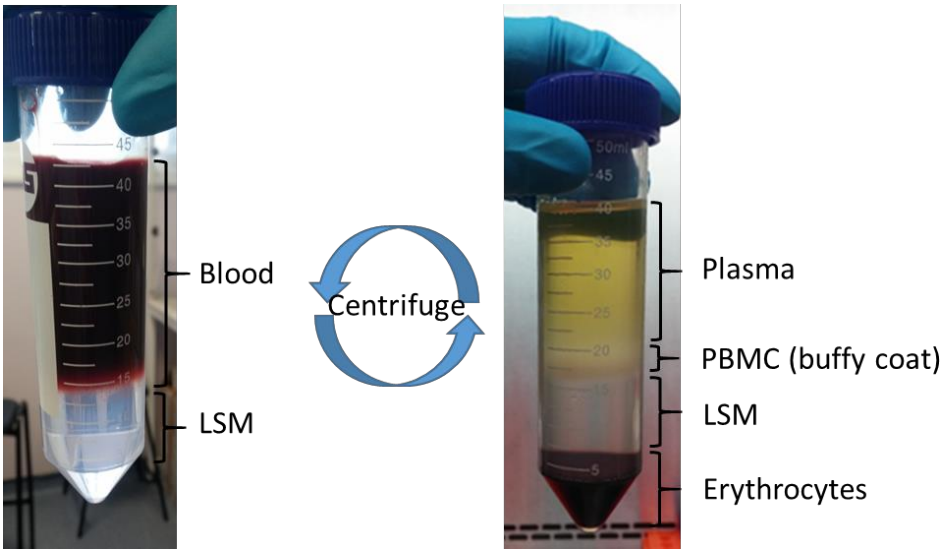


**Figure 2.2: Isolation of PBMC from whole blood by density gradient centrifugation with lymphocyte separation medium 1077 (LSM)**
20 ml of a 1:1 mix of blood and PBS was carefully layered on to 20 ml LSM and centrifuged at 400 x *g* for 30 minutes without brake. Following centrifugation the cells separated and formed layers of plasma, "Buffy coat" peripheral blood mononuclear cells (PBMC), and red blood cells.

### 2.3.2 Isolation of PBMC from leucocyte cones

For leukoreduction prior to transfusion, whole blood is passed through leucocyte cones, filters that trap contaminating white blood cells. These filters provide an enriched source of viable human leucocytes. For assays requiring large numbers of cells or the use of autologous cells on subsequent days (eg CFSE assays; Chapter 3), healthy control PBMC were isolated from leucocyte cones obtained from the National Blood and Transplant service. The cones were securely clamped to a stand as indicated in Figure 2.3, with a 50 ml falcon positioned underneath for the collection of the contents. The tubing at either end of the cone was cut to allow the blood to begin to flow out and, using a needle and syringe, 45 ml PBS was flushed through the cone. To ensure complete removal of the contents a small amount of air was then pumped through the syringe. The isolation of PBMC was carried out as outlined in section 2.3.1.

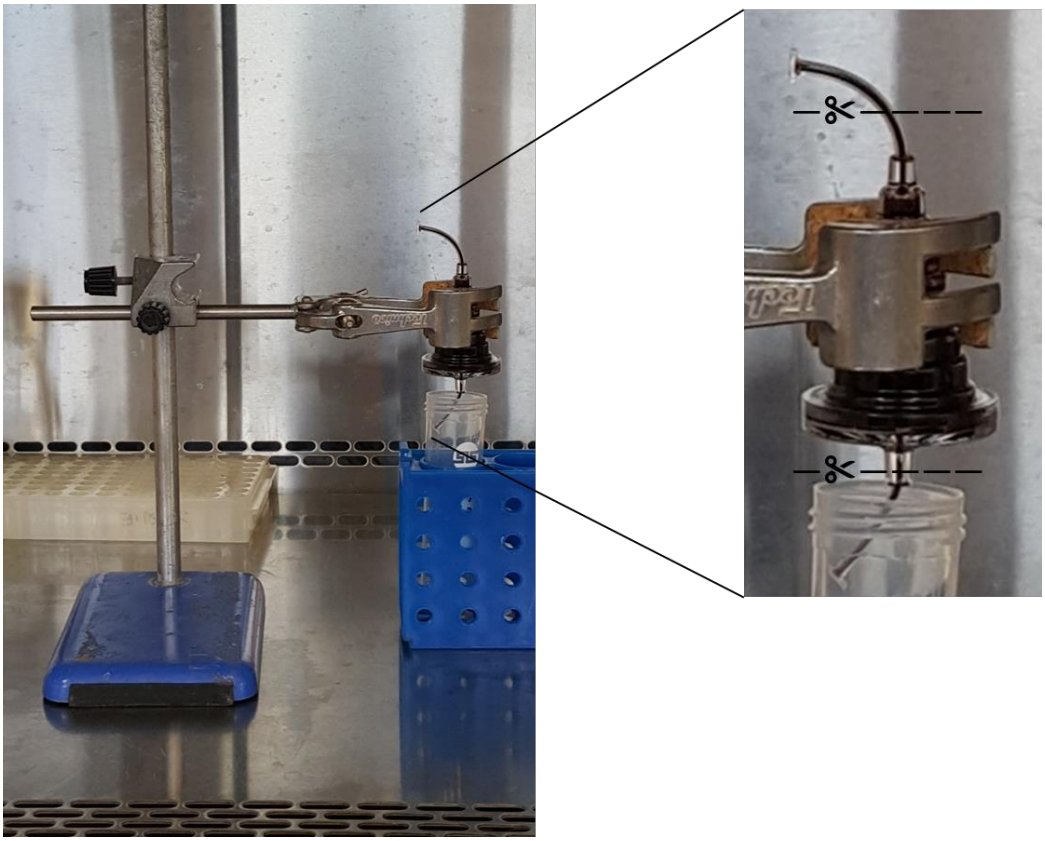

**Figure 2.3: Set up of leucocyte cone with clamp and stand for processing**

### 2.3.3 Culture of PBMC and T cell activation

Freshly isolated PBMC or PBMC that had been cryopreserved and then thawed at room temperature from HNSCC patients, or healthy controls were washed in PBS and cultured in X-Vivo 20 medium (Lonza) containing 5% human AB serum (Invitrogen, Paisley, UK), and 0.1 U/ml penicillin/ 0.1 mg/ml streptomycin (Lonza). Cells were either incubated in the complete lymphocyte growth medium at 37ºC and 5% $CO_2$ in a humidified atmosphere for up to four days or were activated (section 2.3.3.1) and incubated for up to 5 days.

#### 2.3.3.1 *T cell activation*

To activate T cells, whole PBMC or sorted T cell populations were cultured in complete lymphocyte growth medium containing 100 IU/ml IL2 (AbDSerotec, Oxford, UK) and human T activator CD3/CD28 DynaBeads® (1:1, cells:beads; Life Sciences), and incubated at 37ºC and 5% $CO_2$ in a humidified atmosphere for up to 5 days in 96 well round bottom plates (8 x $10^5$ cells/ml in 100µl/well) or 75 $cm^2$ flasks (1 x $10^6$ cells/ml). Following 5 days of culture, the non-adherent lymphocytes were removed and the CD3/CD28 DynaBeads

were detached from the cells by gently pipetting up and down. A Midi MACS separator magnet (Miltenyi Biotech, Woking, UK) was used to separate the cells form the beads and the supernatant containing the cells was removed and centrifuged at 400 x *g* for 5 minutes. The recovered cells were resuspended in PBS for counting using trypan blue exclusion before being used for further experiments.

### 2.3.4 Tumour Dissociation

Immediately following surgery, tumour biopsies were transported in DMEM containing 10% FBS, penicillin/streptomycin (0.1 U/ml and 0.1 mg/ml), L-glutamine (2mM) and Amphotericin B (2.5 µg/ml; Life Technologies) to the laboratory for tissue dissociation (Drennan *et al.*, 2014). The tumour was transferred to a petri dish and kept hydrated while the fat and vascular tissue were removed with scalpels and the tumour was weighed. The tumour was then thoroughly minced using crossed scalpels and transferred to a polypropylene Falcon tube for an antibiotic wash in PBS containing Amphotericin B (2.5 µg/ml) and penicillin/streptomycin (0.1 U/ml and 0.1 mg/ml). The cells were recovered by centrifugation at 400 x *g* for 5 minutes and incubated for 2 hours at 37ºC in medium (DMEM with 10% FBS, 0.1 U/ml and 0.1 mg/ml penicillin/streptomycin and 2.5µg/ml Amphotericin B) containing collagenase type IV (0.2%; Sigma) and DNase (0.02%; Roche, Burgess Hill, UK) on a MACSmix Tube Rotator (Miltenyi Biotech, Woking, UK). The dissociated cells were centrifuged at 400 x *g* and the recovered cells resuspended in 5 ml of complete medium. The cells were washed twice more, before finally plating the cells overnight in a 25 $cm^2$ culture flask. The following day non-adherent cells and CM were collected from the culture flask, centrifuged at 400 x *g* for 5 minutes to pellet the cells and the CM was aliquoted and stored at -80ºC. The pellet was resuspended in PBS and the cell suspension was passed through a 70 µm cell strainer (BD Biosciences) to remove any clumps of cells, before being labelled with fluorescent markers for use in flow cytometry analysis of tumour infiltrating lymphocytes (TIL). Fresh medium was added to the flask for the further culture of tumour-derived fibroblasts.

### 2.3.5 Tumour-derived Fibroblasts

Following enzymatic dissociation of HNSCC tumour biopsies with collagenase IV (Section 2.3.4), flasks of adherent dissociated cells were cultured in conditions favouring the expansion of primary fibroblasts. Every two to three days growth medium was replaced with

fresh DMEM medium containing 10% FBS, penicillin/streptomycin (0.1 U/ml and 0.1 mg/ml), L-glutamine (2mM) and Amphotericin B (2.5 µg/ml; Gibco) and incubated at 37ºC and 5% $CO_2$ in a humidified atmosphere. Once confluent, fibroblasts were trypsinised as outlined in section 2.2.2 sub-cultured at a 1:2 dilution, cryopreserved (Section 2.2.5) or used for further experimentation. For the collection of CM, fibroblasts were seeded at 1 x $10^6$ cells/well in a 6 well plate (Sarstedt) in 1 ml of complete medium. Culture supernatant was collected after 1, 2 or 3 days, centrifuged at 400 x *g* for 3 minutes to pellet cell debris and the resulting CM was aliquoted and stored at -80°C for future use.

## 2.4 Flow Cytometry and fluorescence activated cell sorting (FACS)

Flow cytometry and FACS were carried out on a FACSAria II and analysis completed using FACSDiva software version 6.1.3 (BD Bioscience).

### 2.4.1 Antigen staining

Antibodies were purchased from BD Biosciences, unless otherwise stated. Appropriate IgG isotype matched controls were used as non-specific binding controls for each antibody, at an equivalent concentration.

Antibody staining was carried out in PBS containing 0.25% BSA (Sigma) and 10mM sodium azide (Sigma). Cells were counted using a haemocytometer and trypan blue exclusion, for cell viability, (section2.2.4) and where possible aliquoted into FACS tubes at 1 x $10^6$ in 100 µl PBS/BSA/Azide. Cells were first incubated with surface marker antibodies for 30 minutes in the dark. To remove any unbound antibody cells were washed in (1 ml) PBS/BSA/Azide, centrifuged at 400 x *g* for 5 minutes and the supernatant was discarded. Where required, cells were then permeabilised (section 2.4.1.1), before incubation with antibodies against intracellular antigens for 30 minutes in the dark. Otherwise, cells were resuspended in 100 µl PBS/BSA/Azide and used immediately for flow cytometry analysis.

#### 2.4.1.1 *Cell fixation and permeabilisation*

For the staining of intracellular proteins, cells were fixed and permeabilised using the human FoxP3 buffer set (BD Biosciences), in accordance with the manufacturer's guidelines. Briefly, FoxP3 buffer A was diluted 1:10 with distilled water, and 2 ml was added to each

FACS tube containing 1 x $10^6$ cells in 100 µl PBS/BSA/Azide, for 10 minutes at room temperature. Cells were centrifuged at 400 x *g* for 5 minutes and the cell pellet washed in 1 ml PBS/BSA/Azide. The cells were centrifuged again at 400 x *g* for 5 minutes, and 500 µl of FoxP3 buffer B pre-diluted 1:50 in FoxP3 buffer A was added and incubated at room temperature in the dark for 30 minutes. The cells were centrifuged, washed in 1 ml PBS/BSA/Azide and centrifuged once more at 400 x *g* for 5 minutes to recover the cells. Each pellet of cells was resuspended in 100 µl PBS/BSA/Azide and analysed immediately by flow cytometery.

#### 2.4.1.2 *Antibody titrations*

In order to minimise the amount of non-specific antibody binding while ensuring antigen saturation, antibodies were titrated prior to use in experiments. Starting from the concentration recommended by the manufacturer a 6 point 2-fold serial dilution of stock concentrations was performed of the antibody and matched isotype control. Cells were stained as described above, with equal volumes of each antibody and isotype concentration added to each tube. After analysis by flow cytometry, the staining index (SI) against antibody concentration was plotted to find the optimal antibody concertation for future use (Figure 2.4).

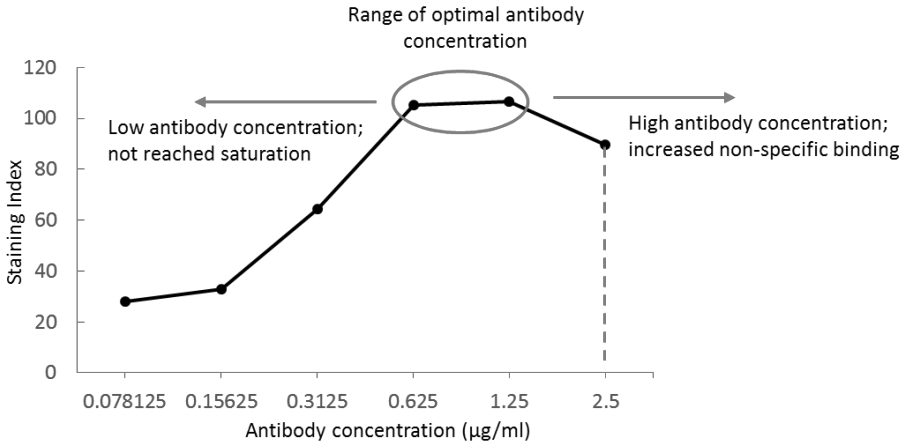


**Figure 2.4: Example of a titration curve used to determine optimal antibody concentration**
Cells were stained with a range of antibody concentrations and matching isotype control (IC) concentrations. Following analysis by flow cytometry, the staining index was calculated for each concentration ([{Median fluorescence intensity of the positively stained population} - {Median fluorescence intensity of the IC}] / [rSD of the IC].

### 2.4.2 Cytometer set up

FACSFlow (BD Biosciences) and 70% ethanol (VWR) were added to appropriate tanks and an empty waste container was connected, before the cytometer and computer were switched on and the FACSDiva software was started up. Once the cytometer had connected, the fluidics start-up was carried out, according to the on-screen instructions. A 70 µm nozzle was inserted and the stream turned on and allowed to stabilise. The lasers were allowed 30 minutes to warm up before a performance check was run using Cytometer setup and tracking (CST) beads (BD Biosciences) to ensure the PMT lasers were in their optimal range and that parameters were consistent between experiments. CST beads were vortexed and one full drop was added to a FACS tube containing 350 µl of FACSFlow, before loading the tube onto the loading port and completing the performance check.

### 2.4.3 Automated compensation set up

To correct for any spill over of fluorescence into the detectors of adjacent fluorochromes when samples were labelled with multiple antibodies, automated compensation was performed using BD CompBeads (BD Biosciences) prior to running samples. BD CompBeads were vortexed thoroughly and one full drop of both negative control and anti-mouse IgG CompBeads were added to FACS tubes containing 100 µl PBS/BSA/Azide. The antibodies for compensation were added to separate tubes at a volume required to label 1 x $10^6$ cells. An additional tube was made up containing 100 µl PBS/BSA/Azide and one drop of CompBeads negative control only. The tubes were incubated for 20 minutes in the dark, washed in PBS/BSA/Azide and centrifuged at 400 x *g* for 5 minutes. The beads were then resuspended in 500 µl PBS/BSA/Azide and used immediately for calculating compensation. Forward and side scatter and fluorescence parameters were set using unstained cells and adjusted with cells labelled with isotype control antibodies, before the compensation procedure was followed. Briefly, the tube containing only negative compensation beads was loaded onto the cytometer, the P1 gate on the FSC/SSC scatter graph was moved to encompass the population of beads and 5000 events were recorded. Each tube of positively labelled beads was then loaded onto the cytometer, the P2 gate was moved so that it encompassed the positively stained peak in the corresponding fluorescence histogram and 5000 events were recorded (Figure 2.5). Once the procedure had been completed for each fluorochrome being used, the compensation was calculated and automatically applied throughout the experiment.

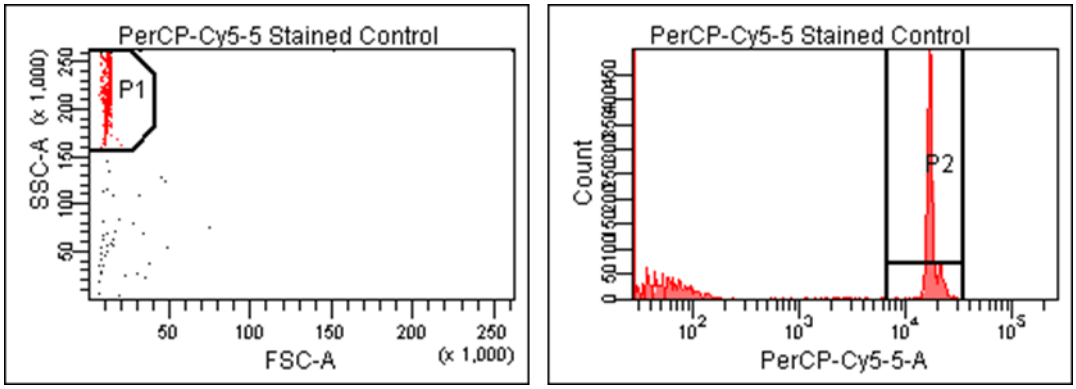


**Figure 2.5: Gating on compensation beads**
The P1 gate was set to enclose the beads based on their forward and side scatter and the P2 gate was set on the positive fluorescent peak, in this case PerCP-Cy5.5 labelled beads.

### 2.4.4 Sample Acquisition

Prepared samples (section 2.4.1) were loaded on to the FACSAria, and 10,000 events were recorded. Lymphocytes were determined based upon characteristic forward and side scatter and gates were applied accordingly (Figure 2.6; P1). For analysis of antigen expression, gates were set against isotype controls to include less than 1% of the cells (Figure 2.6).

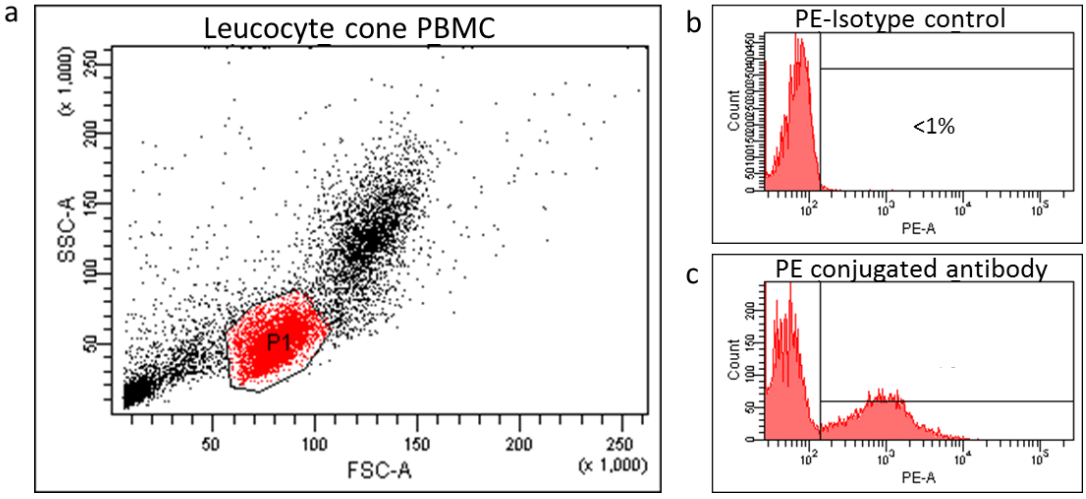


**Figure 2.6: Analysis of PBMC by flow cytometry**
Characteristic forward and side scatter plot of PBMC, with P1 (a; red events) showing the gated lymphocytes. For fluorescent markers, gates were set to contain less than 1% of the cells incubated with the corresponding isotype control (b), the gate was then applied to the sample plot (c).

### 2.4.5 **Fluorescence activated cell sorting (FACS)**

#### 2.4.5.1 *Aseptic clean*

Prior to cell sorting an aseptic clean was carried out according to the manufacturer's instructions, and all surfaces and the sort tube holder were swabbed with 70% ethanol. The set-up procedure was then carried out as previously outlined (section 2.4.2).

#### 2.4.5.2 *Preparation of PBMC for FACS*

PBMC that had either been cryopreserved (section 2.3.1) and thawed at room temperature, or freshly isolated from whole blood were washed in wash buffer (PBS containing 1% human AB serum) and centrifuged at 400 x *g* to recover cells. The cells were counted using trypan blue (section 2.1.4), resuspended in 1 ml of PBS/BSA/Azide and enough antibody was added to label the cells. Following a 30 minute incubation in the dark, cells were washed in wash buffer, centrifuged at 400 x *g* for 5 minutes and resuspended in wash buffer at a concentration of 7.5 x $10^6$ cells/ml. The cell suspension was transferred to a sterile polystyrene FACS tube, through a 70 µm cell straining cap (BD Biosciences) to remove any clumps, before being used immediately. For the collection of sorted cells, polypropylene FACS tubes were coated in 500 µl lymphocyte growth medium (X-Vivo 20; Lonza, containing 5% human AB serum and 0.1 U/ml penicillin/ 0.1 mg/ml streptomycin). Coating medium was discarded and 200 µl of fresh medium was added to each tube, ready to be placed in the collection device.

#### 2.4.5.3 *Setting the accudrop delay*

Following the standard cytometer set up procedure (section 2.3.2), before every sort the amplitude and drop delay were determined. Firstly, empty FACS tubes were inserted into the sort tube holder (Figure 2.7) and the collection device was fitted to the cytometer. To ensure the four side streams were correctly entering the collection tubes the voltage and test sort were turned on, the waste drawer opened and the streams inspected to confirm they were being suitably deflected into the collection tubes. If necessary, the slider controls for the side values were adjusted to achieve accurate deflection (Figure 2.8).

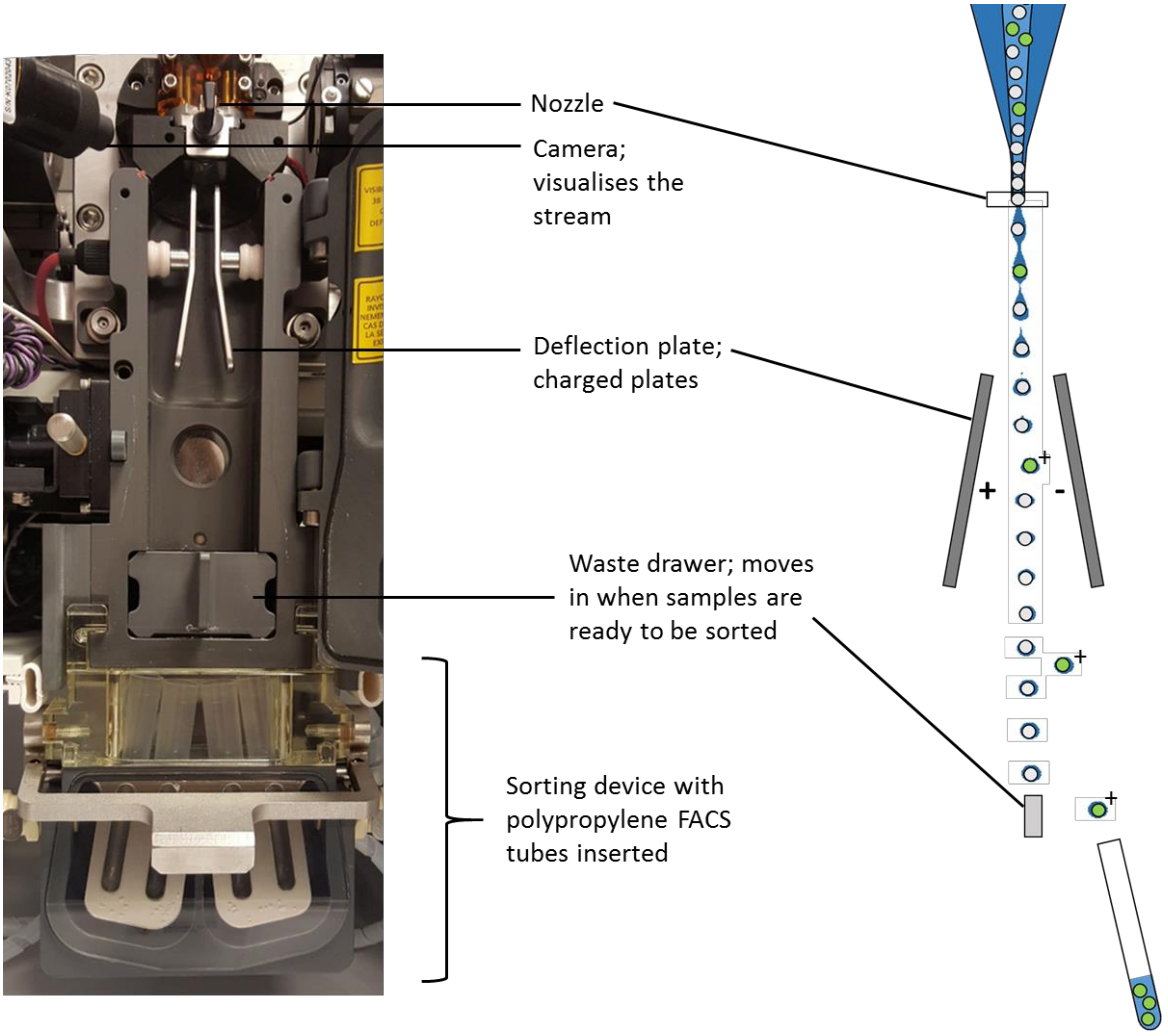


**Figure 2.7: FACS Aria II sort chamber and illustration of the sorting process**
Following cell interrogation, cells pass through the nozzle. The stream separates out into droplets each containing individual cells and the droplets are given a charge based on the information gleaned at interrogation. Droplets containing cells of interest (green fluorescently labelled cells), are deflected by charged plates in the sort chamber into tubes loaded in the FACS sorting device, any other cells (unlabelled) remain uncharged and pass straight into the waste chamber.

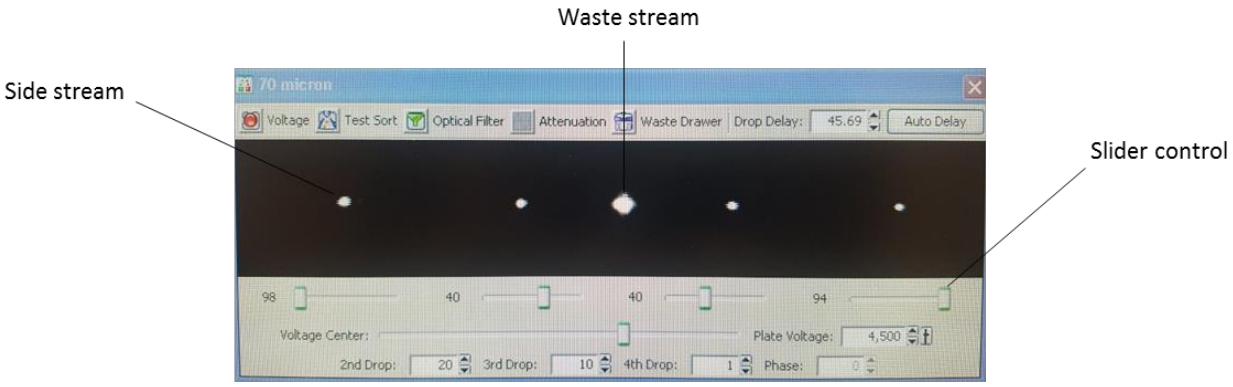


**Figure 2.8: Side stream window**
The central dot shows the waste stream and the four dots at either side are the side streams for sorting into collection tubes. The five streams should appear as separate clearly visible dots as shown.

The amplitude was then adjusted to find the range of values for which the five streams appeared clearly separated in the side stream window (Figure 2.8). The amplitude was set as the central point between these values and the corresponding drop 1 and gap values at this amplitude, given by the software, were inputted into the target fields (Figure 2.9). Once set the "sweet spot" was turned on throughout the sort procedure to ensure the stream remained stable and any fluctuations did not lead to contamination of the sorted sample.

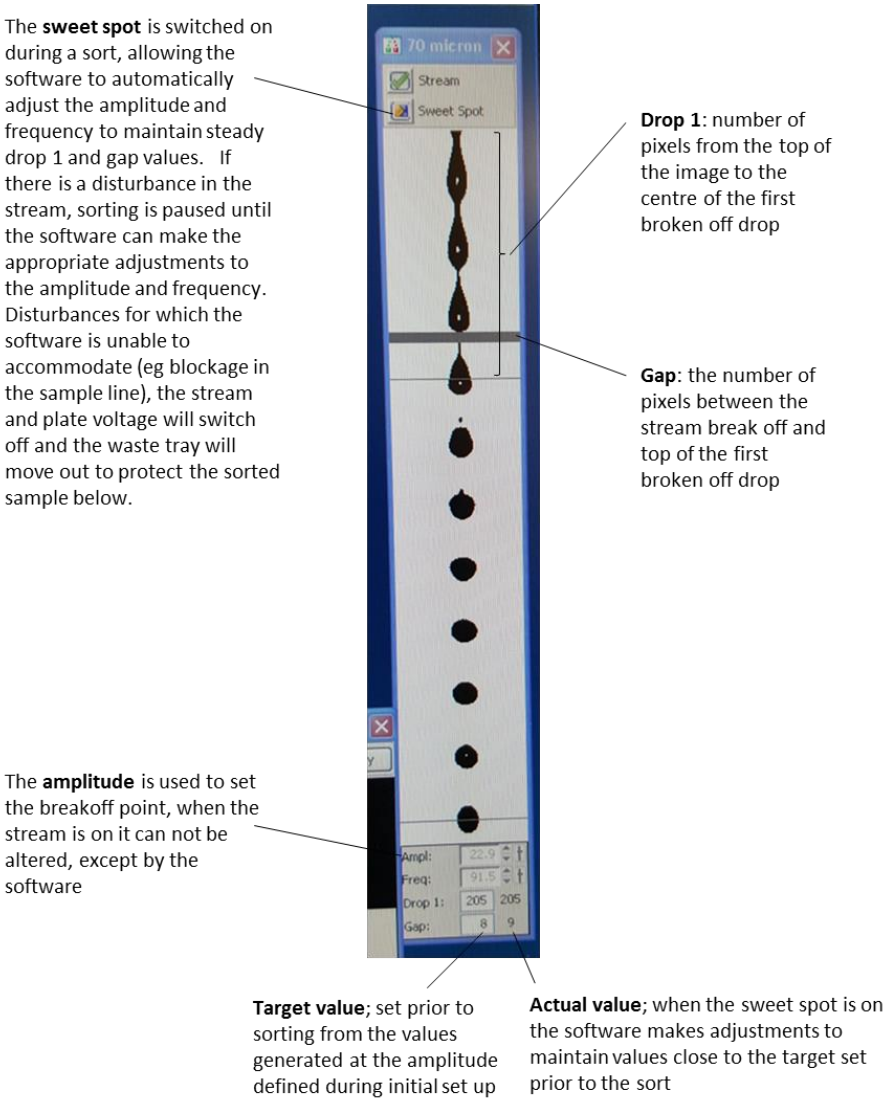


**Figure 2.9: Stream break off window**
The point where the stream separates into single droplets.

Before cell sorting, the stream containing the cells must separate into individual droplets containing the cell of interest so it can be charged and deflected into an appropriate sorting tube (Figure 2.7). The gap between detection of the cell and the formation and charging of the single droplet must be determined to ensure that the cell being collected is the same cell that was detected by the lasers. This was determined by an automated process using fluorescently labelled FACS Accudrop Beads (BD Biosciences). The Accudrop Beads were vortexed and one drop was added to 500 µl of FACSFlow. The tube was loaded onto the cytometer and the flow rate adjusted so the beads ran through the instrument at a rate between 1000 and 3000 events/second. The drop delay was adjusted by the software until nearly all

the beads were entering the side stream and none were visible in the middle waste stream (Figure 2.10).

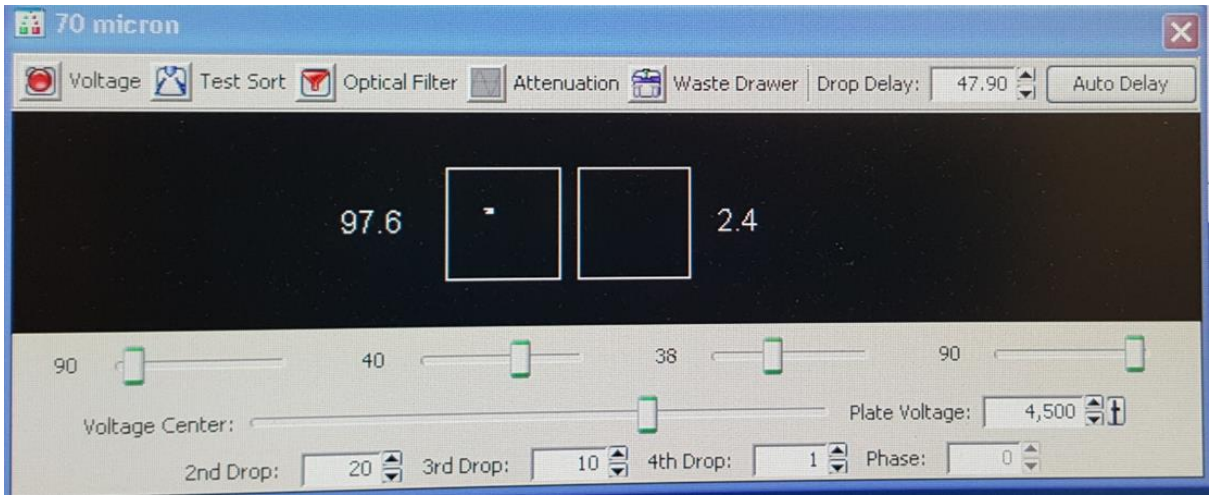


**Figure 2.10: Automated calculation of the drop delay using BD Accudrop Beads**
The drop delay is adjusted to find the optimal value for the settings used so that the majority (>90%) of the sorted population enters the sort tube (left hand box) and very few passes into the waste (right hand box).

### 2.4.5.4 *Setting up a template for FACS*

Following sort set-up, labelled cells (section 2.4.5.22.4.1) were loaded into the machine and the population of interest was gated according to forward and side scatter characteristics. From this population, a plot was made of FSC-W against FSC-A and SSC-W against SSC-A in order to exclude any doublets from the sort (Figure 2.11). Further gating was performed to isolate the cells of interest and the gate with the cell population to be sorted was added to an appropriate tube in the sort layout window (Figure 2.11).

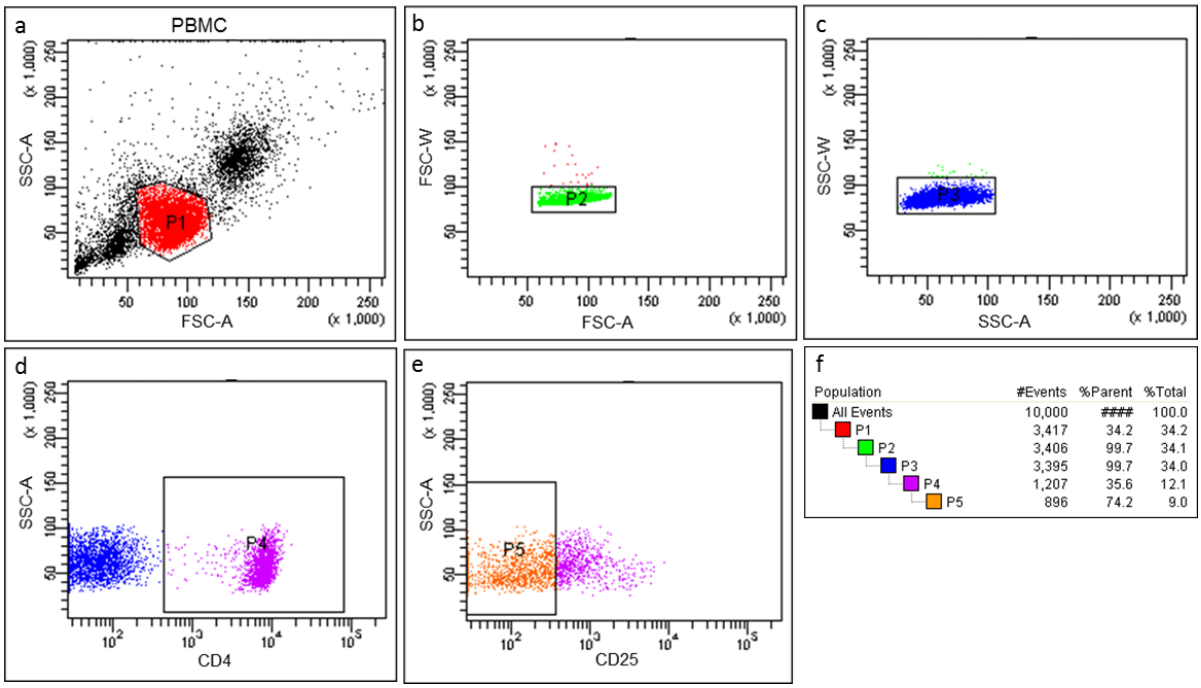


**Figure 2.11: Gating strategy for sorting $CD4^+CD25^-$ lymphocytes from PBMC**
PBMC were labelled with CD4 and CD25 fluorescent conjugated antibodies and events were acquired on a FACS Aria. FSC-A vs SSC-A plots were used to distinguish the lymphocyte population (a; P1). FSC-A vs FSC-W (b) and SSC-A vs SSC-W (c) were plotted using P1 to exclude doublets and from the resulting P3 single cell lymphocyte population, $CD4^+$ cells were selected (d; P4). A $CD25^-$ gate was set using an isotype control, the resulting gate was applied to the stained cells and this $CD4^+CD25^-$ lymphocyte population was sorted (e; P5).

Following the sort procedure, some of the sorted cells were run back through the instrument to check the purity of the sorted population. The collection tubes were centrifuged at 400 x *g* and the recovered cells were counted (section 2.2.4) and used immediately in experiments.

## 2.5 Enzyme-Linked immunosorbent assay

Enzyme Linked Immunosorbent Assay (ELISA; Figure 2.12) kits were used to measure the levels of IL2, TGF-β (human IL2 and human TGF-β1 DuoSet ELISA, R&D Systems, Abingdon, UK) and IL10 (human IL10 ELISA MAX, BioLegend, London, UK) in the conditioned medium from HNSCC cells lines, dissociated tumour tissue and tumour-derived fibroblasts. In addition, levels of IL10 were measured in the medium collected following the culture of $CD4^+CD25^-$ lymphocytes in CM or complete growth medium (GM).

A MaxiSorp® flat bottomed 96-well plate (Nunc, Thermo Fisher Scientific) was coated with capture antibody (100 µl/well; 4 µg/ml anti-IL2 in PBS, 2µg/ml anti-TGF-β in PBS, and 1:200 anti-IL10 in coating buffer: 8.4mg/ml $NaHCO_3$ and 3.56mg/ml $Na_2CO_3$ in $dH_20$) and incubated overnight at room temperature (IL2 and TGF- β) or at -4ºC (IL10). The plate was aspirated and washed three times with 400 µl/ well of wash buffer (0.05% Tween 20; Sigma, in TBS for IL2 and IL10 or PBS for TGF-β) using an automated plate washer (Thermo Fisher Scientific). After the final aspiration, 300 µl of block buffer (1% BSA in PBS for IL2 and IL10 or 5% Tween 20 in PBS for TGF-β) was added to each well and incubated for 1 hour at room temperature (for IL10 all incubations were performed on a shaker at 500 rpm). The plate was washed three times as previously described and the same wash procedure was used throughout.

Before application to the plate, TGF-β samples were activated to an immunoreactive form by the addition of 30 µl of 1 N HCl to 150 µl of sample, mixed thoroughly and incubated for 10 minutes at room temperature. Samples were neutralised by the addition of 30 µl 1.2 N NaOH/0.5 M HEPES, mixed well and 100 µl /well was assayed immediately.

Samples, including a GM control, and standards (a seven-point standard curve using 2-fold serial dilutions in reagent diluent, with a high standard of 1000 pg/ml, 2000 pg/ml and 250 pg/ml for IL2, TGF-β and IL10 respectively and a blank of reagent diluent only) were loaded onto the plate in duplicate (100 µl/well), and incubated at room temperature for 2 hours. The wells were washed three times using an automated plate washer and 100 µl of detection antibody (200 ng/ml IL2, 300 ng/ml TGF-β or 1:200 IL10) was added to wells, before incubation at room temperature for a further 2 hours (IL2 and TGF-β) or 1 hour (IL10).

The wells were washed and incubated with streptavidin-HRP (100 µl/well; 1:200 for 20 minutes for IL2 and TGF-β or 1:1000 for 30 minutes for IL10) at room temperature. Following a further wash step, 100 µl of substrate solution (1:1 mixture of $H_2O_2$ and tetramethylbenzidine; Vector, Peterborough, UK) was added to the wells and incubated for 20 minutes in the dark, before the addition of stop solution (2 N $H_2SO_4$; Sigma, 50 µl for IL2 and TGF-β or 100 µl for IL10).

The absorbance of each well was read and analysed on a Multiskan FC™ microplate reader (Thermo Fisher Scientific) at 450 nm with wavelength correction of 570 nm and a 4-

parameter logistic curve fit was used to plot the standard curve from which the concentrations of the proteins in the samples were determined.

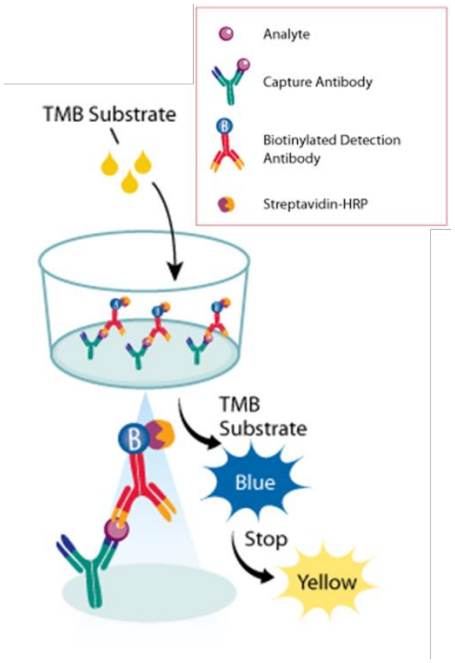


**Figure 2.12: ELISA assay principle**
A plate is coated with a capture antibody specific for the protein of interest. Samples and standards are added and any of the protein present will bind to the plate-bound capture antibody. Unbound protein is washed away and biotinylated detection antibody is added and binds to the protein in the well. Streptavidin horse radish peroxide (HRP) binds to the biotin on the detection antibody and a solution containing tetramethylbenzidine (TMB) and $H_2O_2$ is added. In the presence of the HRP enzyme, the TMB and $H_2O_2$ undergo a reaction that causes a colour change proportionate to the amount of protein in the sample. Addition of a stop solution ($H_2SO_4$) halts the reaction and causes a second colour change to yellow. The absorbance can then be measured on a plate reader at 450 nm. Image taken from R&D Systems website.

## 2.6 Proteome ProfilerTM human chemokine array

A Proteome Profiler$^{TM}$ human chemokine array kit (R&D Systems) was used for the detection of chemokines in the conditioned medium collected from the overnight culture of HNSCC tumours (Section 2.3.4) and UMSCC- cell lines (section 2.2.6). Each kit contained a nitrocellulose membrane on which 31 different chemokine capture antibodies were spotted in duplicate (Table 2. and Figure 2.13).

**Table 2.2: Chemokines detected by the Proteome Profiler™ human chemokine array kit (R&D Systems)**

| | | | |
|---|---|---|---|
| CCL21 | CCL14 | CCL7 | CXCL7 |
| CCL28 | CCL1 | CCL22 | CCL18 |
| CXCL16 | CXCL8 | Midkine | CXCL4 |
| Chemerin | IL-16 | CXCL9 | CCL5 |
| CXCL5 | CXCL10 | CCL3,4 | CXCL12 |
| CCL26 | CXCL11 | CCL15 | CCL17 |
| $CX_3CL1$ | XCL1 | CCL20 | CXCL17 |
| CXCL1 | CCL2 | CCL19 | |

The protocol was followed according to the manufacturer's instructions. Briefly, block buffer (array buffer 6; 2ml) was pipetted in to each well of the 4 well multi dish provided and the 4 membranes were carefully transferred into each separate well of the dish using flat-tip tweezers. The dish was placed on a rocking platform shaker and gently rocked, so that the membranes moved from end to end in their wells, for 1 hour. The samples were prepared by adding 0.5 ml of array buffer 4 and 0.5 ml of array buffer 6 to 0.5 ml of each CM test sample and one GM control. To each sample mix, 15 µl of biotinylated-detection antibody cocktail was added and incubated for 1 hour at room temperature. Block buffer was aspirated from the 4 well multi dish and the prepared sample mixture was added to the appropriate membrane and incubated overnight at 4°C on a rocking platform shaker.

Following incubation, each membrane was removed and transferred to individual petri dishes, where they were washed three times with 20 ml wash buffer to remove any unbound material. For each wash, the membranes and wash buffer were incubated for 10 minutes on a rocking platform before wash buffer was aspirated and replaced with fresh buffer. During the washes, the 4 well dish was thoroughly cleaned with distilled water and dried the washed membranes were transferred back to their original wells and incubated with streptavidin-HRP (2 ml) for 30 minutes at room temperature on the platform rocker. Each membrane was washed as previously described and any excess wash buffer was allowed to drain away before the membranes were placed face up on a sheet of plastic and 1 ml of chemiluminescent reagent mix (equal volumes of Chemi Reagents 1 and 2) was pipetted onto each, ensuring even coverage. Membranes were covered with a second plastic sheet

and incubated for 1 minute. The top plastic sheet was removed and the remaining chemiluminescent reagent mix blotted off before a clean sheet was applied. In the dark, the membranes were immediately placed in an autoradiography film cassette and exposed to X-ray film for 1, 5 and 10 minutes. Following exposure, the X-ray film was carefully removed from the cassette and placed in a tray of developer. The tray was tipped, to ensure the film was fully immersed in the developer for 2 minutes. The film was then immersed in fixer for 2 minutes, followed by acetic acid for a further 2 minutes, before being rinsed in tap water and left to dry.

Developed films were viewed and analysed using the gel doc system (UVP Laboratory products, EPI Chem II Darkroom) and ImageJ Software. The pixel density of each spot was calculated and a mean of the two duplicate spots was taken for each chemokine. The mean pixel densities calculated from the membrane incubated with the GM control were subtracted from the corresponding values from the membranes incubated with each CM sample.

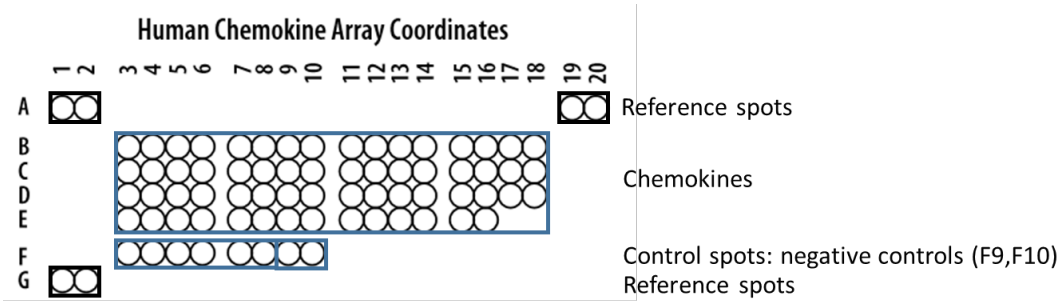


**Figure 2.13 Arrangement of the antibodies on the membranes of the Human Chemokine Array**
Chemokine antibodies are arranged in duplicate in the middle of the membrane. The membrane also includes one pair of negative control spots and three pairs of positive control spots, containing antibodies for three proteins commonly present in cell supernatant. For each separate film, mean results from the negative control spots were subtracted from each chemokine spot. Reference spots in three corners of the membrane are present to aid in orientating the array.

## 2.7 MTS cell proliferation/viability assay

MTS assays (Promega, Southampton, UK) were carried out on PBMC cultured in different CM or GM to determine the effect of CM on PBMC proliferation, according to the manufacturer's guidelines.

### 2.7.1 **Principle of MTS assay**

Metabolically active cells produce the reduced form of the coenzyme nicotinamide adenine dinucleotide (NADH) and are therefore able to reduce methyl tetrazolium salt (MTS) to a soluble coloured formazan product (Figure 2.14). The colour change observed is proportional to the number of viable cells, thus can be used as a measure of cell proliferation.

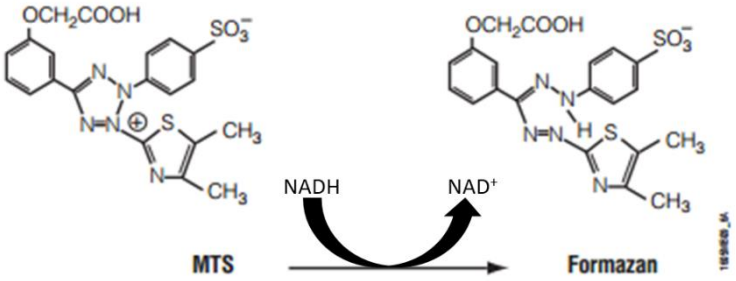


**Figure 2.14: The reduction of MTS to Formazan in the presence of metabolically active cells**
Adapted from Promega.

### 2.7.2 **MTS assay procedure**

PBMC that had been cryopreserved (section 2.2.1) and thawed at room temperature, or that had been previously cultured for 5 days to activate T cells (section2.3.3.1) were washed in PBS and centrifuged at 400 x *g* to recover cells. The cells were counted using trypan blue (section 2.1.2), and were seeded at 8 x $10^4$ cells/well in 66 µl of lymphocyte growth medium and 33 µl complete DMEM medium (section 2.2.5), UMSCC-cell line CM (section 2.2.6), tumour derived fibroblast CM (section 2.3.4) or dissociated tumour overnight CM (2.3.5) in 96 well round bottomed plates. Following culture for 4 days for whole PBMC or 24 hours for pre-activated T cells, 20 µl of MTS reagent (CellTiter 96® $AQ_{ueous}$ One Solution Reagent; Promega) was added to each well and cells were incubated for 4 hours. Following incubation, absorbance was read on a spectrophotometer (Multiskan FC™ microplate reader) at a wavelength of 492 nm.

## 2.8 Carboxyfluorescein succinimidyl ester (CFSE) assay

In order to determine and quantify the suppressive ability of cells ($CD4^+CD25^-$) following culture in dissociated tumour overnight conditioned medium, the preconditioned cells were incubated with freshly sorted $CD4^+CD25^-$ T cells stained with carboxyfluorescein succinimidyl ester (CFSE).

### 2.8.1 Principle of CFSE assay

Carboxyfluorescein diacetate succimidyl ester (CFDA-SE) is a cell permeable molecule that forms the fluorescent CFSE molecule when cleaved by intracellular esterases (Parish, 1999)). The covalent binding of CFSE to intracellular amines prevents the dye exiting the cell and subsequently staining adjacent cells, making it useful for co-culture experiments. The CFSE is divided equally between the daughter cells following each cell division, reducing the fluorescence intensity of the cell by half. This allows the rate of proliferation to be analysed using flow cytometry. The original undivided parent population of cells forms a single bright peak in the FL1/FITC filter, when cells proliferate multiple peaks can be observed, representing the different number of cell divisions that have taken place (Figure 2.15).

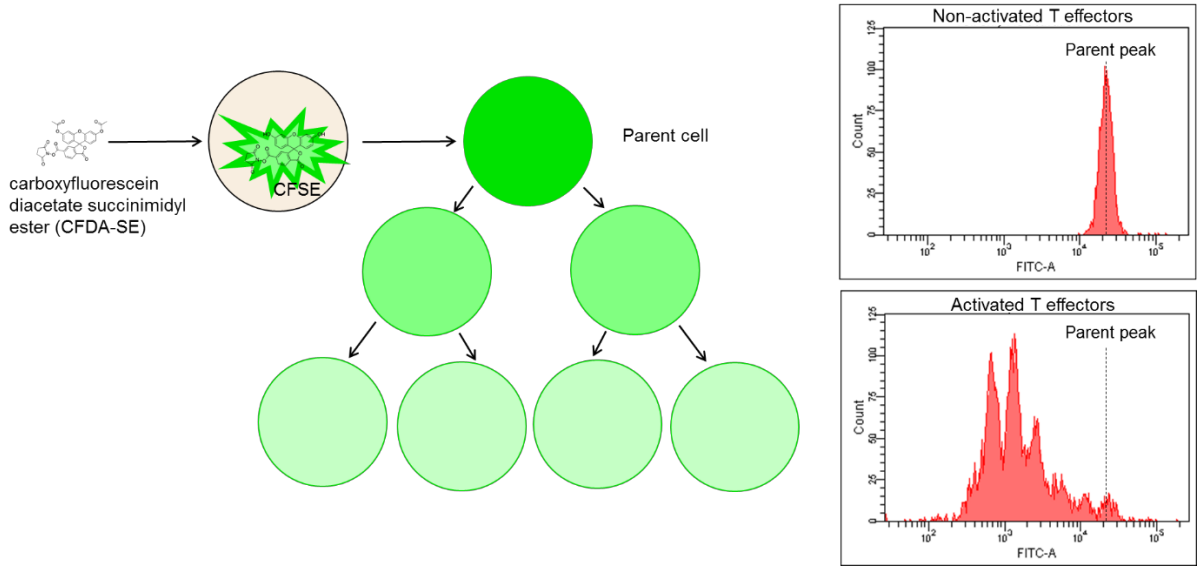


**Figure 2.15: CFSE assay principle**
**Without activation T effectors, undergo little or no proliferation, and one single undivided (parent) peak of cells can be observed. When the cells are activated they proliferate and subsequent progeny form peaks of reduced fluorescence intensity.**

### 2.8.2 **CFSE assay procedure**

#### 2.8.2.1 *Preparation of pre-conditioned (potential suppressive) T cells*

$CD4^+CD25^-$ T cells were sorted from PBMC of healthy control leucocyte cones (section 2.4.52.2.2). Cells were counted using trypan blue exclusion (section 2.2.4), centrifuged at 400 x *g* for 5 minutes and seeded at 8 x $10^4$ cells/well in 66 µl lymphocyte growth medium in 96 well round bottomed plates. An additional 33 µl of complete DMEM growth medium (section 2.2.5), or dissociated tumour overnight CM (2.3.5) were added to the wells, all containing IL2 (final concentration 100 IU/ml; AbDSerotec) and human T activator CD3/CD28 DynaBeads® (1:1, cells:beads; Life Sciences). The cells were incubated for 5 days at 37ºC and 5% $CO_2$ in a humidified atmosphere.

#### 2.8.2.2 *Preparation of responder T cells*

$CD4^+CD25^-$ T cells were sorted from the PBMC of the same healthy control leucocyte cone as was used for the pre-conditioned cells (section 2.4.52.7.2.1). Cells were counted using trypan blue exclusion (section 2.2.4), centrifuged at 400 x *g* for 5 minutes and resuspended in 0.1% BSA in PBS. As a negative control, 5 x $10^4$ cells were transferred to a fresh tube to remain unstained, both tubes of cells were centrifuged at 400 x *g* for 5 minutes and resuspended in 0.1% BSA in PBS at a concentration of 1 x$10^6$ cells/ml, or 1 ml if there were fewer than 1 x $10^6$ cells in total. CFDA-SE (Sigma) was added to the tube of cells to be stained for the assay at a final concentration of 5 µM and both tubes of cells were incubated for 10 minutes at 37ºC. To quench the staining, 2.5 ml of ice cold lymphocyte growth medium was added to the cell suspension and the cells were placed on ice for 5 minutes before being centrifuged at 400 x *g* for 5 minutes and resuspended in lymphocyte growth medium. The cells were washed with growth medium a further 3 times, and then resuspended in the appropriate amount of growth medium to plate cells at 5 x $10^4$ cells/well in 100 µl in a 96 well round bottomed plate.

#### 2.8.2.3 *Co-culture*

The pre-conditioned cells were transferred from wells into 1.5 ml polypropylene tubes following 5 days of culture in either growth medium or tumour overnight CM (section 2.8.2.1). Anti-CD3/CD28 beads were detached from cells by gently pipetting up and down, and magnets were used to separate out the beads from the cell suspension. The supernatant containing the cells was centrifuged at 400 x *g* for 5 minutes and the culture supernatant was removed and stored at -80ºC for future analysis by ELISA (section 2.4). The cell pellet was

resuspended in wash buffer for counting with trypan blue (section 2.2.4). Following centrifugation, the preconditioned cells were resuspended in lymphocyte growth medium and co-cultured with the CFSE stained $CD4^+CD25^-$ lymphocytes, at ratios of 4:1, 1, 2:1, 1:1, 1:2, 1:4, 1:8 and 1:16 (pre-conditioned lymphocytes: $CD4^+CD25^-$ responder lymphocytes:), with 100 IU/ml IL2 and 1:1 CD3/CD28 Dyna Beads for 4 days at 37ºC (Drennan *et al.*, 2014). Some of the $CD4^+CD25^-$ T cells were plated alone with and without the addition of activating factors for a baseline level of T effector proliferation and a non-proliferative parent population, respectively.

Following the co-culture period, the cells were transferred to FACS tubes, centrifuged at 400 x *g* for 5 minutes and the pellet resuspended in 200 µl of PBS/BSA/Azide, before analysis by flow cytometry. Lymphocytes were gated according to characteristic forward and side scatter plots, and of these approximately 3000 CFSE-positive events were recorded.

### 2.8.3 **Analysis of CFSE data with Modfit**

Modfit LT software (Verity Software House, Topsham, USA) was used for the analysis of CFSE data. A scatter diagram of side scatter against forward scatter was plotted from the activated T effector cells that were unstained with CFSE and a gate was set around the lymphocytes (R1; Figure 2.16a). From this lymphocyte gate, a new plot of side scatter against FITC was drawn and a gate was set to the right of the unstained population of cells (R2; Figure 2.16b). Co-cultures of CFSE stained and unstained cells should be clearly distinguishable so that all stained cells are included in the R2 gate (Figure 2.16c).

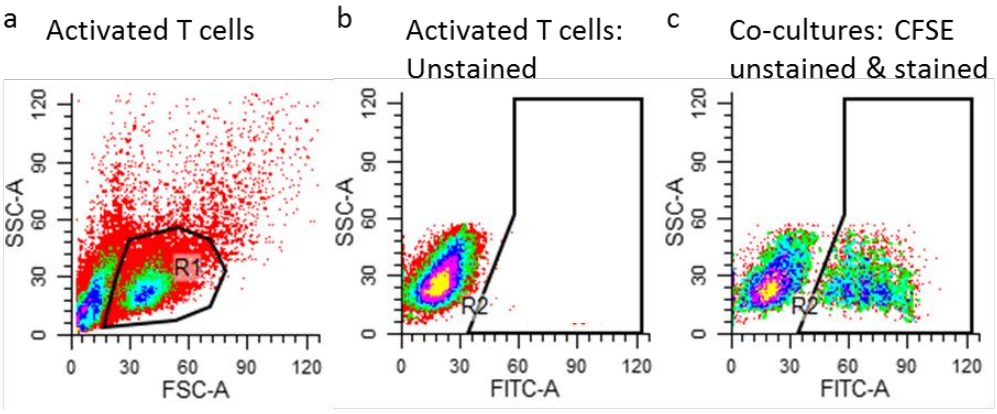


**Figure 2.16: Gating strategy used for Modfit analysis of CFSE assays**
To set the gates for analysis following the co-culture of pre conditioned $CD4^{+}CD25^{-}$ lymphocytes with autologous CFSE stained CD4+CD25- T cells, wells of $CD4^{+}CD25^{-}$ T cells not stained with CFSE were also plated at the same time. These unstained $CD4^{+}CD25^{-}$ T cells were activated for 4 days with CD3/28 DynaBeads and IL2. A gate was set around the lymphocytes (R1; a) and from this gate the gate for CFSE stained cells was set to the right of the unstained cells (b). Co cultures of unstained pre conditioned cells and CFSE stained cells were distinguishable (c).

The gate encompassing the CFSE stained lymphocytes (R2; Figure 2.16) was used to plot histograms of CFSE fluorescence intensity (Figure 2.17a and b). The original parent population was set based on the position of the non-activated CFSE stained T cells, as these cells had undergone no proliferation (Figure 2.17a). The programme then models the subsequent generations, by calculating the spacing between generations (Figure 2.17c). This calculation is based on the number of log decades in the sample, the histogram resolution and the assumption that the fluorescence intensity is halved each generation. Applying this model, the number of cells present in each generation can be determined. From this, it is possible to compute the number of parent cells originally cultured, given that each parent cell will give rise to two daughter cells. A proliferation index was calculated for each tube of cells by dividing the sum of the cells in all the generations by the computed number of cells in the original parent population (Figure 2.17d; Modfit LT User Guide).

The maximum rate of proliferation (100%) was set as the rate of proliferation of the $CD4^{+}CD25^{-}$ T cells cultured alone (Figure 2.17b), and this was used to determine a percentage proliferation for all co cultured cells. The percentage suppression was taken as the percentage of proliferation subtracted from 100 (Figure 2.17d).

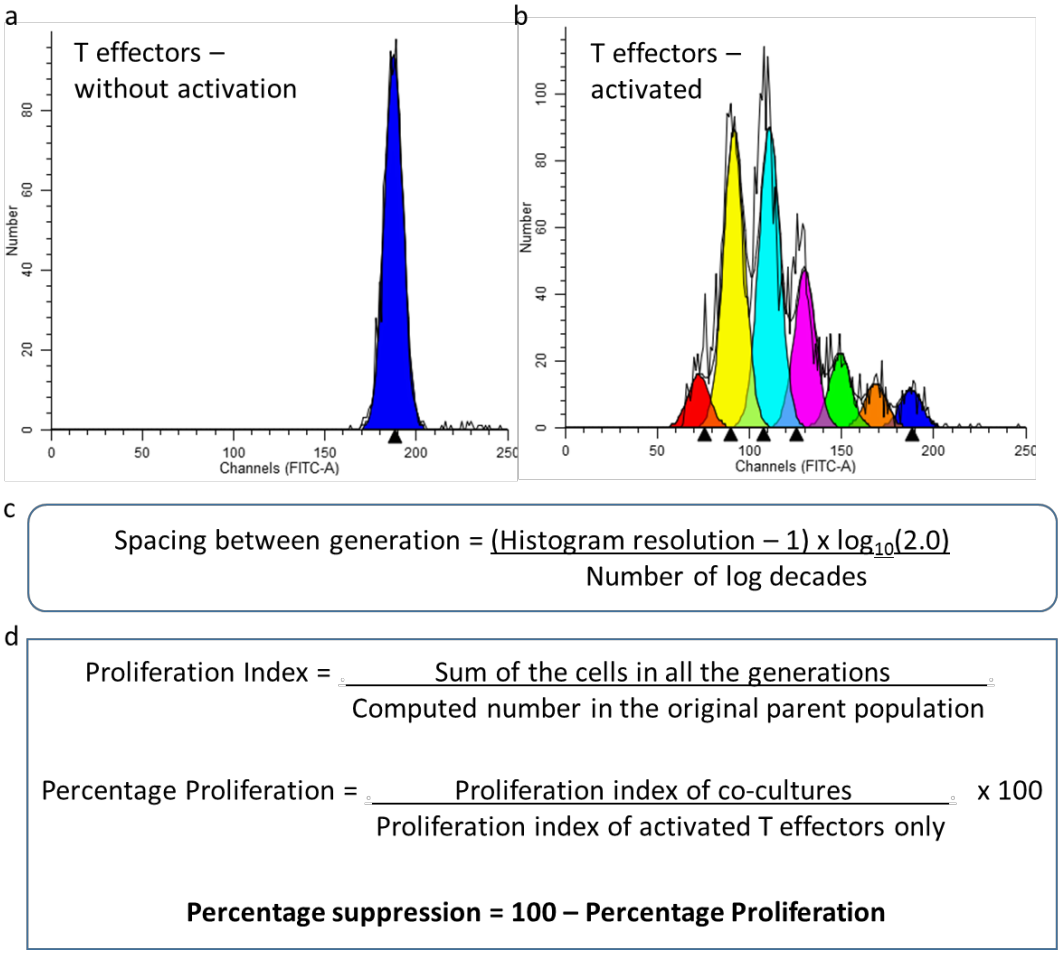


**Figure 2.17: Calculating the percentage proliferation and suppression of a given population of cells using Modfit software**

Modfit software plots histograms showing the intensity of CFSE present in the stained cells (a and b). Using formula (c) the spacing between each generation can be calculated and the number of cells in each generation is determined. This is used to determine the number of cells that were present at the start of the experiment and to calculate a proliferation index. The proliferation index generated by the software is then used to determine the percentage proliferation of the co-cultured $CD4^{+}CD25^{-}$ cells in relation to the proliferation of the T effector cells cultured alone. This is subtracted from 100 to reach a final value for percentage suppression.

## 2.9 *In Vitro* Assays for Measuring Apoptosis

It is possible to distinguish apoptotic cells from those undergoing other types of cell death by looking for the characteristic morphological and biochemical events (Section 1.3.2.1). For example, alterations to the plasma membrane, nuclear condensation and DNA fragmentation have all been exploited in commercially available apoptosis detection kits (Darzynkiewicz *et al.*, 2001; Henry *et al.*, 2013).

One of the markers commonly used to detect apoptotic cells is surface expression of phosphatidylserine (PS). In healthy cells, enzymes known as flippases and floppases control the distribution of lipids in the plasma membrane, holding PS at the cytosolic side of the membrane (Hankins *et al.*, 2015). At the early stages of apoptosis these enzymes are degraded and caspase activated scramblases disrupt plasma membrane asymmetry, translocating PS to the cell surface, which acts as a signal to macrophages for phagocytosis (Fadok *et al.*, 1992; Martin *et al.*, 1995). Annexin V is a phospholipid binding protein that binds to PS at the cell surface and therefore can distinguish cells undergoing apoptosis from healthy cells when conjugated to a fluorophore (Andree *et al.*, 1990; Koopman *et al.*, 1994). A limitation of the use of annexin V is that it can enter necrotic cells through their compromised membranes, where it binds to internal PS. This necessitates the use of viability dyes, such as propidium iodide (PI), which are often used in conjunction with annexin V to help to distinguish necrotic cells from those undergoing apoptosis (Figure 2.18). Propidium iodide is a membrane impermeant fluorescent dye that intercalates with double stranded DNA, resulting in enhancement of its fluorescence. Although these dyes are excluded from cells in the early stages of apoptosis, during late apoptosis the loss of integrity of the cell membrane means that PI will also pass into these cells. Therefore, cells that are positive for both annexin V and PI could be either late apoptotic or necrotic (Figure 2.18; Henry *et al.*, 2013).

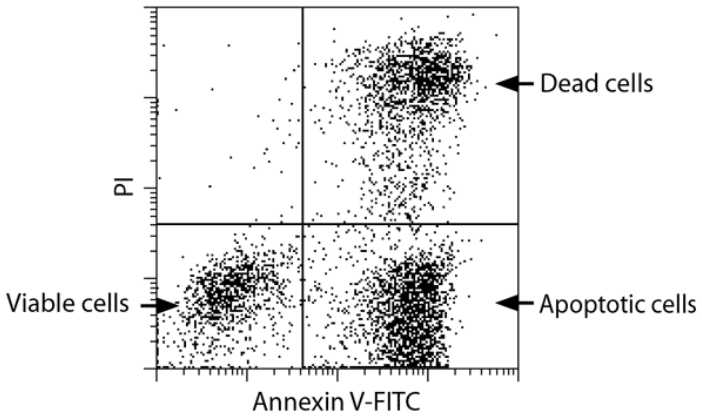


**Figure 2.18: Dual staining of Jurkat cells with PI and FITC- conjugated annexin V**
Viable cells (bottom left) exclude PI and will not bind annexin V. The translocation of PS to the external side of the cell membrane during apoptosis means apoptotic cells (bottom right) bind annexin V but exclude PI. The compromised membranes of necrotic cells and cells in the latter stages of apoptosis will allow PI to pass through and intercalate with nuclear DNA and expose PS to annexin V binding (top right). Figure taken from Miltenyi Biotech website, http://www.miltenyibiotec.com/en/products-and-services/macs-flow-cytometry/reagents/support-reagents/annexin-v-fitc-kit.aspx.

The expression of other proteins with roles in apoptotic pathways can also be measured, but may only be useful if the particular pathways involved are already known. For example, measuring cytochrome c expression will only be informative of activation of the intrinsic pathway (McStay & Green, 2014).

Many apoptosis assays make use of the caspase pathway, which is the converging point of the pathways that trigger apoptosis (Figure 1.15; Section 1.3.2.1). Biochemical substrate assays are popular plate based assays, in which the presence of a particular active caspase causes a colorimetric or fluorescent reaction which can quickly be measured and used to quantify the relative caspase levels present. However, these are often expensive and offer limited scope for further analysis of the cells involved. Fluorescent-conjugated antibodies are available for many of the active caspase enzymes and can be used in conjunction with other antibodies or viability dyes for more detailed observations. Often these antibodies are not cell permeable and require additional fixation and permeabilisation steps. As not all caspases will necessarily by expressed during apoptosis, for example caspase 3 is known to be absent during apoptosis in the breast cancer cell line MCF-7 (Liang *et al.*, 2001), pan-caspase inhibitors that bind with varying affinities to the different caspases can be used. The CaspACE™ FITC-VAD-FMK marker (Promega) is an analogue of the pan caspase inhibitor Z-VAD-FMK. The cell permeable molecule is able to pass into cells were it binds irreversibly to activated caspases. The substitution of the FITC fluorophore for the carbobenzoxy N-terminal group allows apoptotic cells to be detected by microscopy or flow cytometry. The VAD-FMK inhibitor binds with different affinities to most caspases and in the latter stages of apoptosis multiple peaks can be observed (Figure 2.19). The highest fluorescence intensity is seen in late apoptotic cells, and middle peaks represent a mix of cells going through early and late apoptosis. In this study a pan-caspase inhibitor and dual PI/Annexin V staining were used to detect apoptotic cells using flow cytometry.

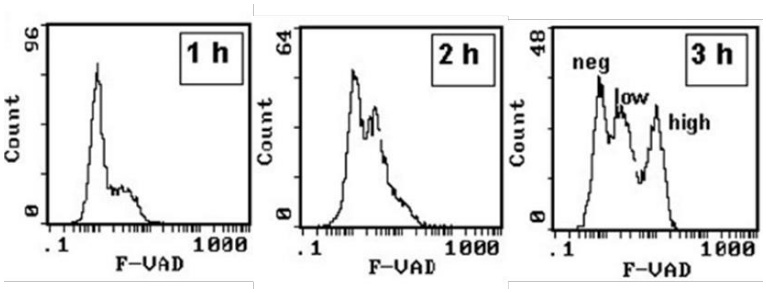


**Figure 2.19: CaspACE™ binding in Jurkats treated with anti-Fas for 1, 2 and 3 hours to induce apoptosis**
Jurkats were stained with CaspACE™, following culture of cells with anti-Fas. CaspACE™ bound the activated caspases in the apoptotic cells. A proportion of the cells in the later stage of apoptosis bound more CaspACE™ as more caspases became activated. Figure taken from Promega website, https://www.promega.co.uk/resources/pubhub/enotes/caspace-fitcvadfmk-in-situ-marker-a-probe-for-flow-cytometry-detection-of-apoptotic-cells/ (Belloc *et al.*, 2000)

### 2.9.1 Induction of apoptosis with etoposide

Etoposide is a chemotherapy agent that induces apoptosis primarily via the intrinsic pathway by disrupting topoisomerase activity. During DNA replication topoisomerases are involved in the winding and unwinding of DNA, necessary for DNA replication, DNA repair, transcription and chromatin remodelling (Vos *et al.*, 2011). Topoisomerase II enzymes induce double stranded DNA breaks, as part of a two-part reaction first breaking DNA and then re-ligating the strands (Montecucco *et al.*, 2015). Etoposide binds to DNA and topoisomerase II preventing DNA re-ligating, resulting in activation of an apoptotic response via cytochrome c and caspase 9.

Etoposide was used to induce apoptosis in Jurkat cells (Section 2.2.3) and activated T cells (Section 2.3.3). Cells were seeded at 1 x $10^6$ cells/well in 1 ml of Jurkat medium (Section 2.1.3) or at 8 x $10^4$ cells/well in 100 µl of complete lymphocyte growth medium in 6 and 96 well plates, respectively. For induction of apoptosis, wells were supplemented with etoposide (final concentration of 10 µM or 5 µM; Sigma), and for control wells the same volume of DMSO was added. Cells were incubated for up to two days at 37ºC, 5% $CO_2$ in a humidified atmosphere. Following 6, 24 or 48 hours incubation cells were counted using trypan blue (Section 2.1.4) and cells were stained with PI/Annexin V or CaspACE™ to measure apoptosis.

### 2.9.2 Measuring cell death and apoptosis

#### 2.9.2.1 *Annexin V and propidium iodide*

Following culture in CM or with etoposide, Jurkats or PBMC were washed in 1x annexin V buffer (Miltenyi Biotech) and transferred to FACS tubes in 100 µl 1x annexin V buffer. FITC conjugated annexin V (10 µl: Miltenyi Biotech) was added to cells and allowed to incubate for 20 minutes in the dark at room temperature. To wash away any unbound annexin V, 1 ml of annexin V buffer was added, the tube was centrifuged at 400 x *g* for 5 minutes and the supernatant was removed. Cells were resuspended in annexin V buffer and propidium iodide (PI; final concentration of 1 ug/ml, Miltenyi Biotech) was added to cells immediately prior to flow cytometric analysis (section 2.3).

#### 2.9.2.2 *Fluorescence compensation using single stained cells*

Automated compensation was set on the FACS Aria using single stained cells taken from the same experiment. Three FACS tubes were prepared containing cells stained with annexin V only, cells stained with PI only and unstained cells. The tube containing unstained cells was used to set the voltages for the forward scatter, side scatter, FITC and PI parameters. For each tube 5000 events were recorded and automated compensation was set up (section 2.3.3).

#### 2.9.2.3 *CaspACE™ FITC-VAD-FMK*

As an additional measure of apoptosis CaspACE$^{TM}$ FITC-VAD-FMK *in situ* marker (Promega; Section 5.1.2) was used to determine the proportion of cells with activated caspases. Following washing in PBS/BSA/Azide (Appendix A), resusupended cells (100 µl) were transferred to FACS tubes and incubated for 20 minutes in the dark at room temperature with a final concentration of 10 µM CaspACE™. Cells were washed in PBS/BSA/Azide, centrifuged at 400 x *g* for 5 minutes and fixed with 0.5% formaldehyde (1 ml; VWR) for 30 minutes. Cells were centrifuged at 400 x *g* for 5 minutes before a final wash step as before, prior to resuspension in 100 µl PBS/BSA/Azide for analysis by flow cytometry (section 2.3).

## 2.10 Migration Assays

Migration assays were performed on PBMC freshly isolated from the peripheral blood of healthy donors or HNSCC patients (section 2.3.1), in order to determine whether CM collected from HNSCC tumour dissociated biopsies (section 2.3.4) contained soluble factors

involved in lymphocyte chemotaxis (Figure 2.20). Due to the presence of chemo attractants in serum, cells were cultured in low serum growth medium (X-vivo 20; supplemented with 0.5% FBS and 0.1U penicillin/0.1 mg/ml streptomycin; Liu *et al.*, 2015).

PBMC were resuspended in lymphocyte growth medium at a concentration of $1x10^7$ cells/ml and plated in 75 $cm^2$ flasks (10 ml). Flasks were incubated for two hours at 37ºC and 5% $CO_2$ to allow monocytes to adhere to the plastic and internalised chemokine receptors to return to the lymphocyte surface. Following incubation, the growth medium containing the suspended lymphocytes was removed from the flask and centrifuged at 400 x *g* to recover the cells. The cells were resuspended in PBS for counting (Section 2.1.4), before being centrifuged and washed once more in low serum growth medium. Following a further centrifugation, cells were resuspended in low serum medium at a final concentration of 2.5 x $10^6$ cells/ml.

Prior to use in the assay 600 µl of low serum medium was added to the bottom wells of a 24 well plate with Transwell® 5 µm pore polycarbonate inserts (Corning, Thermo Fisher Scientific) and the plates were incubated for 1 hour at 37ºC and 5% $CO_2$ to equilibrate. The medium was removed from the wells and replaced with 600 µl of growth medium, either alone or supplemented with 80 ng/ml SDF-1, or dissociated tumour overnight CM (2.3.5) in duplicate.

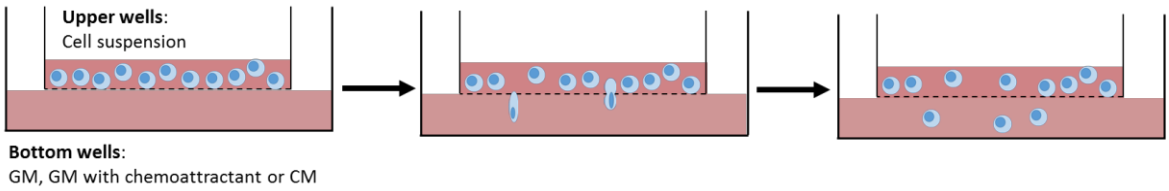


**Figure 2.20: Pricinple of Transwell® migration assay**
Bottom wells were filled with GM alone, GM containing the known activated T lymphocyte chemoattractant SDF-1 or CM from dissociated tumour biopsies. Polycarbonate Transwells® with 5 µm pores were placed in the wells and PBMC were added to this upper compartment. The small pore size in the Transwells® means that lymphocytes can only pass through them by chemotaxis, and will not drop through. Migration can be quantified by counting the number of cells that pass through the pores into the lower chamber of the wells.

The prepared cell suspension (100 µl) was immediately added to the Transwells®, so that each upper well contained 2.5 x $10^5$ cells. The Transwell® plates were then returned to the incubator for 4 hours. Migrated cells were recovered from the bottom wells of the plate by centrifugation. The pelleted cells were resuspended in 100 µl of PBS, counted (section 2.2.4) and transferred immediately to FACS tubes for analysis by flow cytometry (Section 2.4).

## 2.11 Statistical Analysis

Statistical analysis was carried out using SPPS statistics 24 (IBM), or GraphPad Prism 7 (GraphPad Software, Dan Diego, USA) and is described in detail in the relevant chapters. In general, for cell culture experiments, with low n numbers ($n \leq 4$) parametric T tests and ANOVA were used to determine significantly significant diiferences (*$p<0.05$, **$p<0.01$, ***$p<0.001$).

For comparison of receptor expression between the PBMC of healthy controls and HNSCC patients, or between TIL and PBMC from HNSCC patients, normality was tested using a Shapiro Wilks test. Following this either T tests or Mann Whitney U tests were performed, depending on whether the distribution was normal. Where T tests were used Levene's test was carried out to determine whether the data had equal variance and the appropriate *p* value was chosen.

# Chapter 3 Generation of cells with an iTreg phenotype from CD4+CD25- precursors by soluble factors in the HNSCC microenvironment

## 3.1 Introduction

Evasion of the immune system by tumours is one of the emerging hallmarks of cancer (Hanahan & Weinberg, 2011). Alterations to infiltrating immune cell populations in a variety of different cancer settings are mediated by the local tumour environment (Sections 1.2.3-1.2.8). This can involve influencing the cell populations that are drawn in to the tumour, as well as effecting their differentiation and activation (Section 1.3). Furthermore, in addition to manipulating their local immune environment, the tumour can also influence the immune profile in the periphery. For instance, there is a substantial body of evidence showing that levels of Treg are elevated in the peripheral blood of patients suffering from various types of cancer (Woo *et al.*, 2001; Liyanage *et al.*, 2002; Ichihara *et al.*, 2003; Miller *et al.*, 2006; Strauss *et al.*, 2007a; Strauss *et al.*, 2007b; Chi *et al.*, 2010; Jie *et al.*, 2013). There is a growing appreciation of the complexity of this suppressive cell type and the existence of different subsets, which can be broadly divided into those that develop in the thymus and those that are induced in the periphery (Section 1.2.2.4.2). Although there are a number of factors known to be involved in the induction and recruitment of Treg *in vitro*, their contribution to this enrichment *in vivo* in cancer patients requires further investigation. A better understanding as to whether the Treg in HNSCC are primarily nTreg or iTreg induced in the TME could lead to the development of novel ways to prevent Treg enrichment.

### 3.1.1 *In vitro* iTreg induction

A number of cytokines have been implicated in Treg proliferation and induction *in vitro*. Previous studies have noted an increase in Treg following culture of $CD4^+CD25^-$ T cells with TGF-β, usually assessed by an increase in the proportion of $CD25^{+/hi}FoxP3^+$ cells (Tran *et al.*, 2007; Lu *et al.*, 2010a).

#### 3.1.1.1 *The role of TGF-β in Treg induction*

The differentiation of iTreg from precursor $CD4^+CD25^-$ T cells, is among the suspected immunosuppressive roles of TGF-β (Pickup *et al.*, 2013). This role is well established *in vitro*, both for human and mouse cells, where it has been used with IL2 and various methods of TCR activation to induce iTreg (Yamagiwa *et al.*, 2001; Zheng *et al.*, 2002; Chen *et al.*,

2003; Bettelli *et al.*, 2006; Pot *et al.*, 2009; Lu *et al.*, 2010a). The efficacy of TGF-β to induce FoxP3$^+$ iTreg, appears to be lower for human than murine lymphocytes, with many accounts of the resulting human FoxP3$^+$ lymphocytes lacking any suppressive ability, unlike their mouse counterparts (Tran *et al.*, 2007). A more recent study by Lu *et al.* (2010) noted that the level of TGF-β induced FoxP3 expressing cells fell following the removal of TGF-β from cultures, and suggested TGF-β alone may not be sufficient to induce a stable human Treg phenotype. They concluded that the previously observed inability of these cells to suppress CD4$^+$ cells in culture may be because these cells represent partially differentiated Treg that have not yet acquired their full immunosuppressive phenotype (Lu *et al.*, 2010a).

#### 3.1.1.2 *Other cytokines involved in Treg induction*

In addition to TGF-β, both IL10 and IL35 have been associated with immune suppression and Treg induction in humans (Wei *et al.*, 2017). IL10 is an anti-inflammatory cytokine, thought to be involved in the immune dysfunction seen in some cancers (Mannino *et al.*, 2015). Although the suppressive ability of IL10 has been well established (Section 1.3.1), its role in cancer is yet to be fully defined.

As previously discussed, IL10 has been shown to drive the induction of a subset of iTreg, termed Tr1 cells (Section 1.3.1). Whilst in nTreg and some iTreg populations FoxP3 is the master regulator essential for driving their differentiation to functionally suppressive cells, Tr1 cells function independently of FoxP3 (Passerini *et al.*, 2011). This group observed that suppressive Tr1 cells can be generated from the CD4$^+$ naïve T cells of IPEX patients with mutated *FOXP3*, including a *FOXP3*$^{null}$ patient. Although, Tr1 cells are described as having a CD4$^+$FoxP3$^{-/low}$ phenotype (Vieira *et al.*, 2004; Levings *et al.*, 2005), as with other T cell populations, they transiently upregulate FoxP3 following TCR activation (Vieira *et al.*, 2004). Bergmann *et al.* described Tr1 cells generated and expanded from CD4$^+$CD25$^-$ T cells in the presence of IL10, IL15 and IL2 in an *in vitro* system modelling the HNSCC environment. As is the case with TGF-β induction, Tr1 induction with IL10 requires that the T cells are first activated, however unlike other T cells and Treg subsets, this distinct cell type lacks CD25 expression after TCR stimulation (Bergmann *et al.*, 2007). Characteristically Tr1 cells secrete high levels of IL10, and it is primarily this mechanism they utilise for suppression (Haringer *et al.*, 2009).

Another cytokine involved in immunosuppression is IL35, a member of the IL12 family of cytokines. This cytokine family consists of four heterodimeric compounds made up from combinations of five different subunits (Vignali & Kuchroo, 2012). In the case of IL35 these sub units are p35 and Epstein-Barr virus-induced gene 3 (EBI3). In the murine lymphocyte populations, IL35 is primarily produced by Treg (Collison *et al.*, 2010) and as well as having a direct role in the suppression of T effectors, IL35 can also induce Treg via a mechanism of infectious tolerance. Treg induction by IL35 generates potent suppressors, whose mechanism of action is primarily by IL35 secretion that is independent of IL10 and TGF-β (Collison *et al.*, 2010). Human Treg, however, appear not to release IL35, and of the T lymphocyte pool, at least *in vitro*, its secretion seems to be limited to activated T cells (Bardel *et al.*, 2008). High levels of EBI3 and p35 co-expression have been observed in the TME by IHC however, which may contribute toward immune evasion (Zeng *et al.*, 2013; Huang *et al.*, 2017). Colorectal tumour cells have been found to release high levels of IL35 and a positive correlation was observed between levels of IL35 in CRC patient serum and the number of peripheral Treg, suggesting it may be implicated in Treg induction and/or recruitment in the TME (Zeng *et al.*, 2013). IL35 has also been shown to be released at high levels in laryngeal SCC tumours and is present at high levels in patient peripheral blood (Wu *et al.*, 2017). However, its role in human Treg induction remains unclear.

### 3.1.2 **CD39, CD73 and CD26 expression on Treg**

Although, most studies in the past have concentrated on $CD4^+(CD25^{+/hi})FoxP3^+$ Treg, other phenotypes are increasingly being used to define this elusive cell type. For example, the expression of the ectonucleotidase CD39 on $CD4^+$ lymphocytes largely correspond to the $CD4^+CD25^{hi}FoxP3^+$ population observed *in vivo* (Mandapathil *et al.*, 2009). One advantage of the CD39 marker is that its detection does not require cell permeabilisation, so cells can subsequently be used for functional studies. $CD4^+CD25^+CD39^+$ Treg are significantly higher in the PBMC of HNSCC patients (5±3%; mean ±SD) compared with healthy controls (2±1.9%) and further enriched in the HNSCC microenvironment (13±3%; Schuler *et al.*, 2012). CD39 expression has also been observed on iTreg, including *in vitro* induced Tr1 cells (Schuler *et al.*, 2014).

The dual expression of CD39 and CD73 has been observed on the surface of murine $FoxP3^+$ Treg (Deaglio *et al.*, 2007). Although CD73 surface expression was found to be absent on human $FoxP3^+$ Treg (Schuler *et al.*, 2012; Xu *et al.*, 2013), it has been reported to be present

internally in a high proportion of $CD4^+CD39^+$ Treg (Mandapathil *et al.*, 2010a). Furthermore, it has been demonstrated that *in vitro* generated iTreg transiently express surface CD73, which is readily shed following induction (Mandapathil *et al.*, 2010b; Xu *et al.*, 2013).

The absence of CD26 is another characteristic of Treg (Salgado *et al.*, 2012). CD26 is a receptor that binds adenosine deaminase (ADA), which mediates the break-down of immunosuppressive adenosine to inosine (Gorrell *et al.*, 2001). The anchoring of ADA to the surface of T cells, reduces local concentrations of adenosine and thus protects against its immunosuppressive effects (Dong *et al.*, 1996). Most (>80%) T effectors express high levels of CD26, however it is only expressed on a small percentage of Treg, on which expression is much lower (39.4% of $CD4^+FoxP3^+$ Treg and ~15% of $CD4^+CD39^+$ Treg; Mandapathil *et al.*, 2012; Salgado *et al.*, 2012).

The difficulty with the study of Treg is the fact that none of these markers are exclusive to Treg and can be found on one or more other T cell populations. However, when used in combination they are useful for the identification of Treg and may shed light on the different Treg subsets present, their mechanism of action and the factors driving their accumulation.

### 3.1.3 Chapter aims and experimental design

A comparison of the expression of various Treg markers in the paired PBMC and TIL samples collected from eight HNSCC patients was carried out to confirm observation from previous studies. To measure any differences in the proportion of Treg, multicolour flow cytometry was employed. Cells were labelled with either CD25, CD39 and CD73 antibodies or CD25, CD26 and FoxP3 antibodies. These particular antibody panels were chosen, due to the dual CD39 expression and transient CD73 surface expression specific to iTreg, and the lack of CD25 expression that has been noted to be characteristic of Tr1 cells. Given that FoxP3 is still the most widely used marker to define Treg and that $CD25^{hi}FoxP3^+$ lymphocytes are widely accepted as nTreg markers their expression was assessed together, in conjunction with CD26, a negative Treg marker, with expression patterns reciprocal to those of CD39. In subsequent experiments flow cytometry on labelled PBMC and TIL from HNSCC patients was carried out to assess the differences in dual FoxP3 and CD39 expression on T helper cells, using antibodies, for CD4, CD25, FoxP3 and CD39.

A number of cytokines have been implicated in Treg induction. To investigate whether HNSCC tumour cells and the associated stroma release cytokines that may be involved in iTreg induction, ELISAs were carried out on conditioned medium (CM) collected from the culture of dispersed tumour samples, HNSCC cell lines and tumour-derived fibroblasts to quantify the presence of TGF-β and IL10.

Although there are many studies that have highlighted the importance of particular cytokines in the process of iTreg induction *in vitro*, these models do not fully recapitulate the plethora of factors found in the TME. In order to determine whether the array of soluble factors released by HNSCC tumour and stromal cells, were able to influence the induction of iTreg cells, $CD4^{+}CD25^{-}$ cells were sorted from PBMC isolated from leucocyte cones of healthy donors and cultured in CM collected from the culture of dispersed tumour samples, HNSCC cell lines and tumour-derived fibroblasts. The cultured cells were then stained with the two panels of antibodies described above. Healthy control PBMC were used for these experiments, as these cells have not had any previous exposure to cancer cells. Thus avoiding any influences that may already have been induced by the tumour if patient PBMC were used.

Given the increase in Treg in the HNSCC TIL and observations from previous studies, it was hypothesised that soluble factors released from HNSCC and associated stromal cells can cause the induction of Treg from $CD4^{+}CD25^{-}$ T cells.

## 3.2 Methods

### 3.2.1 Flow cytometry to identify Treg in PBMC and TIL

Flow cytometry was carried out on a FACS Aria II using FACSDiva software, following the set up procedure described previously (Section 2.3).

#### 3.2.1.1 *Antibodies used to identify Treg cells*

A panel of antibodies (Table 3.1; BD Biosciences) specific for markers which identify Treg cells was used to label PBMC (Section 2.2.1) and TIL (Section 2.2.4) from HNSCC patients, as well as sorted $CD4^{+}CD25^{-}$ T cells from healthy donors incubated with TGF-β, CM, or complete growth media (GM) and prior to incubation (Section 3.2.4 and 3.2.5).

**Table 3.1*: Antibodies used for the identification of Treg***

| Antibody | Clone | Working concentration |
|---|---|---|
| PerCP Mouse anti-Human CD4 | SK3 | 0.15 µg/ml |
| APC Mouse anti-Human CD25 | M-A251 | 0.15 µg/ml |
| PE Mouse anti-Human CD26 | M-A261 | 0.625 µg/ml |
| Brilliant Violet 421 Mouse anti-Human CD39 | TU66 | 0.625 µg/ml |
| FITC Mouse anti-Human CD39 | TU66 | 0.625 µg/ml |
| PE Mouse anti-Human CD73 | AD2 | 0.3125 µg/ml |
| AlexaFluor488 Mouse anti-Human FoxP3 | 259D/C3 | 2.5 µg/ml |

#### 3.2.1.2 *Measurement of Treg in PBMC and TIL from HNSCC patients*

In order to assess differences in the proportion of Treg in the periphery compared with the TME of HNSCC patients, PBMC from the venous blood and TIL from tumour biopsies collected from the same patients were isolated (sections 2.2.1 and 2.2.4; Table 3.2) and labelled (section 2.3.1) immediately with antibodies for CD4, CD25, CD39 and CD73 or CD4, CD25, CD26 and FoxP3 (Table 3.1). Lymphocytes were gated according to their characteristic side and forward scatter (P1: Figure 3.1a) and 10 000 events were recorded in this gate. Isotype controls were used at the same concentration as antibodies in order to set gates for Treg markers and $CD25^{hi}$ lymphocytes were defined as cells that exceed the level of CD25 expression on the $CD4^{-}$ population (Figure 3.1b).

**Table 3.2: Origin and tumour stage of patient tumour (TR) samples from which TIL and matched PBMC were isolated**

| | HNSCC subsite | Age | Gender | Tumour Origin | TNM Stage |
|---|---|---|---|---|---|
| Primary tumour | Larynx | - | Male | Larynx | T3/4N0 |
| | | 56 | Male | Epiglottis | T4N2 |
| | Oral cavity/ Oropharynx | - | Male | Right lateral tongue | T2N0 |
| | | 51 | Male | Right tonsil | T2N0 |
| | | 56 | Female | Right tonsil | T2N0 |
| Node | | 53 | Male | Unknown primary | T0N2 |
| | | 79 | Male | Unknown primary | T0N3 |
| | | 66 | Male | Left tonsil | T1N2b |
| | | 56 | Male | Epiglottis | T4N2 |

*a and b represent two tumour biopsies taken from the same patient

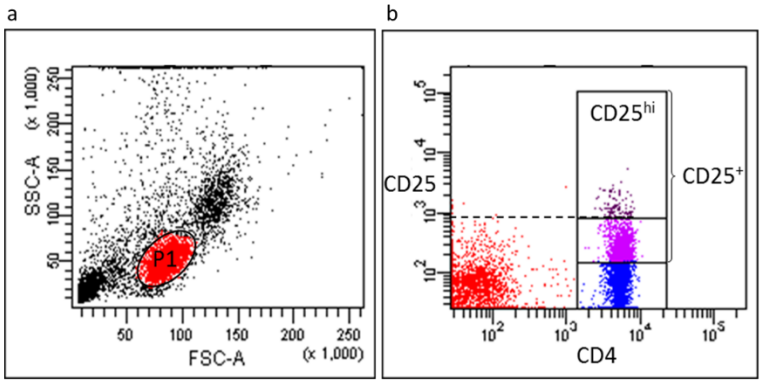


**Figure 3.1: Forward (FSC) and side scatter (SSC) plot of HNSCC patient PBMC (a) and the $CD25^{hi}$ gating strategy (b)**

From the lymphocyte gate (P1; red), a scatter plot of CD25 and CD4 expression was produced. The $CD4^+CD25^+$ gate (pink and dark purple) was set based on corresponding isotype controls and high CD25 expression (dark purple) was defined as the level of $CD4^-$ cells.

In order to determine whether differences in $CD39^+$ expression was limited to the $FoxP3^-$ or $FoxP3^+$ cell fraction in patient PBMC and TIL, venous blood of HNSCC patients and TIL from tumour biopsies were labelled with fluorescent conjugated antibodies for CD4, CD25, CD39 and FoxP3 (Table 3.3) and CD39 and FoxP3 expression was determined on the $CD4^+$ lymphocytes and the $CD4^+CD25^+$ lymphocytes.

**Table 3.3: Origin and tumour stage of patient tumour (TR) samples from which TIL and matched PBMC were isolated for analysing dual FoxP3/CD39 expression**

| | HNSCC subsite | Age | Gender | Tumour Origin | TNM Stage |
|---|---|---|---|---|---|
| Primary tumour | Larynx | 73 | Male | Larynx | T4N2b |
| | | 64 | Male | Larynx | T4N0 |
| | Oral cavity/ Oropharynx | 59 | Male | Left lateral tongue | T1N0 |
| | | 71 | Female | Left lateral tongue | T1N0 |
| | | 56 | Male | Left tonsil | T2N0 |
| | | 51 | Male | Right tonsil | T2N0 |
| | | - | - | Anterior maxilla | T4N0 |
| | | 67 | Female | Right mandible | T4N0 |
| | | 43 | Male | Left posterolateral tongue | T4aN1 |
| Node | | 53 | Male | Unknown | T0N2a |

### 3.2.2 Quantification of TGF-β and IL10 in the conditioned medium from HNSCC cell lines, tumour-derived primary fibroblasts and dissociated tumour tissue

Duoset® ELISA for TGF-β and IL10 were carried out (Section 2.4) on the CM collected from HNSCC cell lines cultured for 1, 2 and 3 days (Section 2.1.6), from the overnight culture of patient dissociated tumour tissue (Section 2.2.4; Table 3.4) and from tumour-derived fibroblasts following 3 days of culture (Section 2.2.5, Table 3.5). Due to the presence of some clumps of cells following tissue dissociation, individual cells were unable to be counted, so concentrations of cytokines in dispersed tumour tissue were standardised by tumour weight to give a value of TGF-β or IL10 released per 100 mg of the initial tissue.

As TGF- β is secreted in a latent form, for the detection of total TGF-β samples were activated to their immunoreactive form by the addition of acid (Section 2.4), before protein concentration was measured by ELISA. All samples were tested both after activation and without activation, in order to establish whether any active TGF-β was already present in the CM.

**Table 3.4: Origin and tumour stage of patient tumour (TR) samples used for the collection of overnight conditioned medium.**

| ID | Origin | Tumour Stage | Nodal status | N |
|---|---|---|---|---|
| L4 | Larynx | T3 | N2c | 1 |
| L5-11 | Larynx | T4 | N0 | 7 |
| L13 | Larynx | T4 | N1 | 1 |
| O3 | Oropharynx | T2 | N0 | 1 |
| O4 | Oropharynx | NA | NA | 1 |
| H1 | Hypopharynx | T3 | N0 | 1 |
| H2 | Hypopharynx | T4 | N2b | 1 |
| N2 | Node (Laryngeal primary) | T3 | N2c | 1 |
| N3 | Node (Hypopharyngeal primary) | T4 | N2b | 1 |
| N4 | Node (unknown primary) | T0 | N2a | 1 |
| N5,6 | Node (unknown primary) | NA | NA | 2 |

**Table 3.5: Origin and tumour stage of patient tumour (TR) samples from which fibroblasts were derived for the collection of conditioned medium**

| ID | Origin | Tumour Stage | Nodal Status | N |
|---|---|---|---|---|
| L1,L2 | Larynx | T4 | N0 | 2 |
| L3 | Larynx | T4 | N1 | 1 |
| O1 | Oropharynx | T2 | N2c | 1 |
| O2 | Oral cavity | T3 | N3 | 1 |
| N1 | Node (unknown primary) | T0 | - | 1 |

* - clinical information unavailable

### 3.2.3 Sorting $CD4^+CD25^-$ T cells from PBMC

Healthy PBMC from leucocyte cones were labelled with antibodies for CD4 and CD25 (0.3 µg/ml and 0.12 µg/ml respectively; BD Biosciences) ready for sorting (Section 2.3.5). Lymphocytes were gated based on their forward and side scatter characteristics, and doublets were excluded prior to gating on $CD4^+$ and $CD25^-$ lymphocytes for selection (Figure 2.11).

### 3.2.4 Addition of TGF-β to $CD4^+CD25^-$ lymphocytes to induce Treg

To establish a positive control for iTreg induction and the corresponding changes in expression of cell markers, sorted $CD4^+CD25^-$ lymphocytes from healthy individuals (Section 2.2.2) were seeded at 8 x $10^4$ cells/well in lymphocyte growth medium (X-Vivo 20 medium; containing final concentrations of 10% human AB serum and 0.1 U/ml penicillin and 0.1 mg/ml streptomycin) in to 96 well round bottom plates. Lymphocytes were stimulated with CD3/CD28 DynaBeads (Gibco) at a ratio of 1:1 (cell:beads), and incubated at 37$^o$C in a 5% $CO_2$ humidified atmosphere in the presence of IL2 (100 U/ml; AbD Serotec) with or without TGF-β (5 ng/ml; AbD Serotec). For each treatment, replicates were set up in at least 8 wells to ensure the required number of cells could be collected for analysis following incubation. The cells were incubated for five days, in line with previous studies that observed this to be a sufficient length of time for cells to adopt a Treg phenotype (Tran *et al.*, 2007; Lu *et al.*, 2010a; Schuler *et al.*, 2012), including CD39 upregulation (Schuler *et al.*, 2012). After 5 days, cells from replicate wells were collected together and separated from CD3/CD28 DynaBeads using a magnet (Section 2.2.3.1), before being labelled with antibodies for flow cytometry (Section 3.2.8).

### 3.2.5 Culture of sorted $CD4^+CD25^-$ lymphocytes in conditioned medium

In order to determine the effect of tumour cell-derived CM on the expression of Treg markers, sorted $CD4^+CD25^-$ lymphocytes from healthy individuals (Section 2.2.2 and 3.2.4) were cultured in lymphocyte growth medium (LGM) or a combination of CM, collected from HNSCC cell lines, tumour-derived fibroblasts or overnight culture of primary HNSCC tumours, and LGM at a ratio of 1:2. (Sections 2.1.6, 2.2.4 and 2.2.5), all supplemented with CD3/CD28 DynaBeads and IL2 (Section 3.2.4). A minimum of eight replicates wells were set up for each treatment.

In addition, in order to determine whether the different growth medium affected the expression of the surface markers of the number of viable cells $CD4^+CD25^-$ cells were cultured in neat LGM, cell line (Section 2.1.1) or fibroblast growth medium (Section 2.2.5), or cell line or fibroblast growth medium diluted at a ratio of 1:2 in LGM. All cells were again cultured with IL2 and CD3/CD28 DynaBeads as previously described.

Following a 5 day incubation, cells from replicate wells were collected together and separated from DynaBeads using a magnet (Section 2.2.3.1), before being labelled with antibodies for flow cytometry (Section 3.2.6).

### 3.2.6 Measurement of Treg induction by flow cytometry

Sorted $CD4^+CD25^-$ lymphocytes, incubated with TGF-β, CM or LGM (Sections 3.2.4 and 3.2.5), were pelleted by centrifugation at 400 x *g* for 5 minutes. The cells were then labelled with antibodies for CD25, CD39 and CD73 or CD25, CD26 and FoxP3 (Table 3.2 and Section 2.3.1). An additional tube of cells was labelled with propidium iodide (1 µg/ml; Sigma) to measure the percentage of dead cells in the cultures. The viable lymphocyte population was gated based on characteristic forward and side scatter (Figure 3.2). All further analysis of marker expression was carried out on the lymphocyte population with all gates set against the corresponding isotype controls (Section 2.3.3 and Figure 2.5).

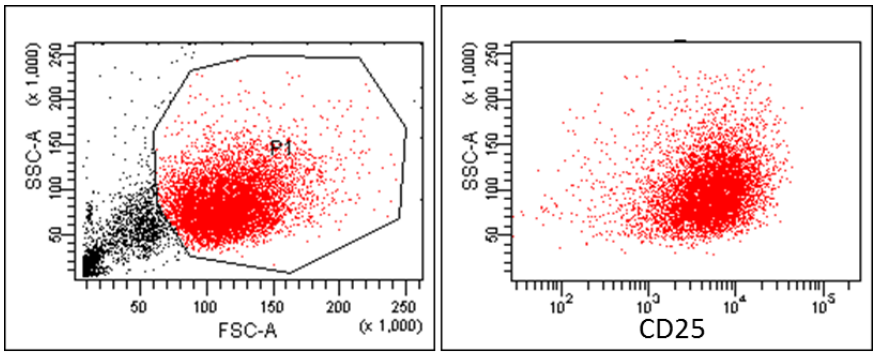


**Figure 3.2: Viable lymphocyte gate (P1) and the corresponding CD25 expression within the lymphocyte gate**

### 3.2.7 Statistical Analysis

For comparisons between marker expression on lymphocytes in HNSCC patient PBMC and the corresponding TIL, Shapiro-Wilks tests were first carried out in order to determine whether the data followed a normal distribution. Datasets that were normally distributed were analysed using independent T tests and for those that did not follow a normal distribution Mann Whitney U tests were performed.

Independent T tests were carried out using SPSS 24 (IBM) in order to compare the expression of Treg markers on cells cultured with TGF-β to those cultured in LGM alone. For comparing $CD4^+CD25^-$ lymphocytes cultured with various CM to those cultured in

LGM alone and for comparing $CD4^+CD25^-$ lymphocytes cultured with different types of growth medium one-way ANOVA with Tukey post-hoc analysis was performed to determine any significant differences. Statistically significant differences are those where *$p$<0.05, **$p$<0.01 and ***$p$<0.001. All error bars show SEM, unless otherwise stated.

## 3.3 Results

### 3.3.1 Treg marker expression on the PBMC and TIL from HNSCC patients

To confirm Treg enrichment in the TME of HNSCC patients, PBMC and TIL were collected from patients and labelled with antibodies for CD4, CD25 and Treg markers (FoxP3, CD39, CD73 and absence of CD26; Figure B.1, Appendix B). Of the $CD4^+$ lymphocytes, a significantly greater percentage expressed CD39 and high levels of CD25 on the HNSCC TIL (30.3±4.1%, $p$=0.001 and 13.0±2.8%, $p$=0.012, respectively) than on PBMC (11.0±2.0% and 5.1±0.8%, respectively) from the same patients (Figure 3.3a). Conversely, $CD26^+$ cells were reduced in the $CD4^+$ lymphocyte pool on the TIL (60.8±8.9%) compared to PBMC (83.0±4.8%, $p$=0.021). No difference was observed between the percentage of $CD4^+$ lymphocytes expressing CD25, CD73 or FoxP3 from patient PBMC compared with TIL.

Within the $CD4^+CD25^+$ lymphocyte gate, there was a greater percentage of cells expressing high levels of CD25 and CD39 compared with on the total $CD4^+$ lymphocytes; similarly the differences in $CD25^{hi}$ and CD39 expression on TIL *vs*. PBMC were more pronounced (Figure 3.3). The percentage of cells that were $CD25^{hi}$ was triple on the TIL (38.6±4.2) compared with the PBMC (11.6±1.8%, $p$<0.001), and the percentage of cells expressing CD39 was more than four times as high on TIL (51.0±6.1%) than PBMC (12.0±2.7%, $p$<0.001; Figure 3.3b). In addition, the percentage of cells expressing FoxP3 was more than double in $CD4^+CD25^+$ lymphocytes from TIL (50.1±6.7%) than in those from PBMC (20.5±5.3%, $p$= 0.013; Figure 3.3b). CD73 expression did not differ between $CD4^+CD25^+$ isolated PBMC or TIL, while significantly fewer cells were $CD26^+$ in TIL (62.8±7.7%) compared with PBMC (89.7±3.1%, $p$=0.002).

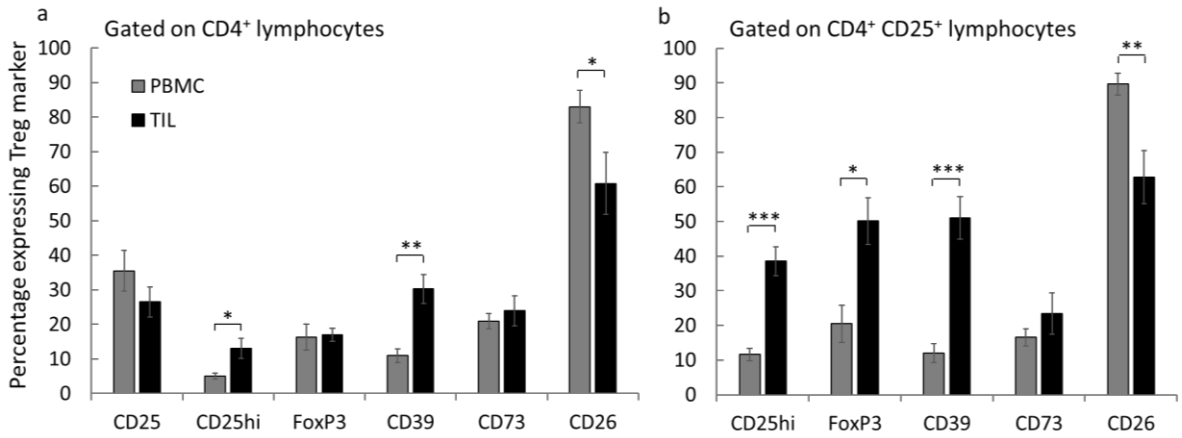


**Figure 3.3: Mean percentage of lymphocytes expressing Treg markers in PBMC and TIL collected from HNSCC patients**

PBMC (n=8) and TIL (n=9) were isolated from whole blood and tumour biopsies collected from eight HNSCC patients and stained for CD4, CD25, FoxP3, CD39 and CD73 (NB. Biopsies from both a primary tumour and metastatic node were collected from one of the 8 patients). Bars represent mean percentage ±SEM of the $CD4^+$ lymphocytes expressing CD25, high levels of CD25, FoxP3, CD39, CD73, and CD26 (a) and $CD4^+CD25^+$ lymphocytes expressing high levels of CD25, FoxP3, CD39 CD73, and CD26 (b). Statistical analysis was carried out using independent T tests to compare CD25, $CD25^{hi}$, FoxP3, CD39 and CD73 expression and Mann Whitney U tests for CD26 expression. Significant results (*) are considered as those where *$p$<0.05, **$p$<0.01 and ***$p$<0.001.

There was no difference observed in the expression of Treg markers on $CD4^+$ lymphocytes from the five primary tumours compared with the four tumour nodes from which TIL were isolated (Figure 3.4). Only FoxP3 was significantly higher on the $CD4^+CD25^+$ cells obtained from the primary tumours (64.3±8.6%) than on those obtained from tumour nodes (35.0±6.5%, $p$=0.014), (Figure 3.4b).

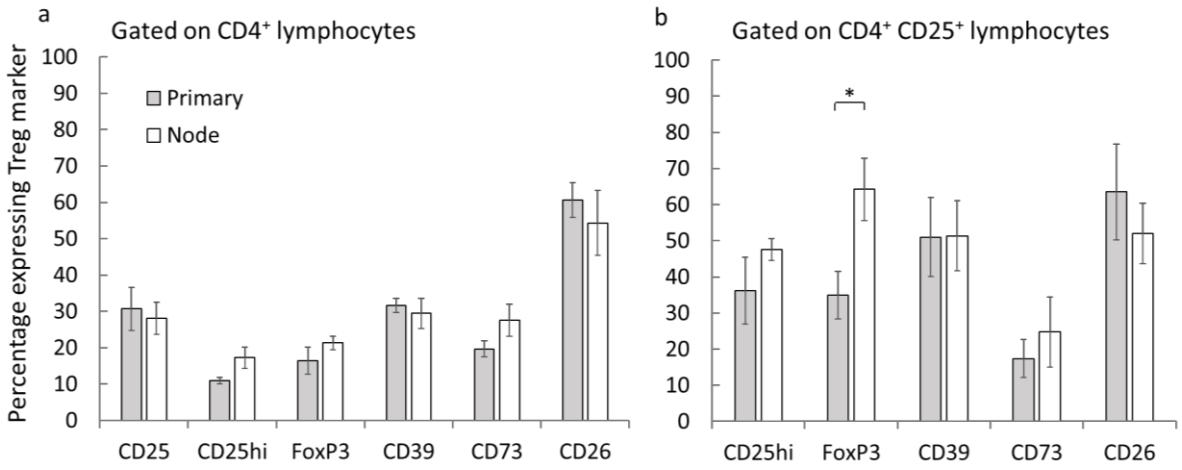


**Figure 3.4: Mean percentage of lymphocytes expressing Treg markers in TIL collected from primary HNSCC tumours and metastatic nodes**

TIL were isolated from tumour biopsies collected from HNSCC patient primary tumours (n=5) and tumour node (n=4) and stained for CD4, CD25, FoxP3, CD39 and CD73. Bars represent mean percentage ±SEM of $CD4^+$ lymphocytes expressing CD25, high levels of CD25, FoxP3, CD39, CD73, and CD26 (a) and $CD4^+CD25^+$ lymphocytes expressing high levels of CD25, FoxP3, CD39 CD73, and CD26 (b). Statistical analysis was carried out using independent T tests to compare CD25, CD25hi, FoxP3, CD39 and CD73 expression and Mann Whitney U tests for CD26 expression. Significant results (*) are considered as those where $p<0.05$.

The previous data has been expressed on the same graph in order to compare the expression of Treg markers on the $CD4^+CD25^+$ lymphocytes collected from PBMC versus primary tumour/metastatic node (Figure 3.5). A greater percentage of $CD4^+CD25^+$ lymphocytes were $CD25^{hi}$, $CD39^+$ and $CD26^-$ on the lymphocytes collected from TIL compared to those from PBMC, this was true regardless of whether the TIL were derived from primary tumour samples or tumour nodes (Figure 3.5). Although FoxP3 was expressed on more $CD4^+CD25^+$ lymphocytes on PBMC than TIL (from combined primary tumour and metastatic node; Figure 3.3b), only the TIL collected from the tumour nodes was observed to have a significantly greater percentage of $FoxP3^+$ cells than patient PBMC ($p=0.017$; Figure 3.5).

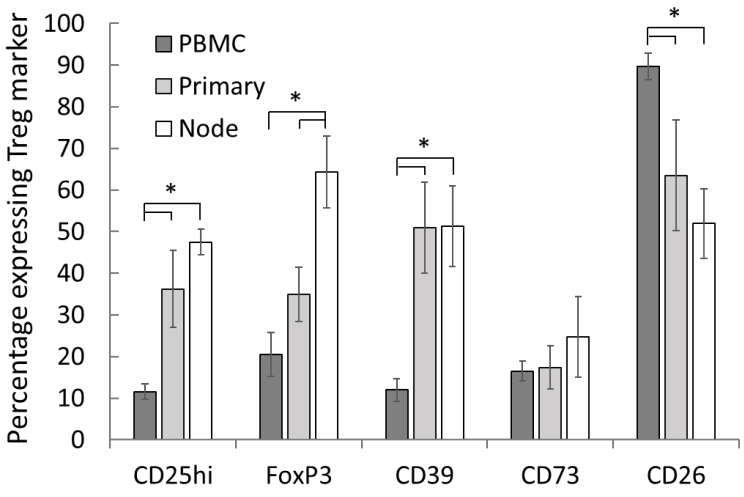


**Figure 3.5: Mean percentage of lymphocytes expressing Treg markers in PBMC and TIL collected from primary HNSCC tumours and meastatic nodes**
PBMC (n=8) and TIL were isolated from whole blood and tumour biopsies collected from HNSCC patient primary tumours (n=5) and tumour node (n=4) and stained for CD4, CD25, FoxP3, CD39 and CD73. Bars represent mean percentage ±SEM of the $CD4^+CD25^+$ lymphocytes expressing high levels of CD25, FoxP3, CD39 CD73, and CD26 (b). Statistical analysis was carried out using a one-way ANOVA. Significant results (*) are considered as those where $p<0.05$.

### 3.3.2 FoxP3 expression on $CD4^+CD39^+$ expressing T lymphocyte populations of HNSCC patient PBMC and TIL

Dual CD39/FoxP3 expression was measured on $CD4^+$ and $CD4^+CD25^+$ lymphocytes from the TIL and PBMC of ten HNSCC patients (Figure 3.6a and b). The percentage of both $CD39^+FoxP3^+$ and $CD39^+FoxP3^-$ in the $CD4^+$ Th cell population was significantly greater in patient TIL than in PBMC (18.8±0.4% of TIL compared to 3.8±0.4% of PBMC were $FoxP3^+CD39^+$, $p<0.001$. and 27.5±9.6% compared to 6.7±0.5% were $CD39^+FoxP3^-$, $p=0.001$; Figure 3.6c and d). As was the case with CD39 alone (Section 3.3.1), the increased percentage of $CD39^+FoxP3^+$ cells in the TIL was more marked on the $CD4^+CD25^+$ T cells, than on the whole $CD4^+$ population (40.1±5.6% on $CD4^+CD25^+$ TIL compared with 8.9±0.9% on PBMC, $p<0.001$; Figure 3.6c). The proportion of $CD39^+FoxP3^-$ cells was similar in the $CD4^+CD25^+$ population as on the whole $CD4^+$ population ($p<0.001$; Figure 3.6d). In contrast, no difference was observed in the percentage of $CD39^-FoxP3^+$ cells between PBMC and TIL (Figure 3.6e) and the percentage of double negative $CD39^-FoxP3^-$ cells was significantly lower in the TIL compared with the PBMC (Figure 3.6f).

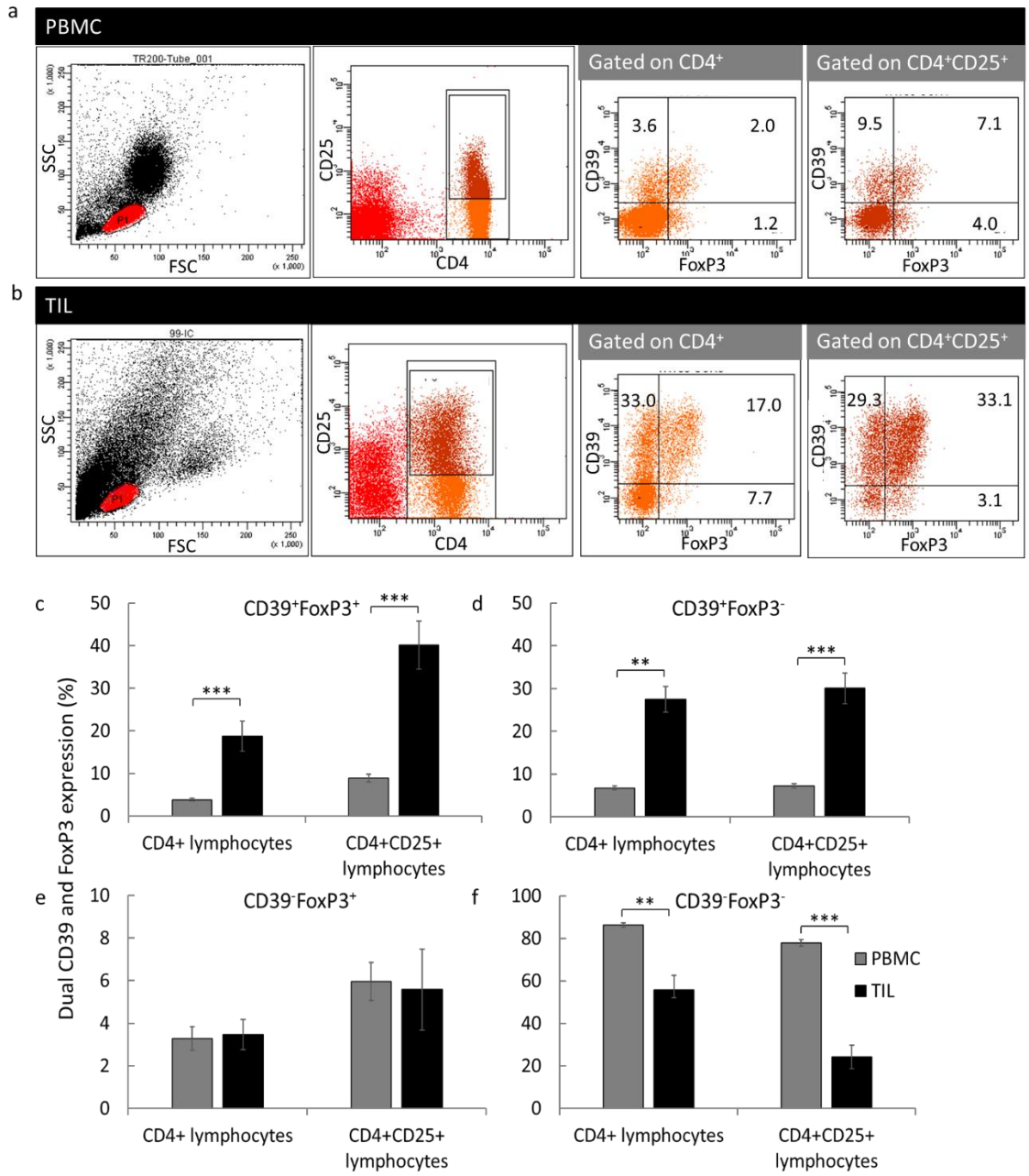


**Figure 3.6: Dual CD39 and FoxP3 expression on CD4+ and CD4+CD25+ lymphocytes of HNSCC patient PBMC and TIL**

PBMC and TIL from 10 HNSCC patients were stained for CD4, CD25, CD39 and FoxP3, gates were set on the $CD4^+$ lymphocyte population (orange) and the $CD4^+CD25^+$ lymphocyte population (brown; a and b) and the percentage of $CD39^+FoxP3^+$ (c), $CD39^+FoxP3^-$ (d), $CD39^-FoxP3^+$ (e) and $CD39^-FoxP3^-$ (f) was determined on cells within the $CD4^+$ and $CD4^+CD25^+$ lymphocyte gates. Bars represent mean percentage of cells ±SEM. Statistical analysis was carried out using independent T tests.

### 3.3.3 TGF-β and IL10 in HNSCC-derived conditioned medium

CM collected from HNSCC cell lines (Table 2.1), HNSCC tumour derived fibroblasts and dispersed tumour biopsies (Table 3.1) were analysed for the presence of TGF-β and IL10

using Duoset® ELISAs and ELISA MAX™, respectively (Section 2.6). CM from seven cell lines (three laryngeal and four oral/oropharyngeal) and five tumour-derived fibroblasts were collected following one, two and three days in culture. For all seven of the cell lines an increase in the concentration of TGF-β was observed in the CM from day one to day three of culture (Figure 3.7a). The cell line CM with the highest level of TGF-β was from the UMSCC 12 cell line (derived from a T3 laryngeal tumour), which had a concentration of 4.6±0.3 ng/ml following three days of culture. The two other laryngeal derived cell lines, both from stage four tumours, had secreted just 7% and 15% as much TGF-β as UMSCC 12 after three days (320±75 pg/ml and 700±200 pg/ml, respectively). Of the oropharyngeal cell lines, UMSCC 4 conditioned media contained the highest level of TGF-β following three days of incubation, though the concentration of 1.4±0.3 ng/ml was less than a third of that observed in the CM from UMSCC 12. The CM collected from UMSCC cell line 81b had the overall lowest level of TGF-β (207±63 pg/ml).

Of the five CM collected from tumour-derived fibroblasts four showed an increase over the three-day culture period. The two fibroblasts that released the most TGF-β were derived from a metastatic node of a patient with an unknown primary tumour and an oropharyngeal T2 primary tumour (1.5±0.2 ng/ml from N1 and 1.6±0.2 ng/ml from O1 after three days).

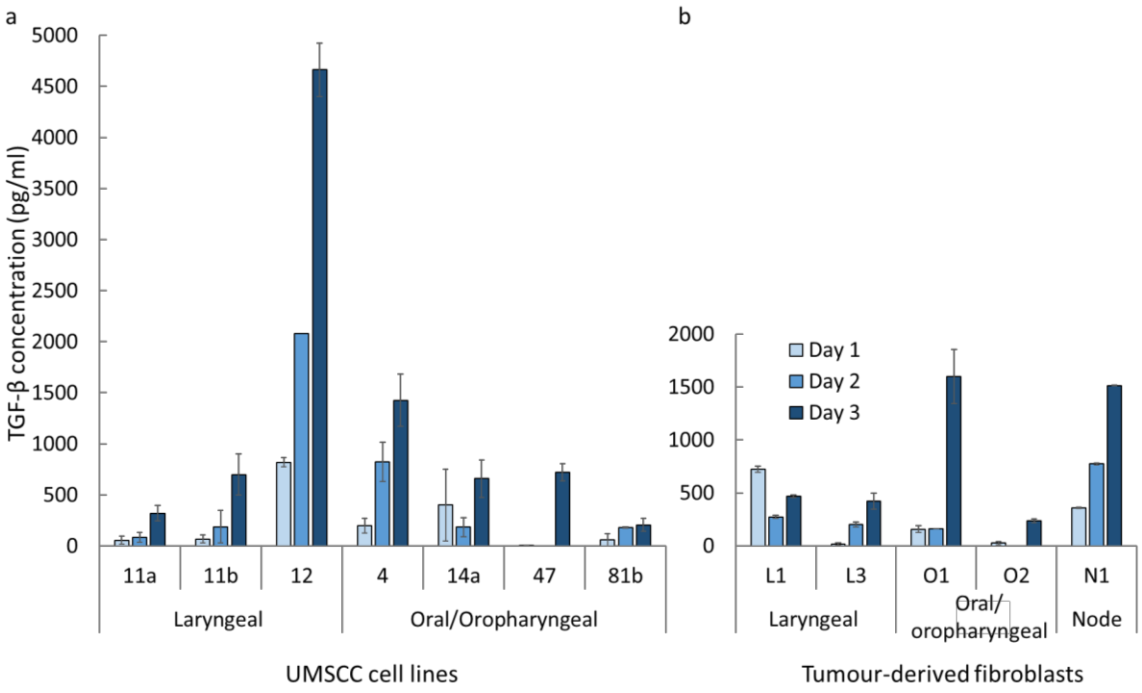


**Figure 3.7: Concentration of TGF-β (pg/ml) in CM collected from HNSCC cell lines and tumour-derived fibroblasts**

Conditioned medium was collected from laryngeal, oral and oropharyngeal cells lines (a) and from two laryngeal and three metastatic node tumour-derived fibroblasts (b) following 1, 2 and 3 days in culture, and TGF-β concentrations were measured by ELISA. Data expressed as means ±SEM from at least two separate ELISA for UMSCC cells, and tumour-derived fibroblasts O1 and N1, and from duplicates taken from one ELISA for tumour-derived fibroblasts L1, L3 and O2.

TGF-β was detected in all nine of the dispersed tumour tissue CM that were tested. The highest concentration of TGF-β was observed in CM derived from a laryngeal primary carcinoma (L5; 565±39 pg/ml), which was approximately twice as much as was observed in CM derived from the malignant node of the same patient (N3; 294±24 pg/ml; Figure 3.8). The CM with the lowest level of TGF-beta was also derived from a primary laryngeal carcinoma (33±4 pg/ml). Similar levels of TGF-β were observed in the CM derived from the primary hypopharyngeal tumour and tumour node of the same patient (H2; 124±4 pg/ml and N2; 101±3 pg/ml, respectively). Overall, there was no significant difference between standardised levels of TGF-β in the CM from the four primary tumours and five tumour nodes (Mann Whitney U).

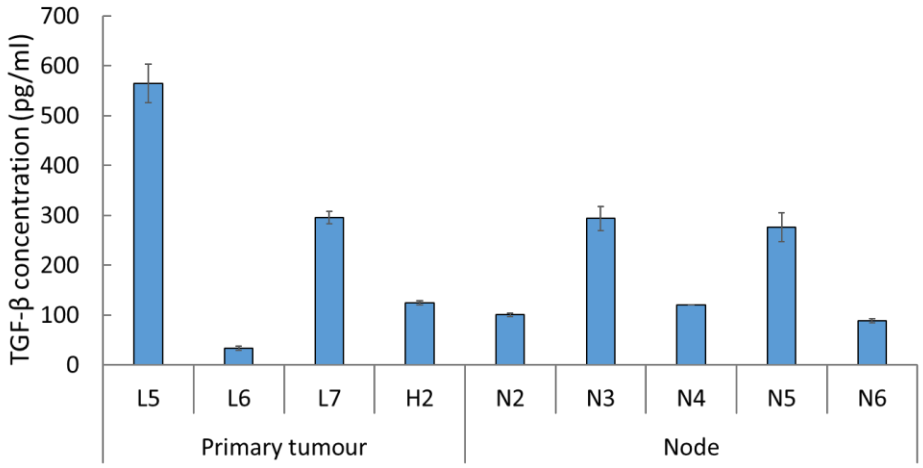


**Figure 3.8 Concentration of TGF-β (pg/ml) per 100 mg tissue in CM collected following the overnight culture of dispersed primary tumour or metastatic node tissue.**
Conditioned medium was collected from one hypopharyngeal (H), three laryngeal (L) primary tumours and metastatic nodes originating from one laryngeal (L), one hypophayngeal (H) or three unknown (U) primary tumours that had been enzymatically dissociated and cultured overnight. TGF-β concentrations were measured by ELISA and results were standardised to represent the concentration (pg/ml) per 100 mg tumour. Data expressed as means ±SEM from two separate experiments on the same CM for L5, L6 primary tumour and N3, N5 metastatic nodes, for all others SEM was taken from duplicates within the same experiment.

There was no IL10 detected in CM from all seven cell lines and four tumour-derived fibroblast cultures by ELISA. However, IL10 was observed in all nine CM collected from dispersed tumour samples (Figure 3.9). The highest concentrations of IL10 was observed in CM derived from two laryngeal primary carcinomas (959.4±150.9 pg/ml and 755.5±0.1 pg/ml). The CM with the lowest level of IL10 was also derived from a primary laryngeal carcinoma (73.5±3.2 pg/ml). Less variation was observed in the level of IL10 in CM derived from the four tumour nodes compared with that in the CM derived from primary tumours, but no significant difference was observed between the two tumour types.

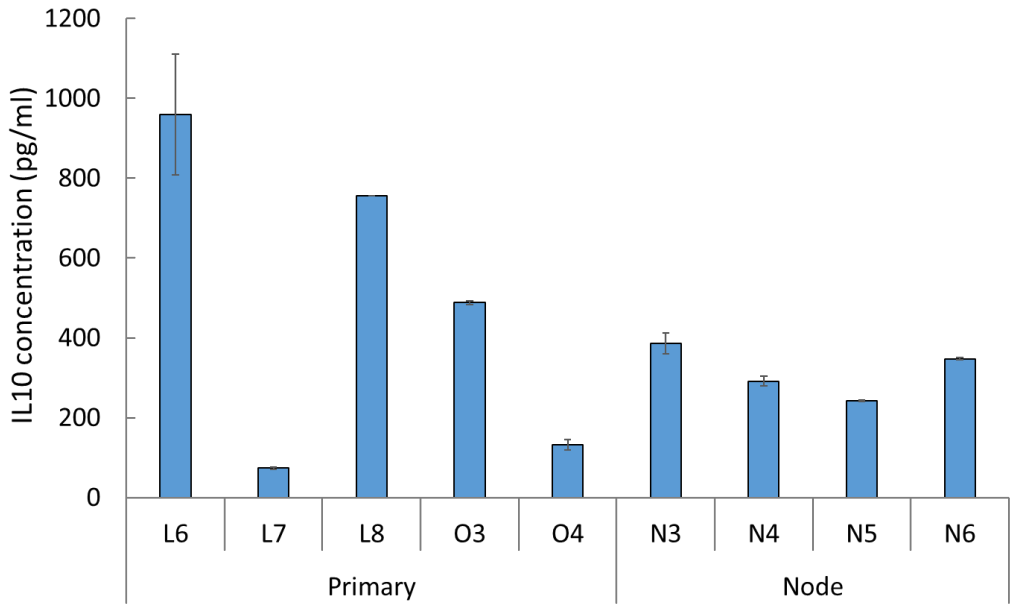


**Figure 3.9 Concentration of IL10 (pg/ml) per 100 mg tissue in CM collected following the overnight culture of dispersed primary tumour (T) or metastatic node (N) tissue**
Conditioned medium was collected from three laryngeal (L), two oropharyngeal (O) primary tumours and metastatic nodes originating from one laryngeal (L) or three unknown (U) primary tumours that had been enzymatically dissociated and cultured overnight. IL10 concentrations were measured by ELISA and results were standardised to represent the concentration (pg/ml) per 100 mg tumour. Data expressed as means ±SEM derived from duplicates of the same experiment.

### 3.3.4 Induction of Treg markers on $CD4^+CD25^-$ lymphocytes by recombinant TGF- β

The addition of TGF-β to $CD4^+CD25^-$ has been shown to induce a Treg phenotype and in some cases a corresponding suppressive function (Section 3.1). Therefore, for a positive control of Treg induction (Section 3.3.5), $CD4^+CD25^-$ cells were sorted from the PBMC of leucocyte cones obtained from healthy donors and cultured in growth medium supplemented with CD3/CD28 DynaBeads and IL2 with or without TGF-β. A combination of positive staining for FoxP3, CD39, CD73 and a lack of CD26 expression was used to identify iTreg following culture. Experiments were repeated a minimum of three times on a total of three leucocyte cones and a mean percentage expression was taken from the three cones.

More than 98% of the viable cell population was $CD25^+$ following culture regardless of whether medium was supplemented with TGF-β or not (Figure 3.10a and b). Of these viable $CD4^+CD25^+$ cells, Treg marker expression was found to be variable between different leucocyte cones both with and without TGF-β, but particularly in those treated with TGF-β, with the proportion of FoxP3 expressing cells ranging between 18.4 and 42.6% compared

with 4.0 and 9.2% in those cultured without TGF-β (n=3). In the proportion of cells expressing the associated Treg marker FoxP3 was higher in the cells cultured with TGF-β than those without, with a mean difference of 20.6% (p=0.046; Figure 3.10c and

Table 3.6). Conversely, the percentage of cells expressing CD26 was significantly lower on cells cultured with TGF-β (61.5±5.6%; p=0.003) than those cultured without (84.5±4.6%; Figure 3.10b). There was no statistically significant difference in the percentage of cells expressing CD39 or CD73 when cells were cultured with or without TGF-β (Figure 3.10 b and c and

Table 3.6). Scatter plots showing the dual expression of FoxP3 and CD26 show a clear shift in expression, with TGF-β increasing the proportion of $FoxP3^{+}CD26^{-}$ cells and decreasing $FoxP3^{-}CD26^{+}$ cells (Figure 3.10b and d).

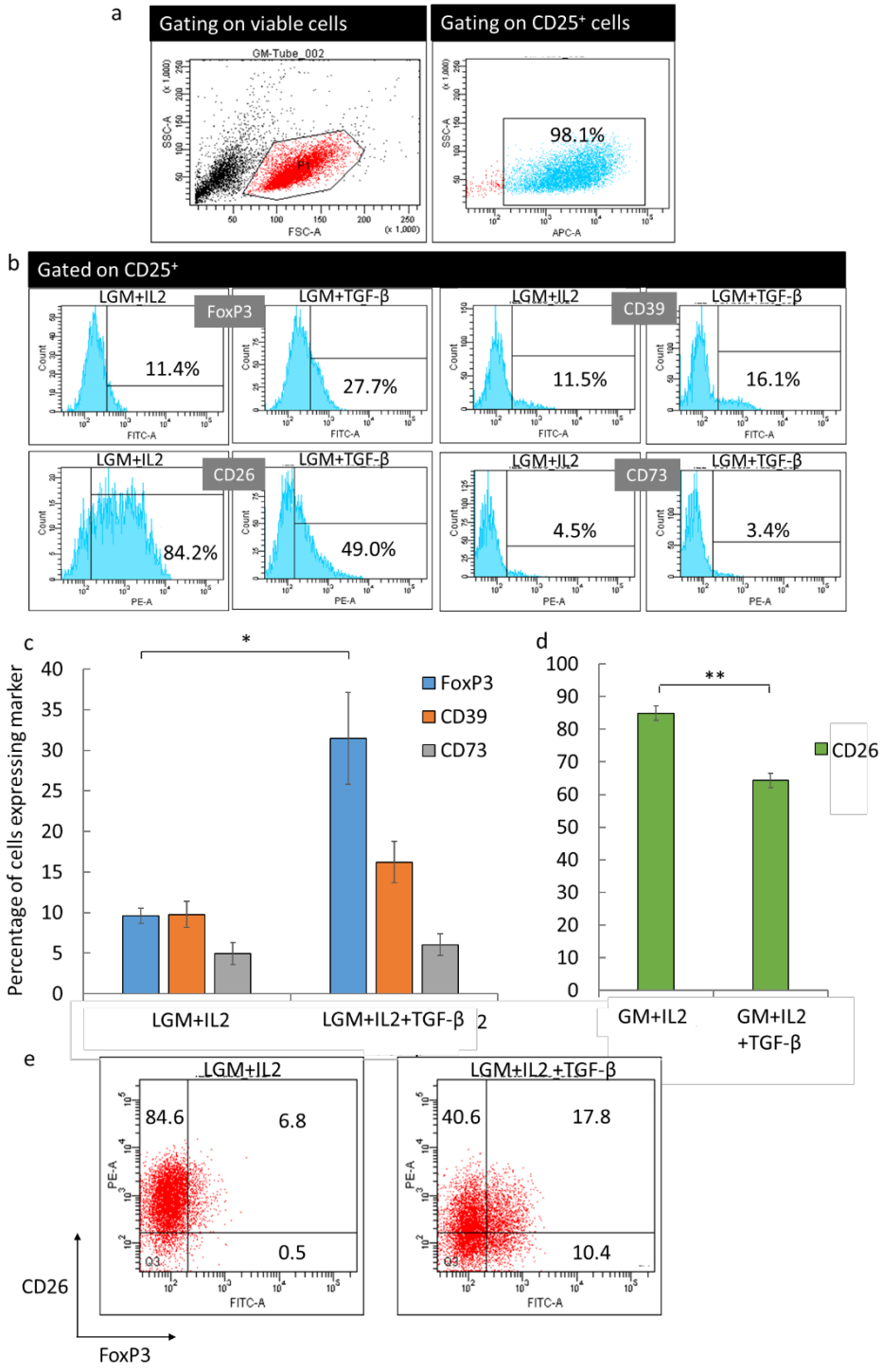


**Figure 3.10: Treg marker expression on CD4+CD25+ lymphocytes cultured with TGF-β**
$CD4^+CD25^-$ lymphocytes sorted from the PBMC of healthy controls (n=3) were cultured for 5 days in medium containing anti-CD3/CD28 DynaBeads and IL2 (100 U/ml), with or without TGF-β (5 ng/ml). Following culture cells were stained for Treg markers for flow cytometry and expression of markers was assessed on the viable $CD25^+$ cells (a). Representative histograms (b) and bar charts of mean (±SEM) percentage of $CD4^+CD25^+$ cells expressing Treg markers (c; FoxP3, CD39 and CD73) and the negative marker CD26 (d). Statistically significant differences (*$p$<0.05) between marker expression were determined using independent T tests. Scatter plots (e) show the difference in the dual expression of FoxP3 (AlexaFluor-488/FITC) and CD26 (PE) when cultured with or without TGF-β; with the percentages of $CD26^+FoxP3^-$ (upper left), $CD26^+Foxp3^+$ (upper right) and $CD26^-FoxP3^+$ (lower right) cells shown in the corresponding quadrants.

**Table 3.6: Percentage of cells with a Treg phenotype following induction with TGF-β in different studies**

| Phenotype | Current study* | | (Tran *et al.*, 2007) | | (Schuler *et al.*, 2012) | | (Lu *et al.*, 2010a) | | (Xu *et al.*, 2013) | |
|---|---|---|---|---|---|---|---|---|---|---|
| | IL2 | IL2+ TGF-β | IL2 | IL2+ TGF-β | IL2 | IL2+ TGF-β | IL2 | IL2+ TGF-β | IL2 | IL2+ TGF-β |
| $CD4^+FoxP3^+$ | - | - | - | - | 6% | 30% | - | - | 3% | 19% |
| $CD4^+CD25^+$ $FoxP3^+$ | 9±2% | 30±7% | 30% | 80% | - | - | 30% | 55% | - | - |
| $CD4^+CD39^+$ | - | - | - | - | 13% | 16% | - | - | - | - |
| $CD4^+CD25^+$ $CD39^+$ | 10±1% | 16±3% | - | - | - | - | - | - | - | - |

Expression of FoxP3 and CD39 on $CD4^+$ and $CD4^+CD25^+$ T cell populations following the culture of $CD4^+CD25^-$ T cells sorted from PBMC with IL2 or IL2 and TGF-β in the current study, compared with representative data from four other studies. All studies were carried out with polyclonal T cell activation to stimulate T cell differentiation and proliferation. The studies by Tran *et al.* (2007), Schuler *et al.* (2012), Lu *et al.* (2010) and Xu *et al*. (2013) used naive T cells, CD4+CD39- T cells CD4+CD25- T cells or CD4+ T cells and cultured for 5, 7, 5, or 4 days, respectively. *Percentages of FoxP3 and CD39 expressing $CD4^+$ cells are approximately the same as for $CD4^+CD25^+$ cells, as more than 98% of $CD4^+$ cells are $CD25^+$.

In order to assess how the expression of FoxP3, CD39, CD73 and CD26 following culture, compared to the expression on the sorted $CD4^+CD25^-$ T cells prior to culture, the percentage of cells expressing the Treg markers was determined on the $CD4^+CD25^-$ lymphocyte population from seven leucocyte cones (Figure 3.11). Mean percentages of FoxP3, CD39 and CD26 expression on $CD4^+CD25^-$ lymphocytes (6.9±1.4%, 3.9±0.7% and 64.4±14.2%; Figure 3.11), were lower than the mean expression of these markers on the $CD4^+$ cells following incubation with or without TGF-β. Contrastingly, the proportion of $CD73^+$ cells was reduced by more than a half following incubation with or without TGF-β compared with on the $CD4^+CD25^-$ lymphocytes from the seven leucocyte cones prior to culture (6.3±1.2% and 5.4±1.5% compared with 17.0±1.4%)

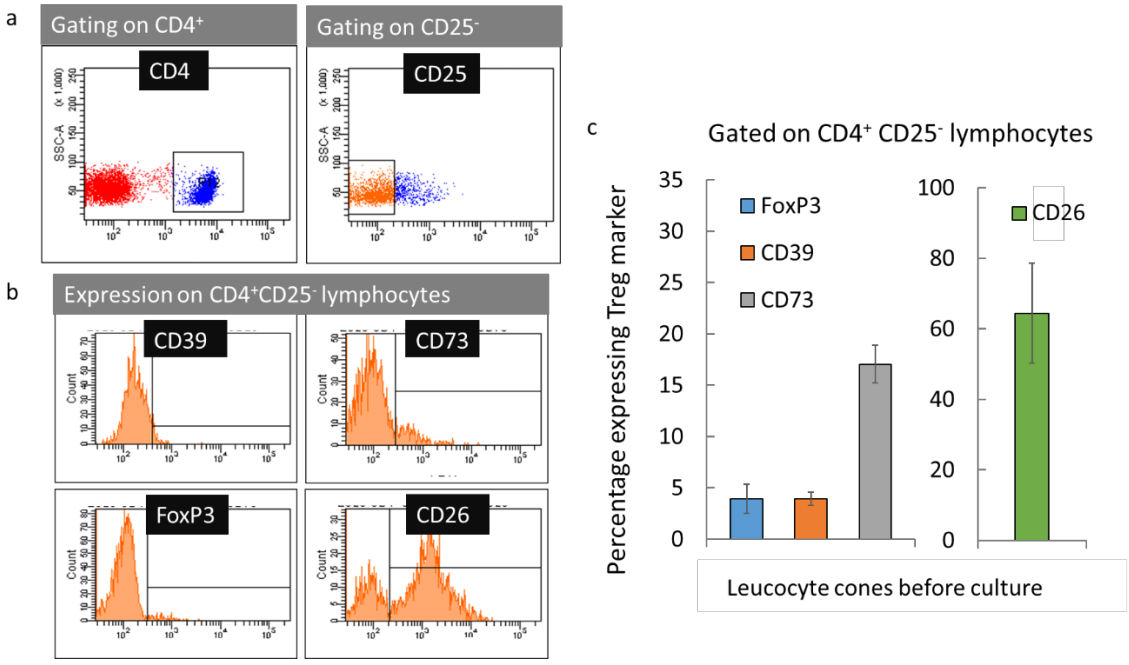


**Figure 3.11: Mean percentage of CD4+CD25- lymphocytes from leucocyte cone PBMC expressing FoxP3, CD39, CD73 and CD26**

PBMC isolated from seven leucocyte cones were labelled with CD4, CD25, FoxP3, CD39 and CD73 fluorescent antibodies. Lymphocytes were gated on $CD4^+$ cells and $CD25^-$ cells were gated from this $CD4^+$ population based upon expression of an isotype control (a). Representative histograms show expression of CD39, CD72, FoxP3 and CD26 on $CD4^+CD25^-$ lymphocytes (b) and bars represent mean percentage (±SEM) of the $CD4^+CD25^-$ lymphocytes expressing these markers (c).

### 3.3.5 Induction of Treg markers on $CD4^+CD25^-$ T cells by HNSCC cell line, tumour fibroblast and overnight dissociated tumour conditioned medium

The effect of culturing $CD4^+CD25^-$ lymphocytes in different CM on the expression of Treg markers was analysed to determine the ability of soluble factors in the medium to induce Treg. In order to ensure there were sufficient nutrients and growth factors for the cells to grow and to dilute any toxic waste products in the CM, cells were cultured in CM diluted at a ratio of 1:2 in LGM or in LGM only. Due to limited CM, experiments were performed on a single occasion on cells isolated from up to three separate leucocyte cones.

The two cell lines from which CM was derived originated from laryngeal tumours and the two fibroblasts from one laryngeal and one unknown node. This was consistent with the CM collected from dispersed HNSCC that were used for these experiments being from laryngeal primary tumours, or nodes with laryngeal or unknown primaries. Although none of the

differences in marker expression between cells cultured in LGM only and those cultured with CM were significant (Figure 3.12), there were more $CD73^+$ cells in cultures with both HNSCC cell line CM (12.6±2.6 and 11.3±3.0%; mean ±SEM) than those in LGM alone (6.5±1.3%), in all three cones (Figure 3.12a). CD26 expression was higher on cells cultured in HNSCC tumour CM and tumour derived fibroblast CM compared with LGM (Figure 3.12b and d). The mean percentage of cells expressing CD39 and FoxP3 was similar across treatment groups (Figure 3.12c).

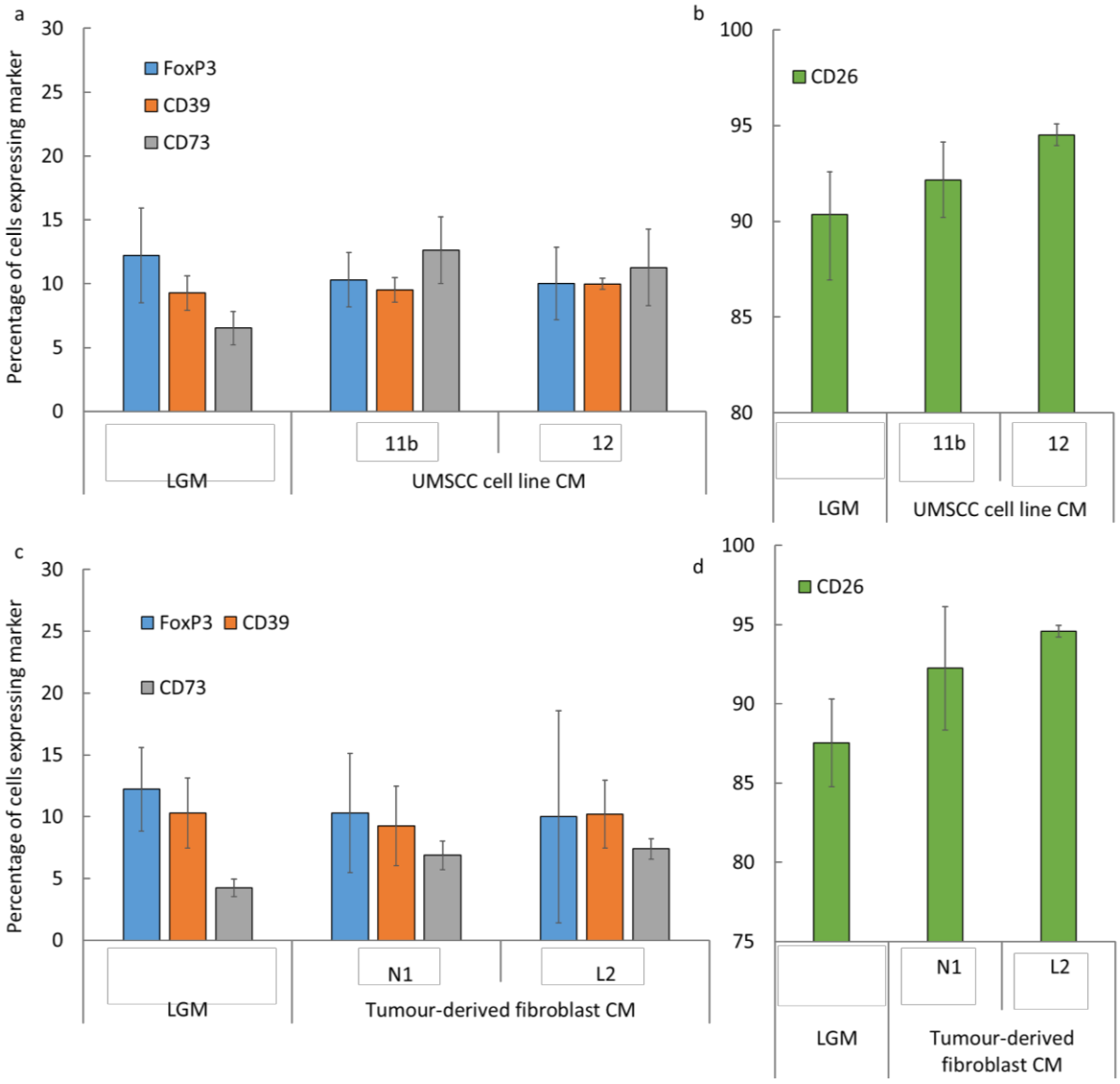


**Figure 3.12: Percentage of CD4+CD25- lymphocytes expressing Treg markers following culture in UMSCC cell line and head and neck tumour derived fibroblast CM**

Mean percentage (±SEM) of $CD4^+CD25^-$ lymphocytes sorted from the PBMC of healthy controls (n=3) expressing Treg markers (FoxP3, CD39 and CD73) and the negative marker CD26. Values are following 5 days of culture in LGM or conditioned medium (CM) collected from 3 day cultures of UMSCC cell lines (a and b) or head and neck tumour-derived fibroblasts (c and d) all supplemented with CD3/CD28 DynaBeads and IL2 (100 U/ml).

A higher proportion of $CD4^+CD25^-$ lymphocytes cultured with CM derived from dissociated tumour tissue expressed CD39 and CD26 than those cultured in LGM only. This was the case for all of the CM tested (Figure 3.13a) and was consistent both between different CM and different leucocyte cones. The mean expression of CD39 and CD26 was higher in all culture conditions than was observed in the $CD4^+CD25^-$ population from seven different leucocyte cones prior to culture (Figure 3.11). A greater number of cells expressed CD73 following culture in CM than LGM. However, this difference was less marked, than with CD39 (Figure 3.13a). Two of the three cones, had CD73 expression lower than that observed on $CD4^+CD25^-$ T cells prior to culture (Figure B.2, Appendix B). In the majority of cases there was no difference in the percentage of cells expressing FoxP3 following culture with CM or LGM.

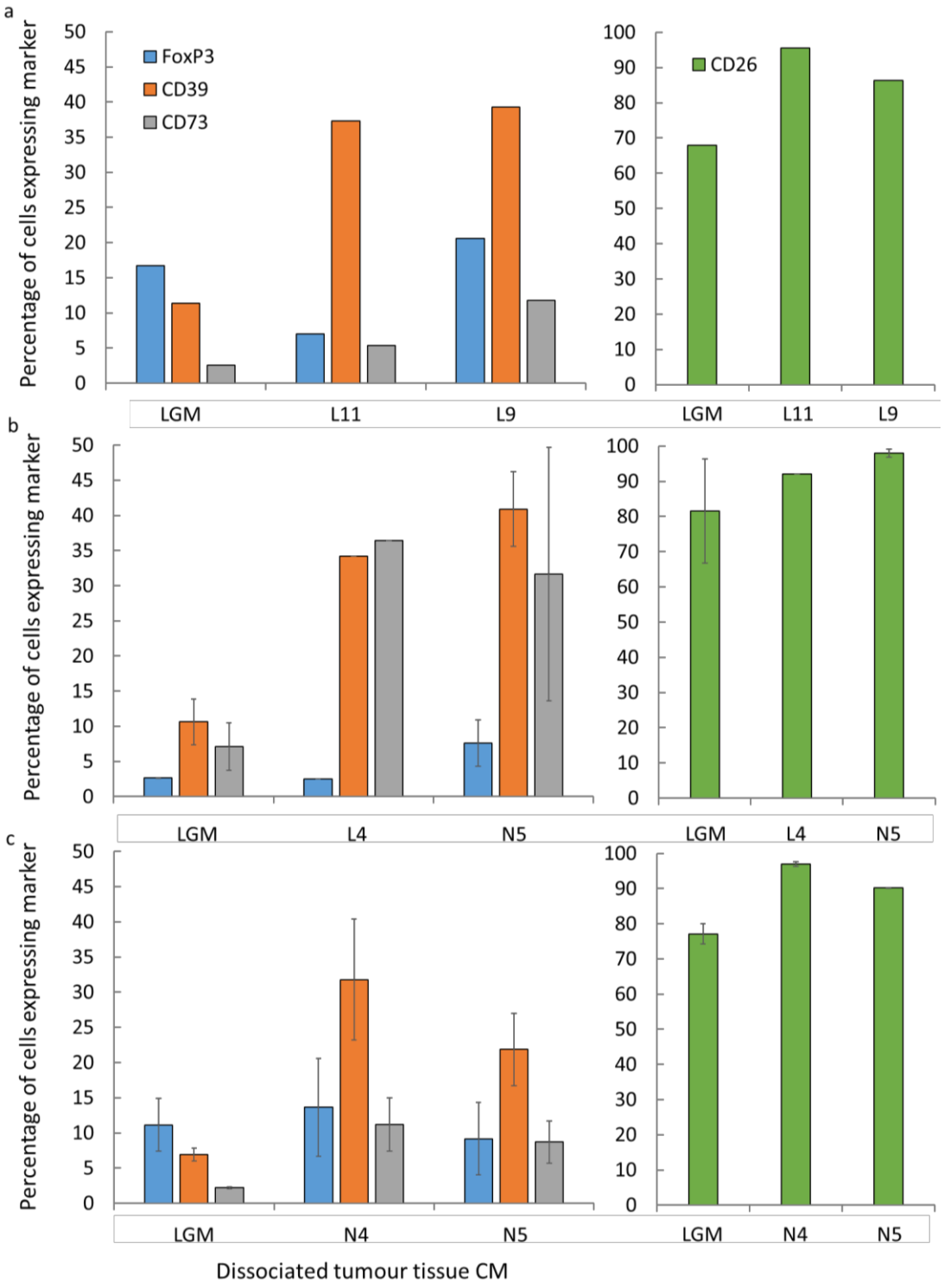


**Figure 3.13: Percentage of CD4+CD25- lymphocytes expressing Treg markers following culture in head and neck dispersed tumour CM**

Mean percentage (±SEM) of $CD4^{+}CD25^{-}$ lymphocytes sorted from the PBMC of three healthy controls (a,b,c) expressing Treg markers (FoxP3, CD39 and CD73) and the negative marker CD26. Expression was measured following 5 days of culture in growth medium (LGM) or conditioned medium (CM) collected from overnight cultures of dispersed tumour tissue, all supplemented with CD3/CD28 DynaBeads and IL2 (100 U/ml). Where present error bars represent SEM from two separate experiments. Statistical analysis could not be carried out due to lack of experimental repeats.

### 3.3.6 The effect of different growth media on cells viability and expression of Treg markers following culture of $CD4^+CD25^-$ T cells

Lymphocytes were cultured in medium optimised for their expansion following TCR activation (lymphocyte growth medium). However, for the collection of CM from cell lines, fibroblasts and dispersed tumour cells were all cultured in complete DMEM. To assess whether the different culture medium affected cell viability or Treg marker expression, $CD4^+CD25^-$ lymphocytes from three leucocyte cones were cultured in the different growth mediums.

Following the five day culture of $CD4^+CD25^-$ lymphocytes in lymphocyte growth medium, cell line medium, fibroblast medium or cell line or fibroblast medium diluted in lymphocyte medium at a ratio of 1:2, cells were removed from wells and counted with trypan blue to determine their viability (Figure 3.14). The number of cells recovered was divided by the number of wells from which the cells were collected to give a standardised value of cells per well for each experiment. The experiment was repeated on cells from three different healthy donors and the mean was taken. Fewer cells were recovered from the wells containing cells cultured in cell line or fibroblast GM ($8.6 \times 10^4 \pm 2.1 \times 10^4$; $p$=0.19 and $8.7 \times 10^4 \pm 1.3 \times 10^4$; $p$=0.16) compared with those cultured in lymphocyte GM ($15.3 \times 10^4 \pm 3.9 \times 10^4$; Figure 3.14a), however the variation was high and the experiment was only carried out on cells from three cones. While the number of cells recovered following culture with the lymphocyte growth medium was close to double the number initially plated ($8.0 \times 10^4$), the number of cells recovered after culture in cell line and fibroblast GM did not change. Diluting either the fibroblast and cell line medium in lymphocyte medium increased the number of cells recovered, but the number of total cells was still lower than when cultured in lymphocyte medium alone. No differences were observed in percentage viability of the cells cultured in different GM, determined by trypan blue exclusion (Figure 3.14b).

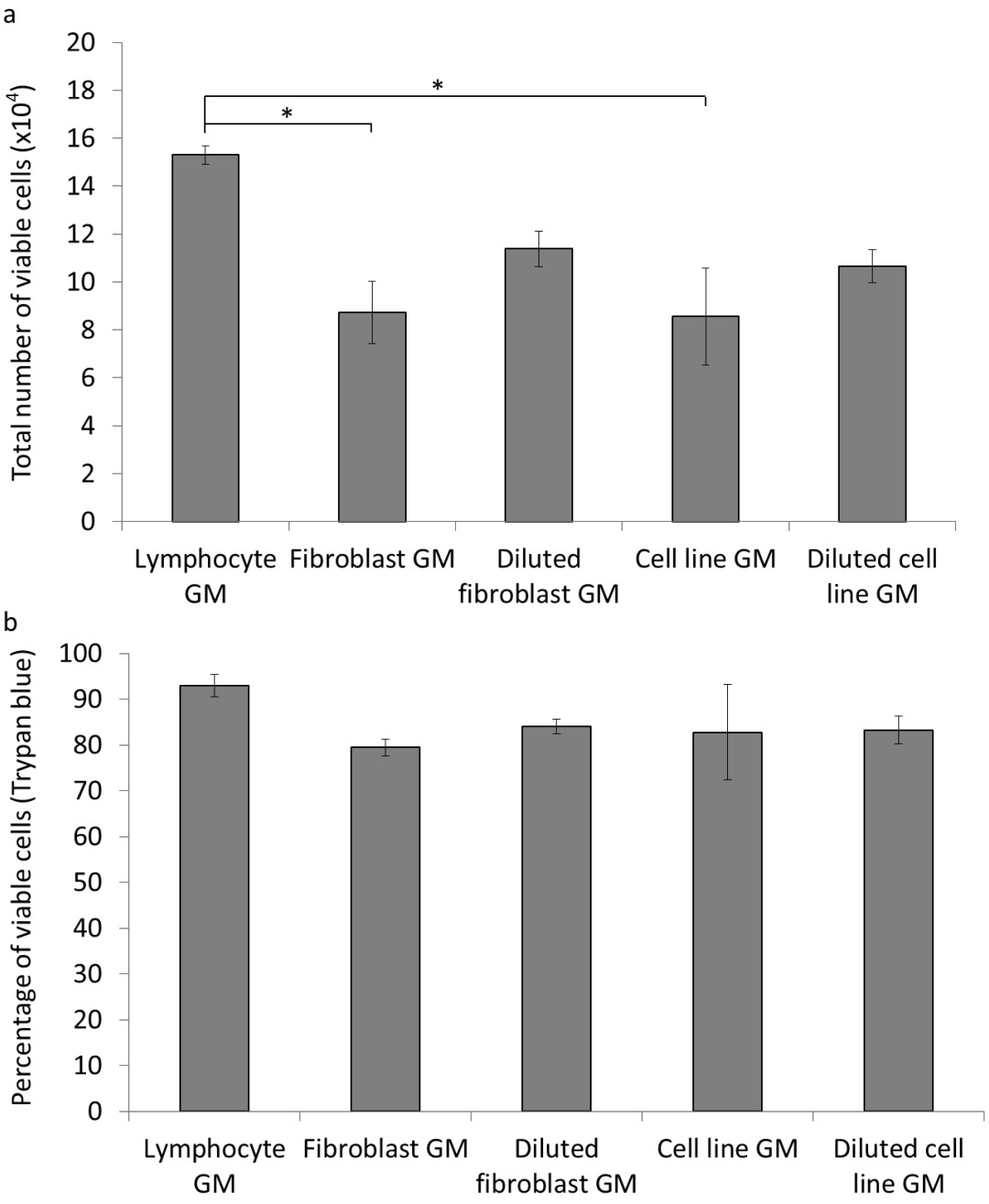


**Figure 3.14: Cell viability following five day culture of CD4+CD25- cells in different growth medium, supplemented with CD3/CD28 DynaBeads and IL2**

$CD4^+CD25^-$ lymphocytes were sorted from leucocyte cones and seeded at $8x10^4$ cells/well in lymphocyte growth medium (X-vivo 20, supplemented with 5% human AB serum), fibroblast growth medium (DMEM, supplemented with 10% FBS), cell line growth medium (DMEM, supplemented with 10% FBS and non-essential amino acids), or fibroblast or cell line GM diluted 1:3 with lymphocyte GM. Following 5 days of culture in GM supplemented with IL2 (100 U/ml) and CD3/CD28 DynaBeads, the mean number of viable cells recovered per well (a) and the percentage viability of the total cells recovered (b) from three separate experiments (±SEM) was determined using Trypan blue exclusion. Statistically significant differences (*$p$<0.05) were determined using one-way ANOVA with Tukey post-hoc test.

There were no statistically different differences in marker expression following culture in the different growth medium (Figure 3.15), however there was considerable variability between FoxP3 expression between donors, and FoxP3 was usually higher in the cells cultured in neat rather than diluted media (Figure 3.15a).

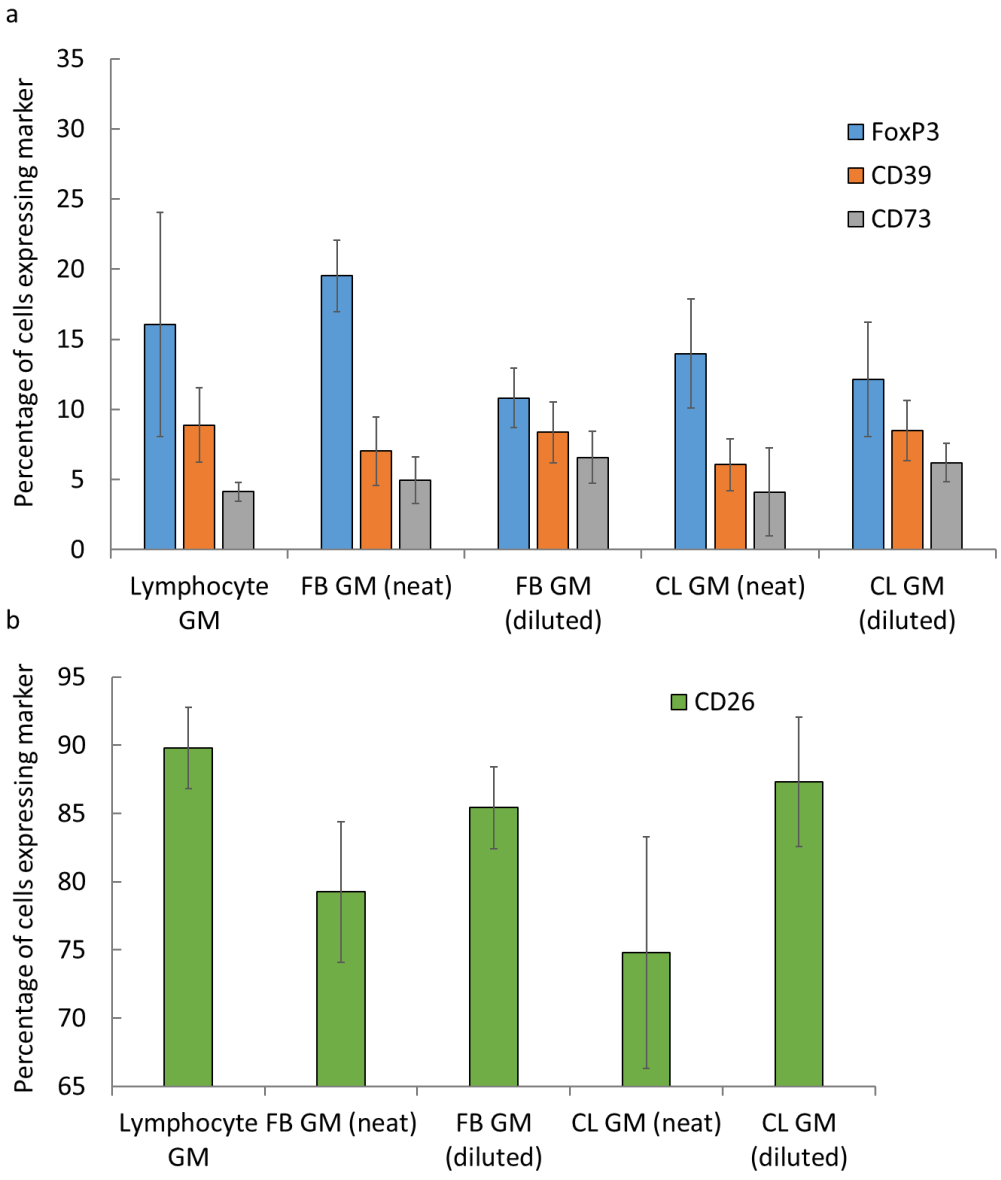


**Figure 3.15: Percentage of CD4+CD25- lymphocytes expressing Treg markers following culture in different growth medium, supplemented with CD3/CD28 DynaBeads and IL2**

$CD4^+CD25^-$ lymphocytes were sorted from leucocyte cones and cultured for 5 days in lymphocyte growth medium (X-vivo 20, supplemented with 5% human AB serum), fibroblast growth medium (DMEM, supplemented with 10% FBS), cell line growth medium (DMEM, supplemented with 10% FBS and non-essential amino acids), or fibroblast or cell line GM diluted 1:3 with lymphocyte GM, all supplemented with IL2 (100 U/ml) and CD3/CD28 DynaBeads. Bars represent the mean (±SEM) percentage of cells from 3 separate experiments, expressing the Treg markers (a; FoxP3, CD39 and CD73) and the negative marker CD26 (b). Statistically significant differences (*$p$<0.05) were determined using one-way ANOVA with Tukey post-hoc test.

## 3.4 Discussion

### 3.4.1 Enhanced Treg levels in the tumour microenvironment of HNSCC patients

The levels of Treg as a proportion of total lymphocytes have previously been found to be enriched in the HNSCC tumour microenvironment compared with peripheral blood (Section 1.2.3.4), a finding confirmed in this study. In particular, increased percentages of lymphocytes with $CD4^+CD25^{hi}$, $CD4^+CD39^+$, $CD4^+CD26^-$, $CD4^+CD25^+CD39^+$ $CD4^+CD25^+CD26^-$ and $CD4^+CD25^+FoxP3^+$ phenotypes were noted on TIL compared with PBMC. Although, there is a consensus among the majority of studies as to the trend in Treg levels, the numbers of Treg observed can be highly variable. Much of this variability can be accounted for by differences in the gating strategies employed between studies (Section 1.2.2.4), though other methodological factors may also contribute.

In contrast to other studies, where a greater frequency of $CD25^+$ lymphocytes has been observed in HNSCC, breast adenocarcinoma and pancreatic adenocarcinoma TIL compared with PBMC (Strauss *et al.*, 2007b, Liyanage *et al.*, 2012), the current study found no difference between the proportion of cells expressing CD25. The percentage of peripheral and tumour infiltrating $CD4^+$ lymphocytes that were $CD25^+$ (36±6% from PBMC and 26±4% from TIL), were also relatively high compared to those observed by others. For example, Liyanage *et al*. (2002) found that 16.6±1.22% and 13.2±1.13% (mean±SEM) of peripheral $CD4^+$ lymphocytes from 35 breast ductal adenocarcinoma and 30 pancreatic adenocarcinoma patients, respectively, expressed CD25, and on breast and pancreatic tumour infiltrating lymphocytes this increased to 20.2±3.93%. In this case this may reflect differences between the different tumour types analysed. In another study assessing Treg populations in HNSCC, the percentages of $CD4^+$ lymphocytes expressing CD25 in both patient PBMC and TIL were much lower than in the current study (3±0.7% in PBMC and 13±3% in TIL; Strauss *et al.*, 2007b). One explanation for the variable expression of CD25 between the Strauss study and this study may be that, unlike CD4 expression, for which separate positive and negative peaks are clearly visible, $CD25^+$ cells are less easily distinguishable (Figure 3.1).

For defining $CD25^{hi}$ cells, different methodologies have been used in different studies (Section 1.2.2.4.4 and Figure 1.10). In the current study, $CD25^{hi}$ cells were considered to be those with CD25 expression exceeding that observed on $CD4^-$ cells. Strauss *et al*. (2007b)

used a cut-off mean fluorescence intensity of 120 to define $CD25^{hi}$ cells based on previous experiments carried out within the group that identified these cells as having a suppressive phenotype (Figure 1.10). In their study fewer $CD25^{hi}$ cells were observed in both the PBMC and TIL of HNSCC patients (1.0±3% and 3±0.5% of $CD4^{+}CD25^{+}$ lymphocytes) compared with the current study (11.6±1.8% and 38.6±4.2). Despite these numerical differences, the enhancement of $CD25^{hi}$ expressing T cells in the tumour infiltrate compared with the periphery of HNSCC patients is a consistent feature of both of these studies. Studies in other cancer types have similarly, noted an increase in $CD25^{hi}$ cells in TIL (Miller *et al.*, 2006; Chi *et al.*, 2010). Chi *et al*. (2010) used the same method to define $CD25^{hi}$ cells as was used in the current study. They found the frequency of $CD25^{hi}$ on peripheral $CD4^{+}$ cells from bladder cancer patients was similar to that found in the current study (8.6±5.4% *vs*. 5.1±2.5%), but only half the frequency of $CD25^{hi}$ cells were observed in the bladder carcinomas (15.4±9.9% *vs*. 30.3±4.1%). However, this could be due to differences between different cancer types and tumour heterogeneity.

It has been observed in some cases that the number of Treg decreases following the cryopreservation of PBMC (Elkord, 2009; Sattui *et al.*, 2012). Sattui *et al*. (2012) saw a decrease in the percentage of $CD4^{+}$ cells possessing a $CD25^{+}FoxP3^{+}$ phenotype of up to 82%, with a reduction noted in both CD25 and FoxP3 expression. Changes to CD25 expression following cryopreservation, could perhaps account somewhat for the differences in the percentages of $CD25^{+}$ and $CD25^{hi}$ lymphocytes between studies. Interestingly, of the results discussed, Strauss *et al.* (2007b), which observed the fewest $CD25^{+}$ and $CD25^{hi}$ cells, was the only other group to use samples that had been cryopreserved prior to staining. FoxP3 expression has also been observed to drop from 5.58% to 3.57% of the $CD4^{+}CD25^{+}$ lymphocyte population three weeks after cryopreservation of PBMC (Elkord, 2009). In contrast, other studies have detected no differences in Treg levels between cryopreserved and fresh PBMC (Van Hemelen *et al.*, 2010; Venet *et al.*, 2010). Venet *et al.* (2010) extended this observation to include whole blood, using a $CD25^{+}CD127^{-}$ phenotype to define Treg within the $CD4^{+}$ pool of cells. Supplementary data collected as part of this study found the percentage of $CD4^{+}$ cells expressing CD25 decreased from 43.2±7.8% to 19.5±4.9% following cryopreservation, however this difference was not significant as the sample size was small (n=3; Figure B.B.3 Appendix B). In the current study there was little or no effect of cryopreservation observed for any of the other Treg markers (FoxP3, CD39, CD73, CD26 and $CD25^{hi}$; Figure B., Appendix B).

An increased frequency of FoxP3 expression was also observed on $CD4^+CD25^+$ lymphocytes in HNSCC TIL compared with PBMC (50.1±6.7% *vs*. 20.5±5.3%), but not in the $CD4^+$ population as a whole (17.0±1.9 and 16.4±3.7). In agreement, Jie *et al*. (2013) noted greater FoxP3 expression on HNSCC TIL compared with peripheral T cells within the $CD4^+CD25^{hi}$ lymphocyte population but not in $CD4^+CD25^{lo}$ pool of cells. Overall, the $CD4^+CD25^{lo}$ population makes up 64.5±5.9% of the $CD4^+$ lymphocyte pool on PBMC and 26.5±4.4% in TIL in the current study and has little FoxP3 expression so it is not surprising that the difference in FoxP3 expression observed on $CD25^{hi}$ lymphocytes of PBMC and TIL becomes masked when considering the entire $CD4^+$ population. FoxP3 has previously been shown to be increased in the peripheral blood of HNSCC compared to healthy controls and this correlated with poor prognosis (Strauss *et al.*, 2007a; Sun *et al.*, 2014). However, when the cohort was divided into different HNSCC subsets, although the percentage of cells positive for FoxP3 expression in the oropharyngeal (n=19), laryngeal (n=36), hypopharyngeal (n=20) and nasopharyngeal (n=18) SCC periphery remained higher than that in healthy controls (n=31), in oral cavity SCC (n=19) peripheral blood there was no difference (Sun *et al.*, 2014). This group also identified an increase in a subset of $FoxP3^+$ Treg that were $CD45RA^-$, in patients with late stage tumours (T3/4; n=66) or tumours with nodal involvement (n=42), compared with those with early stage tumours (T1/2; n=46) or without nodal involvement (n=70), suggesting these cells may be involved in tumour progression. The same group also showed no difference in FoxP3 expression on circulating $CD4^+$ lymphocytes between HNSCC patients and benign counterparts (mean of approximately 7% in each), whereas an increased percentage of $CD45RA^-FoxP3^{hi}$ cells was observed and correlated with a poor prognosis (Ihara *et al.*, 2017). This demonstrates the importance of the classification of the Treg cells and why it is difficult to compare between studies that have used different combinations of markers to identify Treg. Furthermore, it may be that specific subsets of Treg are responsible for the immune dysregulation in cancer.

A similar level of CD39 expression on $CD4^+$ lymphocytes from HNSCC PBMC was observed in the current study compared to that previously described by Mandapathil *et al*. (11±2% *vs*. 13±3%, respectively), where it was nearly double the number observed in the periphery of healthy controls. Furthermore, in the current study $CD4^+CD39^+$ cells were more prevalent in TIL, with three times as many $CD4^+$ lymphocytes in TIL expressing CD39 compared with $CD4^+$ lymphocytes in PBMC. A finding that supports previous observations by Schuler *et al*. (2012)

The lack of CD26 on $CD4^+$ lymphocytes, a trait common to Treg cells, was found to be more pronounced in TIL compared with PBMC, a comparison that has not previously been made. A study by Mandapathil *et al.* (2012), reported CD26 to be expressed on around 60% of $CD4^+$ T effectors from the peripheral blood of HNSCC, considerably lower than the 90% observed in the current study. The same study noted that a greater proportion of peripheral $CD4^+$ lymphocytes express CD26 in healthy controls compared to HNSCC patients (Mandapathil *et al.*, 2012). These findings compliment the results using the positive Treg marker expression and further support the use of CD26 in Treg identification and isolation.

In the current study, the percentage of $CD4^+$ lymphocytes with extracellular CD73 expression was no different between PBMC and TIL. This is perhaps not surprising, as CD73 has only been observed on around 1% of peripheral HNSCC patient and healthy donor $CD4^+CD39^+$ Treg (Schuler *et al.*, 2014) and CD73 has been observed on *in vitro* induced human iTreg where it is expressed only transiently on the surface before being shed (Whiteside *et al.*, 2012). Dual CD39 and CD73 expression was very low on $CD4^+$ lymphocytes in this study, nearly 3% in TIL and approximately 1% of the $CD4^+$ lymphocytes from PBMC (Figure B.4; Appendix B). Of note there were a number of lymphocytes positive for both CD39 and CD73 in HNSCC PBMC and TIL; however, the vast majority of these were $CD4^-$.

Differences between the cohorts in the studies discussed could be responsible for some of the differences observed in the results. For example, all the TIL in the study by Strauss e*t al*. (2007b) were isolated from primary tumours of patients that had undergone no previous treatment, were mostly from the oral cavity (10/15), and the majority were late stage tumours (T3/4; 12/15) (Strauss *et al.*, 2007b). Of the cohort in the study by Jie *et al*. (2013), all but one patient was suffering from tumours of the oral cavity or oropharynx and 9/25 had undergone previous treatments. Comparatively the cohort in this study was much smaller (n=8), and the TIL were taken from a mixture of tumour nodes and primary tumours (two T3/4 laryngeal tumours and three T1/2 oropharyngeal tumours), however all the patients were newly presenting with no previous cancer treatment. It is known that chemoradiotherapy can have effects on immune cell population (Schuler *et al.*, 2013), which could explain some of the differences observed by Jie *et al.* (2013). In this study higher FoxP3 expression was observed on $CD4^+CD25^+$ TIL from nodes than from primary tumours, while all other markers were the same. However, the number of samples compared was small

(n=4 and n=5 in node and primary tumour respectively). Some other cancer studies have shown differences in Treg infiltration between both tumour subsites and tumour stage. For example, Ichihara *et al.* (2003), found that the percentage of $CD4^+CD25^+$ cells in the lymphocyte population was approximately two-fold greater in the TIL from stage 2, 3 and 4 gastric tumours (19.8±4.5%) than from stage 1 tumours (4.6±2.1%). However, Liyanage *et al*. (2002) saw no difference between Treg in TIL from primary tissue or node from breast and pancreatic carcinomas.

### 3.4.2 Both $CD4^+CD39^+FoxP3^+$ and $CD4^+CD39^+FoxP3^-$ T cell populations are enriched in the HNSCC TME

In addition to the increase in $CD4^+CD39^+$ $FoxP3^+$ Treg observed in the TIL of HNSCC compared to the periphery, the percentage of $CD4^+CD39^+FoxP3^-$ T cells was also enhanced. This is consistent with findings by Schuler *et al*. (2012), who found levels of $CD25^+FoxP3^+$ and $CD25^-FoxP3^-$ on $CD4^+CD39^+$ from HNSCC TIL (13.6±9.8% and 12.1±10.1%) to be two-fold that of $CD4^+CD39^+$ from patient PBMC (6.6±3.8% and 5.5±3.3%). More than 72% of peripheral $CD4^+CD39^+$ lymphocytes from the PBMC of healthy donors express FoxP3 (Mandapathil *et al.*, 2012), which is greater than was observed in the patient cohort in the current study (less than 53%). As expected, the increase in $CD4^+CD39^+FoxP3^+$ Treg in the TIL was more marked on the cells that also expressed CD25. Contrastingly, the $CD39^+FoxP3^-$ population of cells were observed at similar levels in the whole $CD4^+$ Th subset as in those expressing the additional CD25 activation marker. These $CD25^-$ and $CD25^+$ populations can contain cells with distinct functions. Schuler *et al*. (2012), have described $CD4^+CD25^-CD39^+FoxP3^-$ non-suppressive T cells that can readily convert to $CD4^+CD25^+CD39^+FoxP3^+$ Treg following culture with TGF-β, however $CD4^+CD25^+CD39^+$ expression may also represent an exhausted phenotype (Fang *et al.*, 2016).

### 3.4.3 Immunosuppressive factors released by cells of the HNSCC tumour microenvironment

Although tumours are known to release soluble factors that manipulate the constituent cells of their environment, whether they induce Treg from precursors or recruit and expand Treg from the periphery is still under investigation. Furthermore the Treg markers used in this study are known to be expressed on both nTreg and some iTreg, so it is unclear as to whether

the increase in Treg discussed above is due to iTreg induction or to expansion of the nTreg subset.

Both TGF-β and IL10 have been implicated in Treg induction *in vitro* (Section 3.1.1). In the current study, TGF-β was released to varying degrees by all the UMSCC cell lines, HNSCC-derived fibroblasts and dissociated HNSCC tissue investigated. Although, TGF-β was detected in the majority of the UMSCC cell line and tumour-derived fibroblast CM after one day in culture, the concentration increased markedly over the three days. The levels of TGF-β found in the CM collected from the laryngeal UMSCC 12 cell line approached similar levels to that used to induce Treg from $CD4^+$ T cells in *in vitro* experiments (Section 3.3.3). TGF-β was also present in the CM collected from dispersed tumour tissue where it was standardised per 100 mg tissue to account for any differences in tumour size. There was a high degree of variability between the concentrations of TGF-β in the CM from different tumours, however no significant difference was observed between samples collected from primary tumours and nodes. The release of TGF-β by HNSCC associated fibroblasts is consistent with observations by Rosenthal *et al.* (2004). In contrast, in a study by Chen *et al.* (1999), ELISA failed to detect TGF-β in CM collected following the 48 hour culture of seven HNSCC cell lines, including two of the same cell lines used in the current study (UMSCC-11a and b, compared with 84 and 188 pg/ml).

The findings of the current study support the ubiquitous nature of TGF-β, which can be expressed by most types of cells. It is frequently upregulated *in situ* in the tumour tissue of various cancer types, including HNSCC (Lu *et al.*, 2004b). The source of this upregulation is likely a combination of cell types within the tumour microenvironment, including the tumour cells and fibroblasts.

IL10 was not detected in any of the CM collected from the UMSCC cell lines or from tumour-derived fibroblasts. However, IL10 was observed in all the CM from the dispersed tumour tissue, this most likely suggests that the IL10 comes from the leucocytes. Leucocytes are known to be the primary producers of IL10, particularly Treg, Th2 cells, and macrophages (Curry *et al.*, 2014), and are prominent in the TME. Previous work carried out in this laboratory has shown that depletion of $CD45^+$ leucocytes from dispersed tumour samples prior to plating the cells, considerably reduces the IL10 in the CM following overnight culture (Smith, 2016).

### 3.4.4 Induction of a Treg phenotype in $CD4^+CD25^-$ lymphocytes by TGF-β

Prior to determining whether the soluble factors found in the conditioned medium from the cell lines, tumour-derived primary fibroblasts and dissociated tumour were capable of inducing Treg, a model was established for the induction of iTreg from healthy donor $CD4^+CD25^-$ lymphocytes. Consistent with findings from other studies the results from the current experiments support a role for TGF-β in inducing Treg from $CD4^+CD25^-$ cells, as shown by a greater proportion of cells with a $FoxP3^+$ and/or $CD26^-$ phenotype following culture with medium containing TGF-β, compared to those cultured without (Liu *et al.*, 2006; Tran *et al.*, 2007; Lu *et al.*, 2010a;

Table 3.6). Few studies have looked at CD39 expression on $CD4^+CD25^-$ cells, following incubation with TGF-β, although these results compliment those reported by Schuler et al. (2010). In the current study, the proportion of $CD39^+$ cells was not significantly increased in cultures supplemented with TGF-β, however the sample size was small (n=3). On the other hand, Schuler *et al.* (2012) induced Treg from a population of $CD4^+CD39^-$, rather than $CD4^+CD25^-$ and reported a significant increase in the proportion of dual FoxP3 and CD39 expressing $CD4^+$ cells with TGF-β (~16%) compared to without (~1%). In the current study there was variability between the percentage of cells expressing FoxP3 and CD26 following culture with TGF-β, between the cells isolated from different leucocyte cones (Figure B.2, Appendix B). However, the same trend was observed in all three healthy controls.

The expression of FoxP3 and CD39 on the $CD4^+CD25^-$ population of lymphocytes collected from leucocyte cones was lower than in the activated cultured cells even without TGF-β, supporting observations that activation induces the expression of some Treg markers (Section 1.2.2.7). CD26 expression was similar on $CD4^+CD25^-$ cells and following their culture with TGF-β. CD26 is normally present on most T helper cells (~75% of $CD4^+CD25^-$ lymphocytes), and is upregulated following TCR activation, while expression of CD26 is low or absent on Treg even after TCR stimulation (Salgado *et al.*, 2012). Similarly, in this study, CD26 expression was induced on the majority of cells following TCR activation in the absence of TGF-β but not when TGF-β was present. The percentage of $CD73^+$ cells was higher in the $CD4^+CD25^-$ T cell population from leucocyte cones than on the same population of cells following culture, suggesting it may be downregulated following TCR

stimulation. Overall the current study supports a role for TGF-β in the induction of Treg, however functional assays are required to confirm these cells are suppressive.

### 3.4.5 The effect of soluble factors released by HNSCC on the induction of Treg markers

Soluble factors, such as TGF-β and IL10, that induce Treg are known to be present in the TME, however it is unlikely to be a single factor, which causes the transformation. How the plethora of factors in the tumour milieu interact and influence Treg induction is unclear, therefore the effect of the whole secretome of the tumour cells and associated stromal cells on the expression of Treg markers was investigated. In the current study, there was an induction of CD39 and CD73 expression following the culture of $CD4^+CD25^-$ lymphocytes in HNSCC dispersed tumour CM. However, no increase in either marker was observed when $CD4^+CD25^-$ lymphocytes were cultured with HNSCC-derived fibroblast or UMSCC cell line CM. This could suggest that it is other cells present in the TME, such as leucocytes, that are key in inducing effects on TIL.

A major factor to bear in mind when drawing conclusions from the observed effects of any tumour dissociated CM is the variation in tumour size. It might be expected that larger tumours with more cells would release cumulatively higher levels of soluble factors, in turn resulting in a greater induction from the CM derived from these larger tumours. However, given the complexity of the tumour microenvironment, the assortment and proportion of different cells types, this correlation is undoubtedly not that straightforward. In support of this, no such relationship was observed in the current study. For example, despite the tumour L9 being one quarter the weight of L11 and L4 being half the weight of N5, there was no marked difference in the expression of the different markers after culture in each of these CM.

Expression of the conventional Treg marker FoxP3 was no different when cultured with CM than LGM, and CD26, which is regarded to be a negative Treg marker was unexpectedly higher in the cells cultured with CM. The percentage of $FoxP3^+$ cells was higher following culture, regardless of the GM or CM used, suggesting this could be the transient upregulation, induced by TCR activation, that has previously been described (Allan *et al.*,

2007). $CD26^+$ cells were also higher following culture, regardless of the CM or GM used, suggesting that the majority of these cells are activated Th cells, rather than Treg.

In addition to the soluble factors, microvesicles isolated from the CM of tumour cells have been shown to have immunoregulatory effects (Czystowska *et al.*, 2009; Szajnik *et al.*, 2010). Szajnik *et al.* (2010), isolated microvesicles from the CM of ovarian cancer cell lines, and observed that they were able to induce $CD25^+FoxP3^+$ Treg *in vitro*. Following five days of culture with the tumour-derived microvesicles, the percentage of $CD4^+CD25^+$ T cells expressing FoxP3 was 41% compared to 30% without. Microvesicles are increased in the serum of HNSCC compared with healthy controls so may contribute to some of the observed induction of Treg in patients (Szajnik *et al.*, 2010). It is possible that if microvesicles are present in any of the CM used in this chapter, it is at too low a concetration to induce any Treg under these conditions. In contrast, other studies isolated microvesicles from CM by centrifugation and used these at higher concentrations. The dilution effect may also be true of any soluble factors, as CM was diluted in GM prior to culturing cells. Dilution of CM in fresh GM was necessary to replenish some of the nutrients that would have been depleted in the spent CM and also to circumvent any detrimental effects on lymphocytes due to the cytotoxic waste products present.

CM collected from HNSCC CAF have also been observed to induce the expression of FoxP3 in $CD4^+$ lymphocytes, compared to CM derived from normal fibroblasts (Takahashi *et al.*, 2015). In the study by Takahashi *et al*. (2015), CM was collected from fibroblasts after three days of culture and diluted 1:1 with fresh GM before use in the culture of healthy control PBMC. The relative gene expression of FoxP3 detected in the PBMC cultured in CAF CM was 1.5-fold higher than in CM from normal fibroblasts. Flow cytometry confirmed a difference in FoxP3 expression on $CD4^+$ lymphocytes, with the mean percentage of $CD4^+FoxP3^+$ cells ranging from around 4% to 7% following culture in CM from normal fibroblasts and 7% to 10% when cultured with CAF CM, values similar to those observed in the current study. Similarly, in a study in lung adenocarcinoma, Treg were found to reside predominantly in the stroma, and CM from CAF were observed to increase FoxP3 expression in naïve $CD4^+$ T cells from healthy controls, when compared with normal fibroblasts (Kinoshita *et al.*, 2013). Furthermore, CM from CAF derived from tumours with high levels of Treg induced significantly more FoxP3 expression than CM from CAF of tumours with low levels of Treg. The CM from CAF of high Treg tumours, induced a four-

fold change in FoxP3 expression in naïve T cells, compared to cultures with normal fibroblast CM, which was also the same level of FoxP3 expression observed when cells were cultured with TGF-β. The observations of Kinoshita *el al*. (2013), suggest a major role for CAF derived soluble factors in Treg induction of lung adenocarcinoma.

Although soluble factors have been implicated in the induction of Treg, *in vivo* this may also rely on, or be enhanced by, cell contact dependent mechanisms and interactions with other factors in the tumour milieu. For example, TGF-β was present in all the CM tested, however, it is secreted in its latent form. Proteins involved in the interaction between cells and the extracellular matrix (ECM), such as thrombospondin I, integrins and metalloproteinases (MMPs) are frequently upregulated in the TME and can induce the activation of TGF-β (Kazerounian *et al.*, 2008; Desgrosellier & Cheresh, 2010; Kessenbrock *et al.*, 2010). However, *in vivo*, the majority of TGF-β is found in its latent form, and following activation is relatively short lived (Stover *et al.*, 2007). It is likely that the majority of TGF-β in the collected CM is not active, and the latent form would require the presence of factors capable of its activation before Treg induction could take place. There are a number of known ways that TGF-β can be activated. For example, metalloproteinases, integrins and reactive oxygen species are all able to induce the conformational change that release TGF-β from its latent complex causing its activation, and are all present in the tumour microenvironment. MMP are secreted by stromal cells, including T cells, macrophages and fibroblasts, however, other inhibitory factors are also released to regulate MMP activation and prevent aberrant protein degradation (Kessenbrock *et al.*, 2010). This highlights that it is likely a balance of factors that determines the induction of iTreg. One reason for the lack of FoxP3 induction noted here, compared with other studies, maybe due to the cell type used in the assays. For example, Takahashi *et al*. (2015), cultured whole PBMC, so other factors may have been present at the start of culture that would not be present in sorted populations of cells. This is corroborated by Melief *et al*. (2013) who observed that co-culture of PBMC with multipotent stromal cells (MSC) or with MSC CM could induce Treg. However, the effect was not seen in monocyte-depleted PBMC. This suggests that in addition to direct mechanisms of Treg induction such as those mediated by TGF-β and IL10, indirect mechanisms exist that may at least be as important. In this case, MSC were promoting the differentiation of macrophages in favour of an M2 phenotype, which were in turn producing factors, promoting the induction of Treg (Melief *et al.*, 2013). In addition to this, Schmidt *et al.* (2016) used conditioned medium from M2 induced macrophages to induce $CD4^{+}FoxP3^{+}$ Treg from naïve T cells

(Schmidt *et al.*, 2016b). Lending further support to the idea that other leucocytes may be important for the induction of Treg.

In the current study, CD39 and CD73 expression were induced on $CD4^+CD25^+$ T cells following culture with dissociated tumour tissue. However, neither are exclusive markers of Treg and are found on other cell types, including other Th subsets. CD39 is found on exhausted $CD4^+$ and $CD8^+$ T cells (Gupta *et al.*, 2015; Fang *et al.*, 2016). T cell exhaustion is a response to the continuous exposure of antigen, such as observed in chronic infection or tumours, were persistent TCR stimulation leads to dysfunction (Catakovic *et al.*, 2017). Fang *et al*. (2016) found that following stimulation of $CD4^+$ memory T cells with CD3/CD28 antibodies, CD39 expression was induced to a greater extent in older individuals. Furthermore, these $CD39^+$ cells were more susceptible to apoptosis and contained a greater percentage of $CD26^+$ cells than their $CD39^-$ counterparts following TCR activation, while percentage of $FoxP3^+$ cells was the same on both $CD39^+$ and $CD39^-$ subsets. In the current study, CD26 was increased following TCR activation. Moreover, although FoxP3 expression was not measured on the $CD39^+$ cells, the proportion of $FoxP3^+$ cells was no different between the cells cultured in tumour CM and those cultured in GM, despite the greater proportion of $CD39^+$ cells in cultures containing CM. Overall, the phenotype of the cells following culture in tumour CM, is more in line with that of exhausted T cells, than iTreg.

There was an increase in CD73 expression on $CD4^+CD25^+$ cells following culture in all of the CM. CD73 is known to be abundantly expressed by human Treg, however, is usually intracellular. It is also found in other T lymphocyte subsets and its overexpression has been observed on cancer cells, where it is associated with promoting tumour growth and immune suppression by production of adenosine (Allard *et al.*, 2012). Although in mice it is co-expressed on Treg, CD73 is rare on the surface of human Treg, with fewer than 1% of peripheral $CD4^+$ T cells co-expressing CD39 and CD73 (Dwyer *et al.*, 2010; Schuler *et al.*, 2014). Their co-expression has been observed on T cells from human gastric tissue and is upregulated on nTreg following TCR activation *in vitro* (Alam *et al.*, 2008; Schuler *et al.*, 2014). Studies have observed that surface CD73 expressed on *in vitro* induced iTreg is shed soon after its expression, so may have been missed in this study (Schuler *et al.*, 2014). However, CD39 and CD73 do not need to be co-expressed on the same cell to have an immunosuppressive effect; different cells expressing each of the markers can collaborate

and mediate the breakdown of ATP to adenosine and therefore induce immune suppression (Schuler *et al.*, 2014).

Using an *in vitro* co-culture system consisting of irradiated HNSCC tumour cells, immature dendritic cells, $CD4^+CD25^-$ T cells, IL2, IL10, and IL15 to model the HNSCC TME, Bergman *et al.* (2007) observed the induction of Tr1 cells, with a $CD4^+CD25^-CD39^+$ phenotype. In this study, the dissociated tumour tissue derived CM were the only CM to contain IL10. However, as the vast majority of cells observed in this study expressed CD25 following culture with CD3/CD28 activation beads, it is unlikely that the cells collected after culture with CM are the IL10/IL15-induced Tr1 cells described by Bergmann *et al.* (2007). In addition to $CD4^+CD39^+FoxP3^+$ Treg, a second population of $CD39^+$ T helper cells has been identified that are $CD25^-FoxP3^-$ and have a memory phenotype (Moncrieffe *et al.*, 2010). These cells are thought to act as reserves, able to convert to $CD39^+FoxP3^+$ Treg following activation (Moncrieffe *et al.*, 2010; Schuler *et al.*, 2012).

Although there are changes in the expression of some of the markers that are associated with Treg, following culture with overnight tumour CM, whether these changes are truly representative of an increase in the level of functional Treg will require further investigation.

### 3.4.6 Different culture medium had no effect on expression of markers

The DMEM based growth medium impeded the proliferation of lymphocytes compared with the specialised lymphocyte growth medium. Interestingly culture in the different medium did not affect the overall viability of the cells. Diluting the cell line and fibroblast GM with lymphocyte GM, alleviated their effects and was comparable to culturing lymphocytes in lymphocyte GM alone. Furthermore, no differences were observed in the expression of Treg markers between the cells cultured in the different GM, indicating that any effects from the CM were likely due to factors released by the HNSCC tumour cells and not due to the differences in the medium used to culture the cells.

### 3.4.7 Conclusion

T cells expressing FoxP3, CD39 and high levels of CD25 are increased in the TIL of HNSCC patients compared with the periphery, indicating enrichment of Treg by the tumour. Although, tumour cells and stroma secrete immunosuppressive TGF-β and IL10, there was

no induction of a Treg phenotype by soluble factors released from HNSCC and associated stromal cells.

# Chapter 4 The effect of soluble factors in the HNSCC microenvironment on the generation of functionally suppressive iTreg from $CD4^+CD25^-$ precursors

## 4.1 Introduction

An increase in the proportion of CD39 expressing cells was observed following culture of $CD4^+CD25^-$ lymphocytes in conditioned medium (CM) from dissociated tumour tissue (Chapter 3). However, studies of human induced Treg (iTreg) have shown that induction of Treg marker expression does not always confer the expected suppressive function. In the current chapter, the association between phenotype and functional iTreg induction was investigated.

### 4.1.1 Analysis of Treg function

It has been shown that TGF-β can induce $FoxP3^+$ cells both in this study (Chapter 3) and in the literature (Section 1.2.2.4.4). However, in some studies these cells were found not to be functionally suppressive. While FoxP3 expression is a specific marker of mouse Treg, in humans it is also found transiently expressed in other activated Th cells (Allan *et al.*, 2007). It has been suggested that these TGF-β induced $FoxP3^+$ cells represent only partially differentiated cells and that in addition to TGF-β, other factors may be required for human $CD4^+$ T cells to become fully differentiated /stable Treg (Lu *et al.*, 2010b). Both retinoic acid, a vitamin A metabolite, and the immunosuppressive mTOR inhibitor rapamycin have been shown to enhance the induction of $FoxP3^+$ T cells when used in combination with TGF-β (Wang *et al.*, 2009a; Kawamoto *et al.*, 2010; Lu *et al.*, 2010b; Hippen *et al.*, 2011; Schmidt *et al.*, 2016a; Candia *et al.*, 2017). Although functionality was not assessed in all of these studies, those that did, confirmed the induced cells to be functionally suppressive. Some studies have even observed just IL2 and rapamycin to be sufficient for *de novo* Treg induction (Valmori *et al.*, 2006; Long & Buckner, 2008), however this may require repeated stimulation. Furthermore, it is understood that there may be other factors present in the TME *in vivo* that are also involved in Treg induction.

In addition to the proportion of Treg, there may also be differences in their suppressive ability. Studies comparing peripheral $CD4^+CD25^{hi}$ and $CD4^+CD25^+CD127^-$ Treg from HNSCC patients to those of healthy controls observed that Treg from patients mediate greater suppression of autologous T effectors than their healthy counterparts (Strauss *et al.*,

2007a; Drennan *et al.*, 2013). Different subsets of Treg (nTreg, FoxP3$^+$ iTreg, Tr1, Th3) have been identified that can differ both phenotypically and functionally, including in their mechanism of action and potency of suppression (Section 1.2.2.4.4). For example, the iTreg subsets Th3 and Tr1 rely heavily on secretion of the suppressive cytokines TGF-β and IL10 respectively (Section 1.2.2.4.3). Understanding the role these subsets may play in cancer is hindered by the fact that these cells are not well defined and specific markers have not been identified. Furthermore, many of the markers traditionally used to identify Treg, such as FoxP3, CTLA-4 and GITR, are also upregulated on other activated Th effector cells. Therefore, conclusions from changes to the overall number of Treg defined by marker expression should be made cautiously. *In vitro* suppression assays and the secretion of certain cytokines are useful in measuring the suppressor function of potential Treg cells.

#### 4.1.1.1 *Suppression assays*

Tregs can cause suppression by a variety of mechanisms; however, the end result is anergy and/or death of the responder cell (Section 1.2.2.4.5). *In vitro* suppression assays use fluorescent dyes, such as CFSE to measure the rate of proliferation of responder cells in the presence of suspected Treg populations (Section 2.7). These functional assays remain the best method of identifying Treg due to the lack of a definitive phenotypic marker.

Both nTreg and *in vitro* induced iTreg have been shown to successfully suppress CD4$^+$ and CD8$^+$ T effectors. It is thought that the primary mechanism of suppression may vary between Treg, particularly between nTreg and iTreg, and understanding this will aid in the further identification of Treg subset roles in causing immunosuppression.

#### 4.1.1.2 *Soluble factors and iTreg*

Induced Treg are thought primarily to use cytokine mediated suppression mechanisms. For example, Tr1 and Th3 release high levels of IL10 and TGF-β, respectively. Interestingly, Tr1 cells are also FoxP3$^-$ and CD39 has been shown to be present on a high proportion of these cells in HNSCC patients. Given that in the current study, culture with tumour CM induced expression of CD39 on CD4$^+$CD25$^-$ precursors, without effecting FoxP3 expression, it was of particular interest to investigate IL10 secretion by these cells.

### 4.1.2 Chapter aims and experimental design

To assess whether an increase in CD39 expression on $CD4^+CD25^-$ lymphocytes cultured in CM collected from dissociated tumour biopsies is representative of an increase in Treg, their ability to suppress autologous $CD4^+CD25^-$ T cells was assessed. In addition to CFSE suppression assays, medium was collected following the culture of $CD4^+CD25^-$ lymphocytes in either growth medium (GM) or tumour biopsy derived conditioned medium (CM) and the level of IL10 was assessed by ELISA (Figure 4.1). TGF-β was not measured as it is secreted in an inactive form so was not expected to contribute toward suppression under these conditions, (Section 3.4.4). The CD39 expression following culture of $CD4^+CD25^-$ cells with GM or CM previously measured by flow cytometry (Section 3.3.5) and was correlated with IL10 secretion.

Given the suspected role of tumour derived soluble factors in the induction of iTreg, it was hypothesised that cells cultured with CM collected from HNSCC and stromal cells could induce suppressive iTreg that prevent the proliferation of responder T cells in co-culture and release high levels of suppressive cytokines.

## 4.2 Methods

### 4.2.1 Induction of Treg from $CD4^+CD25^-$ lymphocytes using TGF-β and rapamycin

In order to ensure the CFSE assays were properly set up to detect any suppression due to induction of iTreg by CM, a positive iTreg control was required. Some studies have reported that TGF-β alone is inadequate for the induction of Treg *in vitro* (Tran *et al.*, 2007), therefore rapamycin was also added to cultures. Sorted $CD4^+CD25^-$ lymphocytes from healthy individuals (Section 2.2.2) were seeded at 5 $x10^4$ cells/well in lymphocyte growth medium (X-Vivo 20 medium; containing 10% human AB serum and 0.1 U/ml penicillin and 0.1 mg/ml streptomycin) in 96 well round bottom plates. Lymphocytes were stimulated with anti-CD3/anti-CD28 DynaBeads (Gibco) at a ratio of 1:1 (cell: beads) and IL2 (100 U/ml; AbD Serotec) only, or with additional TGF-β (5 ng/ml; AbD Serotec) with and without rapamycin (100 ng/ml; Thermo Fisher Scientific). Following five days incubation at 37˚C in a 5% $CO_2$ humidified atmosphere, cells were collected, separated from DynaBeads using a

magnet (Section 2.2.3.1) and either used in CFSE assays (Section 2.7) or labelled with antibodies for CD25, CD39, CD73, CD26 and FoxP3 for flow cytometry (Section 3.2.8).

### 4.2.2 CFSE assays to determine the suppressive ability of $CD4^+CD25^-$ lymphocytes following culture in CM or with TGF-β and rapamycin

CFSE assays were carried out according to Section 2.7.2. $CD4^+CD25^-$ T cells from leucocyte cones of healthy donors were cultured with TGF-β, or TGF-β and rapamycin to induce iTreg (Section 4.2.1) or with CM (Section 2.7.2.1) herein called "pre-conditioned" cells, before co-incubation with CFSE-stained autologous $CD4^+CD25^-$ T cells (Sections 2.7.2.2 and 2.7.2.3).

CFSE co-cultures were incubated for four days before cells were analysed by flow cytometry (Section 2.7.2.3). Given that the number of $CD39^+$ cells induced following culture in CM varied between experiments (ranging from 20 to 40%; Chapter 3) a range of ratios of preconditioned T effector cells to T responder cells was used (Table 4.1).

**Table 4.1: Ratios of preconditioned cells to CFSE stained T responder cells used in CFSE assays and the corresponding cell numbers that were plated**

| Pre-conditioned cells : T responder cells | |
|---|---|
| **Ratio** | **Numbers plated ($x10^4$)** |
| 4:1 | 20 : 5 |
| 2:1 | 10 : 5 |
| 1:1 | 5 : 5 |
| 1:2 | 2.5 : 5 |
| 1:4 | 1.25 : 5 |
| 1:8 | 0.63 : 5 |
| 1:16 | 0.31 : 5 |

Analysis of CFSE data was carried out using Modfit software (Section 2.7.3). The percentage suppression by pre-conditioned $CD4^+CD25^-$ T lymphocytes was defined relative to that seen in the population of $CD4^+CD25^-$ T responder cells cultured alone with IL2 and CD3/CD28 DynaBeads (Section 2.7.3).

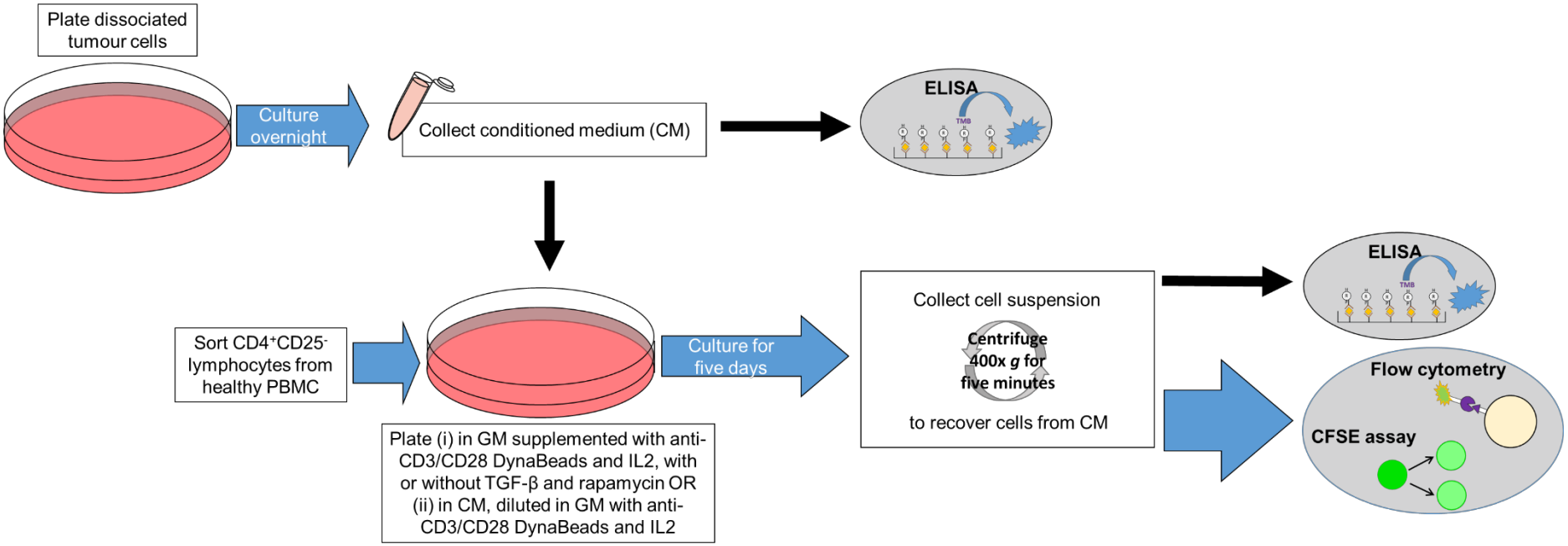


**Figure 4.1: Schematic overview of methods and analysis used in Chapter 4**

HNSCC tumour biopsies were dissociated and cells were plated in GM and incubated overnight at 37°C, 5% $CO_2$ in a humidified atmosphere. Conditioned medium was collected the next day and centrifuged at 400 x *g* for five minutes to remove any cells and debris, before being stored in aliquots at -80°C. When required CM was thawed and the levels of IL10 and TGF-β were measured by ELISA. As a positive control for iTreg induction (i) $CD4^+CD25^-$ T lymphocytes were sorted from healthy PBMC and cultured in GM supplemented with and without TGF-β and rapamycin and with CD3/CD28 DynaBeads and 100 U/ml IL2 for T cell activation. To assess the ability of soluble factors in the CM to induce Treg, (ii) $CD4^+CD25^-$ T lymphocytes from healthy PBMC were cultured with CM diluted 1:3 in GM supplemented with CD3/CD28 DynaBeads and 100 U/ml IL2. Following five-day incubation at 37°C, 5% $CO_2$ in a humidified atmosphere the cells suspension was collected and centrifuged at 400 x *g* for five minutes. The CM was stored in aliquots at -80 °C and IL10 and TGF-β levels were determined by ELISA. The recovered T cells, were stained for Treg markers for flow cytometry (Chapter 3) or co-incubated with CFSE-stained $CD4^+CD25^-$ autologous T responder cells for suppression assays.

### 4.2.3 Measurement of IL10 secretion by ELISA

As some iTreg secrete high levels of IL10, ELISA were carried out on the CM collected from tumour-dissociated tissue (Table 4.2; Section 2.2.4), and on the medium collected after the five day culture of $CD4^+CD25^-$ lymphocytes with CM or GM (Figure 4.1), to measure the levels of IL10 (human IL10 ELISA MAX, Biolegend; Section 2.4). Samples were diluted 1 in 8 prior to being tested as this had been determined from previous experiments to give values within the range detectable by ELISA.

**Table 4.2: Origin and tumour stage of patient tumour samples from which conditioned medium was derived**

| Origin | Tumour Stage | Nodal Status | N |
|---|---|---|---|
| Larynx | T3 | N0 | 1 |
| Larynx | T3 | N2c | 1 |
| Larynx | T4 | N0 | 4 |
| Larynx | T4 | N2b | 2 |
| Node (unknown primary) | T0 | N2 | 2 |

### 4.2.4 Statistical Analysis

Statistical analysis was carried out using SPSS 24 (IBM). A one-way ANOVA with Tukey's post hoc test was used to compare differences in Treg marker expression on $CD4^+CD25^-$ lymphocytes cultured in GM alone or GM supplemented with TGF-β with and without rapamycin. For percentage suppression caused by cells cultured in GM alone, GM with TGF-β or TGF-β and rapamycin, a two-way ANOVA was carried out with Tukey's post hoc tests. For comparisons between the percentage suppression of $CD4^+CD25^-$ lymphocytes cultured in various dissociated tumour CM and those cultured in GM, statistical analysis was not carried out due to small sample numbers. In order to determine any correlation between the percentage of cells expressing the surface marker CD39 following culture, and IL10 secretion, a Pearson's correlation was performed. Statistically significant differences (*) are those where $p<0.05$ (**$p<0.01$, ***$p<0.001$). All error bars show SEM.

## 4.3 Results

### 4.3.1 Inducing Treg with TGF-β and rapamycin

$CD4^+CD25^-$ lymphocytes from four healthy donors were cultured with TGF-β or TGF-β and rapamycin to induce Treg. Lymphocyte populations cultured with TGF-β or with TGF-β and rapamycin had a greater percentage of $FoxP3^+$ (25.2±10.6% and 26.6±6.8%) and $CD39^+$ (7.8±2.5 and 9.7±2.1) cells compared with those cultured in GM alone (11.5±3.8% and 3.9±1.7%; Figure 4.2a), however the difference was not significant. Little or no effect on FoxP3 and CD39 expression was observed following the addition of rapamycin to the cultures, compared with TGF-β alone. CD73 expression was very similar between the cells cultured in GM, TGF-β or TGF-β and rapamycin (2.9±0.8%, 3.0±0.9% and 3.35±1.1%, respectively). CD26, which is usually absent on Treg, was significantly lower in cultures incubated with TGF-β and rapamycin compared with those incubated in GM alone (Figure 4.2b; $p$=0.006). The percentage of cells expressing FoxP3 varied considerably between cells from different donors, ranging from 4.8 to 25.3% in the GM only cultures, 5.1 and 53.1% in cultures supplemented with TGF-β and 12.8 and 39.2% in cultures supplemented with TGF-β and rapamycin. In cells from three of the donors, FoxP3 expression approximately doubled in cells cultured with TGF-β, compared to those in GM alone (Figure B.5, Appendix B). In the fourth donor (Figure B.5, Appendix B) the percentage of $FoxP3^+$ cells was not different when TGF-β was added to cultures but did increase following the addition of rapamycin. Rapamycin also caused a further increase compared to using TGF-β alone in two of the other three donors, and in the third the percentage of $FoxP3^+$ cells was reduced with rapamycin treatment. The change in CD26 expression was much more consistent between donors, with cells from all four donors showing a decreased percentage of $CD26^+$ lymphocytes when cultured with TGF-β than without, and the lowest percentages when cultured with TGF-β and rapamycin.

There was considerable difference in the dual expression of CD26 and FoxP3 between the three different conditions (Figure 4.2c). TGF-β in the GM led to a greater percentage of $FoxP3^+CD26^-$ cells than in cultures without (4.7±2.3% *vs*. 0.5±0.2%). The addition of rapamycin further increased the number of $FoxP3^+CD26^-$ cells from all four donors (8.7±3.3%) to a level which was significantly greater than control cultures ($p$=0.06). Furthermore, a clear decrease in the level of CD26 expression was observed in the cells cultured with rapamycin and TGFβ compared to those in TGFβ alone. Extending the Treg

gate to also include FoxP3$^{+}$ cells with low CD26 expression, in addition to no CD26 expression, further increases these differences. For example, using an arbitrary cut-off point just below $10^{3}$ for CD26$^{low}$, the mean percentages of FoxP3$^{+}$CD26$^{-/low}$ Treg become 1.1±0.3%, 8.9±2.7% and 14.3±4.9% for GM only, GM+TGF-β and GM+TGF-β+rapamycin, respectively. Dual expression of CD39 and CD73 was not observed on any cells under any of the culture conditions.

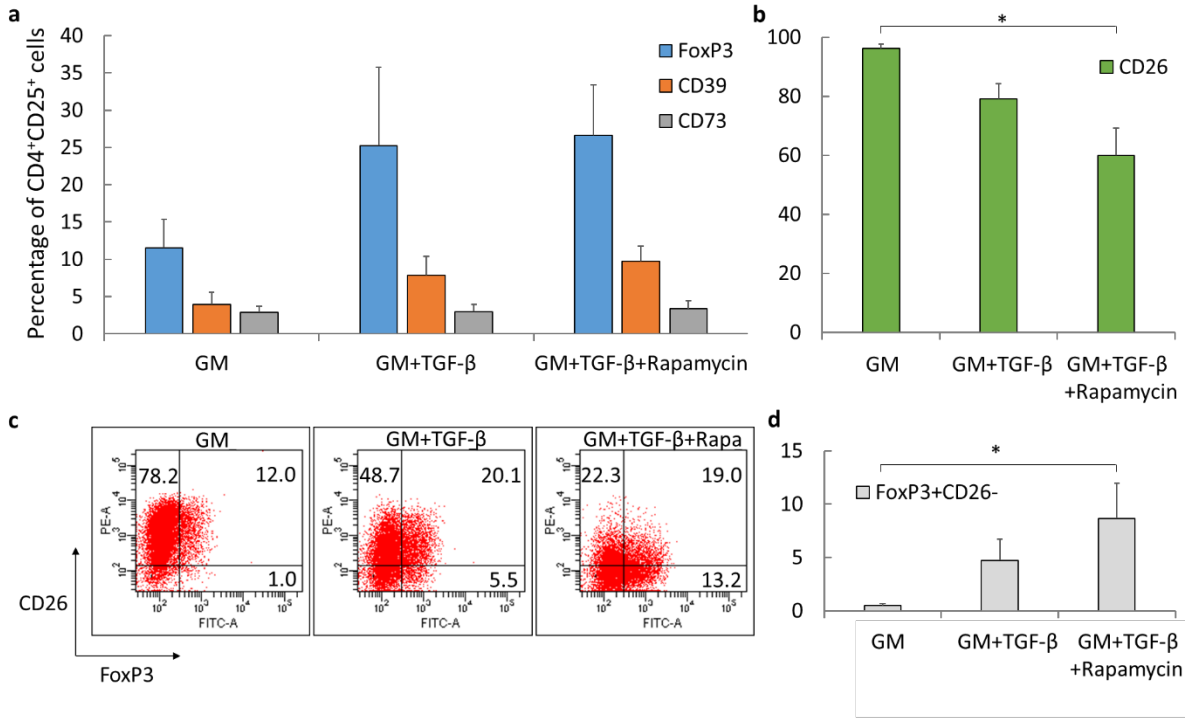


**Figure 4.2: Induction of Treg makers on CD4$^{+}$CD25$^{+}$ lymphocytes by TGF-β and TGF-β with rapamycin**
Mean percentage of CD4$^{+}$CD25$^{+}$ lymphocytes expressing Treg markers a) FoxP3, CD39 and CD73 and b) the negative marker CD26 and c) representative scatter plots and d) mean percentage of dual CD26 and FoxP3 expression, following 5 day culture of CD4$^{+}$CD25$^{-}$ from the PBMC of healthy controls (n=4) in growth medium containing anti-CD3/CD28 DynaBeads and IL2 (100 U/ml), with or without TGF-β (5 ng/ml) and rapamycin (100 ng/ml). Statistical analysis was carried out using a one-way ANOVA with Tukey's post hoc test. Significant results (*) are considered as those where $p<0.05$.

### 4.3.2 Suppressive activity of iTreg induced with TGF-β and rapamycin

Due to previous reports that TGF-β alone may be insufficient to produce suppressive Treg, rapamycin was also added to some CD4$^{+}$CD25$^{-}$ cells in order to generate a positive control for CFSE suppression assays. Control cultures of CFSE-stained CD4$^{+}$CD25$^{-}$ activated T responders only, contained up to seven peaks that were distinguishable from unstained cells after four days (Figure 2.17; Section 2.7.3). All cultures with pre-conditioned cells, including GM control cultures, caused considerable suppression of responder cells in co-cultures,

particularly at the higher ratios (76.4±2.8% at 4:1 and 10.4±4.4% at 1:16 GM+IL2 pre-conditioned cells: T responders; Figure 4.3). As the number of pre-conditioned cells decreased so did the suppressive effects. In all cases cultures containing TGF-β caused significantly more suppression than those without; however at the highest ratios of pre-conditioned cells to T responders, the difference was smaller. At all but the lowest ratio, the cells pre-conditioned with rapamycin and TGF-β showed the greatest suppression, although the difference between that and TGF-β alone was not significant. The biggest relative difference in suppression between TGF-β and rapamycin pre-conditioned cells compared with GM controls was observed at a 1:8 ratio, with a 2.2-fold increase in suppression between cultures with TGF-β and rapamycin and those without.

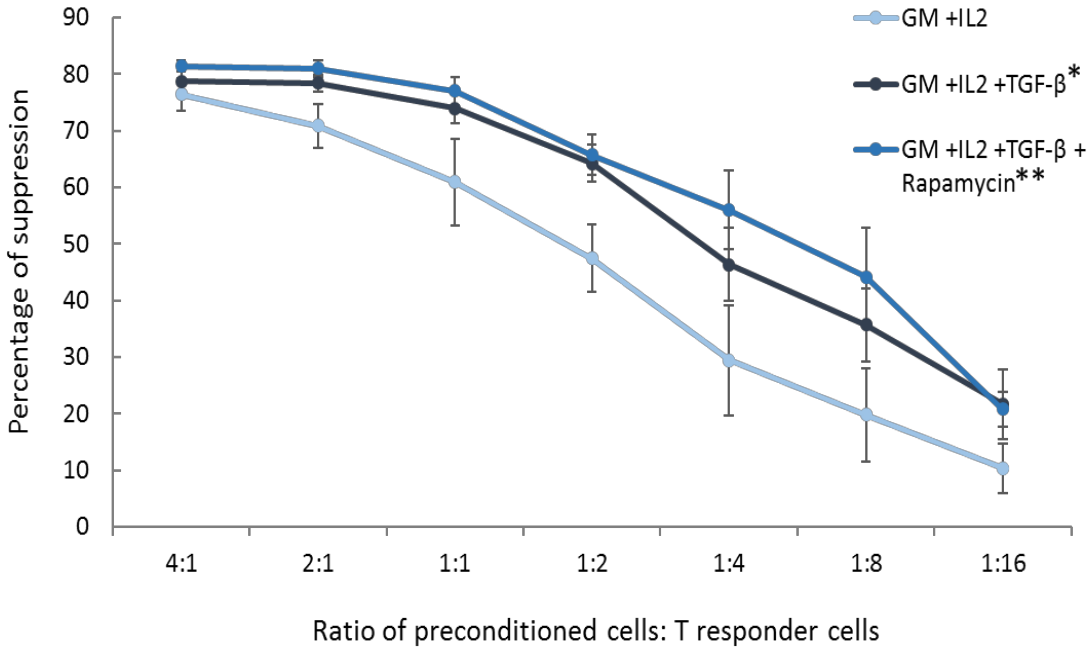


**Figure 4.3: Percentage suppression of autologous T helper cells by pre-conditioned $CD4^+CD25^-$ cells**
Mean percentage suppression of $CD4^+CD25^-$ T responder cells (n=4) by autologous "pre-conditioned" $CD4^+CD25^-$ cells that had undergone five days of culture in growth medium containing IL2 (100U/ml) and anti-CD3/CD28 DynaBeads (GM), GM with TGF-β (5ng/ml) and GM with TGF-β (5ng/ml) and rapamycin (100ng/ml). Pre-conditioned T cells and CFSE-stained responder cells were co-cultured for 4 days at a variety of ratios, with anti-CD3/CD28 DynaBeads and IL2 (100U/ml), before analysis by flow cytometry and Modfit software. Statistically significant differences between the control GM only group and cultures containing TGF-β or TGF- β and rapamycin (*$p<0.05$ and **$p<0.01$) were determined by two-way ANOVA with Tukey's post hoc test, no significance was observed between cultures with TGF-β and those with TGF-β and rapamycin.

### 4.3.3 Suppressive activity is not induced in $CD4^+CD25^-$ T cells by soluble factors in tumour-derived conditioned medium

Due to limited amount of dissociated tumour CM, CFSE assays for each CM (n=4) were carried out on T cells isolated from only two healthy controls. Overall, there was no increased suppression of T responder cell by cells preconditioned with CM compared to those cultured in GM (Figure 4.4). Suppression decreased with increasing responder cell proportion for all pre-conditioned cells cultured in GM but incubating the cells with tumour CM showed variable results. In the case of one of the CM greater suppression was observed from the cells cultured in GM than those cultured in CM at all four co-culture ratios, with the percentage suppression decreasing with increasing responder cell proportions (Figure 4.4a). The results with the other three CM were less consistent, with the greatest suppression differing at different ratios. There was considerable variability in the percentage of suppression between the different donors. At the highest ratio of GM pre-conditioned cells to responder cells (2:1) the percentage of expression ranged between 55% and 86% and this difference increased to between 60% and -12% (ie a rate of proliferation exceeding the T responder cells cultured in the absence of any pre-conditioned cells) at the lowest ratio of 1:4.

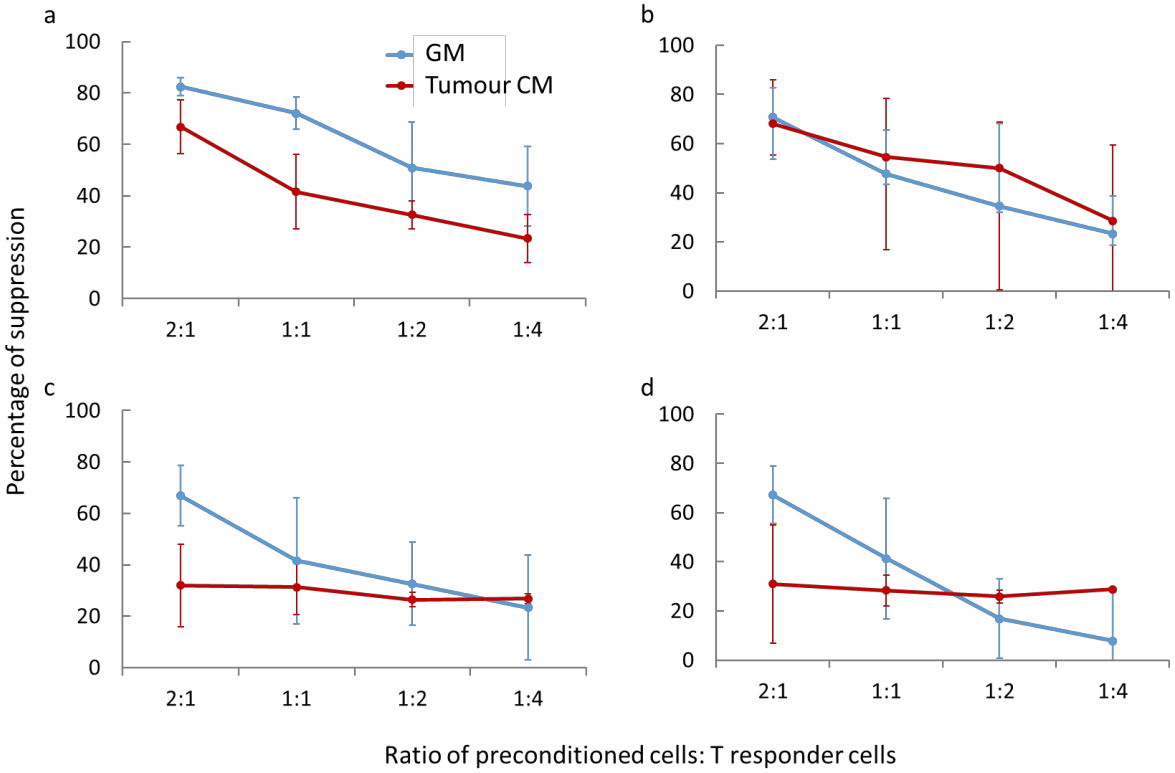


**Figure 4.4: Percentage suppression of autologous T helper cells by autologous pre-conditioned $CD4^+CD25^-$ cells cultured with tumour-derived CM**

Mean percentage suppression of $CD4^+CD25^-$ T responder cells (n=2) by autologous $CD4^+CD25^-$ cells that had undergone five days of culture in growth medium containing IL2 (100U/ml) and anti-CD3/CD28 DynaBeads (GM; blue), or tumour dissociated CM diluted (1:3) in growth medium containing IL2 (100U/ml) and anti-CD3/CD28 DynaBeads (red). Pre-conditioned T cells and CFSE-stained responder cells were co-cultured for four days at a variety ratios, with anti-CD3/CD28 DynaBeads and IL2 (100U/ml), before analysis by flow cytometry and Modfit software. Charts a-d represent results from $CD4^+CD25^-$ cells incubated with four different tumour-derived CM.

### 4.3.4 Soluble factors in tumour CM do not induce IL10 secretion from Th cells

All tumour dissociated CM tested (n=8; Table 4.2) contained IL10, while IL10 was not detectable in GM (Figure 4.5). The IL10 in the diluted CM before culture, ranged from 37.4±2.3 pg/ml to 442.7±0.1 pg/ml. $CD4^+CD25^-$ lymphocytes from healthy donors (n=7) were incubated in either GM alone or in 1 in 3 diluted CM from dissociated tumours (n=8). In every experiment, the level of IL10 was greater in the cells cultured in GM than those cultured with any of the CM. The level of IL10 following culture of $CD4^+CD25^-$ cells in GM varied greatly between the different healthy samples (from 260.9±18.0 pg/ml to more than 2000 pg/ml). Cells from three of the donors released a moderate level of IL10 following culture in GM, with cultures secreting less than 600 pg/ml (Figure 4.5a, b and c), while cells

from the other four donors secreted much higher levels of IL10, over 1500 pg/ml (Figure 4.5 d, e, f and g).

The levels of IL10 detected following culture of the $CD4^+CD25^-$ T cells from healthy donors with CM in 7/18 cases was lower or similar to the levels in the medium prior to culture. In 11/18 cases IL10 was higher following culture, however, the increase in IL10 was lesser (up to 851±38 pg/ml; Figure 4.5g), than that seen in the cells cultured in GM (>2000 pg/ml). There was a considerable amount of variability between the effect of the same CM on different $CD4^+CD25^-$ donor T cells and on the effect of different CM on the same donor cells. The biggest increase in the level of IL10 following culture was seen in cells from the donors represented by Figure 4.5 f and g. In these two cases all the CM induced IL10 secretion from these cells, with between 2.7 and 23.7-fold more IL10 in the medium after culture. The effect of CM on cells from the other five donors was less consistent as there was not always an increase in IL10 concentration after culture. Interestingly the CM that induced the greatest increase in IL10 concentration (37.4 prior to culture *vs* 887.9 pg/ml after culture Figure 4.5g), was used to culture cells from two other donors and in both cases it was the only CM of those tested to induce an increase in IL10 release (4.6-fold and 3.3-fold that prior to culture; Figure 4.5a and c).

The highest level of IL10 was always observed following the culture of $CD4^+CD25^-$ lymphocytes with GM only, rather than with the tumour-derived CM. This finding was consistent between the cells of different donors.

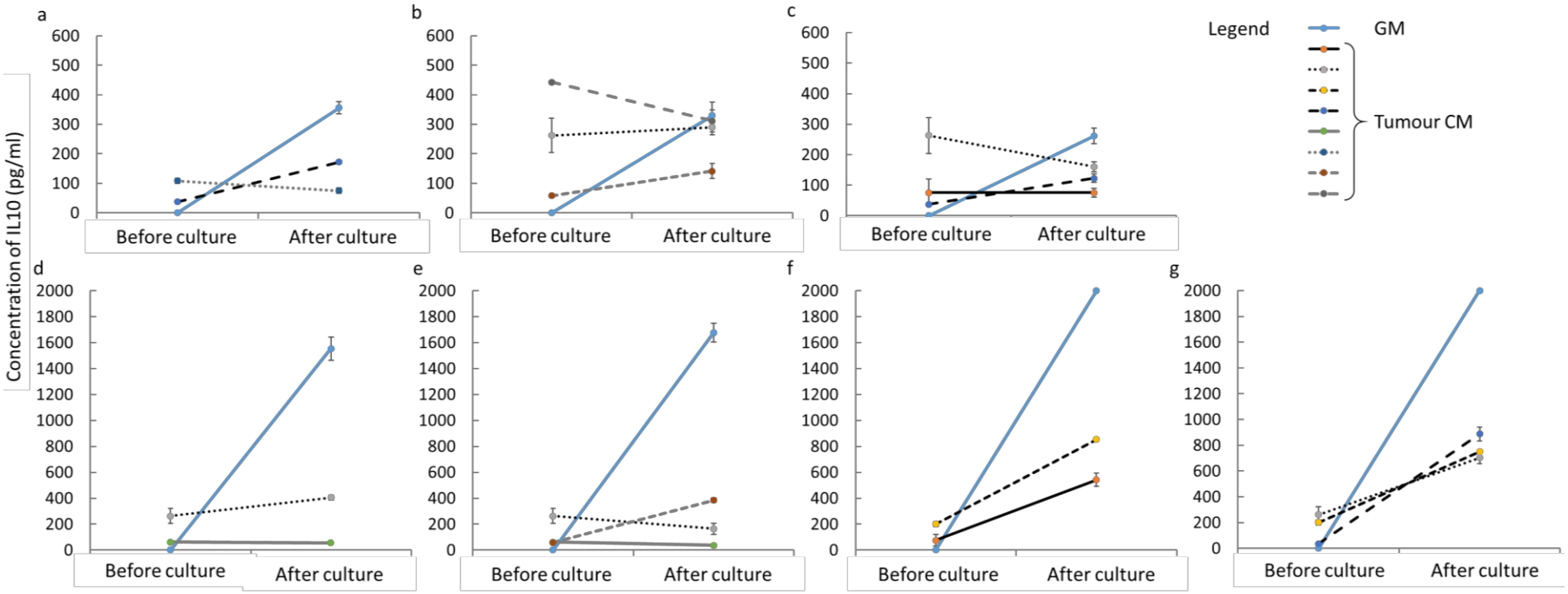


**Figure 4.5 IL10 concentration (pg/ml) in GM or CM used to culture healthy $CD4^{+}CD25^{-}$ T lymphocytes and in the medium collected following 5 days incubation**
$CD4^{+}CD25^{-}$ T lymphocytes from healthy PBMC (a-g) were cultured in CM from eight dissociated tumour diluted 1:3 in GM (black and grey lines) or GM alone (blue line), all with IL2 (100U/ml) and CD3/CD28 DynaBeads. IL10 concentration was measured in the medium before and after culture. Each graph shows mean data from duplicate wells of an experiment carried out on one healthy donor ±SD. NB. In graphs f and g the level of IL10 in the medium collected from the cells cultured in GM exceeded the level of 2000pg/ml that could be measured by the BioLegend ELISA MAX kit.

In order to determine whether the percentage of cells expressing CD39 (Section 3.3.4) was associated with the level of IL10 secreted following incubation of $CD4^+CD25^-$ T cells with GM or dissociated tumour CM, a Pearson's correlation was performed. The concentration of IL10 in the CM prior to culture was subtracted from the concentration after culture, in some cases this gave a negative value as the level of IL10 was lower following culture. Overall, there was a negative correlation between the percentage of CD39 expression and the IL10 secreted over the 5-day culture period (Figure 4.6; r = -0.604 $p$<0.001).

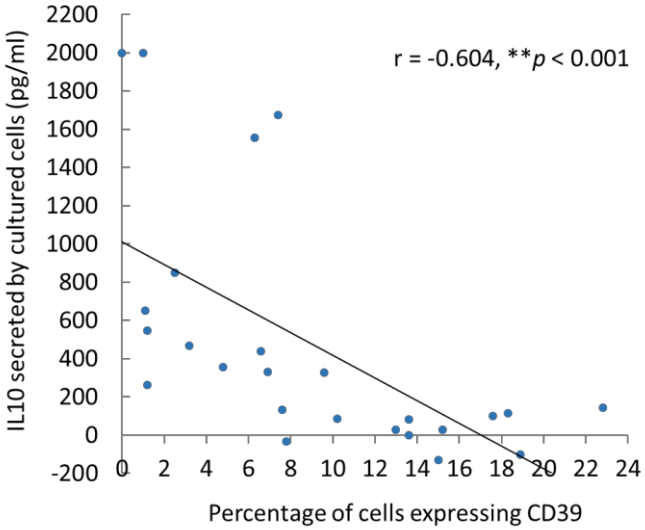


**Figure 4.6: Scatter plot of the secretion of IL10 in cultures of $CD4^+CD25^-$ lymphocytes cultured with GM or dissociated tumour CM against the percentage of $CD39^+$ cells after culture**

$CD4^+CD25^-$ lymphocytes sorted from healthy individuals were cultured for five days with 1 in 3 diluted dissociated tumour CM or in GM alone, in the presence of IL2 and CD3/CD28 DynaBeads. Cells were stained for CD25 and CD39 to determine the percentage of the $CD39^+$ lymphocytes in the $CD25^+$ gate after culture. IL10 secretion during the culture period was calculated as the difference between the level of IL10 in the medium prior to and after culture measured by ELISA. Pearson's correlation was performed to investigate the correlation between the factors.

## 4.4 Discussion

### 4.4.1 TGF-β and rapamycin-induced FoxP3+ T cells are suppressive Treg

The culture of $CD4^+CD25^-$ T lymphocytes with TGF-β and rapamycin led to a significantly greater percentage of Treg in the cultures, measured by an increase in the percentage of $CD4^+CD25^+$ T cells with a $FoxP3^+CD26^-$ phenotype compared to control cultures. Following the method used by Mandapathil *et al*, (2012), the current study defined Treg as $CD26^-$, using the isotype control to define $CD26^+$ expression (Section 2.3.4) and thus gating the cells that did not exceed the level of fluorescence of the isotype. In contrast, Salgado *et al.* (2012) have described Treg as being $CD26^{-/low}$, and included cells with low levels of CD26 expression in their Treg gate. Depending on where the cut off for low expression is placed this would increase the percentage of iTreg. Interestingly, in the current study the only single marker to show a statistically significant difference when cultured with TGF-β and rapamycin was CD26. In contrast to the previous observations of Treg marker expression following the culture of $CD4^+CD25^-$ T cells with TGF-β (Section 3.3.3), neither FoxP3 nor CD26 were significantly different when cultured with TGF-β alone compared to the control cultures. However, the same overall trend was observed in the expression of all the markers, with more cells expressing CD39 and FoxP3 and fewer expressing CD26 when cultured with TGF-β than without. The addition of rapamycin to cultures made little difference to the percentage of cells expressing the positive Treg markers (FoxP3 and CD39), however, did considerably increase the proportion of cells with a $CD26^-$ phenotype. The failure to observe a significant difference in FoxP3 and CD26 expression following culture with TGF-β compared to media alone, could be due to differences between donors. The $CD4^+CD25^-$ lymphocytes used in this chapter were isolated from the peripheral blood of four different healthy donors to those used in chapter 3. The profile of these donors is unknown, and factors such as differences in age and sex may contribute toward the different responses observed *in vitro*. Although, overall the mean percentage of cells expressing FoxP3 when cultured with TGF-β alone, and when cultured without TGF- β, was similar to results in the previous chapter (Section 3.3.3), the variability between the percentage of cells expressing FoxP3 was much greater in the cells from the four donors in the current chapter.

Both treatment with TGF-β and TGF-β/rapamycin not only induced an iTreg phenotype but these cells were suppressive compared with control cultures for all four donors, despite variability in marker expression. Rapamycin did not significantly increase the suppressive

capacity of cells compared to TGF-β alone. This contradicts previous studies that have observed an increase in suppressive function of cells cultured with rapamycin and TGF-β, compared to TGF-β only (Hippen *et al.*, 2011; Candia *et al.*, 2017). For example, despite finding no increase in the percentage of $FoxP3^+$ Treg with the addition of rapamycin and TGF-β to cultures of naïve T cells, compared to just TGF-β (~50-60%), Candia *et al.* (2017) observed the cells cultured with rapamycin were more suppressive. The additional presence of rapamycin caused the induction of cells that were roughly four times as suppressive of $CD4^+CD25^-$ proliferation, at 1:16 ratio of suppressors to responders, compared to those cultured with TGF-β only. Schmidt *et al*. (2016) compared different methods of iTreg induction and found no difference between suppression induced by cells stimulated in the presence of TGF-β and those without. However, the addition of both rapamycin and retinoic acid led to the induction of suppressive iTreg, down to ratios of 1:4 suppressor T cells: T responders in CFSE assays.

In the current study, the levels of $FoxP3^+$ lymphocytes induced following the culture of $CD4^+CD25^-$ cells with TGF-β with and without rapamycin failed to reach the levels observed by either Candia *et al*. (2017) or Hippen *et al*. (2011). However, in the study by Hippen *et al*. (2011), a similar percentage of $FoxP3^+$ cells was observed following the culture of $CD4^+CD25^-CD45RA^+$ lymphocytes with IL2 alone as was seen on the $CD4^+CD25^+$ investigated in the current investigation (11±1% *vs*. 11.5±3.8% respectively). Hippen *et al*. (2011) noted that the addition of rapamycin led to a considerable increase in the percentage of cells expressing high levels of FoxP3 (31±12%), whereas without rapamycin the majority of cells were $FoxP3^{lo}$ with only 5±2% expressing high levels. The same study, co-cultured CFSE stained autologous PBMC with the cells pre-treated with and without TGF-β and/or rapamycin, and found that $CD4^+CD25^-CD45RA^+$ that were TCR stimulated and cultured with IL2 and TGF-β were no more suppressive than those cultured with IL2 alone. However, in line with the increased expression of FoxP3, the addition of rapamycin led to an approximate doubling in percentage suppression.

Differences between the current study and those discussed could be attributable to differences in the methods used for the generation of iTreg. For instance, all of the other studies induced Treg from naïve T cells, either by sorting out $CD4^+CD25^-CD45RA^+$ or $CD4^+CD45RA^+$ cells. The $CD4^+CD25^-$ cells used in this thesis may also include some $CD45RA^-CD45RO^+$ memory T cells, which may respond differently in the presence of these

cytokines. Hippen *et al*. (2011) also cultured cells for a longer period of seven days, compared to the five days used in the current study, in order to induce Treg. Following the induction of iTreg, Candia *et al*. sorted $CD4^+CD25^{hi}CD127^-$ cells from the induced cultures for use in suppression assays; however, neither the current study nor Hippen *et al*. accounted for the proportional differences of Treg in different culture conditions. Additional differences between the types of responder cells used in the CFSE co-cultures may contribute to the discrepancies observed between this study and others. Overall, although there were differences between the marker expression, the current study observed little benefit of adding rapamycin to the cultures, over using TGF-β alone in terms of suppression.

### 4.4.2 $CD39^+$ T cells induced by dissociated tumour CM were not suppressive

Soluble factors released by dissociated tumour cells induced the expression of CD39, an ectonucleotidase associated with iTreg, on $CD4^+CD25^+$ T cells. However, CD39 expression is not exclusive to Treg, therefore this upregulation may not be solely indicative of Treg induction. In order to clarify this, the suppressive activity of these $CD39^+$ cells was determined. There was little difference in suppression induced by cells cultured in three out of the four dissociated tumour-derived CM compared with GM controls, while cells cultured in the fourth CM were surprisingly less suppressive than controls. Due to the variation in the percentage of $CD39^+$ cells in the cultures, a range of ratios were used, between 2:1 and 1:4 preconditioned T cells: T responder cells. All preconditioned cells suppressed responder $CD4^+CD25^-$ T lymphocytes in co-cultures, particularly at high ratios. This is supported by other studies, for example in the studies described above (Section 4.4.1) cells cultured in GM with IL2 were observed to suppress proliferation of $CD4^+CD25^-$ lymphocytes by up to 25% (Hippen *et al.*, 2011; Schmidt *et al.*, 2016a; Candia *et al.*, 2017).

Overall, the results of suppression assays in the current study suggest that the $CD4^+CD25^+CD39^+$ T cells induced by tumour CM are not suppressive Treg. However, it is worth noting that these assays do not fully recapitulate the plethora of factors in the TME and the additional factors present *in vivo* may contribute to making this population a suppressive group that could work in concert with other Treg subsets to exert an immunosuppressive environment. For example, CD73 found on tumour cells may be required to mediate the complete breakdown of ATP to adenosine (Section 3.3.4).

### 4.4.3 **Suppressive factors released by $CD4^+CD25^-$ T cells when cultured with CM**

Release of certain cytokines, is more strongly associated with some cell types compared to others, for example Treg release high levels of TGF-β and IL10 while Th1 cells release much lower levels of these cytokines and high levels of IFN-γ. No active TGF-β was detected in CM following the culture of $CD4^+CD25^-$ T cells with either GM or CM so could not contribute to immunosuppression in these conditions. ELISA were performed to detect the level of IL10 in the medium prior to and following the culture of $CD4^+CD25^-$ T cells, in order to determine whether the cells were releasing a factor characteristic of Tr1 cells. In all cases, control cultures in GM alone released more IL10 than any of the cultures containing CM. Although not entirely expected this is in line with a study by Schmidt *et al.* (2016), where higher levels of IL10 mRNA were observed in cultures stimulated in the presence of IL2 alone, compared with IL2 and TGF-β or IL2, TGF-β and rapamycin. The levels of IL10 detected following culture of the $CD4^+CD25^-$ T cells from healthy donors with CM in some cases was lower or similar to the levels in the medium prior to culture. This suggests that IL10 is not being released by these cells, or is being released at a rate comparable to or less than the rate at which it is being depleted from or broken down in the medium. IL10 is a pleiotropic protein and has roles in addition to that of immunosuppression (Section 1.3.1.2). Furthermore, IL10 is also released by other immune cells, including Th2 cells, and so its presence may not be indicative of the presence of Treg. A lot of variability was observed in the suppressive activity of the cells following culture in CM (section 4.4.2) and this was mirrored in the results observed in the measurements of IL10 secretion. An alternative hypothesis to the reduced IL10 production in the populations of cells cultured with CM could be that the proliferation of other IL10 secreting cells (primarily Th2) is being suppressed by factors in the CM. This seems a favourable hypothesis, over that of increased iTreg production in the control cultures due to both resulting populations of cells, showing no differences in ability to suppress responder T cells in co-cultures.

In contrast to the current study, previous research has observed an induction of IL10 producing cells by soluble factors in the TME. Liu *et al.* (2007), observed an increase in IL10 secreted from $CD4^+CD25^-$ T lymphocytes of mice following culture in CM derived from a murine prostate cancer cell line, TRAMP-C2, compared to control cells which had been cultured with GM alone. In these experiments, cells were cultured for five days with CM or GM and then reactivated for two days with antibodies for CD3 and CD28, before

medium was collected and protein IL10 measured by ELISA. This difference may reflect an intrinsic difference between murine and human cells, rather than small methodological variations between studies.

Induced Treg produce high levels of suppressive cytokines. Treg isolated from the TIL of HNSCC patients have been observed to rely primarily on the release of IL10 and TGF-β to mediate suppression, with the addition of neutralising antibodies completely inhibiting the suppression observed in CFSE assays (Strauss *et al.*, 2007b). In order to determine whether the increase in Treg markers following the culture of $CD4^+CD25^-$ T cells with tumour dissociated CM could be due to the TGF-β released by these cells, supernatant was collected after the 5 days of culture and the presence of any active TGF-β was determined by ELISA. No active TGF-β was found to be present in any of the supernatants, suggesting that the increase in Treg markers observed after culture with CM was not dependent on TGF-β. The phenotype of the cells cultured in tumour dissociated CM is also different from that induced by TGF-β, with a much more notable increase in expression of the Treg associated ectonucleotidase, CD39, and little difference in FoxP3 and CD26 expression. TGF-β has been shown to be upregulated in tumours and may contribute to suppression *in vivo*, where activating factors are present. However, due to the lack of activated TGF-β in the conditioned medium following culture with $CD4^+CD25^-$ T cells, its presence in the CM was not suppressive.

In chapter 3, the whole tumour derived CM was the only CM found to contain IL10 (Section 3.3.2), a cytokine that is known to play a role in the conversion of naïve T cells to Tr1 cells. Neither tumour-derived fibroblasts nor UMSCC cell lines secreted detectable levels of IL10. However, the concentrations of IL10 used by others for the induction of Tr1 cells *in vitro* are higher than the levels observed in the tumour-derived CM, between 1.4 ng/ml and 100 ng/ml (Bergmann *et al.*, 2007; Martinez-Forero *et al.*, 2008; Hsu *et al.*, 2015). Although $CD4^+CD25^-$ lymphocytes expressed CD39 following culture in tumour derived CM, a characteristic of Tr1 cells, their failure to suppress autologous $CD4^+CD25^-$ responder cells in co-culture experiments suggest they are unlikely to be functional Tr1 cells.

There is evidence that CD39 expression is upregulated on exhausted T cells. T cell exhaustion is commonly seen in chronic infection and in cancer patients, where due to repeated stimulation, T cells lose their effector function (Wherry, 2011). Increased levels of

$CD8^+CD39^+$ have been observed in patients with the chronic viral infections HIV and hepatitis C (HCV), compared to healthy controls, and their presence correlates with viral load (Gupta *et al.*, 2015). These cells were found to be upregulated in mice after viral infection, and were functionally impaired compared with their $CD8^+CD39^-$ counterparts, suggesting that CD39 expression can represent an exhausted phenotype (Gupta *et al.*, 2015). A greater induction of CD39 expression on $CD4^+$ T cells following activation has also been observed in older individuals; approximately 50% more on those cells from 65-85 year olds than 20-35 year olds. These $CD4^+CD39^+$ cells were not suppressive but instead were metabolically stressed effector cells that were more prone to apoptosis (Fang *et al.*, 2016). Alternatively, it has been suggested that the $CD39^+FoxP3^-$ population of Th cells could be reserves for $FoxP3^+$ iTreg. These cells are not suppressive but can be induced to become suppressive Treg given the correct conditions (Schuler *et al.*, 2012). However, this particular cell population also lacks CD25 expression so is unlikely to be the cells observed following culture of $CD4^+CD25^-$ T cells with CM in the current study, as these were $CD25^+$.

### 4.4.4 **Conclusion**

Soluble factors released by HNSCC and associated stromal cells were not able to induce suppressive iTreg. An induction of CD39 expression on $CD4^+$ T cells was previously observed by soluble factors released by tumour cells; however, $CD4^+CD39^+$ T cells are known to include multiple distinct cell types with various different functions. Given the CD25 expression observed on these cells, they most closely resemble the exhausted phenotype described by Fang *et al*. (2016). Tumours can induce apoptosis or inactivation of T effector cell populations, which may contribute to the shift toward an immunosuppressive microenvironment and evasion of the immune system. Given that some $CD39^+$ Th cells may be more prone to apoptosis (Fang *et al.*, 2016), it may be worth investigating, whether the soluble factors in the CM are enhancing immunosuppression by inducing T cell exhaustion.

# Chapter 5 The effect of soluble factors in the tumour micro-environment on PBMC Viability and Apoptosis

## 5.1 Introduction

Initiation of T cell apoptosis is one of the pathways exploited by tumours to evade the immune system. Furthermore, the immune checkpoints essential for maintaining healthy T cell levels, such as PD1/PDL1 and CTLA-4, have been successfully targeted for cancer therapy in a subset of HNSCC patients (Postow *et al.*, 2015; Zou *et al.*, 2016). However, the contribution of these pathways to tumour evasion is not consistent between tumours and correspondingly these types of therapies are not always appropriate. There has been some evidence for the role of tumour derived soluble factors in apoptosis (Section 1.3.2.4), though further investigation is required. The current chapter aims to determine whether soluble factors released by cells of the TME can induce T cell apoptosis, using the distinctive features of apoptotic cells as a tool for analysis.

### 5.1.1 Soluble factors involved in apoptosis in HNSCC

There is evidence that peripheral lymphocytes from cancer patients, including HNSCC patients, are more prone to apoptosis than those from healthy controls (Saito *et al.*, 1999; Hoffmann *et al.*, 2002). Furthermore, in the study by Hoffmann *et al* (2002), the levels of annexin V binding by $CD8^+$ CTL, measured by multicolour flow cytometry, was greater than that of $CD4^+$ Th from the peripheral blood of HNSCC patients, indicating that CTL are particularly susceptible to apoptosis. The same study also observed that the percentage of $CD3^+$ T cells expressing the Fas receptor was greater in PBMC from HNSCC patients than healthy controls, suggesting a role for the Fas/FasL interaction in T cell apoptosis in HNSCC. Some tumour cells, including HNSCC express FasL on their surface (Feldman *et al.*, 2016), which may disable activated T cells via receptor binding, in the TME (section 1.3.2.4). Furthermore, soluble FasL (sFasL) can be found in patient serum and is released by prostate and colon tumour cells *in vitro* (Liu *et al.*, 1998; Song *et al.*, 2001). An environment supporting T cell apoptosis would perhaps be expected to be high in sFasL, however sFasL is lower in the serum of patients with solid tumours such as HNSCC (Baron *et al.*, 2007), breast cancer, prostate cancers (Kavathia *et al.*, 2009) and thyroid cancer (Owonikoko *et al.*, 2013) compared with healthy controls. Although some have speculated that this may be due to sFasL being bound by the increased number of cells with upregulated Fas expression (Hoffmann *et al.*, 2002), others have observed a protective effect, with sFasL

unable to trigger an apoptotic signal (Tanaka *et al.*, 1998; Hohlbaum *et al.*, 2000). Any sFasL therefore, competes with the more potent pro-apoptotic membrane bound FasL, preventing apoptosis. Other cytokines, such as TNF-α and TNF-α related apoptosis inducing ligand (TRAIL), are also able to activate apoptosis of immune cell via their corresponding receptors (Section 1.3.2.2.1). Co-culture experiments with OSCC cell lines have found evidence of both TRAIL and TNF-α mediated apoptosis of Jurkats (Kassouf & Thornhill, 2008).

Cytokine deprivation can also cause T cell apoptosis, suggesting that the fate of the T cell is in the balance of the cytokine milieu in which it is present. For example, lack of the growth factor IL2 can lead to T cell apoptosis, a proposed mechanism of Treg suppression (Section 1.2.2.4.5). Paradoxically, IL2 increases FasL expression by $CD4^+$ T cells following repeated TCR stimulation, increasing apoptosis (Refaeli *et al.*, 1998). The apparent dichotomy in the role of IL2 in apoptosis highlights the complicated nature of cytokines and the difficulties involved in elucidating their effects.

Although the majority of studies have concentrated on apoptosis induced by cancer cells themselves there is also evidence that soluble factors released by CAF can induce T cell apoptosis. Conditioned medium (CM) from HNSCC CAFs has been found to promote apoptosis of T cells when compared with CM from normal fibroblasts collected from the same patient (Takahashi *et al.*, 2015), highlighting the need to investigate the soluble factors released by the different cells within the TME.

### 5.1.2 **Chapter aims and Experimental Design**

The aim of the current chapter is to determine whether soluble factors released from cells in the TME of head and neck tumours can induce apoptosis of T cells and/or reduce their viability. Thus, PBMC were cultured in CM collected from the overnight culture of dissociated primary tumour, tumour-derived fibroblasts and HNSCC cell lines to assess whether these cells release factors that are able to induce apoptosis. In order to limit the effects caused by reduced growth factors and nutrients as well as toxic waste products in the CM, PBMC or T cells were only cultured for up to 48 hours in CM diluted in complete growth medium (GM). Following culture in CM, cells were collected and incubated with FITC labelled annexin V and PI or with a FITC labelled pan-caspase inhibitor to detect apoptosis using flow cytometry. MTS assays were carried out to determine whether soluble factors in CM impeded T cell growth. It was hypothesised that soluble factors released by

HNSCC and associated stromal cells could induce apoptosis of T cells and reduced their viability.

## 5.2 Materials and Methods

### 5.2.1 Culturing PBMC with conditioned medium for apoptosis assays

PBMC were isolated from leucocyte cones (n=3) from the blood of healthy donors (n=2) and cryopreserved (section 2.1.5). When required, cells were thawed, washed in 10 ml of PBS and centrifuged at 400 x *g* for 5 minutes. Supernatant was removed and cells were resuspended in PBS and counted using trypan blue exclusion (section 2.1.4). PBMC were seeded into 96 well round bottomed plates at 8 x $10^4$ cells/well in 66 µl of complete lymphocyte growth medium (X-Vivo 20 medium containing 5% human AB serum and 0.1 U/ml penicillin/ 0.1 mg/ml streptomycin; section 2.2.3). An additional 33 µl of either complete DMEM GM or CM (Table 5.1), all supplemented with IL2 (final concentration per well of 100 IU/ml; AbD Serotec) and human T activator CD3/CD28 DynaBeads® (1:1, cells:beads; Life Sciences), were added to each well and cells were incubated for up to four days at 37$^o$C, 5% $CO_2$ in a humidified atmosphere. Cells were removed from wells, separated from the CD3/CD28 activation beads using a magnet (Section 2.2.3.1) and washed in PBS, before apoptosis was measured (Section 5.2.4).

**Table 5.1: Characteristics of the dissociated tumour tissue, UMSCC cell lines and tumour-derived fibroblasts that were used for the collection of CM for apoptosis and MTS assays**

| | | HNSCC subsite or cell line origin | ID | Age | Gender | Tumour Origin | TNM Stage |
|---|---|---|---|---|---|---|---|
| **Dissociated tumour tissue** | **Primary tumour** | Larynx | L1 | NA* | Male | Larynx | T3/4N0 |
| | | Oral cavity/ Oropharynx | O1 | NA | Male | Oral | T2N0 |
| | | | O2 | 51 | Male | Right tonsil | T2N0 |
| | | | O3 | NA | Male | Right lingual sulcus | T2N0 |
| | | | O4 | 67 | Female | Right mandible | T4N0 |
| | **Node** | Unknown | N1 | 70 | Male | Unknown | T0N3 |
| | | Larynx | N2 | 55 | Male | Pirriforma fossa | T1N2b |
| **UMSCC cell line** | | Larynx | 12 | 71 | Male | Larynx | T2N1a |
| | | | 11a | 65 | Male | Epiglottis | T2N2a |
| | | Oral cavity/ Oropharynx | 81b | 53 | Male | Tonsillar pillar | T2N0 |
| | | | 47 | 53 | Male | Lateral tongue | T3N0 |
| **Tumour-derived fibroblasts** | | Larynx | L2 | 71 | Male | Right supraglottic larynx | T4N1 |
| | | | L3 | 56 | Male | Supraglottic laryngeal surface of epiglottis | T4N2c |
| | | Oral cavity/ Oropharynx | O1 | NA | Male | NA | T1N0 |
| | | | O5 | 51 | Male | Right tonsil | T2N0 |
| | | Node | N3 | 56 | Male | Supraglottic laryngeal surface of epiglottis | T4N2c |
| | | NA | U1 | 71 | Male | NA | NA |

*NA – information not available

### 5.2.2 **Induction of Jurkat cell death with etoposide**

In the current study, etoposide was used to establish a positive apoptotic control to confirm the PI/annexin V and CaspACE™ binding were working appropriately and gates on apoptotic cells for flow cytometry analysis were set correctly.

Jurkat T cells were seeded into 6 well plates (Sarstedt) at 1 x $10^6$ cells/well in 1 ml of X-vivo 20 medium (Lonza) supplemented with 10% FBS (Biosera), 0.1 U/ml and 0.1 mg/ml penicillin/streptomycin (Lonza) and either etoposide (final concentration of 10 μM; Sigma) or the equivalent volume of DMSO, before being incubated for up to two days at 37ºC, 5% $CO_2$ in a humidified atmosphere. Cells were collected from duplicate wells after 6, 24 and 48 hours incubation, were counted using trypan blue and the number of apoptotic cells was measured using PI/Annexin V and CaspACE™ (section 2.9.2).

### 5.2.3 **Culturing activated T cells with etoposide or conditioned medium for apoptosis assays**

To allow the T cells to proliferate and the proportion of non-viable cells to decrease, PBMC from the blood of healthy donors (n=4) were seeded in complete lymphocyte growth medium supplemented with IL2 (final concentration of 100 IU/ml) and human T activator CD3/CD28 DynaBeads® (1:1, cells:beads), and incubated at 37ºC and 5% $CO_2$ in a humidified atmosphere in 75 $cm^2$ flasks (1 x $10^6$ cells/ml). After 5 days, the non-adherent (activated) lymphocytes were removed and separated from the CD3/CD28 beads using a magnet (section 2.2.3.1). Cells were washed in PBS and counted by trypan blue exclusion (section 2.1.4).

The activated T cells were then seeded in 96 well round bottomed plates at 8 x $10^4$ cells/well in lymphocyte growth medium (section 5.2.2) supplemented with IL2 (100 U/ml), and 5 μM etoposide, or the equivalent volume of DMSO; or in 66 μl of complete lymphocyte growth medium and 33 μl of either complete DMEM GM or CM, supplemented with IL2 (100 IU/ml). The cells were incubated for one day at 37ºC, 5% $CO_2$ in a humidified atmosphere before cells were analysed (section 5.2.4).

### 5.2.4 **Measuring cell death and apoptosis with Annexin V/PI and CaspACE™ FITC-VAD-FMK**

Following culture in CM or with etoposide, Jurkats or PBMC were collected from wells and stained with either PI and Annexin V or CaspACE$^{TM}$ (Section 2.8.2), before analysis by flow cytometry. The proportion of dead cells was defined as those that were $PI^{+}AnnexinV^{+}$ and apoptotic call as $PI^{-}AnnexinV^{+}$ or $CaspACE^{TM+}$.

### 5.2.5 **MTS assay**

To measure the effect of CM on lymphocyte proliferation, PBMC from leucocyte cones were cultured for 5 days in lymphocyte GM, supplemented with IL2 (10 U/ml) and CD3/CD28 DynaBeads for activation (section 2.2.3.1) before being cultured for 24 hours in 33 µl CM (Table 5.1) diluted in 66 µl GM at 37ºC and 5% $CO_2$ (Section 2.6.2). Following incubation, 20 µl MTS reagent (Section 2.6.2) was added to each well for 4 hours at 37ºC and 5% $CO_2$, after which the absorbance of each well was measured on a spectrophotometer at a wavelength of 492 nm.

### 5.2.6 **Statistical analysis**

Statistical analysis was carried out with SPSS 24 (IBM), using parametric tests due to the small n numbers in the experiments (Section 2.10). Independent T tests were used to compare results from PBMC cultured with and without etoposide. To compare differences in PBMC cultured with CM to those cultured in GM alone one way ANOVAs were performed with Tukey post hoc tests. Results were considered statistically significant (*) when $p<0.05$. All error bars show ± SEM. Statistical analysis was not performed on the experiments carried out with Jurkats due to the low number of repeats (n=2) as they were solely used for optimisation.

## 5.3 Results

### 5.3.1 The effect of tumour-derived conditioned medium on PBMC apoptosis

To analyse the effect of soluble factors released by cells in the TME of HNSCC on the apoptosis of healthy immune cells, PBMC from leucocyte cones were cultured for one or two days in CM collected from dissociated tumour biopsies, tumour-derived fibroblasts and UMSCC cells lines. At both time points, the percentage of $PI^+$ cells was always greater in the cells cultured in CM than the corresponding GM controls (Figure 5.1a and c). The number of cells recovered after culture and the viability measured by trypan blue exclusion showed no differences between the cells cultured in CM to those cultured in GM (data not shown).

Fewer cells were $PI^-$/annexin $V^+$ following culture in CM alone when compared to GM after both day one and day two (Figure 5.1a and c). Although, none of the differences between GM and CM were significant, the cells cultured in UMSCC-11a CM came close, and using an independent T test this result was significant ($p$=0.013). Apoptosis, measured by CaspACE, was higher in the PBMC cultured in dissociated tumour tissue CM at days one and two (Figure 5.1b and d). The proportion of CaspACE-positive cells was higher in three out of four of the PBMC cultured in cell line or fibroblast CM when compared with the corresponding GM controls (Figure 5.1b), and lower in all four by day two (Figure 5.1d). The overall number of cells that appear to be apoptotic according to the presence of caspases is greater in all cases than the number estimated using PI and annexin V. The proportion of apoptotic cells increases at day two when measured by either marker. There were no significant differences in the percentage of $PI^+$/annexin$V^+$, $PI^-$/annexin$V^+$ or Casp$ACE^+$ cells when cultured in any of the CM compared with GM controls.

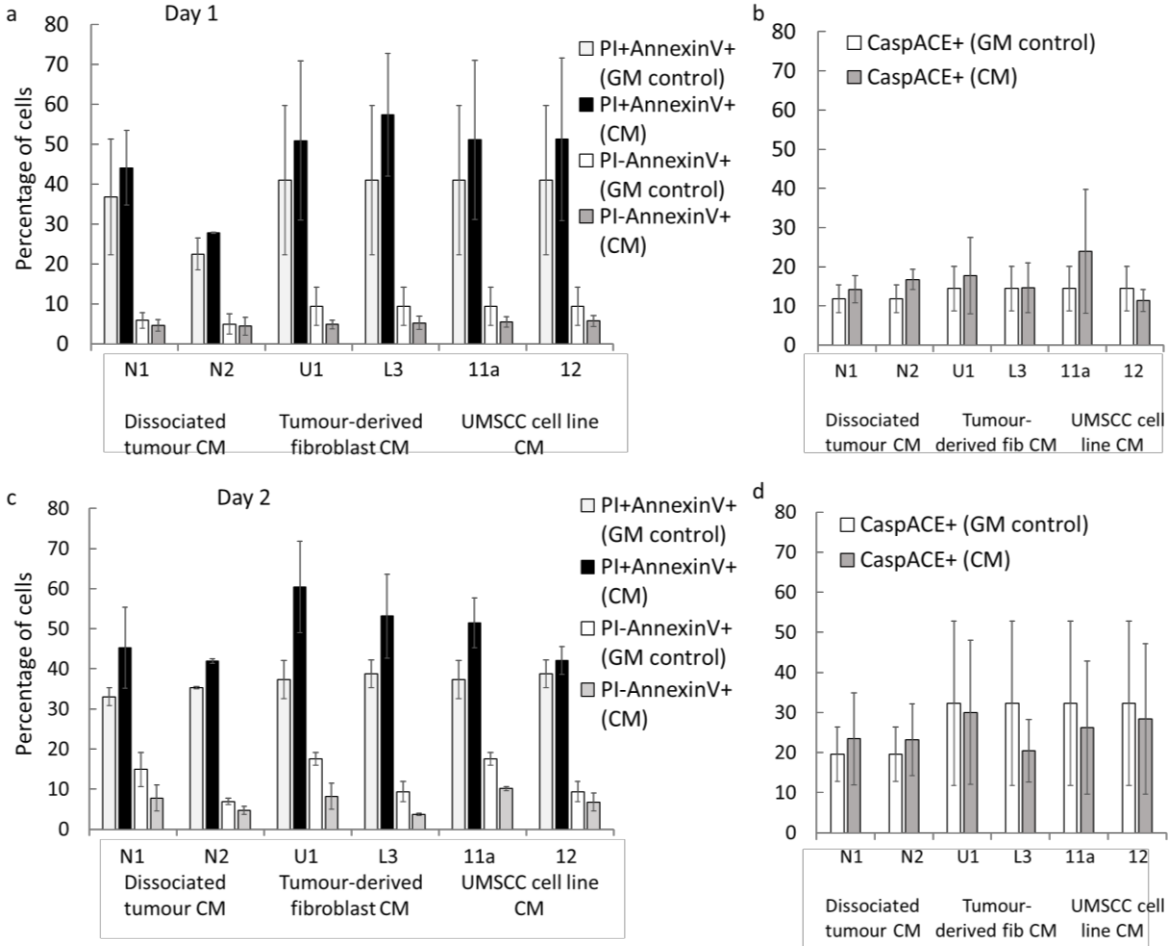


**Figure 5.1: Mean percentage of PBMC that bound PI and annexin V or CaspACE™ following culture with dissociated tumour, tumour-derived fibroblast or UMSCC cell line CM.**
PBMC from healthy controls were cultured in GM supplemented with IL2 and CD3/28 Dynabeads, with or without CM and stained with PI and annexin V (n=3 for N1, UI1, L3, UMSCC-11a and UMSCC-12 and n=2 for N2) or FTC-VAD-FMK CaspACE™ inhibitor (n=3) following incubation for one (a and b) or two (c and d) days. PBMC that bound PI and annexin V (black; a and c) represent late apoptotic/necrotic cells and PBMC that bound annex V only (grey; a and c) are apoptotic. Solid bars represent cells cultured in CM, while the shaded bars represent the corresponding GM controls from experiments using the same healthy PBMC. Statistical analysis was carried out using a one-way ANOVA with Tukey's post hoc test.

### 5.3.2 The viability of PBMC cultures

Due to unexpectedly high proportions of dead cells in cultures of whole PBMC, further investigations were carried out to determine if longer culture periods or the use of freshly isolated cells would give better viability. Following thawing and plating of 8 x$10^4$ leucocyte cone PBMC in 96 well plates and culture for two days in GM with IL2 and CD3/CD28 DynaBeads, the percentage of viable cells ($PI^-annexinV^-$) was relatively low (between 37.6% and 52.5% for the three cones used above; Figure 5.2). Culturing PBMC over a four-day period showed that in two of the three leucocyte cones the proportion of viable cells

decreased over the first two days of culture, before increasing over the remaining culture time (Figure 5.2a). In the third leucocyte cone the percentage of viable cells dropped to its lowest viability after one day of culture and then began to increase thereafter. The overall number of cells per well, determined by counting using trypan blue exclusion, remained low after one, two and three days of culture, before increasing considerably by day four for all the leucocyte cones investigated (Figure 5.2b).

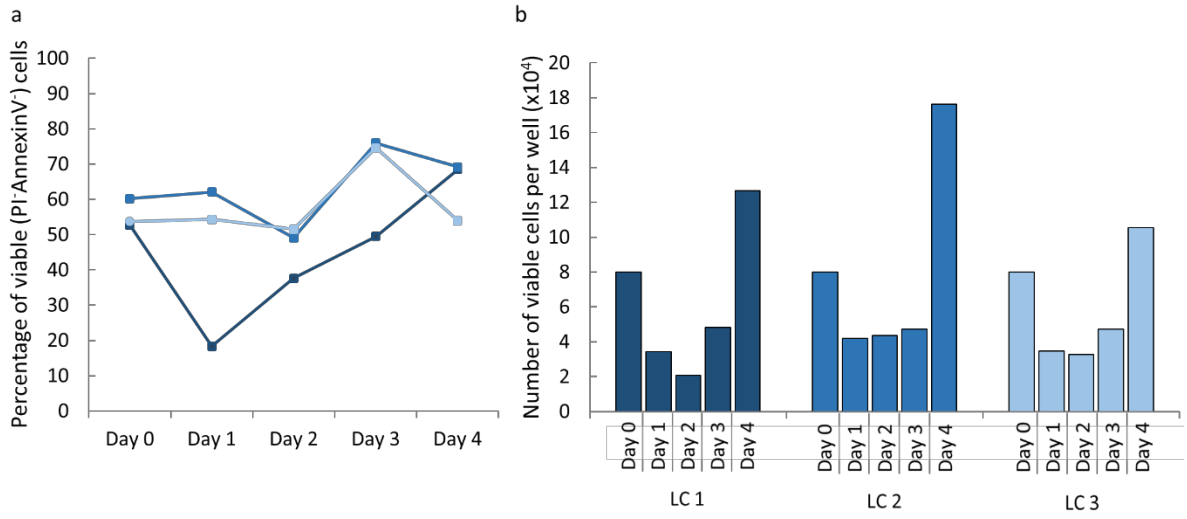


**Figure 5.2: Change in the percentage and number of viable PBMC following culture over a 4-day period in GM supplemented with IL2 and CD3/CD28 DynaBeads**
Results are from three separate experiments using leucocyte cones (LC) from different healthy controls. Following culture, cells were collected from 18 wells, stained with PI and annexin V and counted with trypan blue exclusion. The percentage of viable cells was defined as the percentage of the total cells that were $PI^-$ $AnnexinV^-$ (a) and the corresponding total viable cell counts are calculated by trypan blue exclusion (b).

Due to the low viability of frozen leucocyte cone PBMC over the first two days of culture PBMC were collected from two healthy donors and immediately cultured for two days in GM with IL2 and anti-CD3/28 activation beads in order to avoid any cell death caused by freeze/thawing. Staining with PI showed the percentage of viable cells in the freshly isolated PBMC was greater than 95% prior to culture, greater than the 50 to 60% observed in the freeze/thawed leucocyte cones (Figure 5.2a, Day 0). Following two days of culture the percentage of viable ($PI^-AnnexinV^-$) cells from the two, fresh, healthy control PBMC had fallen to 50% and 80% (Figure 5.3). Although, in the latter case this was markedly higher than the viability observed following two days of culture of frozen/thawed leucocyte cone PBMC, the other fresh PBMC samples showed similar viability to those seen in with

leucocyte cone PBMC following two days in culture thus work continued using the cones due to the number of cells easily available.

In order to try and increase the viability in the cultured LC PBMC, dead cells were removed, either by density gradient centrifugation or by sorting $PI^-$ cells following their staining with PI (1µg/ml; Figure B.6, Appendix B). In both cases however, the PBMC viability following two days of culture in GM supplemented with IL2 and CD3/28 DynaBeads was no greater than when whole PBMC were cultured (Figure 5.6, Appendix B).

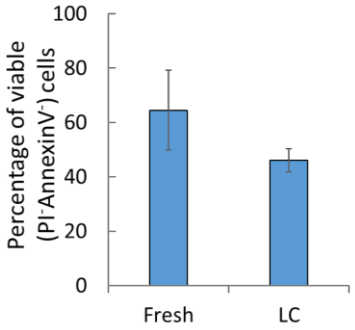


**Figure 5.3 Mean percentage of viable ($PI^-AnnexinV^-$) PBMC freshly isolated from healthy controls or thawed from frozen leucocyte cone PBMC following two days of culture in growth medium supplemented with IL2 and anti-CD3/CD28 DynaBeads**
The percentage of viable cells was determined in healthy PBMC freshly isolated from venous blood (n=2) or from those isolated from leucocyte cone blood, frozen and thawed (LC; n=3). The fresh or freeze/thawed PBMC were cultured in GM supplemented with IL2 and CD3/28 DynaBeads and incubated for two days before being stained with PI and annexin V.

### 5.3.3 Culture of Jurkats with etoposide to induce apoptosis

For a positive control of apoptosis, Jurkat cells were cultured in GM with 10 µM etoposide or a corresponding control of GM with the equivalent volume of DMSO for 6, 24 or 48 hours. The number of live and dead cells were counted with trypan blue exclusion and used to calculate the percentage viability. Following 6 hours in culture, the number of viable cells recovered from control cultures (GM) was almost two times greater than the cultures containing etoposide (Figure 5.4a). The number of viable cells increased after 24 hours and again at 48 hours when cultured in GM, whereas cultures containing etoposide decreased over the 48 hours. The percentage viability of all the cells recovered remained above 90% in control GM cultures over the 48 hours (Figure 5.4b).. However, when etoposide was

added a sharp decrease in percentage viability was observed after 24 hours in culture (decreased by 75%) and this remained low up to 48 hours.

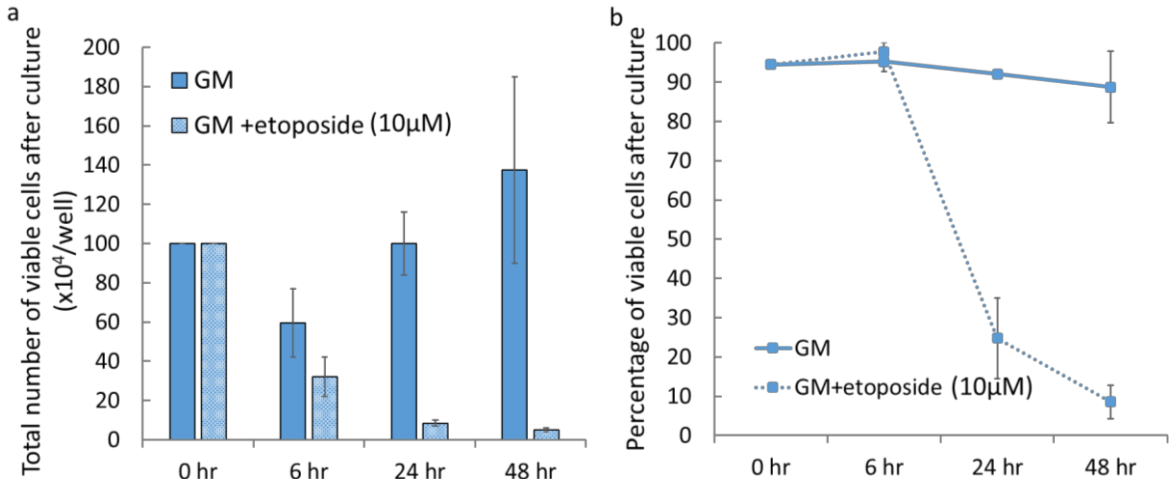


**Figure 5.4: The effect of etoposide on Jurkat viability**
Mean number of viable Jurkat cells recovered per well (a) and percentage viability (b) following culture for 6, 24 and 48 hours in GM with or without 10 µM etoposide or a GM control, determined by trypan blue exclusion. Results show the mean and SEM from two separate experiments.

The percentage of apoptotic Jurkat cells was determined using PI exclusion and annexin V binding, as well as the binding of the CaspACE™ fluorescent caspase inhibitor. After 6 hours of culture there was no obvious difference between the mean percentage of late apoptotic/necrotic cells ($PI^+annexinV^+$) cultured with etoposide (25.7 ±6.7%) compared to those cultured without (21.8 ±3.7%), and the mean percentage of early apoptotic cells ($PI^-annexinV^+$) was only slightly higher in the Jurkats incubated with etoposide (17.9 ±11.1% compared to 3.8 ±2.6%; Figure 5.5). There was no difference between the percentage of $CaspACE^+$ apoptotic cells in Jurkats cultured with etoposide compared with the control cells (18.6 ±1.9% and 23.2 ±5.6%, respectively; Figure 5.6). At 24 hours, the percentage of dead ($PI^+annexinV^+$) and apoptotic ($PI^-annexinV^+$) cells was similar to that at 6 hours in the control cultures (22.8 ±0.3% and 4.9 ±3.7%), however in the presence of etoposide almost all the cells recovered were dead or apoptotic (84.8 ±3.5% and 11.4 ±2.0%, respectively; Figure 5.5). In contrast, over 50% of the recovered cells were found to be apoptotic using CaspACE™, following culture with etoposide, which was approximately double compared with the GM control (53.1 ±0.8% and 21.9 ±6.8%; Figure 5.6). By 48 hours, almost all Jurkats recovered were dead (necrotic/late apoptotic) when cultured with etoposide (97.8 ±1.2%), while the cells cultured in GM alone, contained a much lower percentage of dead

cells (13.6 ±4.1%; Figure 5.5). Although the number of CaspACE$^+$ apoptotic cells remained higher in the Jurkats cultured in etoposide for 48 hours compared with those cultured in GM, this difference was less marked than at 24 hours (Figure 5.6).

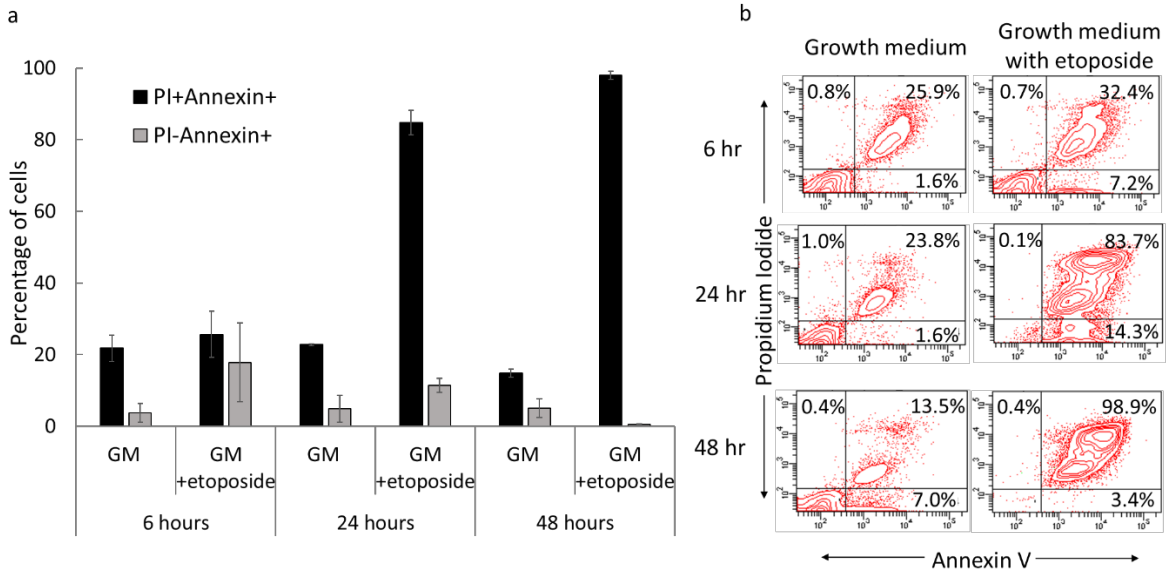


**Figure 5.5: Dual PI/annexin staining of Jurkats following 6, 24 and 48 hours of culture in GM with or without etoposide**

Jurkats were cultured in GM with 10 µM etoposide or the equivalent volume of DMSO as a control for up to 48 hours, before staining with PI and annexin V. Results show the mean percentage of Jurkats (n=2) that bound PI and annexin V, or annexin V alone from two separate experiments (a) and representative contour plots of PI/Annexin V binding.

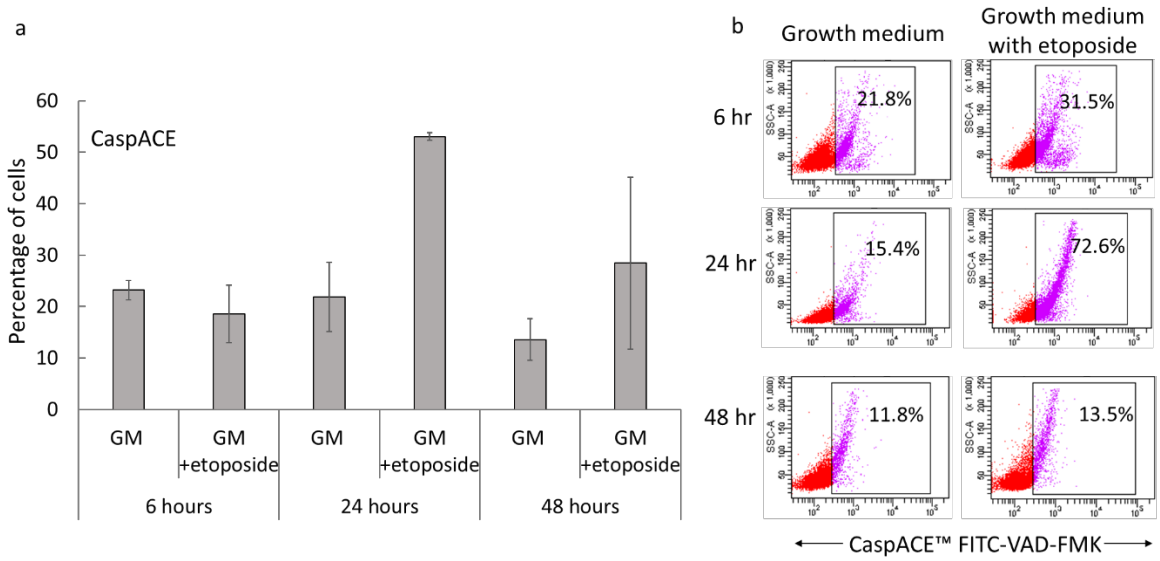


**Figure 5.6 CaspACE™ staining of Jurkats following 6, 24 and 48 hours of culture in GM with or without etoposide**

Jurkats were cultured in GM with 10 µM etoposide or the equivalent volume of DMSO as a control for up to 48 hours before staining with CaspACE™ for analysis. Results show the mean percentage of Jurkats (n=2) that bound CaspACE™ from two separate experiments (a) and representative scatter plots (b).

### 5.3.4 Culture of activated T cells with etoposide to induce apoptosis

PBMC from leucocyte cones (n=4) were activated with CD3/CD28 DynaBeads and IL2 and incubated for five days to allow the T cells to proliferate and improve the viability of cultures prior to their use in experiments. After five days, viability of the cells was >87.5% in cell cultures from three of the donors and 70% in the fourth. Following this, the non-adherent T cells were removed and cultured for a further 24 hours in GM with or without etoposide to induce apoptosis. In an initial experiment PBMC were cultured with 10µM etoposide and were all dead at 24 hours, so the etoposide concentration was reduced to 5µM for subsequent experiments. After 24 hours, the number of viable cells (Figure 5.7) and percentage viability, determined by trypan blue exclusion, was lower in T cells cultured with 5µM etoposide ($0.8x10^4 \pm 0.2x10^4$ cells and 44.8 ±7.0%) compared to control cells ($13.6x10^4 \pm 2.1x10^4$ cells and 94.0 ±1.2%).

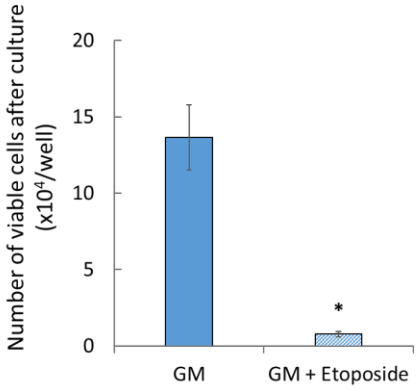


**Figure 5.7: Trypan blue staining of activated T lymphocytes following 24 hours of culture in GM with or without etoposide**

Mean (±SEM) number of viable healthy PBMC (n=4) recovered per well following a 5 day incubation with IL2 and CD3/CD28 DynaBeads and a further 24 hours in GM with 5 µM etoposide or the same volume of DMSO. Statistically significant results (*$p<0.05$) were determined using independent T tests.

The percentage of dead ($PI^+AnnexinV^+$) cells significantly increased from 14.5±2.1% to 77.9±2.2% following the addition of etoposide to the activated T cells (Figure 5.8a). In addition the percentage of apoptotic cells detected either with Annexin or CaspACE™ also increased significantly with etoposide however the increase was most evident (3-fold) using the CaspACE™ reagent (Figure 5.8b).

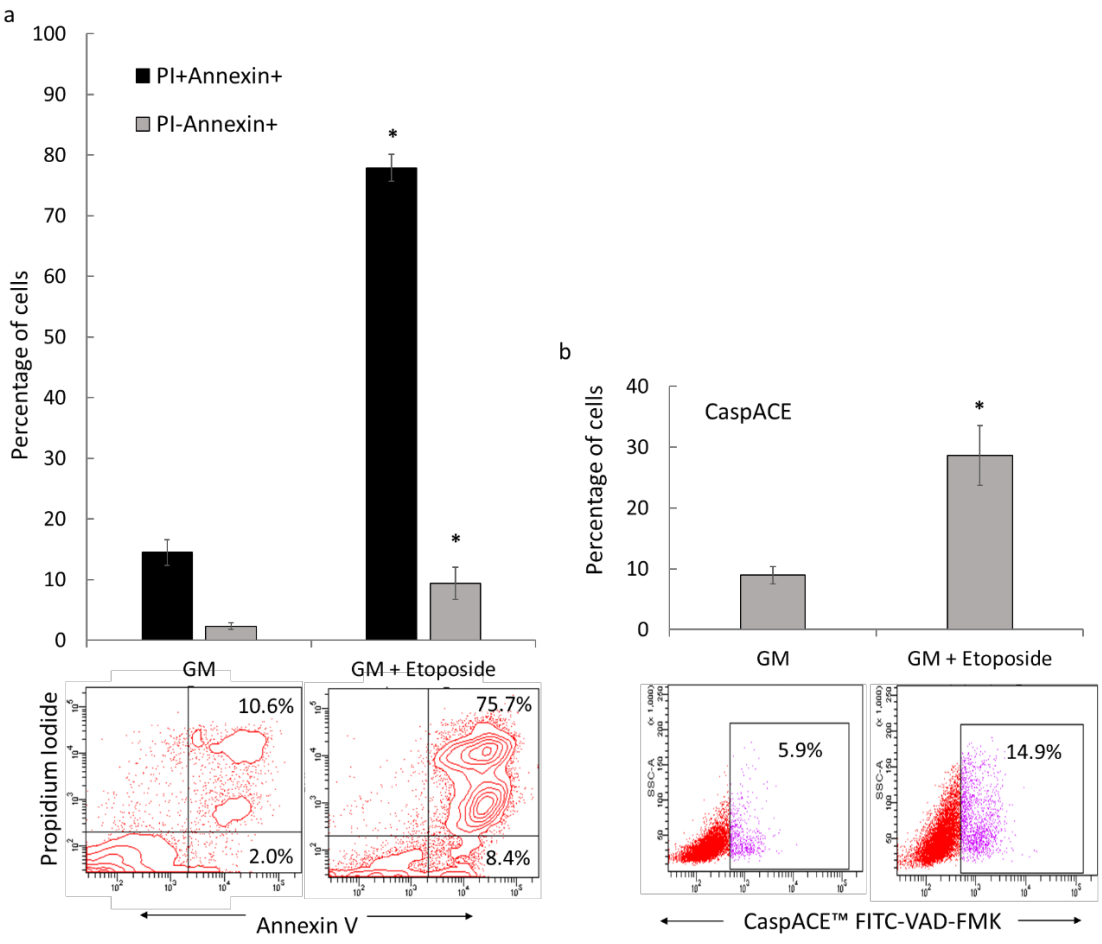


**Figure 5.8: Dual PI/annexin V and CaspACE™ staining of activated T lymphocytes following 24 hours of culture in GM with or without etoposide**

Mean (±SEM) percentage and representative contour and scatter plots of healthy PBMC (n=4) labelled with both PI and annexin V (a) or CaspACE™ (b) following a 5 day incubation with IL2 and CD3/CD28 DynaBeads and a further 24 hours in GM with 5 µM etoposide or the same volume of DMSO. Statistically significant results (*p<0.05) were determined using independent T tests.

### 5.3.5 The effect of conditioned medium on the induction of apoptosis of T cells

Healthy PBMC (n=4) were cultured with anti-CD3/CD28 DynaBeads and IL2 for 5 days and the activated T cells were collected and cultured with CM. Due to limited CM, cells were cultured at the single time point of 24 hours in these experiments. A short culture time was chosen to limit any effect caused by the lack of factors required for sustaining cell viability in the CM. No statistically significant differences in the proportion of dead ($PI^+AnnexinV^+$) and apoptotic ($PI^-AnnexinV^+$) cells were observed when the T cells were cultured with dissociated tumour CM, UMSCC cell line CM or tumour-derived fibroblast CM compared with GM alone (Figure 5.9a-c). Similiarly, no statistically significant differences in the proportion of dead cells ($PI^+AnnexinV^+$) was observed when the PBMC

were cultured with dissociated tumour CM, UMSCC cell line CM or tumour-derived fibroblast CM compared with GM alone with the mean percentage of dead cells varying between 15.5±3.4% and 19.6±1.9% compared to 15.1±2.1% in the GM control. Finally, no statistically significant differences in the proportion of apoptotic cells ($PI^-AnnexinV^+$) was observed when the PBMC were cultured with dissociated tumour CM, UMSCC cell line CM or tumour-derived fibroblast CM compared with GM alone with the mean percentage of dead cells varying between 2.9% to 3.2% in the dissociated tumour CM, 2.1% to 2.7% in the UMSCC cell line CM and 1.8% to 2.7% in the tumour-derived fibroblast CM compared with a mean of 2.1% in the GM.

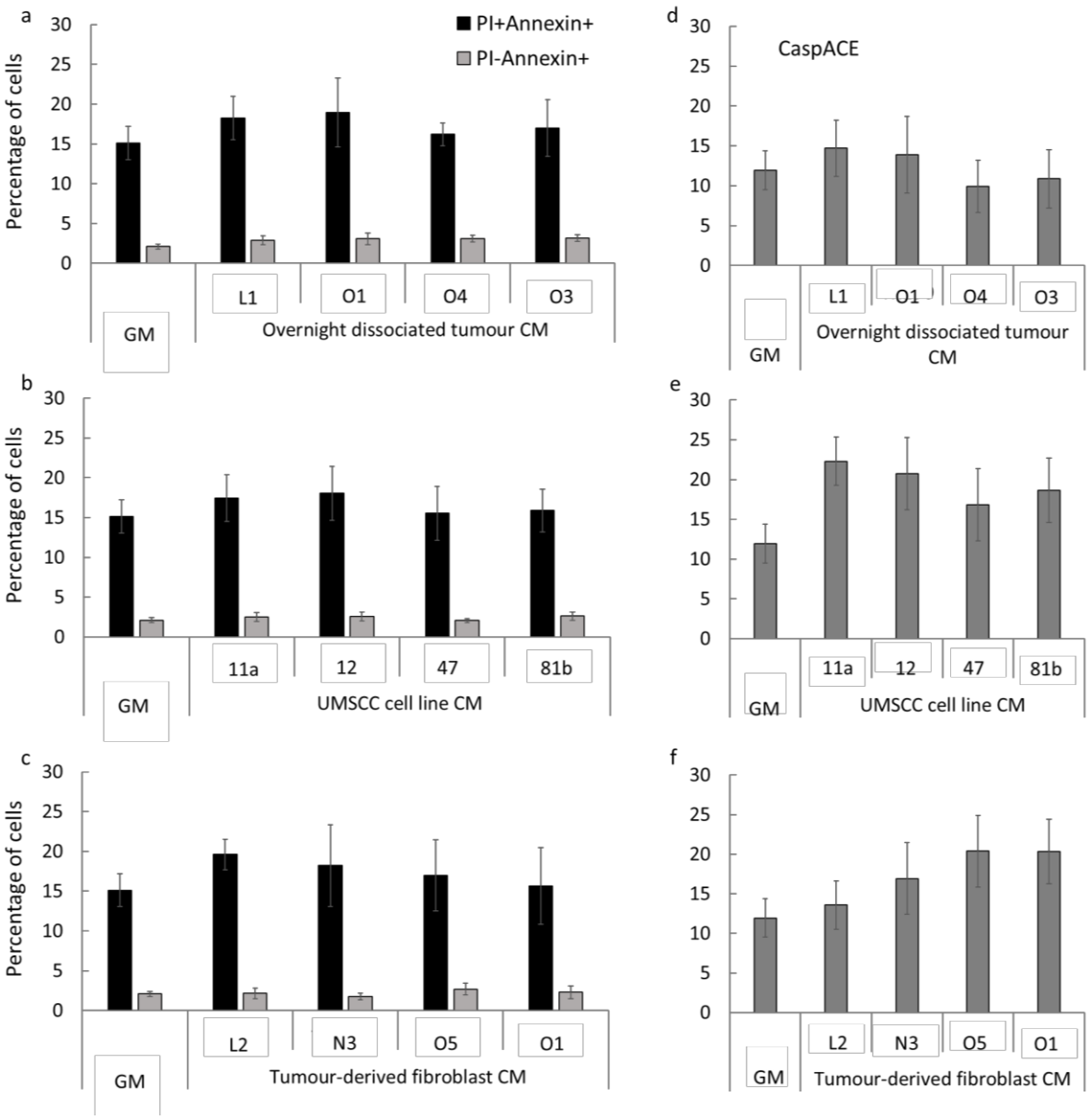


**Figure 5.9: Mean percentage of activated T lymphocytes cultured in dissociated tumour, UMSCC cell line and tumour-derived fibroblast CM**

Healthy PBMC (n=4) were labelled with annexin V and PI or CaspACE™-FITC-VAD-FMK following 5 days of culture in GM supplemented with IL2 and CD3/CD28 DynaBeads and a further 24 hours culture in CM collected from the overnight culture of four dissociated tumours (a and d), four UMSCC cell lines (b and e) and four tumour-derived fiboblasts (c and f). Bars represent mean values ±SEM. Statistical analysis was carried out using a one-way ANOVA with Tukey's post hoc test.

Binding of the pan-caspase inhibitor, CaspACE$^{TM}$, showed greater variability between the leucocyte cones, than PI$^{-}$AnnexinV$^{+}$ staining, and was present in a greater proportion of cells (Figure 5.9). For example, the percentage of apoptotic cells detected using CaspACE™ in the GM control was 12.0±2.4% compared to the 2.1±0.3% detected using PI exclusion and

Annexin V binding. All the UMSCC cell line CM (22.3 ±3.0%, 20.8 ±4.5%, 16.8 ±4.5% and 18.6 ±4.1%) and tumour-derived fibroblast CM (13.6 ±3.7%, 16.9 ±4.7%, 20.4 ±6.7% and 20.3 ±6.5%) and two of the four overnight dissociated tumour CM (14.7 ±3.5% and 13.9 ±4.8%) caused an increase in activated caspases compared with GM alone (12.0 ±2.4%), though none of these results were statistically significant (Figure 5.9d-f). The greatest increase in apoptosis was induced by UMSCC-11a CM; cells cultured with this media had a 1.87-fold higher percentage of CaspACE$^{+}$ cells than those cultured in GM alone ($p$=0.039, independent T test).

### 5.3.6 The effect of conditioned medium on cellular activity

MTS assays were carried out to assess the effect of CM from dissociated tumours, UMSCC cell lines and tumour-derived fibroblasts on the proliferation of healthy PBMC (n=4). Leucocyte cone PBMC were cultured for five days with CD3/CD28 DynaBeads and IL2 to activate the T cells, before a 24 hour incubation with CM. Mean absorbance of the formazan product from the cells cultured with two of the dissociated tumour CM (O4, 1.59±0.15 and O3, 1.72±0.10) were found to be lower than for the GM only control (1.83±0.08; Figure 5.10a), but the difference was not significant. In the case of both of these CM, the same effect was seen consistently from the T cells of all four healthy donors. The two other dissociated tumour CM showed little difference in mean absorbance (L1, 1.83±0.13 and O1, 1.82±0.13), compared with the GM control and there was no consistent effect on absorbance between the cones.

The mean absorbance values of the formazan product following culture of T cells with CM collected from the culture of four UMSCC-cell lines (UMSCC-11a, 1.55±0.15; UMSCC-12. 1.66±0.17; UMSCC-47, 1.50±0.20; UMSCC-81b, 1.80±0.08) were all lower than the GM control (Figure 5.10b), however the results were not significant. In three of the four donors, the cell line CM in general had the biggest effect on the absorbance values, reflected in the mean values (Figure 5.10), however for one of the cones the greatest effect was observed from the tumour derived-fibroblast CM. Overall there was no significant difference in mean absorbance between the cells cultured with fibroblast CM and those cultured in GM, though again all were lower when cultured with CM (L2, 1.74±0.08; N3, 1.68±0.07; O2 1.77±0.09, O1, 1.66±0.05; Figure 5.10c).

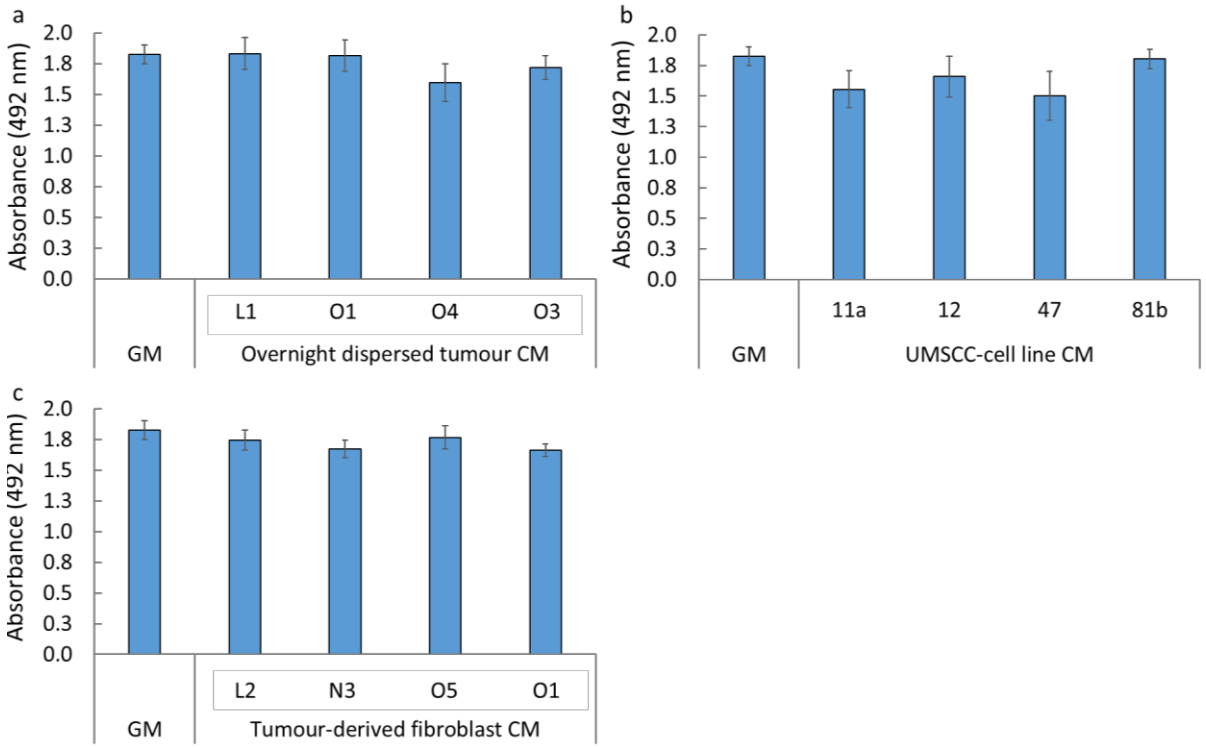


**Figure 5.10: Mean absorbance of the formazan product following MTS assays on activated T lymphocytes cultured in dissociated tumour, UMSCC cell line and tumour-derived fibroblast CM**

Healthy PBMC (n=4) were cultured for 5 days in GM supplemented with IL2 and CD3/CD28 DynaBeads and then for a further 24 hours with dissociated tumour overnight CM (a), UMSCC cell line CM (b) and tumour-derived fibroblast CM (c) or GM only. MTS reagent was added (20 µl/well) and cells were cultured for 4 hours before absorbances were read at 492 nm. Statistical analysis was carried out using a one-way ANOVA with Tukey's post hoc test.

## 5.4 Discussion

### 5.4.1 The effect of tumour-derived soluble factors on PBMC apoptosis

The induction of T cell apoptosis by tumours is likely a contributing factor in immune evasion. Co-culture experiments with various HNSCC cell lines and the upregulation of apoptotic receptors have implicated FasL, TRAIL and TNF-α in lymphocyte apoptosis (Kassouf & Thornhill, 2008). The role of soluble forms of these factors is controversial; however, there is evidence that soluble factors from HNSCC CAF are able to induce apoptosis *in vitro* (Takahashi *et al.*, 2015). Discrepancies in experiments using conditioned medium collected from tumour cell lines compared with co-culture experiments may likely be due to the relatively reduced potency of the soluble form of some ligands, compared to their membrane bound counterparts. For example, a study that observed apoptosis of T cells and Jurkat when co-cultured with HNSCC cell lines, failed to detect any effect from CM collected from the same cells (Gastman *et al.*, 1999). Cell lines transduced with FasL were able to generate CM capable of inducing apoptosis in 39±1% Jurkat, however this still failed to reach the levels (66%) observed in co-culture experiments using the same cells.

In the current chapter initial experiments comparing the level of apoptotic markers expressed on whole PBMC cultured in GM alone, or with CM found no significant difference in apoptosis or cell death. However, the results were highly variable and levels of cell death were much higher than expected. Takahashi *et al.* (2015), compared the effect of CM from HNSCC derived fibroblasts to that of normal fibroblasts, derived from pieces of non-cancerous tissue from the same patients. They observed PBMC cultured with CM from HNSCC CAFs had significantly more CaspACE$^+$ cells than cultures with CM-derived from normal fibroblasts (an approximate increase of 50%). Their results appear in contrast to observations in this chapter, where tumour-derived fibroblast CM did not cause any increase in either binding of caspACE or annexinV. However, given the use of different control cultures (GM only vs normal fibroblast CM) it is not possible to compare directly between the studies. The levels of CaspACE$^+$ cells observed in the study by Takahashi *et al.* (2015) (15-40%), were similar to those of the current study (19-33%). However, much fewer cells bound the viability marker, 7-AAD, compared with PI in this study, indicating they observed fewer dead cells overall. This could be because they gated on CD3$^+$ cells, which may have been more viable.

A recent paper, that compared PBMC cultured with CM from two HNSCC cell lines (UMSCC-1 and UMSCC-22B) with that of PBMC cultured in complete GM also found there was no difference in apoptosis (de Medeiros *et al.*, 2017). A combination of annexin V and 7-AAD was used to identify apoptotic cells and both 7-AAD$^+$/annexinV$^+$ and 7-AAD$^-$/annexinV$^+$ cells were defined as apoptotic. In the study, de Medeiros *et al*., (2017), observed around 35-40% of cells were 7-AAD$^-$/annexinV$^+$ following two days of culture, which was markedly greater than the PI$^-$/annexinV$^+$ population in the current study (<20%), and only 15-20% of cells were 7-AAD$^+$/annexinV$^+$. This could be attributable to differences in the experimental set up as although, both studies used PBMC from healthy donors, de Medeiros *et al*., (2017), used the mitogenic lectins concanavalin A (ConA) and phytohemagglutinin (PHA) in combination with IL2 for T cell stimulation, rather than the more physiologically relevant stimulation using CD3/CD28 antibodies.

In the current study the sum of the PI$^+$AnnexinV$^+$ and PI$^-$AnnexinV$^+$ populations were similar in all cultures. In all culture conditions, the percentage of the apoptotic cells, identified by CaspACE binding, was greater than those defined as PI$^-$AnnexinV$^+$. This is not surprising, as some apoptotic cells will fall into the PI$^+$AnnexinV$^+$ gate, therefore defining apoptotic cells as PI$^-$AnnexinV$^+$ will underestimate the number of apoptotic cells compared to using CaspACE.

Due to the unexpectedly large proportion of dead cells in the cultures established in the current study, it was postulated that these could have been obscuring any effect the CM may have been having on PBMC viability. Therefore, efforts to remove dead cells were made in order to improve the chance of observing an effect from the CM. The removal of dead cells by sorting out the viable (PI$^-$) PBMC using FACS (Section 2.3.5) or by density centrifugation (Section 2.2.1), prior to culture were however unsuccessful in reducing the number of dead cells following culture (Figure B.6; Appendix B). Freshly isolated PBMC initially were more viable than PBMC that had been through a freeze/thaw cycle, and there was a slight improvement in the viability of cells following two days in culture, however, there were still a considerable percentage of dead cells in these cultures. Without T cells markers, such as CD3, it is not possible to identify if the dead cells are T cells or other cells in the PBMC. Therefore, it was decided to expand the lymphocyte population from the PBMC to use in subsequent assays, which would also results in a more viable starting population of cells. PBMC were cultured for 5 days until they were in the exponential growth

phase and these cells were used for experiments. Following 5 days the percentage of viable cells was between 70 and 90%.

### 5.4.2 The induction of apoptosis by etoposide

In order to better define any apoptotic cells and to optimise the experimental setup to measure any apoptosis induced by CM, etoposide was used as a positive control to induce apoptosis. Jurkat that were cultured with etoposide contained a greater number of dead and apoptotic cells, compared to controls, after 6 hours. By 48 hours the majority of the cells cultured with etoposide were dead. This correlated with the results of CaspACE binding, where the percentage of cells that were CaspACE$^+$ was greatest in etoposide cultures at 24 hours (53.1±5.6%) and by 48 hours the number of apoptotic cells had dropped to 28.6±16%. The decreased presence of caspases in cells cultured with etoposide between 24 hours and 48 hours, is likely to be due to the cells being dead at this point (97.8 ±1.2%) and no longer detectable. This highlights the transient nature of apoptosis and reinforces the importance of looking at markers that can detect apoptotic cells at different stages as well as using viability markers in conjunction with these markers. Other papers looking at T cells and Jurkats, culture cells for between 24 and 48 hours (Karpinich *et al.*, 2006; Sato *et al.*, 2009; Takahashi *et al.*, 2015). In a study by Karpinich *et al*. (2006), using MTS assays, the viability of Jurkats was observed to be 20% following 24 hours incubation with 10μM etoposide (Karpinich *et al.*, 2006), while Sato *et al*. (2009) detected differences in cell viability from 6 hours post treatment with etoposide, measured by PI staining using flow cytometry. By 9 hours, Sato *et al*. (2009) observed both annexin V and caspase-3 levels were significantly greater than in control cultures, reaching approximately 3% and 18% respectively.

T cells were cultured for 24 hours with etoposide, following their 5-day activation and expansion from PBMC. In an initial experiment using 10 μM etoposide the majority of cells were dead after 24 hours, so etoposide was reduced to 5μM. At this concentration significant differences were observed with both apoptotic markers (annexin V and CaspACE) and in the viability marker PI between PBMC cultured with and without etoposide. Given these results further experiments with CM were carried our following 24 hours of culture with CM.

### 5.4.3 **The effect of tumour-derived soluble factors on T cell apoptosis and viability**

Having optimised the assays, the effect of CM on expanded populations of T cells, was assessed using PI/annexinV staining, CaspACE staining and MTS metabolism. No difference was observed in the proportion of cells with an apoptotic phenotype $PI^{-}Annexin^{+}$ or $CaspACE^{+}$ following culture of cells with any of the twelve CM tested (4 dispersed tumour CM, 4 UMSCC cell line CM and 4 tumour-derived fibroblast CM). Both surface expression of PS and caspase activation are events in the early stages of apoptosis; PS translocation from the cytoplasmic side of the plasma membrane to the external side can be initiated by either caspase-dependent or caspase intendent pathways (Nakano *et al.*, 2001; Marino & Kroemer, 2013). It is therefore possible if any apoptotic cells were present that had entered the late stages of apoptosis the cells may appear as necrotic $PI^{+}annexin^{+}$ cells, however, there was also no difference in the percentage of these cells present when cultured with or without CM.

Similarly, none of the CM induced an effect on the viability of T cells, compared with culture in GM alone according to observations from MTS assays. However, overall there was a trend toward decreased viability of cells cultured in CM, particularly that derived from UMSCC cell lines. It could be that diluting the CM has diluted any effect of the soluble factors. The study by Takahashi *et al*. (2015) used up a 2:1 ratio of CM:GM, however CM will also be depleted of some of the necessary factors for cell growth, which could also contribute to any detrimental effects observed. Alternatively CM may effect particular subsets of T cells differently, this could also account for some of the variation between the effects on different donor cells. For example if some of the donor contained high proportions of a subset that is particularly susceptible to the effect of CM it would appear to have a bigger effect overall.

### 5.4.4 **Conclusion**

There was no effect of soluble factors from dissociated HNSCC tumours, tumour-derived fibroblasts and UMSCC cell lines on T cell death and apoptosis. CM may effect different cell types differently, and effects may be masked when looking at mixed cell populations. In the future it would be of interest to look at the effect of apoptosis on different T cell subsets, by sorting out the different T cell populations prior to culture with CM. In particular,

it may be interesting to look at the effect on Treg and $CD8^+$ CTL, as the balance of these two populations are known to be predictive of prognosis.

# Chapter 6 Expression of Chemokine Receptors on T Lymphocytes of HNSCC patients

## 6.1 Introduction

Chemotaxis plays an essential role in establishing an immune response; ensuring the appropriate cells are in the correct place as and when required (Section 1.3.3). It is by this mechanism that circulating immune cells are directed to migrate from the bloodstream and infiltrate the tumour mass. The proportions of different immune cells in the TME differ considerably to those seen circulating in the periphery, and the resulting cell balance is insufficient to elicit effective tumour rejection (Section 1.2.2.9). Furthermore, variations in the immune infiltrate can be seen throughout the tumour and associated stromal regions and the localisation of immune cells may determine their influence on prognosis (Mizukami *et al.*, 2008b). Differences in this immune profile may in part be attributable to the variation in chemokine receptors present on the different immune cells (Curiel *et al.*, 2004; Mizukami *et al.*, 2008b; Tan *et al.*, 2009; Shields *et al.*, 2010; Parsonage *et al.*, 2012; Liu *et al.*, 2015; Zhang *et al.*, 2015). Given that there was no induction of functionally suppressive iTreg observed following culture in CM (Section 4.4.2), the current chapter will investigate whether variation in specific chemokine receptor expression on different immune cells may cause preferential recruitment of Treg.

### 6.1.1 Chemokine expression in HNSCC

The role chemokines play in the selective recruitment of T cells into the tumour mass of HNSCC is not clear. However, differences have been observed in chemokine profiles in HNSCC patient serum and tumour tissue. CXCL8, CCL4 and CCL5 are increased in HNSCC patient serum compared to that of healthy controls (Hathaway *et al.*, 2005; Trellakis *et al.*, 2011). In addition CXCL8 expression is upregulated in HNSCC tumours compared with healthy tissue (Hasina *et al.*, 2008). The upregulation of CCL20 mRNA and downregulation of CCL19 and CCL21 in LSCC tissue compared with adjacent normal tissue from the same patient has also been observed, (Chen *et al.*, 2013). In the same study, expression of the CCL20 chemokine receptor CCR6 was found to be expressed on an increased percentage of circulating Treg from patients with laryngeal squamous cell carcinoma (LSCC) compared with those of healthy controls. No such difference was observed in the expression of CCR7, a receptor for CCL19 and CCL20. Thus, the high expression of CCL20 in the tumour may contribute to the accumulation of Treg in the TME.

An expression signature of 12 genes, CXCL9, CXCL10, CXCL11, CXCL13, CCL2, CCL3, CCL4, CCL5, CCL8, CCL18, CCL19 and CCL21, associated with a T cell inflamed phenotype was originally described in melanoma and has also been found in a subset of HNSCC patients (Messina *et al.*, 2012; Kang *et al.*, 2015). This profile was associated with high $CD8^+$ lymphocyte infiltration and PD-L1 expression, suggesting it may be a useful indicator as to a patient's suitability for immunotherapy (Kang *et al.*, 2015).

### 6.1.2 The role of chemokine receptors in leucocyte recruitment to the TME

The majority of research into chemokines and chemokine receptor expression in cancer, particularly HNSCC, focusses on tumour invasion and metastasis (da Silva *et al.*, 2016; Section 1.3.3.1). As a result, there are several chemokine/receptor axes currently under investigation as targets for cancer therapy; antibodies targeting CXCL12/CXCR4 in leukemia and multiple myeloma patients, CCL2/CCR2 in patients with bone metastases, and CCL22/CCR4 in patients with recurrent metastatic tumours are all currently undergoing clinical trials (Vela *et al.*, 2015). Some studies have investigated the chemokine receptor profiles of immune cells and the resulting influence on migration, in various diseased and healthy settings (O'Garra *et al.*, 1998; Charo & Ransohoff, 2006). However, how this relates to the HNSCC microenvironment is currently unclear.

Differences have been observed in receptor expression in the TIL and circulating T cells of HNSCC, nasopharyngeal carcinoma (NPC), oesophageal squamous cell carcinoma (ESCC) and non-small cell lung carcinoma (NSCLC) patients (Strauss *et al.*, 2007b; Parsonage *et al.*, 2012; Liu *et al.*, 2015; Zhang *et al.*, 2015). CXCR5 and CXCR6 have been implicated in the recruitment of lymphocytes in NPC, with levels of CCR5 expressing $CD8^+$ memory T cells and $CD4^+$ conventional Th cells and CXCR6 expressing $CD8^+$ memory T cells, $CD4^+$ conventional Th cells and $FoxP3^+$ Treg greater in TIL compared to matched patient PBMC (Parsonage *et al.*, 2012). Lui *et al*. (2015), observed increased CCR5 on $CD8^+$ CTL and CCR6 expression on Treg from ESCC TIL compared with PBMC. Additionally, in ESCC tissue the expression of CD8 and FoxP3 correlated with expression of the CCR5 ligand, CCL4, and the CCR6 ligand, CCL20, respectively, suggesting that these receptors may be actively involved in the recruitment of CTL and Treg in ESCC. High CCL4 to CCL20 expression in ESCC tumours was associated with better prognosis for ESCC patients, indicating that these chemokine/receptor interactions may be a potential target for future therapy. The CCL20/CCR6 chemokine axis has also been associated with Treg recruitment

to NSCLC tumours, with a greater number of Treg in TIL expressing CCR6 compared with in the periphery and more CCL20 expression on patient tumours compared with healthy tissue (Zhang *et al.*, 2015).

CCL22, a ligand of the receptor CCR4, has also been implicated in the recruitment of $FoxP3^+$ Treg to the tumour site in ovarian, gastric and breast cancers (Curiel *et al*, 2004, Mizumaki 2008, Gobart, 2009). Furthermore, Curiel *et al*. (2004) were able to inhibit Treg recruitment to human ovarian tumours in a mouse xenograft model using a CCL22 antibody, while $CD3^+CD25^-$ migration was unaffected. An increase in the proportion of CCR4 expression on Treg has also been observed on T cells in the peripheral blood of HNSCC patients compared to healthy controls (Strauss *et al.*, 2007b). However, whether the increased CCR4 expression on Treg of HNSCC patients is responsible for their preferential recruitment by the CCL22/CCR4 was not investigated.

There is redundancy between chemokines and their receptors (Section 1.3.3) so targeting of a single chemokine/receptor axis may not necessarily prevent cells migrating. Furthermore, in addition to migration, chemokine receptors can be responsible for T cell retention and activation (Franciszkiewicz *et al.*, 2012). Therefore, an enrichment of cells expressing a specific chemokine receptor does not necessarily indicate it is solely involved in the migration of those cells. Ondondo *et al*. (2015) observed that, despite increased CXCR3 expression on T cells in the tumour of mice with fibrosarcomas, downregulation of CXCR3 on cells prior to their adoptive transfer had no effect on T cell migration to the tumour. Furthermore, despite different chemokine profiles in tumours, spleens, and lymph nodes $CD4^+FoxP3^+$ and $CD4^+FoxP3^-$ T cells with receptors for the prevalent tumour inflammatory chemokines were equally enriched in tumours in comparison to spleen and lymph nodes (Ondondo *et al.*, 2015). Thus, indicating that none of the chemokines investigated were causing selective recruitment of Treg.

Some of the disparities between studies may be due to the dynamic nature of the immune-tumour interaction and the heterogeneity between tumours (Franciszkiewicz *et al.*, 2012). A number of studies have also observed that the method used to process and isolate leucocytes may affect the expression of chemokine receptors (Berhanu *et al.*, 2003; Nieto *et al.*, 2012).

### 6.1.3 Effects of analysis on chemokine receptor expression

Chemokine receptor expression is dynamic; their up- and downregulation often linked to activation status and maturation (Franciszkiewicz *et al.*, 2012). The method of PBMC isolation, including temperatures and reagents used, may influence receptor expression. Nieto *et al*. (2012), saw a reduction of CCR4 expressing T cells following leucocyte isolation using density gradient centrifugation from 90% to 55% and a reduction of mean fluorescence intensity of CCR2, CXCR3 and CXCR4. A study by Berhanu *et al*. (2003) investigated the percentage expression of 13 chemokine receptors following the isolation of PBMC by eight different protocols and compared this to percentage expression in whole blood. In some cases, more expression of chemokine receptors was found on the cells in whole blood, this was thought to be due to the higher presence of contaminating blood cells. As some chemokines are only expressed on a small percentage of T cells, any contamination from other cell types that express high levels of the same receptor could give misleading results. Berhanu *et al*. (2003) observed that highly auto fluorescence granulocytes and monocytes in the blood was contributing to the perceived increase in $CXCL1^+$ and $CXCL2^+$ T cells. In the same study it was concluded that the method of cell isolation and staining that gave the greatest sensitivity varied depending on the chemokine receptor being investigated, therefore caution must be applied when studying these proteins.

### 6.1.4 Aims and experimental design

This chapter aims to address whether differential chemokine receptor profiles on CTL, Th cells and Treg contribute to the enrichment of T cell populations in the HNSCC TME. The expression on the $CD4^+CD25^-CD39^+$ population was also assessed; as this is a phenotype associated with Tr1 cells and has been suggested to include a memory T cell population that act as a potential reserve for $FoxP3^+$ iTreg induction (Moncrieffe *et al.*, 2010). In order to choose candidate chemokine receptors for analysis Proteome Profilers™ were used to identify chemokines that were released by dissociated tumour samples from nine HNSCC patients. Chemokine receptors for analysis were chosen based on identification of their ligands in the CM. HNSCC PBMC, HNSCC TIL and healthy control PBMC were stained for these chemokine receptors in addition to a combination of CD3 and CD8, or CD4, CD25, FoxP3 and CD39. This enabled a comparison of the chemokine receptor expression on the T cell subsets between the periphery and local tumour environment in an attempt to establish how these cells are recruited into the tumour. The chemokine receptor expression on

peripheral T cells of HNSCC and healthy controls was investigated so any wider systemic effect from the tumour on chemokine receptor expression could be observed.

Following this, Transwell migration assays were used to determine whether CM from tumour dispersed tissue contained soluble factors that could actively recruit $CD8^+$ T cells, $CD4^+$ T cells and $CD4^+CD25^+CD127^-$ Treg populations. Establishing how chemokine receptor profiles differ between $CD8^+$ CTL, $CD4^+$ Th cells and Treg may provide an insight into how the suppressive HNSCC microenvironment is shaped and how it can be manipulated to promote tumour destruction.

Due to the lack of iTreg induction noted in previous chapters, and observations of differential chemokine receptor profiles on TIL compared to peripheral blood lymphocytes in other cancer types, it was hypothesised that soluble factors released by cells of the TME cause the preferential recruitment of Treg to the tumour site.

## 6.2 Materials and Methods

### 6.2.1 Detection of chemokines in tumour overnight conditioned medium

To determine the relative levels of 31 chemokines (Table 6.1) in the conditioned medium collected following the overnight culture of nine different dissociated tumour biopsies (Section 2.2.4), a Proteome Profiler$^{TM}$ human chemokine array kit (R&D Systems) was used (Section 2.5). The background levels of chemokines present in the growth medium (GM) used to culture the cells were also measured.

Following acquisition of pixel densities for all the duplicate chemokine spots using ImageJ software, the mean result from the negative control spots was subtracted from each of these values. The mean pixel density was taken from the duplicate data for the GM control for each chemokine and these were subtracted from the corresponding chemokines in each CM. A mean was then calculated for each chemokine duplicate for each of the CM. These results were standardised by tumour weight so that the result was expressed per 100 mg of tumour.

**Table 6.1: Chemokine receptors and their ligands that are detected by the Proteome Profiler**

| Receptor | Chemokines | Major associated T cell population(s) | Expression on other cell types found in the TME |
|---|---|---|---|
| CXCR1 (CD181) | CXCL1, CXCL5, CXCL8 (IL8) | Activated CTL | Monocytes, neutrophils |
| CXCR2 | CXCL1, CXCL2, CXCL5, CXCL7, CXCL8 | Negligible | Monocytes, neutrophils, eosinophils, endothelial cells |
| CXCR3 | CXCL4, CXCL9 (MIG), CXCL10 (IP10), CXCL11 (I-TAC) | Activated Th1 cells, CTL and a subset of Treg | B cells, NK cells, endothelial cells, mast cells |
| CXCR4 (CD184) | CXCL10, CXCL11, CXCL12 (SDF-1) | Naïve T cells | Immature DC, monocytes, B cells |
| CXCR6 (CD186) | CXCL16 | Activated Th1 and CTL | NK cells |
| CXCR7 | CXCL11, CXCL12 | None reported | None reported |
| CCR1 | CCL3, CCL4, CCL5, (RANTES), CCL7 (MCP-3), CCL14, CCL15 | Activated T cells | Monocytes, immature DC, basophils, neutrophils, eosinophils |
| CCR2 | CCL2, CCL7 | Activated T cells | Monocytes, immature DC, basophils, neutrophils, NK cells, endothelial cells, fibroblasts |
| CCR3 | CCL5, CCL7, CCL14, CCL15, CCL26, CCL28 | Th2 cells | DC, basophils, eosinophils, mast cells |
| CCR4 | CCL2, CCL3/CCL4 (MIP-1α/MIP-1β), CCL5, CCL17, CCL22 | Th2 cells and Treg | Immature DC, basophils |
| CCR5 (CD195) | CCL3/CCL4, CCL5, CCL14 | Th1 cells, CTL | Monocytes, immature DC, NK cells |
| CCR6 (CD196) | CCL20 (MIP-3α) | Activated T cells | Immature DC, B cells |
| CCR7 (CD197) | CCL19, CCL21 | Naive and memory T cells | Mature DC, B cells |
| CCR8 (CDw198) | CCL1, CCL4, CCL17 | Th2 cells, Treg | Monocytes, B cells |
| CCR9 (CDw199) | CCL20 | T cells | Macrophages, DC |
| CCR10 | CCL28 | Activated T cells, Treg | Dermal endothelial cells, fibroblasts |
| CCR11 | CCL19, CCL21 | None | None |
| XCR1 (GPR5) | XCL1 (SCM-1α), XCL2, XCL1 | Resting T cell | None |
| $CX_3CR1$ (GPR13) | CCL26, $CX_3CL1$ | Th1 cells | Monocytes, neutrophils, NK cells |
| CMKLR1 | Chemerin (TIG-2) | Unstimulated Th cells | Macrophages, immature DC, endothelial cells |

Adapted from (Tanaka, 2001; Takata *et al.*, 2004; Yoshimura & Oppenheim, 2011; Ha *et al.*, 2017)

**Table 6.2: Characteristics of the patients from which tumour tissue and blood samples were obtained and how the samples were used in the chemokine study**
For the Proteome Profiler CM was collected from dissociated tumour tissue. PBMC and TIL collected from patients were stained with fluorescent antibodies for CTLs and/or Treg with chemokine receptor antibodies.

| | Subsite | ID | Age | Gender | Tumour Origin | Stage | Experiments | | | | |
|---|---|---|---|---|---|---|---|---|---|---|---|
| | | | | | | | Proteome Profiler | PBMC | TIL | | Migration Assays |
| | | | | | | | | | CTL | Treg | |
| Primary tumour | Larynx | L1 | NA | NA | Larynx | T1aN0 | ✓ | | | | |
| | | L2 | 64 | Male | Larynx | T4N0 | | ✓ | | ✓ | |
| | | L3 | 71 | Female | Larynx | T4N0 | ✓ | | | | |
| | | L4 | 61 | Male | Piriformfossa | T4N0 | | ✓ | ✓ | | ✓ |
| | | L5 | NA | NA | Larynx | T4N0 | ✓ | | | | |
| | | L6 | 63 | Male | Larynx | T4N2 | | ✓ | | | ✓ |
| | | L7 | 73 | Male | Larynx | T4N2b | | ✓ | | ✓ | ✓ |
| | | L8 | 56 | Male | Supraglottis | T4N2c | ✓ | | | | ✓ |
| | | L9 | 65 | Female | Larynx | Unknown | | ✓ | | ✓ | |
| | Oropharynx | O1 | 56 | Male | Left tonsil | T2N0 | ✓ | ✓ | ✓ | ✓ | |
| | | O2 | 51 | Male | Right tonsil | T2N0 | | ✓ | ✓ | ✓ | |
| | | O3 | 56 | Female | Right tonsil | T2N0 | ✓ | | | | ✓ |
| | | O4 | NA | NA | Soft pallet | T2N0 | | ✓ | | ✓ | |
| | | O5 | 60 | Female | Base of tongue | T4N2b | | ✓ | ✓ | | |

| | | | | | | | | | | | |
|---|---|---|---|---|---|---|---|---|---|---|---|
| | Oral | O6 | 59 | Male | Left lateral tongue | T1N0 | | ✓ | ✓ | | ✓ |
| | | O7 | 71 | Female | Left lateral tongue | T1N0 | | ✓ | ✓ | | |
| | | O8 | NA | Male | Right lateral tongue | T1N0 | | ✓ | | | |
| | | O9 | 55 | Male | Right mandible | T1N2b | | ✓ | | | |
| | | O10 | NA | Male | Right lingual sulcus | T2N0 | | ✓ | ✓ | | |
| | | O11 | NA | NA | Anterior maxilla | T4N0 | | ✓ | | ✓ | |
| | | O12 | 67 | Female | Right mandible | T4N0 | | ✓ | ✓ | ✓ | |
| | | O13 | 43 | Male | Left posterolateral tongue | T4aN1 | | ✓ | ✓ | ✓ | |
| | Hypopharynx | H1 | NA | Male | Hypopharynx | T4N0 | ✓ | | | | ✓ |
| **Metastatic Lymph Node** | | N1 | 55 | Male | Piriformfossa (Larynx) | T1N2b | ✓ | | | | |
| | | N2 | 56 | Male | Supraglottis (Larynx) | T4N2c | ✓ | | | | ✓ |
| | | N3 | 66 | Male | Left tonsil (Orophaynx) | T1N2b | | | | | ✓ |
| | | N4 | 53 | Male | Unknown | T0N2a | | ✓ | ✓ | ✓ | |

*NA – information not available

### 6.2.2 Staining whole blood and PBMC for chemokine receptors

In order to determine whether PBMC isolation led to a significant reduction in the expression of the selected chemokine receptors in the protocol used in this study, whole blood and PBMC from the same patients were labelled with antibodies directed against chemokine receptors for comparison (Section 2.3.1). PBMC from HNSCC (Section 2.2.1) were re-suspended in PBS/BSA/Azide at $5x10^6$ cells/ml and transferred (100µl) to FACS tubes as was whole venous blood (100µl). Antibodies for chemokine receptors (CXCR3, CCR4, CCR5 and CCR6, Miltenyi Biotech; Table 6.3 and Table 6.4) were added to the tubes of cells and incubated at room temperature in the dark for 30 minutes.

For whole blood, 1xFACS lysing solution (2 ml; BD Biosciences) was added to each tube of cells to lyse erythrocytes. Following incubation for 10 minutes in the dark at room temperature, immune cells were recovered by centrifugation at 400 x *g* for 5 minutes. The supernatant was discarded and the cell pellet washed in 1 ml PBS, centrifuged to recover cells and resuspended in 200 µl of PBS for analysis by flow cytometry (Section2.3.4). Results from flow cytometry were compared with the PBMC isolated and stained from the venous blood of the same patient.

### 6.2.3 Multicolour staining of PBMC and TIL for chemokine receptors and T cell markers

For the investigation of chemokine receptor expression PBMC from healthy donors and HNSCC patients (Section 2.2.1) and TIL from HNSCC dissociated tumours (Section 2.2.4). were stained with a combination of antibodies for CD3 and CD8 or CD4, CD25, CD39 and FoxP3 in conjunction with the various chemokine receptor antibodies (Table 6.3 and Table 6.4). Following antibody staining (Section 2.3.1), cells were analysed by flow cytometry (Section 2.3.2-2.3.4).

**Table 6.3 Antibodies used for the analysis of chemokine receptor expression**

| Antibody | Clone | Concentration |
|---|---|---|
| Brilliant Violet 421 Mouse anti-Human CD3 | UCHT1 | 1.25 µg/ml |
| FITC Mouse anti-Human CD8 | RPA-T8 | 3.13 µg/ml |
| PerCP Mouse anti-Human CD4 | SK3 | 0.15 µg/ml |
| APC Mouse anti-Human CD25 | M-A251 | 0.15 µg/ml |
| PE Mouse anti-Human CD26 | M-A261 | 0.625 µg/ml |
| Brilliant Violet 421 Mouse anti-Human CD39 | TU66 | 0.625 µg/ml |
| AlexaFluor488 Mouse anti-Human FoxP3 | 259D/C3 | 2.5 µg/ml |
| PE CXCR3 anti-Human CXCR3 (CD183) | REA232 | 2.75 µg/ml |
| PE anti-Human CCR4 (CD194) | REA279 | 2.75 µg/ml |
| PE anti-Human CCR5 (CD195) | REA 245 | 2.75 µg/ml |
| PE anti-Human CCR6 (CD196) | REA190 | 2.75 µg/ml |

**Table 6.4: Antibody combinations used to analyse chemokine receptor expression on CTL and Treg**

| T cell subset | Antibodies | |
|---|---|---|
| | T cell markers | Chemokine receptor |
| CTL | CD3, CD8 | CXCR3 |
| | CD3, CD8 | CCR4 |
| | CD3, CD8 | CCR5 |
| | CD3, CD8 | CCR6 |
| Treg | CD4, CD25, CD39, FoxP3 | CXCR3 |
| | CD4, CD25, CD39, FoxP3 | CCR4 |
| | CD4, CD25, CD39, FoxP3 | CCR5 |
| | CD4, CD25, CD39, FoxP3 | CCR6 |

### 6.2.4 Migration of PBMC towards CXCL12 and conditioned medium

To determine whether chemokines released by dispersed HNSCC tumour samples (Section 2.2.4) were able to actively induce the chemotaxis of $CD4^+$, $CD8^+$ CTL or Treg, migration assays were carried out using CM (Section 2.8). As a positive control to measure T cell migration, GM supplemented with 80 ng/ml CXCL12, a known T cell chemoattractant (Yonezawa *et al.*, 2000), was added to specific wells. PBMC were incubated for two hours at 37$^o$C and 5% $CO_2$ before seeding into transwells in low serum medium at a final concentration of 2.5 x $10^6$ cells/ml (Section 2.8). Low serum GM with or without CXCL12, or dissociated CM was added to the bottom wells of the plate. Following a 4 hour incubation

at 37°C and 5% $CO_2$, cells that had migrated through into the bottom well of the plates were collected, counted with trypan blue (Section 2.1.4) and transferred immediately to separate FACS tubes for staining.

#### 6.2.4.1 *Multicolour staining of migrated cells for T cell markers*

Cells were incubated in PBS/BSA/Azide with a combination of antibodies for CD3, CD4, CD8 and the negative Treg marker CD127. Due, to the small number of cells recovered from the wells, the Treg marker FoxP3 was not used in order to avoid any additional loss of cells during the fixation and permeabilisation procedure. Following a final washing step, cells were resuspended in 100µl PBS/BSA/Azide and analysed by flow cytometry (Section 2.3.1). As many cells as possible were acquired, for around 5 to 6 minutes, and to compare the number of migrated cells between treatments this was normalised to the number of $CD3^+$ cells acquired/minute.

### 6.2.5 **Statistical analysis**

Statistical analysis was carried out using GraphPad Prism 7 (GraphPad Software). For the comparison of chemokines in the CM from early/late stage tumours Mann Whitney U tests were performed. To identify differences between chemokine receptor expression on TIL and PBMC and between HNSCC patient and healthy donor PBMC, Shapiro-Wilks tests were first carried out to determine whether the data were normally distributed. For normally distributed data, significant differences were determined using unpaired T tests for data that were not normally distributed the non-parametric Mann Whitney U test was used. For the analysis of chemokine receptor expression on matched PBMC and TIL samples, Sharpiro-Wilks tests were again carried out, and normally distributed data were analysed using paired T tests. For datasets that did not follow a normal distribution, the non-parametric match paired Wilcoxon test was used. Statistical analysis was not performed on results from migration assays due to the small numbers. All error bars represent SEM, and statistically significant differences are those where *$p$<0.05, **$p$<0.01, ***$p$<0.001 and ****$p$<0.0001.

## 6.3 Results

### 6.3.1 Chemokines released by cells of the HNSCC microenvironment

Proteome Profiler™ human chemokine array kits (R&D Systems) were used to measure the relative expression levels of 31 chemokines in CM from four laryngeal, two oropharyngeal and one hypopharyngeal primary tumour and two metastatic nodes; Table 6.2). Most of the chemokines were detectable to some degree in all of the CM, however in many cases the level of bound protein was very low (Figure 6.1a). There was clear variation in the chemokines released between individual tumours. With one laryngeal sample (L1) and the hypopharyngeal sample, showing very little detectable levels of any chemokines other than CXCL8, while the other two laryngeal samples (L3 and L5) contained much higher levels of all the other chemokines.

CXCL28, CCL16, CCL26, CXCL16, CCL14, CCL1, CXCL10, CXCL11, XCL1, CCL7, CXCL9, CCL15, CCL18, CXCL12, CCL17 and CXCL17 all had mean pixel densities below 10 in at least five out of nine CM studied. Conversely, Midkine, CXCL1 and CCL19, were present at levels high enough to give a mean pixel density over 10 in five of nine CM. All other chemokines (CXCL4, CXCL5, CXCL7, CXCL8, CCL2, CCL3/4, CCL5, CCL20, CCL21, CCL22, Chemerin and IL16) were observed at notable levels (mean pixel density>10) in at least six CM and gave mean pixel densities above 150 in at least one CM (Figure 6.1b).

Of the chemokines tested CXCL8 was the only one to be detected at notable levels in CM derived from all nine of the dispersed tumour samples with mean pixel densities ranging from 110 to 580 (Figure 6.1). The highest levels of CXCL8, CCL2, CCL3,4, CCL20 and CCL22 were detected in the same CM (O3), derived from a T2 oropharyngeal primary tumour and the lowest levels were observed in the CM derived from a hypopharyngeal tumour (Figure 6.1b). Grouping of the tumours according to subsite and stage revealed no difference in secretion of the most detectable chemokines (Figure 6.2 and Figure 6.3).

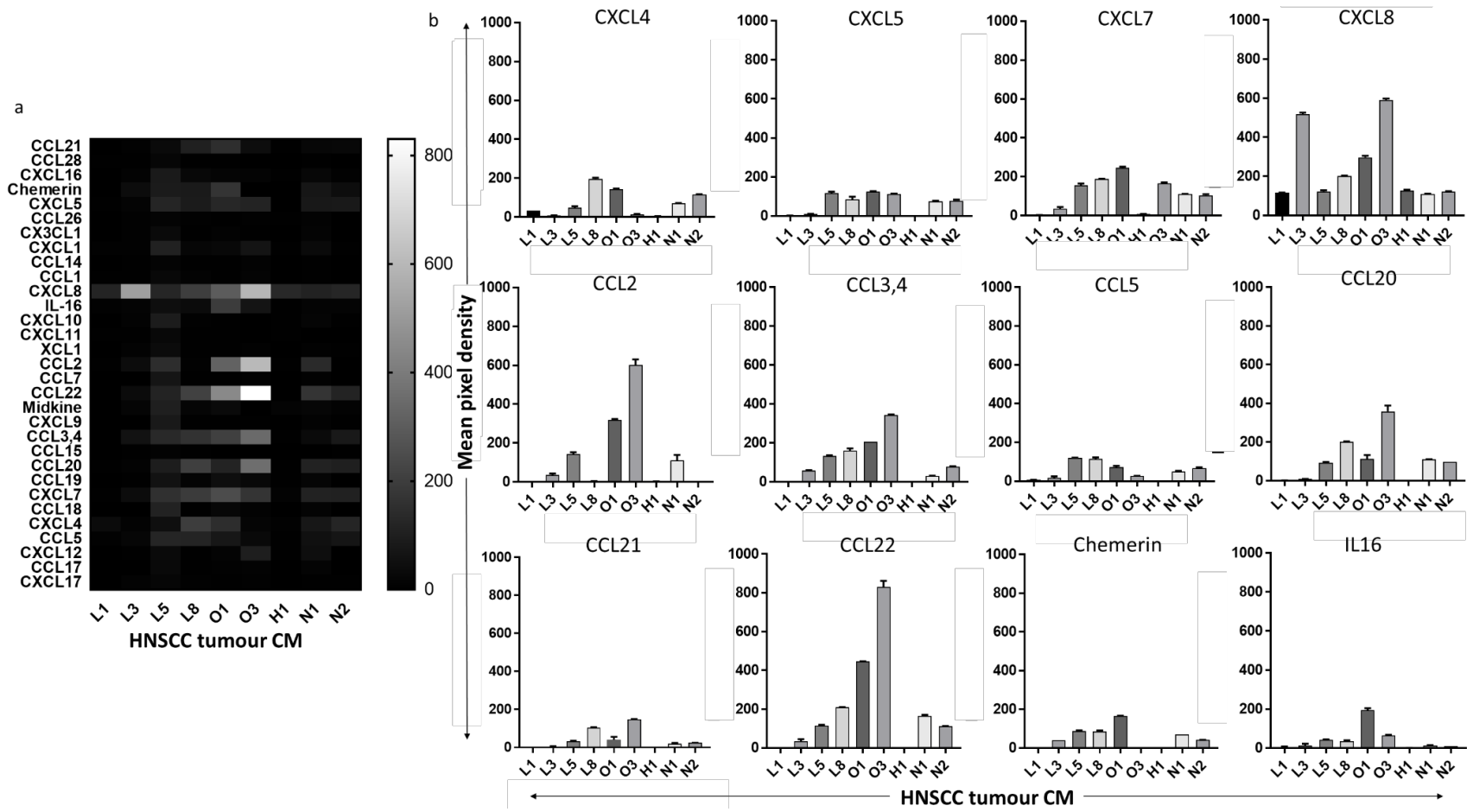


**Figure 6.1: Detection of chemokines in CM collected form the overnight culture of nine dissociated tumour biopsies**

A Proteome Profiler™ human chemokine array kit (R&D systems) was used to detect chemokines in the CM. The heat map shows the mean pixel density from duplicate wells for each chemokine (a) and bar charts represent the mean (±SEM) pixel density of the most frequently expressed chemokines (b).

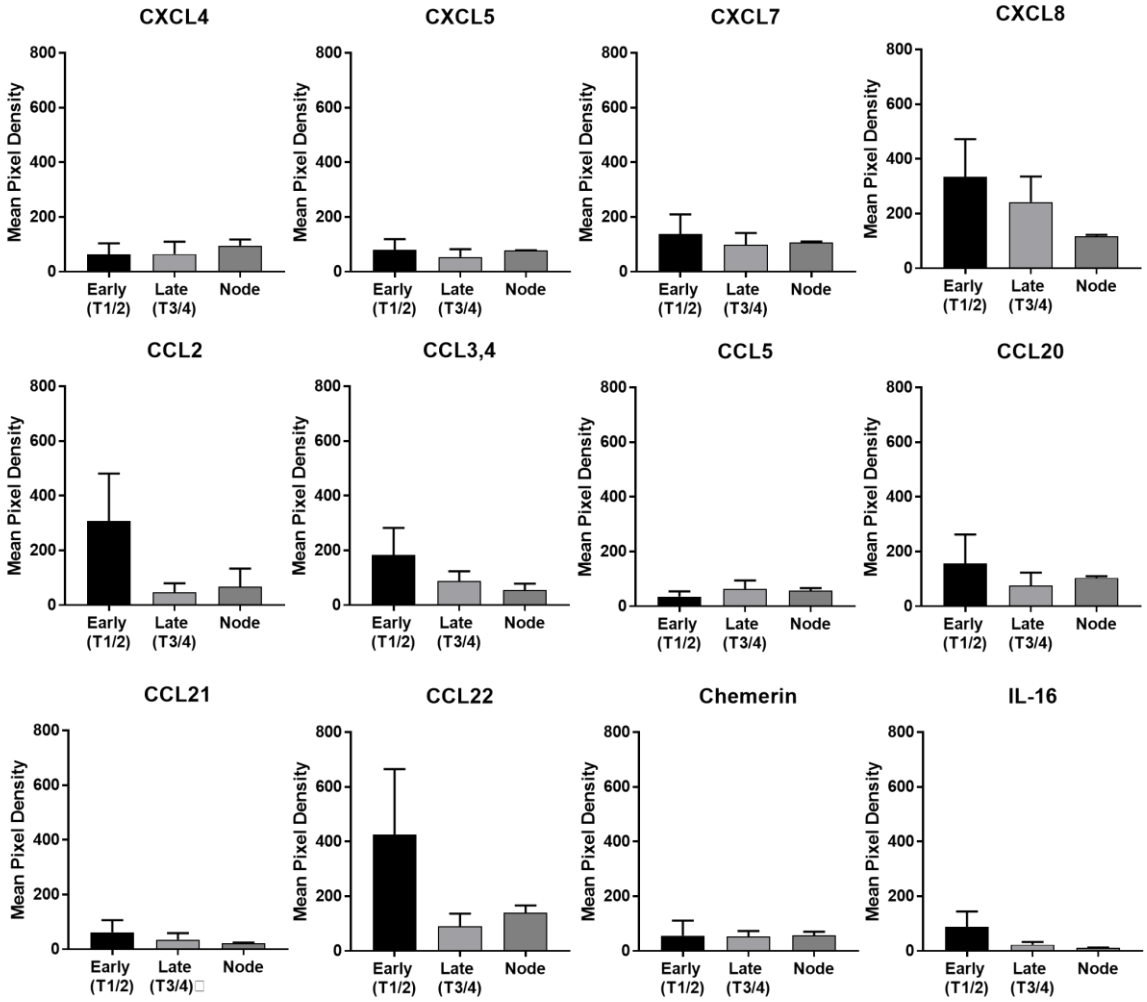


**Figure 6.2: Comparison of chemokine production from early and late tumour stages and nodal metastases**
Mean pixel density of twelve chemokines in CM from the overnight culture of dissociated early stage (tumour stage 1 and 2; n=3) and late stage (tumour stage 3 and 4; n=4) primary HNSCC tumour tissue and metastatic node (n=2). To compare differences between early and late stage tumours Mann Whitney U tests were performed.

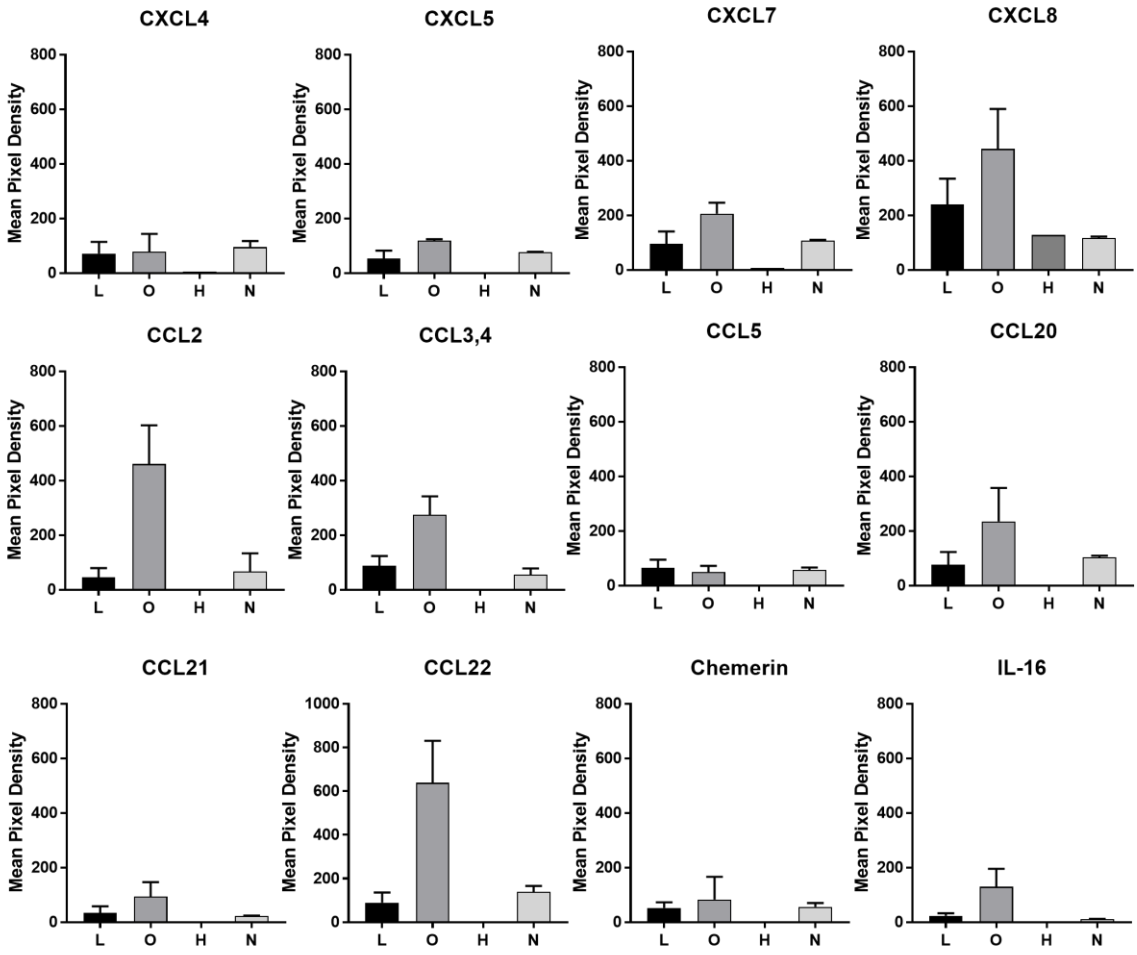


**Figure 6.3: Comparison of chemokine production from different HNSCC sub sites**
Mean pixel density of twelve chemokines in CM from the overnight culture of dissociated laryngeal (n=4), oropharyngeal (n=2), hypopharyngeal (n=1) primary HNSCC tumour tissue and metastatic node (n=2).

### 6.3.2 Chemokine receptor expression on whole blood and PBMC

To determine whether the isolation of PBMC using this method reduced the percentage of T cells expressing the chemokine receptors CXCR3, CCR4, CCR5 and CCR6, whole venous blood and PBMC from three donors were stained with antibodies for the receptors and percentage of lymphocytes expressing each receptor was compared. No difference was observed between the percentage expression of CXCR3 (39.1±6.1% on whole blood *vs*. 37.1±1.2 on PBMC), CCR4 (13.0±3.4% on whole blood *vs*. 14.9±0.9% on PBMC) and CCR6 (21.4±2.6% on whole blood *vs*. 22.0±2.4% on PBMC) on lymphocytes in whole blood compared to following PBMC isolation (Figure 6.4). The mean percentage of lymphocytes expressing CCR5 was slightly lower in PBMC than whole blood (13.3±10.9%

on whole blood *vs*. 8.8±8.1% on PBMC), due to a lower level of expression on the cells from one of the three patients.

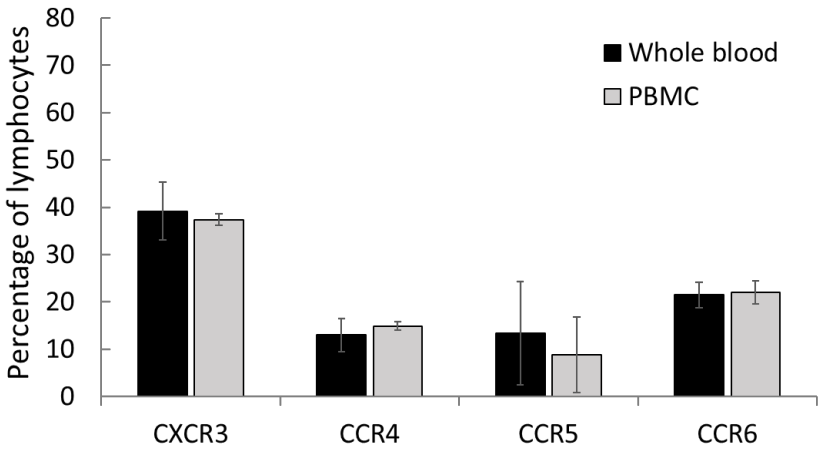


**Figure 6.4: Mean percentage of lymphocytes expressing the chemokine receptors CXCR3, CCR4, CCR5 and CCR6 on whole blood and following isolation of PBMC**
Venous blood collected from HNSCC patients (n=3) was stained with antibodies for chemokine receptors, either immediately or following PBMC isolation by density gradient centrifugation. Bars represent the mean (±SEM) percentage of cells expressing chemokine receptors on T lymphocytes.

### 6.3.3 CXCR3, CCR4, CCR5 and CCR6 in T lymphocyte subsets of HNSCC patient PBMC and TIL

The percentage of each T cell subset expressing the different chemokine receptors was compared between PBMC and TIL from peripheral blood and tumour biopsies of HNSCC patients Figure 7.7 and Figure B.8, Appendix B). Due to the small number of TIL recovered from some tumour biopsies, it was not always possible to stain for all the antibodies in each patient. Therefore, chemokine receptor expression on TIL was measured in fewer patients than chemokine receptor expression on PBMC. For staining of cells with antibodies for CD3, CD8 and each of the chemokine receptors PBMC from fifteen HNSCC patients (5 laryngeal SCC, 9 oral/oropharyngeal SCC, 1 metastatic node) and TIL from seven HNSCC patients (2 laryngeal SCC, 4 oral/oropharyngeal SCC, 1 metastatic node) were used. Although, there was a slightly lower mean percentage of $CD3^+$ lymphocytes expressing the chemokine receptor CXCR3 in PBMC (42±2.7%, n=15) than TIL (54.1±6.3, n=7) from HNSCC patients, the difference was not statistically significant (p=0.0793; Figure 6.5a). However, in matched PBMC and TIL samples, six of the seven patients had a higher percentage of CXCR3 expression on $CD3^+$ lymphocytes from TIL compared to PBMC and

this difference was statistically significant ($p$=0.0313; Figure 6.5b). There was no overall difference between the expression of CXCR3 on $CD3^+CD8^+$ TIL compared to PBMC in unpaired and matched paired samples. The expression of chemokine receptors on Th cells and Treg was analysed in eighteen PBMC samples (5 laryngeal SCC, 12 oral/oropharyngeal SCC, 1 metastatic node) and ten TIL (2 laryngeal SCC, 7 oral/oropharyngeal SCC and 1 metastatic node). CXCR3 expression was significantly higher in the $CD4^+$ Th cells from TIL compared to those isolated from PBMC ($p$=0.0235 in unpaired and 0.0270 in paired samples), with five of the ten patients having between 0.5-fold and 1.4-fold more CXCR3 expressing $CD4^+$ Th cells in the TIL compared with PBMC and the remaining five patients showing little difference, or in one case moderately less, CXCR3 expression on $CD4^+$ lymphocytes from TIL. $CD4^+CD25^{hi}FoxP3^+$ Treg isolated from TIL also contained a greater proportion of $CXCR3^+$ cells than from PBMC ($p$=0.0104 in unpaired and 0.0278 in paired samples). There was no significant difference between expression of CXCR3 on the $CD4^+CD25^-CD39^+$ population from PBMC and TIL, with greater levels of expression on the TIL from five of the patients, reduced expression in two patients and similar levels of expression in the final two patients. Overall the expression of CXCR3 on Th cells and Treg ($CD4^+CD25^{hi}FoxP3^+$) was similar (42.2±3.0% and 43.4±2.9% in PBMC, respectively), and slightly higher on the $CD4^+CD25^-CD39^+$ (55.4±3.1% in PBMC and 62.7 ±8.3% in TIL). The greatest proportion of $CXCR3^+$ cells was observed on $CD8^+$ CTL (66.3±3.9% in PBMC and 79.0±3.3% in TIL).

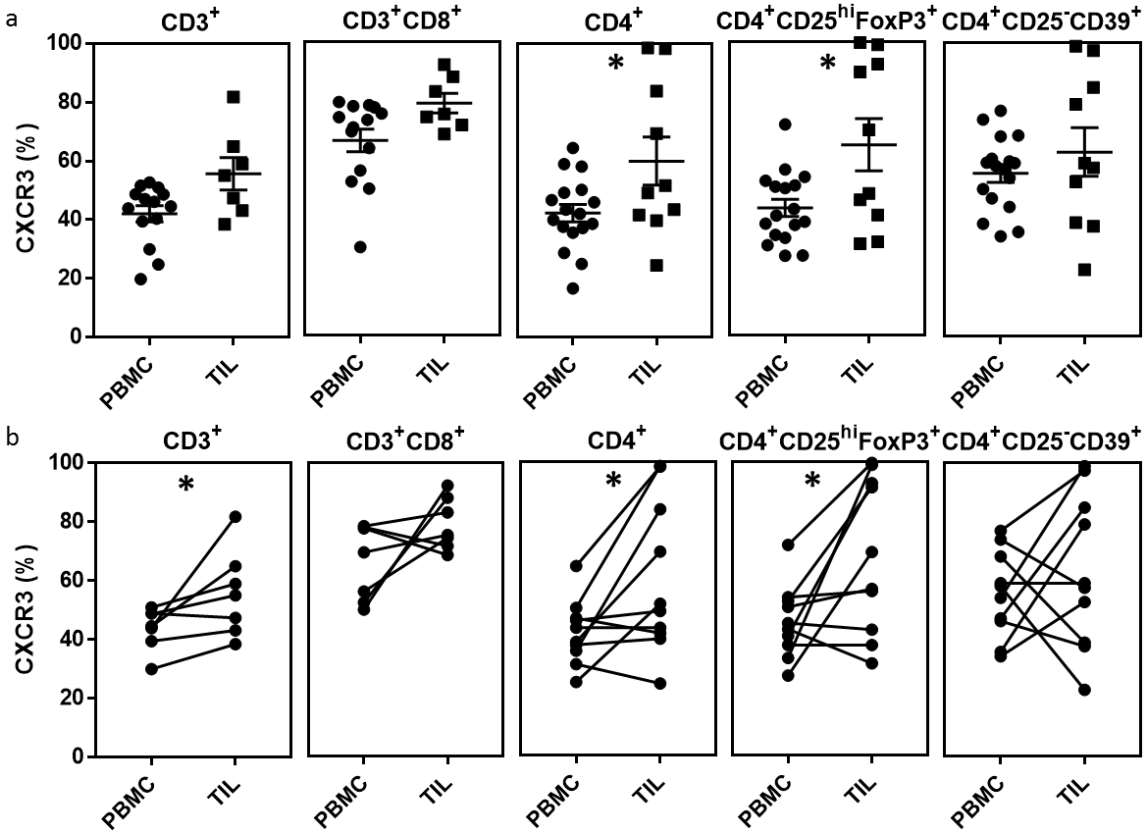


**Figure 6.5: Mean percentage of cells expressing the chemokine receptor CXCR3 on PBMC and TIL from HNSCC patients**

PBMC and TIL were isolated from whole blood and tumour biopsies collected from HNSCC patients and stained for either CD3, CD8 and CCR4 (PBMC;n=15 and TIL; n=7) or CD4, CD25, FoxP3, CD39 and CCR4 (PBMC; n=18 and TIL; n=10 ). Dots represent the percentage of $CD3^+$, $CD3^+CD8^+$, $CD4^+$, $CD4^+CD25^{hi}FoxP3^+$ and $CD4^+CD25^-CD39^+$ lymphocytes from individual donors expressing CCR4 (a) and the percentage of $CD3^+$, $CD3^+CD8^+$ (n=6), $CD4^+$, $CD4^+CD25^{hi}FoxP3^+$ and $CD4^+CD25^-CD39^+$ lymphocytes (n=10) expressing CCR4 from matched PBMC and TIL samples (b). Bars represent the mean percentage ±SEM and significant results are considered as those where $*p<0.05$, $**p<0.01$, $***p<0.001$ and $****p<0.0001$. Statistical analysis was carried out using independent T tests (a) and paired T tests for matched patient samples (b).

Overall, there was no difference in the expression of CCR4 on $CD3^+$, $CD3^+CD8^+$, $CD4^+$, or $CD4^+CD25^{hi}FoxP3^+$ T cell populations between PBMC and TIL (Figure 6.6a and b). In all of these cell types there was no consistent trend between receptor expression on TIL and PBMC, with some patients having higher expression on TIL and others higher on PBMC. In contrast CCR4 expression was significantly lower on $CD4^+CD25^-CD39^+$ cells from TIL ($p$=0.0007 on unpaired and $p$=0.0201 on paired samples from the same patients), with a lower proportion of CCR4 expressing cells in TIL compared with those from PBMC in seven of the ten patients. On average, CCR4 expression was highest on Treg and lowest on CTL

in both PBMC (89.3±1.7% and 30.5±4.8%) and TIL (78.0±7.8% and 32.3±10.8%). Considerable variation in expression of CCR4 was also observed between patients.

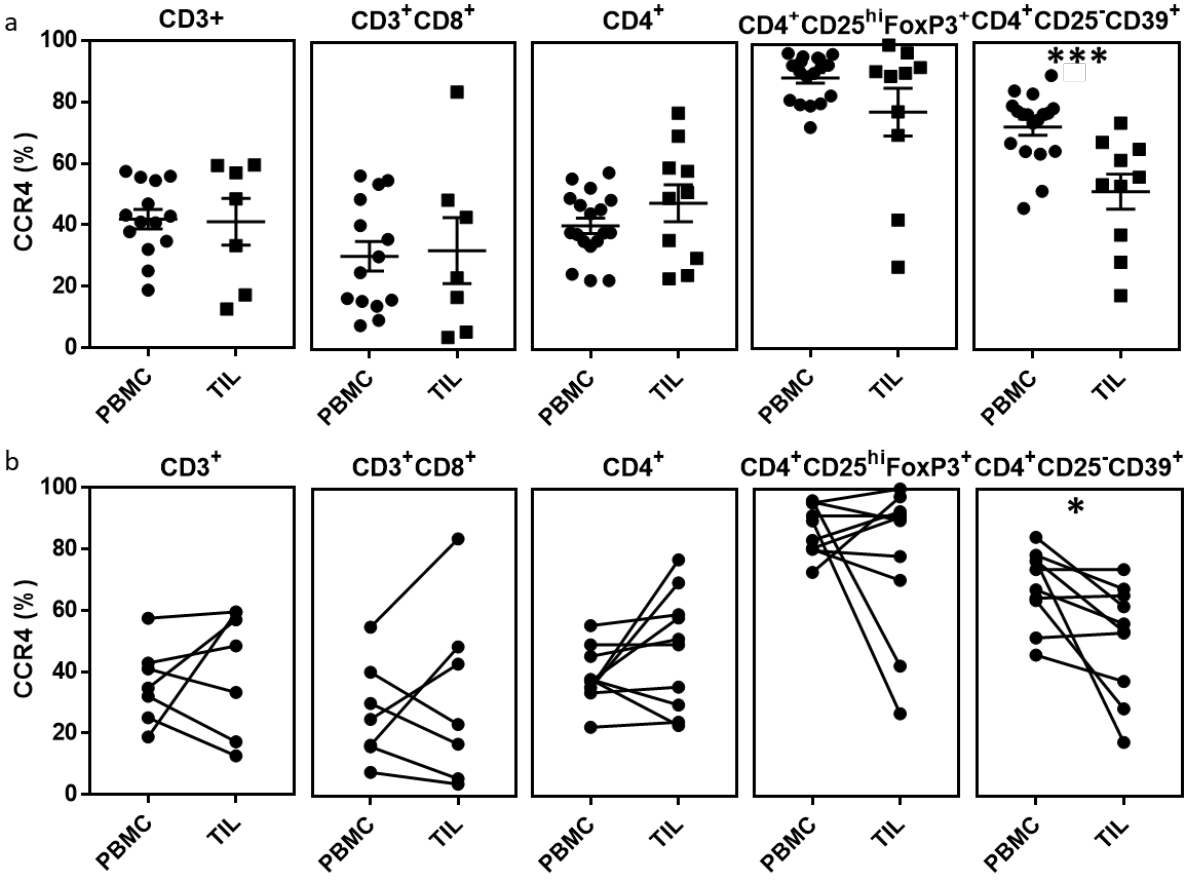


**Figure 6.6: Mean percentage of cells expressing the chemokine receptor CCR4 on PBMC and TIL from HNSCC patients**

PBMC and TIL were isolated from whole blood and tumour biopsies collected from HNSCC patients and stained for either CD3, CD8 and CCR4 (n=15 and n=7, PBMC and TIL) or CD4, CD25, FoxP3, CD39 and CCR4 (n=18 and n=10, PBMC and TIL). Dots represent the percentage of $CD3^+$, $CD3^+CD8^+$, $CD4^+$, $CD4^+CD25^{hi}FoxP3^+$ and $CD4^+CD25^-CD39^+$ lymphocytes from individual donors expressing CCR4 (a) and dots represent the percentage of $CD3^+$, $CD3^+CD8^+$ (n=6), $CD4^+$, $CD4^+CD25^{hi}FoxP3^+$ and $CD4^+CD25^-CD39^+$ lymphocytes (n=10) expressing CCR4 from matched PBMC and TIL samples (b). Bars represent the mean percentage ±SEM and significant results (*) are considered as those where *$p$<0.05, **$p$<0.01, ***$p$<0.001 and ****$p$<0.0001. For statistical analysis of the expression of CCR4 on $CD4^+CD25^{hi}FoxP3^+$ cells a Mann Whitney U test and a Wilcoxon test were performed on unpaired and paired data respectively. All other statistical analysis was carried out using independent T tests (a) and paired T tests for matched patient samples (b).

CCR5 expression was significantly higher on $CD3^+$ ($p$=0.002) and $CD3^+CD8^+$ cells ($p$<0.0001; Figure 6.7a), extracted from TIL compared with those from PBMC, with a greater proportion of $CCR5^+$ cells in TIL from all seven tumours compared to matched PBMC from the same patients ($p$=0.0156 and $p$=0.0156, for $CD3^+$ and $CD3^+CD8^+$ T cells respectively; Figure 6.7b). $CD4^+$ Th cells also contained a greater percentage of CCR5

expressing cells in the TIL compared to the PBMC ($p$=0.0013; Figure 6.7a); with nine of the ten paired samples having markedly higher expression of CCR5 on TIL than PBMC ($p$=0.0043; Figure 6.7b). This same trend was seen on $CD4^+CD25^{hi}FoxP3^+$ Treg ($p$=0.0004 unpaired; n=18 and $p$=0.0030 paired; n=10 paired) and $CD4^+CD25^-CD39^+$ T cells ($p$=0.0123 unpaired and 0.0198 paired samples). One of the patients had very little CCR5 expression on $CD4^+$ Th cells in both PBMC and TIL. The mean percentage of CCR5 expression was highest on CTL (53.5±3.0% in PBMC and 86.6±2.2% in TIL) and Treg (58.0±4.5% in PBMC and 77.5±8.2% in TIL).

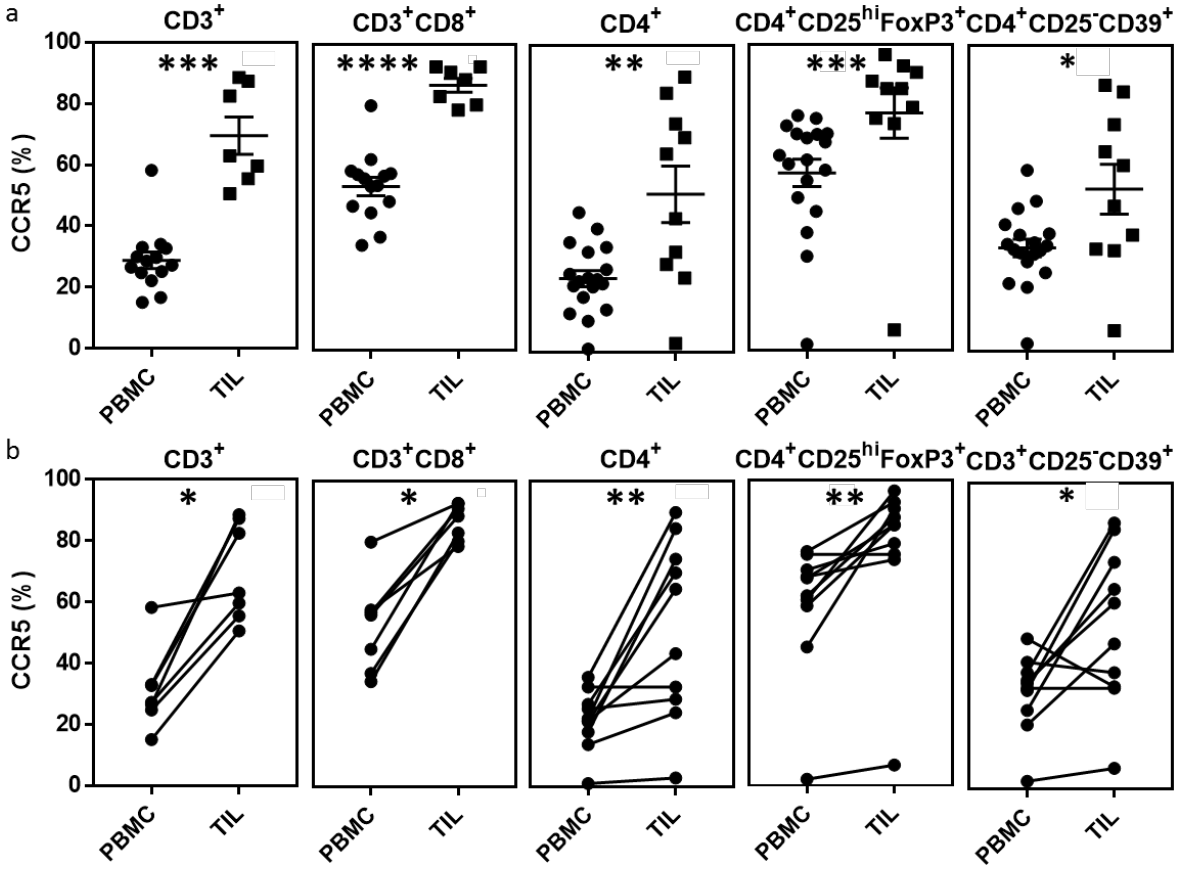


**Figure 6.7: Mean percentage of cells expressing the chemokine receptor CCR5 on PBMC and TIL from HNSCC patients**

PBMC and TIL were isolated from whole blood and tumour biopsies collected from HNSCC patients and stained for either CD3, CD8 and CCR5 (PBMC; n=15 and TIL; n=7) or CD4, CD25, FoxP3, CD39 and CCR5 (PBMC; n=18 and TIL; n=10). Dots represent percentage of $CD3^+$, $CD3^+CD8^+$, $CD4^+$, $CD4^+CD25^{hi}FoxP3^+$ and $CD4^+CD25^-CD39^+$ lymphocytes from individual donors expressing CCR5 (a) and the percentage of $CD3^+$, $CD3^+CD8^+$ (n=6), $CD4^+$, $CD4^+CD25^{hi}FoxP3^+$ and $CD4^+CD25^-CD39^+$ lymphocytes (n=10) expressing CCR5 from matched PBMC and TIL samples (b). Bars represent the mean percentage ±SEM and significant results are considered as those where *$p$<0.05, **$p$<0.01, ***$p$<0.001 and ****$p$<0.0001. For statistical analysis of the expression of CCR5 on $CD4^+CD25^{hi}FoxP3^+$ cells a Mann Whitney U test and a Wilcoxon test were performed on unpaired and paired data respectively. All other statistical analysis was carried out using independent T tests (a) and paired T tests for matched patient samples (b).

Although there were significantly fewer CCR6$^+$ cells on CD3$^+$ lymphocytes from TIL than PBMC (18.0±4.0% *vs* 30.6±2.1%, $p$=0.0387; Figure 6.8), there were no significant differences in percentage of CCR6 expression observed between PBMC and TIL in any of the specific T cell populations investigated, either overall or within the matched samples. The greatest proportion of CCR6$^+$ cells was observed on the CD4$^+$CD25$^{hi}$FoxP3$^+$ population (67.2±2.6% in PBMC and 75.8±4.8% in TIL).

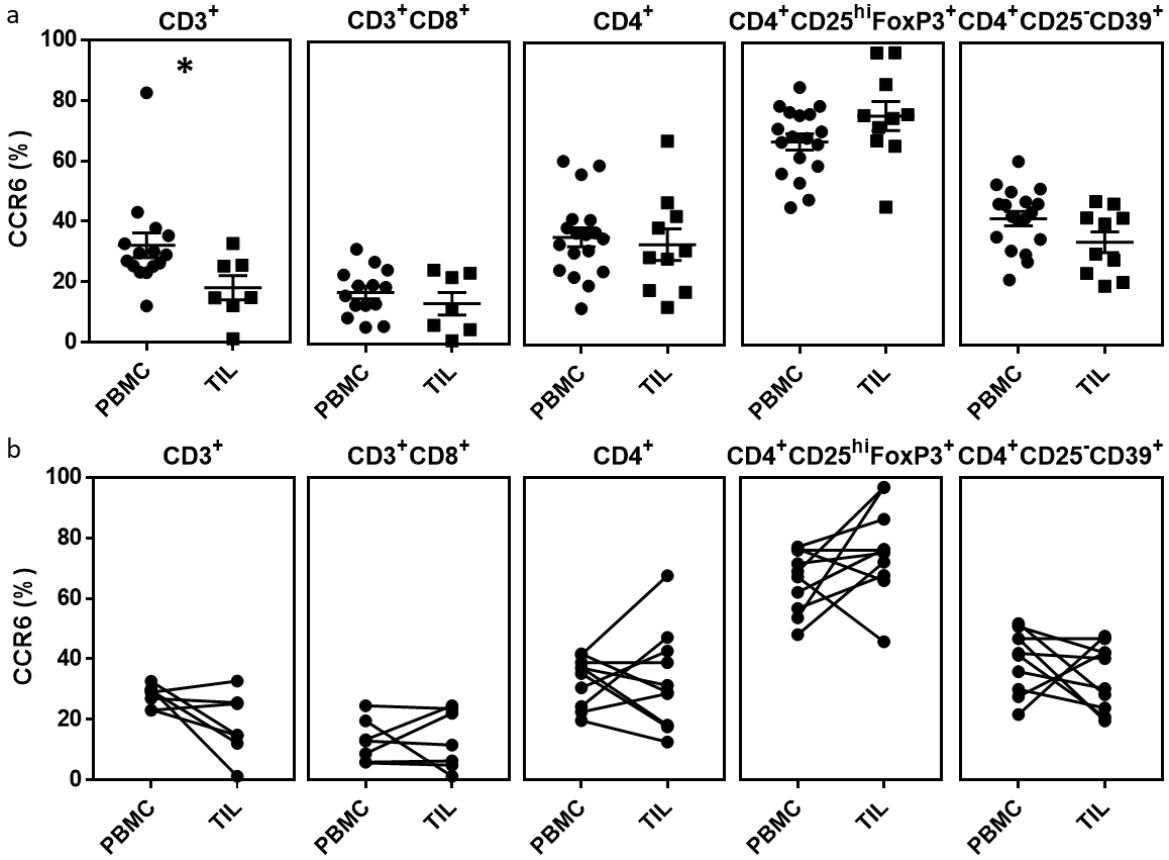


**Figure 6.8: Mean percentage of cells expressing the chemokine receptor CCR6 on PBMC and TIL from HNSCC patients**

PBMC and TIL were isolated from whole blood and tumour biopsies collected from HNSCC patients and stained for either CD3, CD8 and CCR6 (PBMC; n=15 and TIL; n=7) or CD4, CD25, FoxP3, CD39 and CCR6 (PBMC; n=18 and TIL; n=10). Dots represent percentage of CD3$^+$, CD3$^+$CD8$^+$, CD4$^+$, CD4$^+$CD25$^{hi}$FoxP3$^+$ and CD4$^+$CD25$^-$CD39$^+$ lymphocytes from individual donors expressing CCR6 (a) and the percentage of CD3$^+$, CD3$^+$CD8$^+$ (n=6), CD4$^+$, CD4$^+$CD25$^{hi}$FoxP3$^+$ and CD4$^+$CD25$^-$CD39$^+$ lymphocytes (n=10) expressing CCR6 from matched PBMC and TIL samples (b). Bars represent the mean percentage ±SEM and significant results are considered as those where *$p$<0.05, **$p$<0.01, ***$p$<0.001 and ****$p$<0.0001. Statistical analysis was carried out using independent T tests (a) and paired T tests for matched patient samples (b).

### 6.3.4 **CXCR3, CCR4, CCR5 and CCR6 in T lymphocyte subsets of HNSCC patient PBMC and healthy PBMC**

The differences between the expression profile of chemokine receptors on circulating T cells from eighteen HNSCC patients and twelve healthy controls was investigated (Figure 6.9). Percentage expression of CXCR3 was significantly lower on the $CD3^+$ T lymphocyte populations in the peripheral blood of HNSCC patients compared to healthy controls (HC; 42.0±2.7% vs 51.0±3.1%, $p$=0.049; Figure 6.9a). However, there was no difference between the percentage expression of CXCR3 on the $CD3^+CD8^+$ CTL or $CD4^+$ Th subsets between patient and healthy samples.

CCR4 was expressed on a significantly greater percentage of $CD3^+$, $CD4^+$ and $CD4^+CD25^{hi}FoxP3^+$ immune cells from HNSCC patient PBMC compared to those from healthy control PBMC (41.7±4.1% *vs*. 28.9±3.4%, $p$=0.0264; 40.4±2.5% *vs*. 31.2±1.7%, $p$=0.0128; and 89.3±1.7% *vs*. 74.1±3.9%, $p$=0.001 respectively; Figure 6.9b). There was no difference between levels of $CCR4^+$ expressing cells on $CD3^+CD8^+$ CTL and on $CD3^+CD25^-CD39^+$ T cells from healthy control PBMC or HNSCC patient PBMC (21.8±4.2% *vs*. 30.5±4.8%, $p$=0.292 and 64.9±3.6% *vs*. 72.5±2.6%, $p$=0.195).

The expression of CCR5 was no different on any of the T cell populations isolated from HNSCC PBMC or PBMC from healthy controls (Figure 6.9c). The percentage of $CCR6^+$ cells was significantly higher in $CD4^+CD25^{hi}FoxP3^+$ Treg from HNSCC patient PBMC compared with those from healthy controls (67.2±2.6% *vs*. 53.7±4.4%, $p$=0.0085; Figure 6.9d). In the entire $CD3^+$ population there was no overall difference in CCR6 percentage expression between PBMC from patients and controls, and this was also the case for the $CD3^+CD8^+$, $CD4^+$, $CD4^+CD25^{hi}FoxP3^+$ T cell subsets.

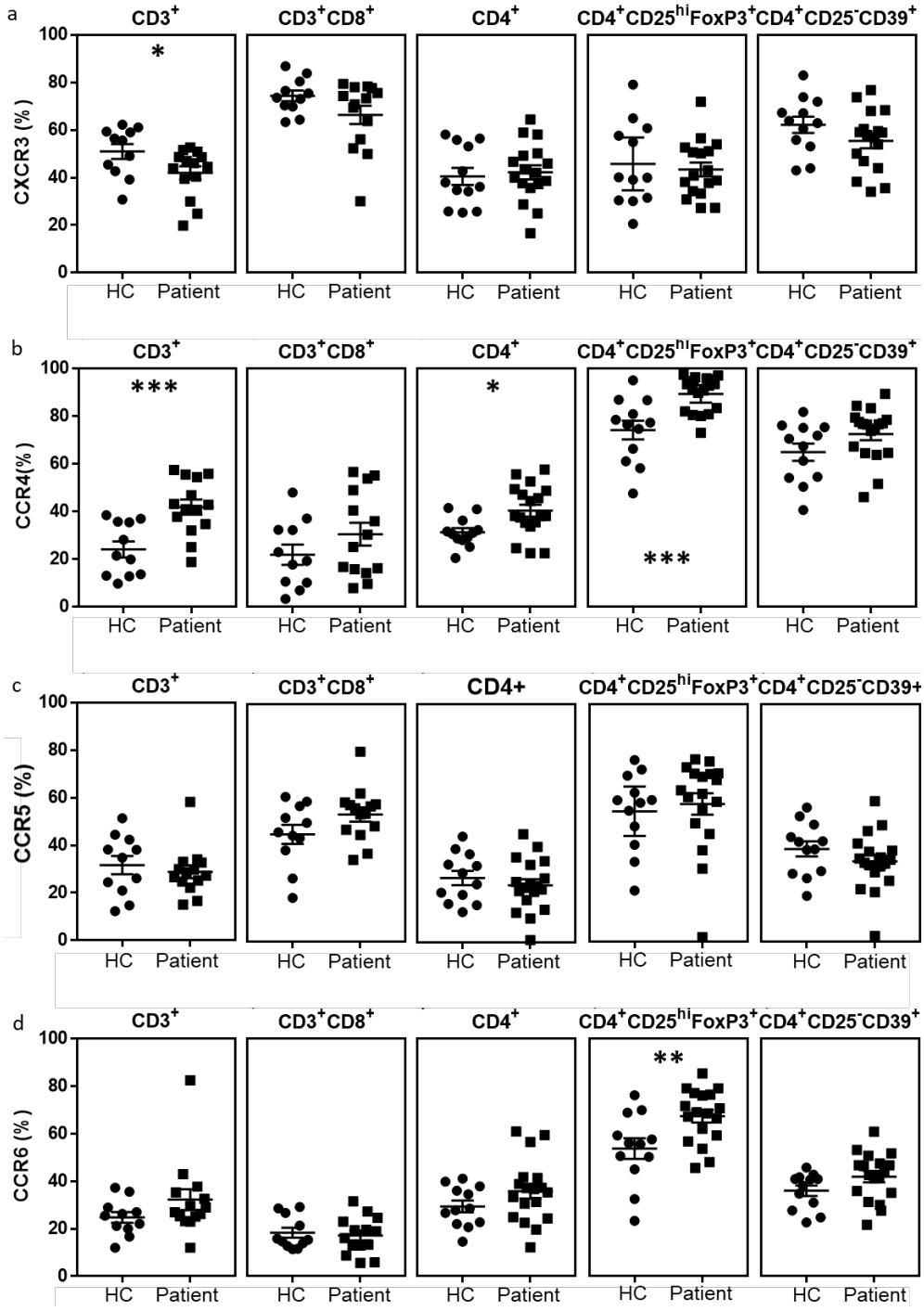


**Figure 6.9: Mean percentage of cells expressing the chemokine receptors CXCR3, CCR4, CCR5 and CCR6 on PBMC from healthy donors and HNSCC patients**

PBMC were isolated from whole blood of healthy controls (HC) and HNSCC patients and stained for a chemokine receptor (CXCR3/CCR4/CCR5/CCR6), in addition to either CD3 and CD8 (HC; n=11 and patient PBMC; n=15,) or CD4, CD25, FoxP3 and CD39 (HD; n=12 and patient PBMC; n=18). Dots represent the percentage of $CD3^+$, $CD3^+CD8^+$, $CD4^+$, $CD4^+CD25^{hi}FoxP3^+$ and $CD4^+CD25^-CD39^+$ lymphocytes expressing CXCR3 (a), CCR4 (b), CCR5 (c) and CCR6 (d) from individual donors and bars represent mean percentage ±SEM. For statistical analysis of the expression of CXCR3 expression on $CD3^+$ and $CD3^+CD8^+$ cells, and CCR5 expression on $CD3^+$ and $CD4^+CD25^{hi}FoxP3^+$ cells Mann Whitney U tests were performed. All other statistical analysis was carried out using independent T tests. Significant results are considered as those where *$p$<0.05, **$p$<0.01, ***$p$<0.001 and ****$p$<0.0001.

**Table 6.5: Percentage expression of CXCR3, CCR4, CCR5 and CCR6 on T cells from healthy control PBMC, HNSCC patient PBMC and HNSCC patient TIL**

| | Healthy Control PBMC | | HNSCC Patient PBMC | | HNSCC Patient TIL |
|---|---|---|---|---|---|
| | Mean±SEM | *P* | Mean±SEM | *p* | Mean±SEM |
| **CXCR3** | | | | | |
| CD3+ | 51.0±3.1% | **0.049** | 42.0±2.7% | **ns** | 54.1±6.3% |
| CD3+CD8+ | 74.3±2.2% | **Ns** | 66.3±3.9% | **ns** | 79.0±3.3% |
| CD4+ | 40.5±3.6% | **Ns** | 42.2±3.0% | **0.024** | 60.0±8.2% |
| CD4+CD25hiFoxP3+ | 45.7±5.0% | **Ns** | 43.4±2.9% | **0.010** | 67.76±8.4% |
| CD4+CD25-CD39+ | 62.2±3.4 | **Ns** | 55.4±3.1% | **ns** | 62.7±8.3 |
| **CCR4** | | | | | |
| CD3+ | 28.9±3.4% | **0.026** | 41.7±4.1% | **ns** | 45.0±7.7% |
| CD3+CD8+ | 21.8±4.2% | **Ns** | 30.5±4.8% | **ns** | 32.3±10.8% |
| CD4+ | 31.2±1.7% | **0.013** | 40.4±2.5% | **ns** | 47.7±6.0% |
| CD4+CD25hiFoxP3+ | 74.1±3.9% | **0.001** | 89.3±1.7% | **ns** | 78.0±7.8% |
| CD4+CD25-CD39+ | 64.9±3.6% | **Ns** | 72.5±2.6% | **<0.001** | 51.5±5.7% |
| **CCR5** | | | | | |
| CD3+ | 31.6±3.8% | **Ns** | 30.1±3.5% | **0.002** | 66.33±6.1% |
| CD3+CD8+ | 45.2±4.0% | **Ns** | 53.5±3.0% | **<0.0001** | 86.6±2.2% |
| CD4+ | 27.1±3.0% | **Ns** | 24.0±2.6% | **0.001** | 51.5±9.2% |
| CD4+CD25hiFoxP3+ | 54.9±4.7% | **Ns** | 58.0±4.5% | **<0.001** | 77.5±8.2% |
| CD4+CD25-CD39+ | 39.1±3.2% | **Ns** | 33.8±2.9% | **0.012** | 53.0±8.2% |
| **CCR6** | | | | | |
| CD3+ | 24.8±2.3% | **Ns** | 30.6±2.1% | **0.039** | 18.0±4.0% |
| CD3+CD8+ | 18.3±2.1% | **Ns** | 17.1±2.1% | **ns** | 13.4±3.7% |
| CD4+ | 29.3±2.5% | **Ns** | 35.7±3.1% | **ns** | 32.8±2.6% |
| CD4+CD25hiFoxP3+ | 53.7±4.4%, | **0.009** | 67.2±2.6% | **ns** | 75.8±4.8 |
| CD4+CD25-CD39+ | 35.9±2.2% | **Ns** | 41.9±2.4% | **ns** | 34.1±3.4 |

*ns represents non-significant differences

### 6.3.5 **Migration of T cells toward soluble factors released by the TME**

Prior to assessing the effect of tumour CM on T cell migration, experiments were carried out using CXCL12 as a positive control. In all cases, $CD3^+$ lymphocytes from both healthy controls (n=3) and HNSCC patients (n=2), migrated more toward GM supplemented with CXCL12 compared to GM alone (Figure 6.10). The migratory potential of these cells varied considerably between individuals, with between three times (Figure 6.10a and d) and 42 times (Figure 6.10b and e) the number of cells migrating towards GM containing CXCL12 than towards GM only. Overall, there was less migration of HNSCC patient $CD3^+$ lymphocytes than healthy controls, with the mean number of healthy lymphocytes migrating toward GM alone 3.6 times that of the patient lymphocytes (111.0±65.6% *vs.* 30.8±15.6%).

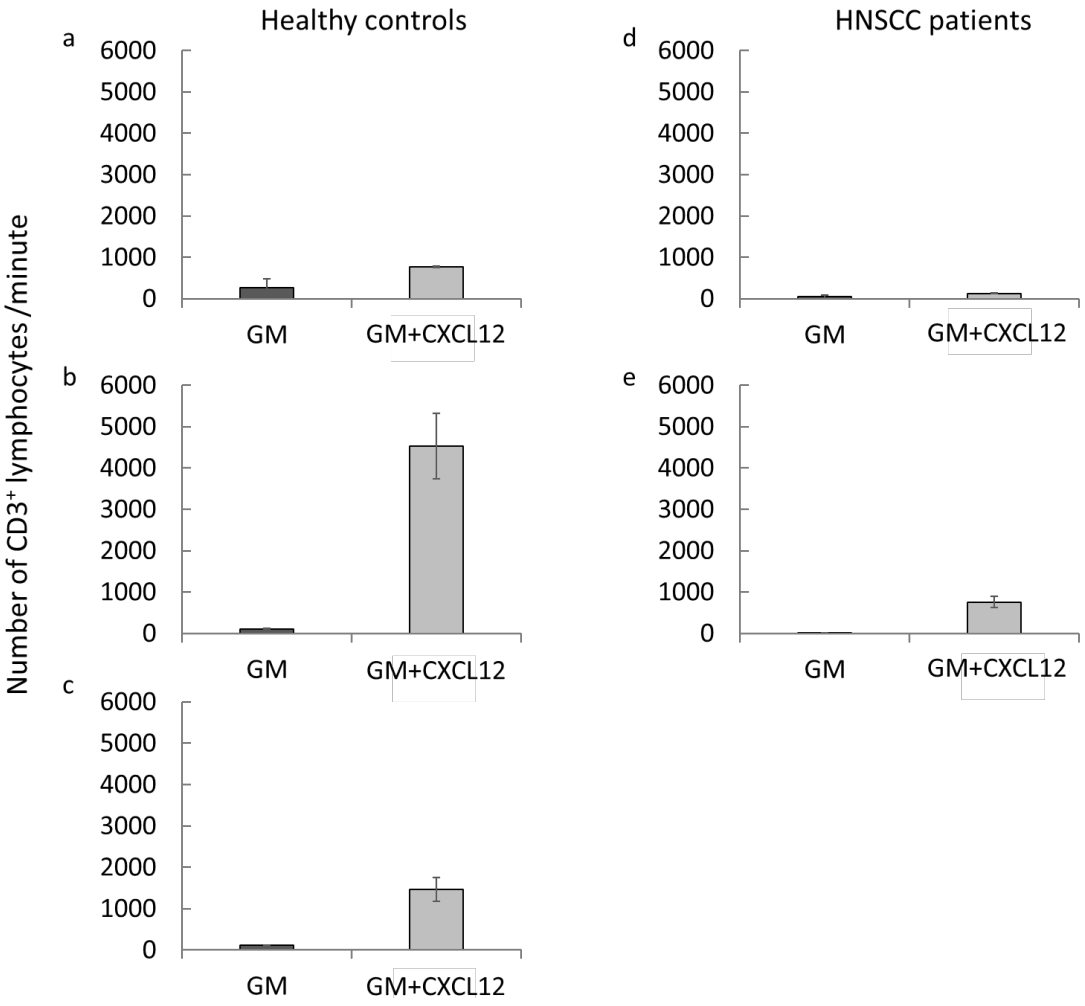


**Figure 6.10: Migration of CD3$^+$ T cells toward CXCL12**
PBMC from healthy controls (n=3) and HNSCC patients (n=2) were seeded into transwells with GM supplemented with or without CXCL12 in the wells underneath. Following 4-hours incubation, the migrated cells were collected, labelled with a CD3 antibody and analysed by flow cytometry. The number of CD3+ lymphocytes acquired per minute was determined. Bars represent mean data from duplicate wells ±SEM.

In addition to differences in the absolute numbers of CD3$^+$ T cells, differences in the proportion of T cell subsets was investigated. The percentage of cells expressing CD4 was increased in the CD3$^+$ lymphocyte population that had migrated toward the GM containing CXCL12, compared to GM alone in all three healthy individuals and both cancer patients (Figure 6.11). In the two donors with the biggest difference in the proportion of CD4$^+$ cells between the GM with and without CXCL12, there was a corresponding lower percentage of CD8$^+$ cells (Figure 6.11b and e). The proportion of Treg that had migrated towards the medium containing CXCL12 was slightly lower than those which had migrated towards the GM alone for two of the healthy PBMC and one patient (Figure 6.11a,b,d). For the second patient PBMC a slightly greater proportion of Treg had migrated toward the GM with

CXCL12 tan that without (Figure 6.11e) and was no difference in the proportion of Treg migrating toward GM with or without CXCL12 for the final healthy sample (Figure 6.11c). Overall, although a greater number of CTL, Th and Treg had migrated toward the CXCL12 supplemented GM in all five experiments, there was a trend toward a reduced proportion of CTL and increased Th cells in the resulting lymphocyte population.

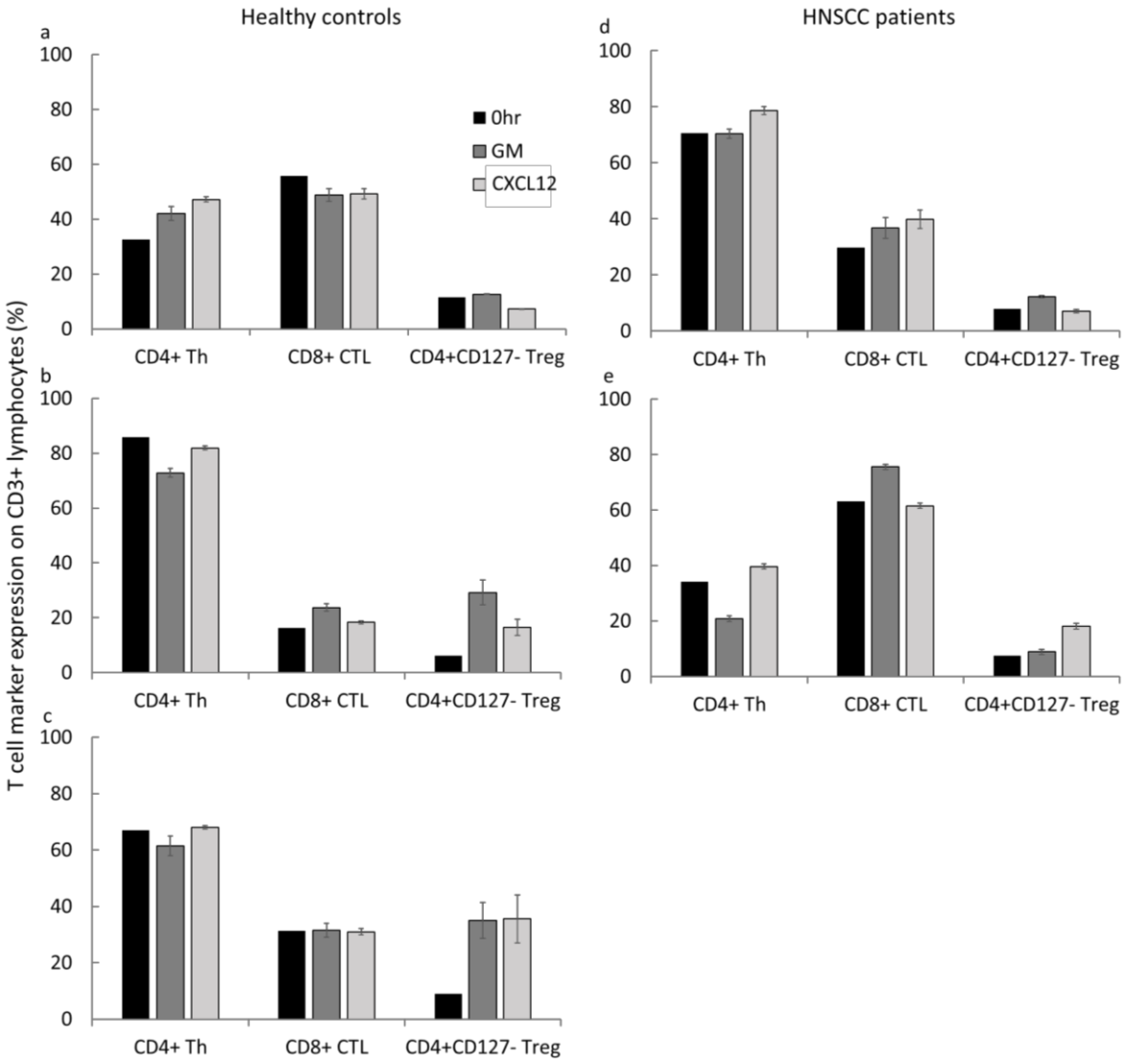


**Figure 6.11: Migration of Th cells, CTL and Treg towards CXCL12**
PBMC from healthy controls (n=3) and HNSCC patients (n=4) were seeded into transwells with GM supplemented with or without CXCL12 (80 ng/ml) in the wells underneath. Following 4-hours incubation, the migrated cells were collected, labelled with specific T cell antibodies and the percentage of $CD4^+$ cells, $CD8^+$, and $CD4^+CD127^-$ cells within the $CD3^+$ T cell population was determined by flow cytometry and compared with the proportions in the whole PBMC (black). Bars represent mean data from duplicate wells ±SEM.

Migration assays were then carried out to determine the ability of soluble factors present in the tumour CM to recruit T cells actively from the PBMC isolated from four healthy controls and two HNSCC patients. The number of $CD3^+$ lymphocytes from three healthy donors and two HNSCC patients that had migrated following culture was the same between GM and CM (Figure 6.12).

When individual subsets of lymphocytes were labelled, there was an overall trend toward a higher proportion of $CD4^+$ Th cells in the $CD3^+$ migrated cells (Figure 6.13). Of the healthy controls, for three of the donors, the proportion of $CD4^+$ cells that had migrated toward the CM was higher in all cases than in the GM control (Figure 6.13a, b and d). For the final healthy donor, T cells that had migrated to three of the four CM contained a greater percentage of $CD4^+$ T cells, compared to the GM control, and in the final CM there was no difference between the proportion of $CD4^+$ cells compared to those which had migrated toward the GM (Figure 6.13c). In both experiments using the patient PBMC, all but one CM induced migration of a greater proportion of $CD4^+$ cells compared to the proportion seen attracted to GM alone (Figure 6.13d and e).

The proportion of $CD8^+$ lymphocytes that had migrated toward CM compared to GM was more variable, however it was generally opposing to the $CD4^+$ results (Figure 6.14). For example, the majority of samples in which a high proportion of $CD4^+$ lymphocytes had migrated towards the CM, e.g. H1, tended to have the lowest proportion of $CD8^+$ cells (Figure 6.13c). For the cells collected from healthy controls, the percentage of CTL that migrated toward the CM was lower or the same as those which migrated towards GM alone in all but one CM (H1; Figure 6.13a-d). This was also the case for the lymphocytes from one of the two HNSCC patients where three out of CM caused a decreased proportion of $CD8^+$ cells to migrate (Figure 6.13f). In the second patient PBMC sample a greater percentage of $CD8^+$ lymphocytes was observed migrating toward six of the eight CM, compared to GM alone (Figure 6.13e)

The percentage of $CD4^+CD127^-$ Treg in the migrated T lymphocyte population was only measured in three experiments using healthy donor PBMC. The proportion of lymphocytes which were $CD4^+CD127^-$ Treg and had migrated out of the transwell followed the general trend observed in $CD4^+$ migration in some experiments, with a greater or similar percentage of Treg migrating toward the CM, compared with the GM (Figure 6.15a, b and d). However,

in some cases the level of Treg that had migrated toward the CM was lower than the levels observed migrating toward GM (Figure 6.15b and c).

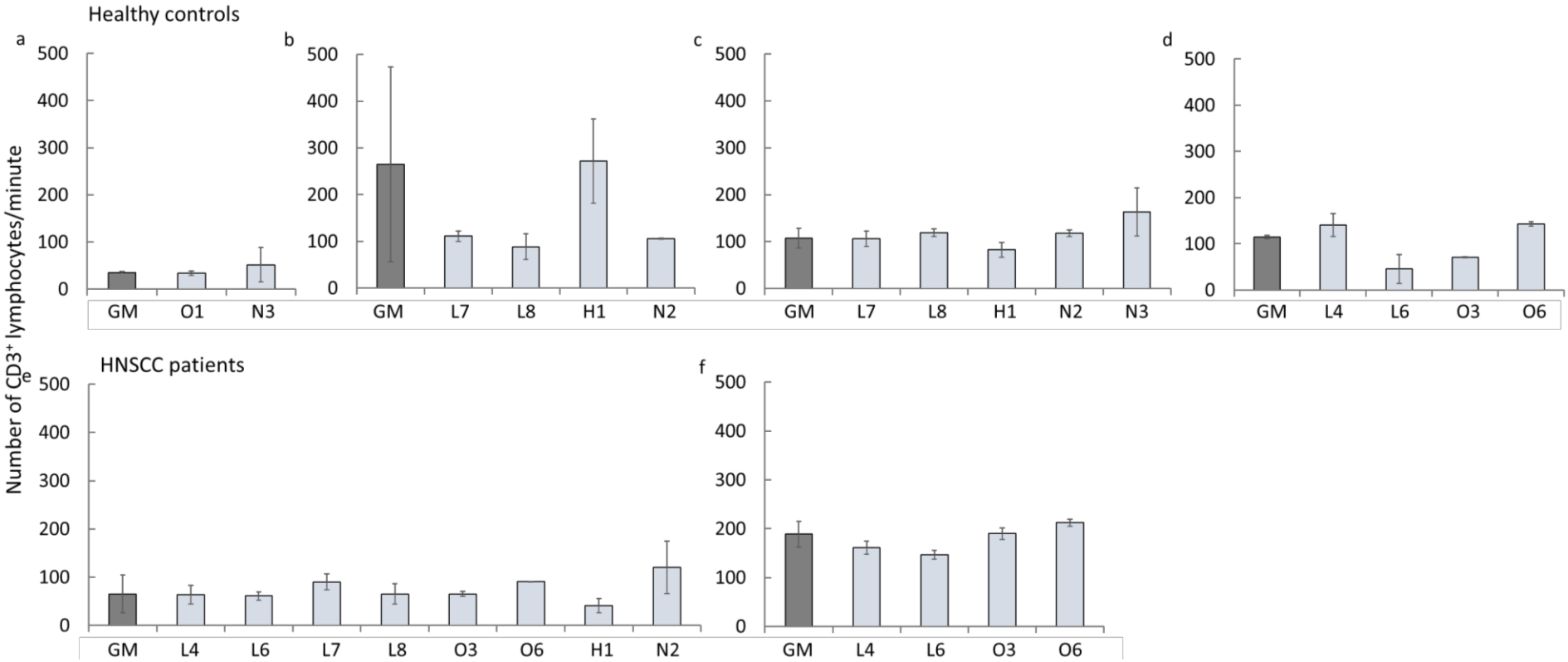


**Figure 6.12: Migration of CD3⁺ T cells toward tumour CM**

PBMC from healthy controls (n=4) and HNSCC patients (n=2) were seeded into transwell plates with GM or tumour CM (derived from 4 laryngeal (L) SCC; 1 hypopharyngeal (H) SCC, 3 oral/oropharyngeal (O) SCC; and 2 tumour nodes (N); in the wells underneath. Following 4-hours incubation, the migrated cells were collected, labelled with a CD3 antibody and the number of CD3+ lymphocytes acquired per minute was determined using flow cytometry. Bars represent mean data from duplicate wells ±SEM.

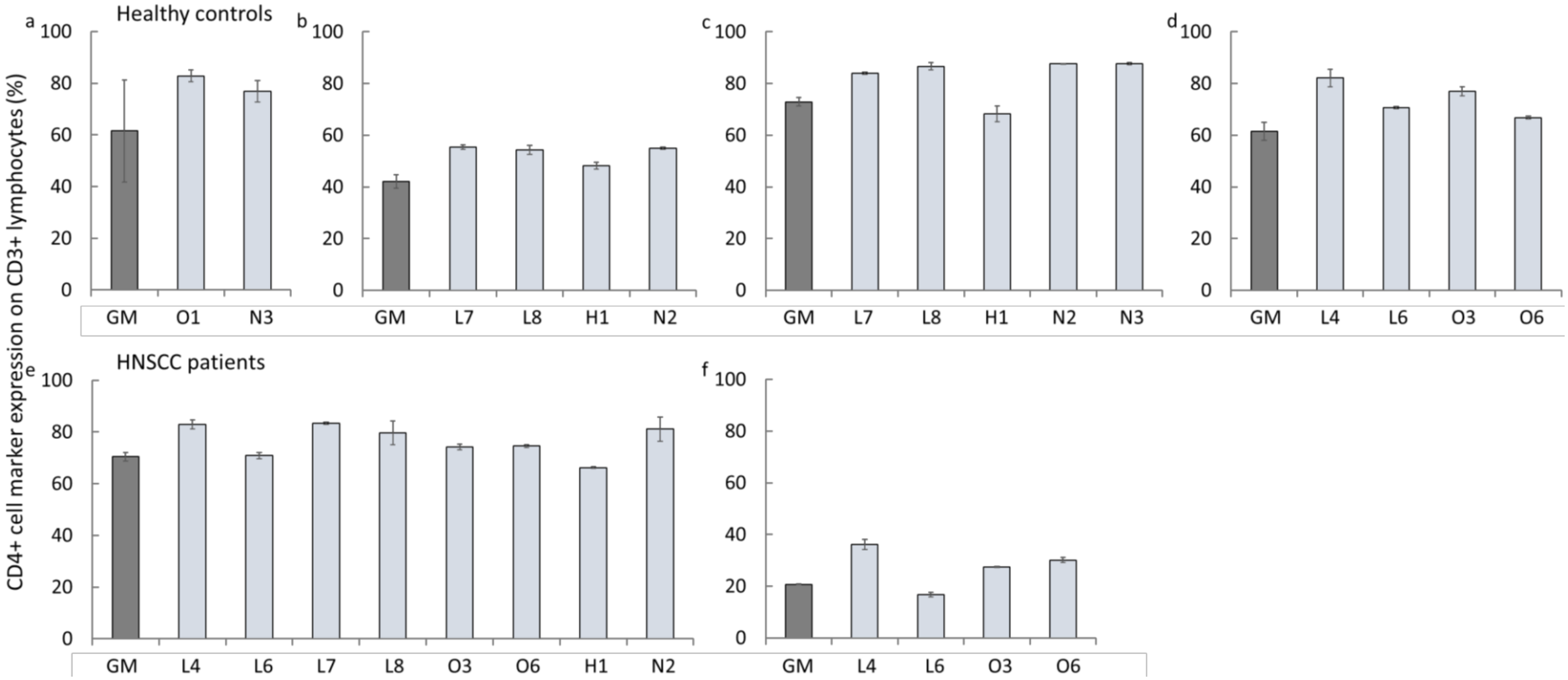


**Figure 6.13: Migration of CD4⁺ Th cells toward tumour CM**

PBMC from healthy controls (n=4) and HNSCC patients (n=2) were seeded into transwell plates with GM or tumour CM (derived from 4 laryngeal SCC (L); 1 hypophayrngeal SCC (H), 3 oral/oropharyngeal SCC (O); and 2 tumour nodes (N)) in the wells underneath. Following 4-hours incubation, the migrated cells were collected, labelled with specific T cell antibodies and the percentage of $CD4^+$ cells within the $CD3^+$ T cell population was determined by flow cytometry. Bars represent mean data from duplicate wells ±SEM.

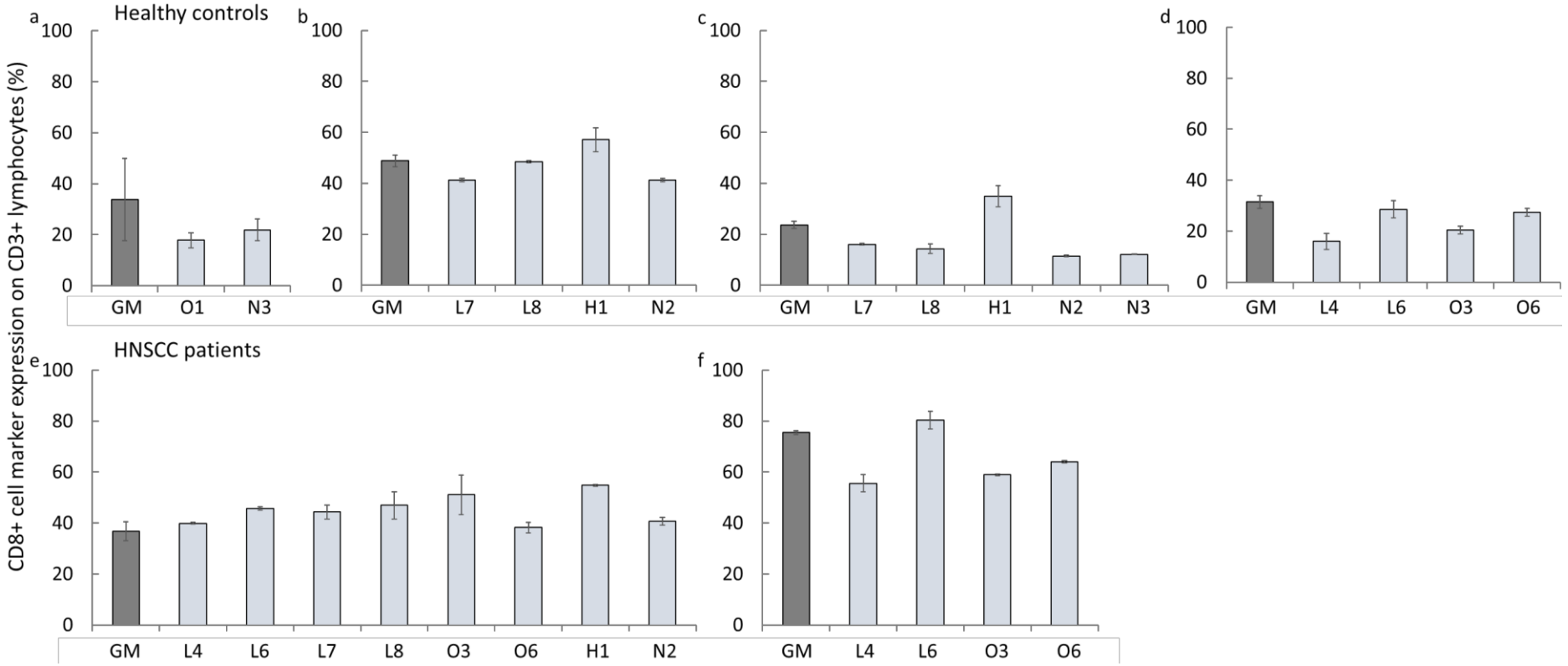


**Figure 6.14: Migration of CD8⁺ CTL toward tumour CM**

PBMC from healthy controls (n=4) and HNSCC patients (n=2) were seeded into transwell plates with GM or tumour CM (derived from 4 laryngeal SCC (L); 1 hypophayrngeal SCC (H), 3 oral/oropharyngeal SCC (O); and 2 tumour nodes (N)) in the wells underneath. Following 4-hours incubation, the migrated cells were collected, labelled with specific T cell antibodies and the percentage of $CD8^+$ cells within the $CD3^+$ T cell population was determined by flow cytometry. Bars represent mean data from duplicate wells ±SEM.

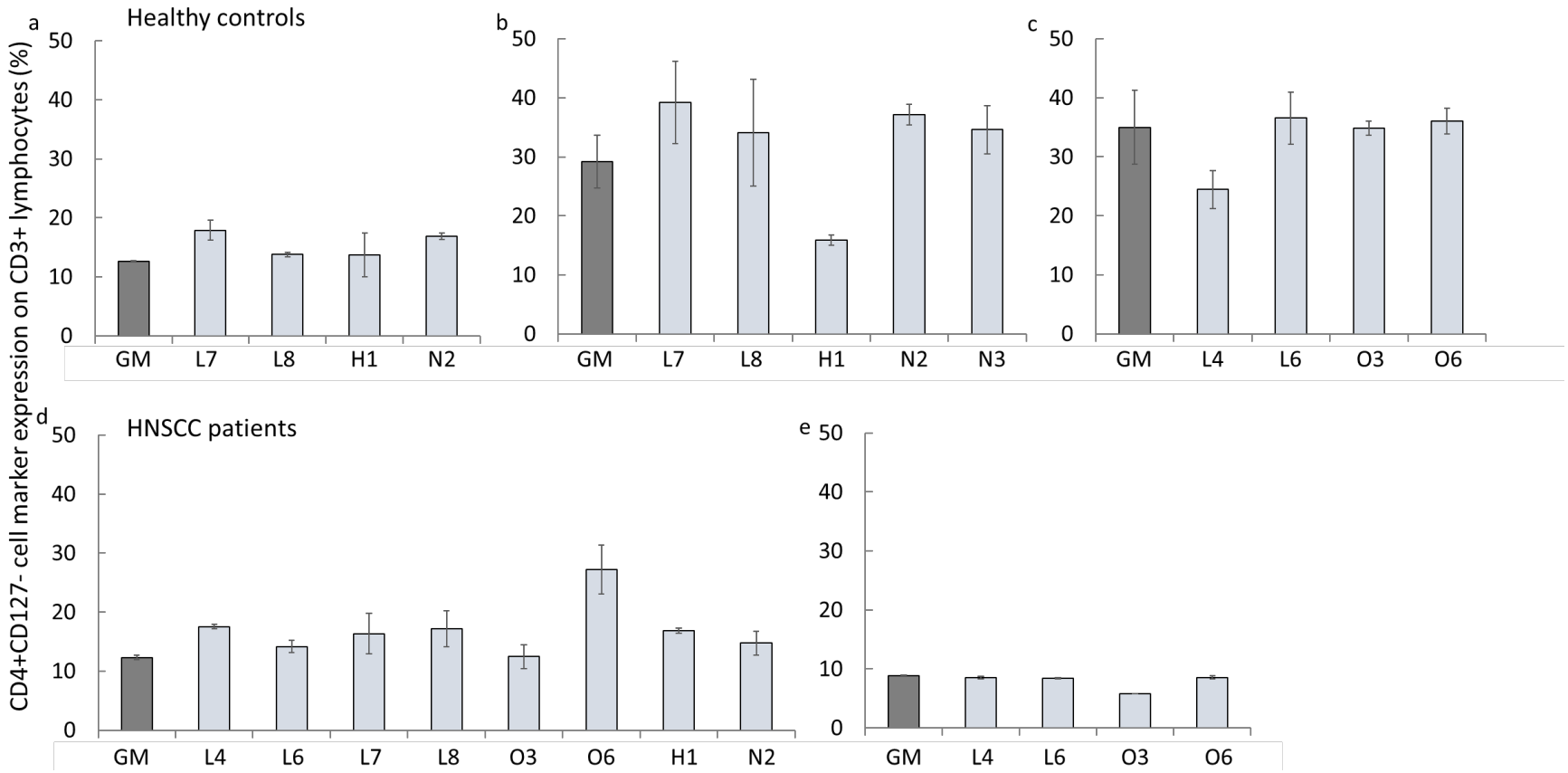


**Figure 6.15: Migration of $CD4^+CD127^-$ Treg toward tumour CM**

PBMC from healthy controls (n=4) and HNSCC patients (n=2) were seeded into transwell plates with GM or tumour CM (derived from 4 laryngeal SCC (L); 1 hypophayrngeal SCC (H), 2 oral/oropharyngeal SCC (O); and 2 tumour nodes; (N)) in the wells underneath. Following 4-hours incubation, the migrated cells were collected, labelled with specific T cell antibodies and the percentage of $CD4^+CD127^-$ cells within the $CD3^+$ T cell population was determined by flow cytometry. Bars represent mean data from duplicate wells ±SEM.

## 6.4 Discussion

### 6.4.1 Chemokines released by cells of the HNSCC microenvironment

Chemokines are prevalent in the tumour microenvironment, where they contribute to the recruitment, retention and activation of T cells. Given the differences observed in chemokine receptor expression on different T cell populations, it has been speculated that chemokines released by tumours may be involved in the preferential recruitment of certain cell types, such as Treg, that contribute to the establishment of an immunosuppressive environment. This chapter aimed to further elucidate the role of chemokines and their receptors in HNSCC. Specifically, to determine whether it is the preferential recruitment of immunosuppressive T cells from the periphery by chemokines in the TME or whether the TME changes the expression of the chemokine receptors in order to retain the immunosuppressive T cells, leading to their accumulation. To identify which chemokines are present in the HNSCC microenvironment and therefore the relevant associated chemokine receptors to investigate on the T cells, Proteome Profiler™ human chemokine array kits were used to determine the presence of chemokines in CM from dispersed HNSCC biopsies.

From the data collected, twelve chemokines were identified that were present at notable levels (mean pixel density >10) in more than five of the CM investigated. Of these, CXCL5, CXCL7 and CXCL8 bind the receptors CXCR1 and CXCR2. Although CXCR1 has been observed on T cells, very few T cells express CXCR2, and both receptors are primarily associated with the chemotaxis of monocytes and neutrophils (Takata *et al.*, 2004). Of the remaining nine chemokines, four (CCL2, CCL3/CCL4, CCL5, CCL22) are able to bind the receptor CCR4, and two (CCL3/4 and CCL5) bind CCR5; both receptors implicated in the recruitment of Treg and CTL into the TME respectively (Section 6.1.3). CCR6 has also been identified as having a role in Treg recruitment (Yamazaki *et al.*, 2008) and its sole ligand (CCL20), was detected in six of the nine tumour CM. Other receptors that can also recognise the chemokines detected in the tumour CM (CCL2, CCL3,4, CCL5, CCL21, CXCL4), are CCR2, CCR8, CCR7 and CXCR3; all receptors found on various T cell subsets. CCR7 is expressed on naïve and central memory T cells and on dendritic cells, where it facilitates their migration to secondary lymphoid tissue (Forster *et al.*, 2008). In gastric cancer the majority of tumour infiltrating Treg are $CCR7^-$ (approximately 90%; Mao *et al.*, 2017). CCR2 and CXCR3 are found on activated T cells, and CCR8 are associated with Th2 cells,

however all three receptors are also found on Treg. Only one ligand for each of the receptors CCR2, CCR7, CCR8, and CXCL3 was detected in the CM.

The data in part, supports that published by other authors investigating chemokines in HNSCC. For example, CXCL5 and CXCL8 are upregulated in tumour tissue and were detected in CM from OSCC cell lines by Western blot (Miyazaki *et al.*, 2006; Christofakis *et al.*, 2008; Lo *et al.*, 2013). CCL2 expression has been observed in both LSCC and OSCC using IHC, with OSCC metastatic tumours containing a significantly greater percentage of $CCL2^+$ cells than either LSCC or OSCC primaries (Ferreira *et al.*, 2008), suggesting it may play a role in tumour metastasis. Similarly, CCL3 expression was also increased in OSCC tissue compared to healthy control oral tissue, and has been observed to be expressed at great levels in nodes compared to primary tumour tissue (Silva *et al.*, 2007). CCL5 mRNA and protein have been observed in OSCC cell lines, and the protein was detected in CM from these cells by ELISA (Chuang *et al.*, 2009). CCL22 is released by HNSCC cell lines (Schott *et al.*, 2010), and increased levels of CCL20 have been observed in nasopharyngeal and OSCC samples compared to normal tissue, suggesting it may favour the recruitment of $CCR6^+$ immune cells (Chang *et al.*, 2008; Chang *et al.*, 2011). CCL21 has been observed in OSCC, however expression was not found to be significantly different to that in healthy control tissue. This may suggest that any role CCL21 has in immune cell recruitment may not contribute to establishing the unique immune environment observed in tumours (Oliveira-Neto *et al.*, 2013). In these studies, the authors look at the expression of one or two chemokines, rather than a panel of multiple chemokines, as was done in the present study. This limits the conclusions that can be drawn as it is the combination of the chemokines present that will ultimately determine the immune cells that are attracted to the tumour.

A study by Wolff *et al*. (2011), measured RNA levels of a panel of chemokine receptors in fifteen HNSCC cell lines and observed that all of them expressed CCL5 and CCL20 and none expressed CCL3 and CCL4. This could indicate that the source of CCL3/4 detected in the present study are stromal cells rather than the tumour cells themselves.

There are also some differences between the observations in this study and those of others. For example, few of the CM in the current study contained notable levels of CXCL9 and CXCL10, each being found in the CM from a single tumour exceeding a mean pixel density

of 10 on the Proteome Profiler. Other studies have found both CXCL9 and CXCL10 to be upregulated in OSCC tissue (Chang *et al.*, 2013; Rentoft *et al.*, 2014). Although, no OSCC CM were used in this study, only very low levels of CXCL9 and CXCL10 were detected in the CM from LSCC, oropharyngeal SCC or metastatic nodes. Perhaps most surprisingly, little CXCL12 was detected in the current study. The CXCL12/CXCR4 chemokine axis has been widely studied in various different cancers, including HNSCC. A study using IHC to look at CXCL12 expression on 233 HNSCC samples found CXCL12 in 43.3% (Rave-Frank *et al.*, 2016).

The differences observed when comparing the presence of chemokines in tumours between studies are probably due in part to the different methods used to detect chemokines. In the current study, secreted soluble factors were measured in the CM from dissociated tumour samples. In most of the other studies discussed here, chemokine expression was determined by IHC or by measuring the total mRNA or protein in the tumour lysate. For IHC the chemokine may be bound to the surface of tumour cells or expressed intracellularly, whilst the current study relies on the active secretion and release of the chemokine from the tumour cells into the surrounding milieu. These secreted chemokines more accurately represent the factors potentially involved in mediating migration to the TME as it is these that will have the chemotactic effects.

The majority of published HNSCC studies have looked at chemokine receptors on tumour cells and how their expression correlates with invasion and metastasis with very limited data on the affect these chemokines have on the attraction and retention of immune cells. However, some of the chemokines found in the CM in the current study, have been implicated in studies of other cancers, where the chemokine/receptor axis has been investigated in relation to leucocyte recruitment. The most extensively studied is the CCL22/CCR4$^{+}$ Treg axis. For example, CCL22 is expressed by many tumour types and correlates with FoxP3$^{+}$ Treg levels in ovarian, prostate, gastric, oesophageal and breast cancers (Curiel *et al.*, 2004; Miller *et al.*, 2006; Mizukami *et al.*, 2008a; Maruyama *et al.*, 2010; Li *et al.*, 2013b). CCL20 has also been observed on ESCC and NSCLC, where it has been found to correlate with the accumulation of Treg, while CCL4 expression in ESCC correlated with CTL recruitment (Liu *et al.*, 2015; Zhang *et al.*, 2015).

Some of the chemokines identified in the tumour CM in the current study have also been observed to be increased in the HNSCC periphery compared to that of healthy controls. Trellakis *et al*. (2011) found levels of CCL4, CCL5 and CXCL8 were higher in serum from the peripheral blood of HNSCC patients than from healthy controls, suggesting tumours have wider systemic effects on immune cell function. CCL20 is increased in the serum of patients with active NPC compared to healthy controls and patients in remission, and correlated with a worse prognosis (Chang *et al.*, 2008). CCL20 is the sole ligand recognised by CCR6 and has been implicated in tumour cell migration and invasion. However, CCR6 is also expressed on Treg, the accumulation of which may contribute to tumour immune evasion. CXCL9 was observed to be higher in OSCC patient serum compared with healthy controls (Chang *et al.*, 2013), while Schott *et al*. (2010) observed no difference in the CCR4 ligand, CCL22, in the serum of HNSCC, compared with healthy controls.

Chemokine secretion was highly variable between individual tumours, with some showing very limited expression, and others containing a wide variety of chemokines. This variation reflects the heterogeneity of tumours and may be indicative of the amount of leucocyte infiltration. The number of CM analysed in the study was low, so statistical analysis to compare the secretion of chemokines between different HNSCC subsites could not be carried out. Although the early tumours appeared to have higher levels of chemokines present in the CM this increased level was not statistically significant, again probably due to the small sample size. Furthermore, of the three early stage tumours, two are OSCC, which also appeared to release increased levels of chemokines compared with any of the laryngeal tumours, hypopharyngeal tumour and metastatic nodes. If these are real differences, it is not clear whether it is a difference between sub sites or tumour stage. However, oropharyngeal tumours have been associated with higher levels of $CD4^+$ and $CD8^+$ T cell infiltration compared with other sub sites (Green *et al.*, 2013), this may be due to the high prevalence of HPV in this cancer type. $HPV^+$ tumours also generally have an increased immune cell infiltrate, including increased $CD8^+$ and $CD4^+$ T cells (Partlova *et al.*, 2015), in which case it seems likely that there would be greater levels of chemokines released from $HPV^+$ oropharyngeal tumours. An increase in chemokines released from early stage tumours, particularly in CCL2 and CCL22 could be indicative that increased recruitment of the corresponding immune cells is controlling the progression of these tumours.

The expression of the receptors CCR4, CCR5 and CCR6 were chosen for further investigation on T cells in HNSCC, as all their corresponding chemokines were present in the CM (Table 6.6), and they have been previously associated with the accumulation of Treg and CTL in other types of tumour. In addition, it was chosen to look at the expression of CXCR3 as this chemokine receptor is well known to be important in the recruitment of T cells to inflammatory sites (Lacotte *et al.*, 2009; Chen *et al.*, 2010). CXCR3 is highly expressed on a subset of Treg that specialises in mediating the Th1 response (Koch *et al.*, 2009), and has been associated with the accumulation of a Treg in ovarian carcinoma (Redjimi *et al.*, 2012). Although, CXCL9 and CXCL10 have previously been shown to be up regulated in HNSCC tumours and are associated with high T cell infiltration (Chang *et al.*, 2013; Rentoft *et al.*, 2014; Kang *et al.*, 2015), the expression of their receptor, CXCR3, on the different T cell subsets in HNSCC required further investigation.

**Table 6.6 Chemokines identified in tumour CM by Proteome Profilers and their associated receptors**

| Chemokine | Chemokine Receptor |
|---|---|
| CXCL1 | CXCR1, CXCR2 |
| CXCL4 | CXCR3 |
| CXCL5 | CXCR1, CXCR2 |
| CXCL7 | CXCR2 |
| CXCL8 | CXCR1, CXCR2 |
| CCL2 | CCR2, CCR4 |
| CCL3,4 | CCR4, CCR5, CCR8 |
| CCL5 | CCR3, CCR4, CCR5 |
| CCL20 | CCR6 |
| CCL22 | CCR4 |
| IL16 | NA |
| Chemerin | CMKLR1 |

### 6.4.2 Chemokine receptors on PBMC and whole blood

Previous studies have observed the internalisation of chemokine receptors following the isolation of PBMC by density gradient centrifugation (Section 6.1.3). In contrast, in the current study there was little difference between percentage expression of chemokine

markers on lymphocytes in whole blood compared to those following isolation of PBMC, suggesting the density centrifugation protocol used here did not cause internalisation of the receptors. PBMC were therefore isolated for the analysis of chemokine receptor expression, as the method was well established and reduces the possibility of contamination from other cells in the blood, such as granulocytes. Furthermore, PBMC will be used for subsequent migration assays so the results for those assays will be more relevant. Berhanu *et al.* (2003) looked at the sensitivity, of different methods of T cell isolation and their effect on the sensitivity of measuring chemokine receptor expression. In their study, density gradient centrifugation was the best method for isolating PBMC for the analysis of CCR6 expression. Red blood cell lysis following staining of whole blood was the best method for analysing CXCR3 and CCR5, with the loss of expression following PBMC isolation determined to be between 1 and 24% and between 24 and 39% respectively. Contrastingly, Nieto *et al*. (2012), observed no effect of density gradient centrifugation on CCR5 expression. CCR4 expression was not analysed in the study by Berhanu *et al.* (2003) but has been observed to decrease from 90 to 55% following density gradient centrifugation (Nieto *et al.*, 2012). In the three donors from which PBMC and whole blood were stained for CXCR3, CCR4, CCR5 and CCR6, no difference was observed, this was also the case for TIL that had been isolated using the same methods from just one sample (data not shown). Another study, investigating chemokine receptor expression in multiple sclerosis, also noted that there was no significant difference between expression of chemokine receptors, which included CXCR3, CCR4 and CCR5, on whole blood compared with on PBMC that had been isolated by density gradient centrifugation (Krakauer *et al.*, 2006). The isolation of PBMC from whole blood via density gradient centrifugation is also the method most widely used by others prior to chemokine receptor analysis (Parsonage *et al.*, 2012; Liu *et al.*, 2015; Zhang *et al.*, 2015).

### 6.4.3 Chemokine receptors on circulating T cells and TIL from HNSCC patients

#### 6.4.3.1 *CXCR3 on circulating T cells and TIL from HNSCC patients*

To determine whether differences in the chemokine receptor profiles of T cells could contribute to the accumulation of different T cell populations in the HNSCC microenvironment, the percentage of cells expressing CXCR3, CCR4, CCR5 and CCR6 on different T cell populations in PBMC and TIL isolated from HNSCC tissue was analysed. Despite five out of six patients having a greater proportion of $CD3^{+}CXCR3^{+}$ cells in their TIL compared to the PBMC, this was not a significant difference; perhaps due to the numerical differences and sample size being small. Although CXCR3 is primarily associated

with CTL and Th1 cells, which are involved in promoting an anti-tumour response, it is also expressed on a subset of Treg (Hoerning *et al.*, 2011). The exact contribution of Treg in cancer is controversial, although they have an opposing action to CTL and Th1 and the resulting immunosuppression is generally considered to be tumour promoting. In some cases immunosuppression may be detrimental to tumour progression, controlling the damaging inflammation that contributes its growth (Erdman & Poutahidis, 2010). Using flow cytometry, Redjimi *et al*. (2012), showed an increase in $CXCR3^+$ memory Treg (mTreg; with a $CD4^+CD45RA^-CD25^+CD127^-$ phenotype) in ovarian carcinoma TIL (~75%) compared to the proportion in the patient periphery (~25%), which correlated with an increase in conventional memory T cells. Both these findings and the ones of the current study support the role of CXCR3 in Treg and general Th cell recruitment. However, Redjimi *et al*. (2012) did not look at the expression of CXCR3 in CTL, so whether this recruitment is general to all T cells or just Th cells cannot be concluded. In gastric cancer increased CXCR3 in tumour tissue correlated with both increased Th1 and increased CTL infiltration, analysed by IHC (Li *et al.*, 2015a). Strongly linked with T cell activation, CXCR3 is upregulated on Th1 and CTL effector cells following TCR stimulation of their naïve precursors (Groom & Luster, 2011). In the current study, although not always significant, CXCR3 expression was found on a greater proportion of $CD3^+CD8^+$, $CD4^+$, $CD4^+CD25^{hi}FoxP3^+$ and $CD4^+CD25^-CD39^+$ cells in the TIL compared to the PBMC. This could be due to increased recruitment of these cells or it may be indicative of the high levels of T cell activation in the HNSCC microenvironment.

In a study looking at the analysis of gene expression in 33 HNSCC tumour biopsies, a trend toward higher CXCR3 expression in $HPV^+$ tumours, compared with $HPV^-$ tumours was observed, although this difference was not significant (Russell *et al.*, 2013). Interestingly, five of the patients in the current study had a markedly greater proportion of CXCR3 expression on both Th1 cells and Treg in TIL compared to PBMC, while five of the patients showed little difference between CXCR3 expression on these T cell populations in TIL and PBMC. Of the five patients with increased $CXCR3^+$ Treg in the TIL three had T4 OSCC, one had a T4 LSCC and one a metastatic lymph node (suggesting a more aggressive phenotype), whereas the other five patients included two with T1 OSCC, two T2 oropharyngeal SCC with the other being a T4 LSCC. Although, the oral cavity and oropharynx are the sub sites predominantly associated with $HPV^+$ tumours, LSCC has also been associated with HPV infection (Li *et al.*, 2013a). It would therefore be of interest to

know the HPV status of the two sets of patients, as this information was not available to the author. It is of note that, in addition to increased T cell infiltration, $HPV^+$ tumours also have a better prognosis (Dok & Nuyts, 2016), which seems to contradict the finding that the five patients with increased $CXCR3^+$ expressing TIL apparently have the most aggressive tumours (although again this may reflect a lack of knowledge of other competing influences).

CXCR3 was found to be expressed on similar proportions of Treg as in the whole $CD4^+$ Th cell population in both PBMC and TIL, which perhaps suggests that CXCR3 ligands do not selectively recruit Treg over other Th cells. The $CD8^+$ cells in the TIL investigated in the current study did not contain an increased percentage of CXCR3 expressing cells, which could indicate that Th cells are being preferentially selected for over CTL, however the sample size was small.

#### 6.4.3.2 *CCR4 on circulating T cells and TIL from HNSCC patients*

CCR4 has previously been observed on Treg infiltrating ovarian cancer, where recruitment is primarily thought to be by CCL22, which was detected in CM in the current study, and CCL17 (Curiel *et al.*, 2004). In mice, blocking CCL22 reduced Treg recruitment into ovarian tumours, without reducing $CD3^+CD25^-$ recruitment (Curiel *et al.*, 2004). Additionally, in a 3D migration model of melanoma, CCL2 released from tumour cells has been observed to induce the migration of $CCR4^+$ CTL (Zhang *et al.*, 2006). Given this, it may be expected that the percentage of Treg cells expressing CCR4 would be greater in TIL than in PBMC, but this was not the case. This result is consistent with findings from a previous study which investigated the chemokine receptor expression on $CD4^+CD25^{hi}$Treg from the PBMC and TIL of HNSCC patients, where CCR4 expression was observed in both cases on nearly all Treg (Strauss *et al.*, 2007b). Redjimi *et al*. (2012) found lower CCR4 expression on mTreg in PBMC than TIL from patients with ovarian cancer suggesting it may not play a role in the recruitment of these cells. Given that $CCR4^+$ Treg had not accumulated in the in the TIL of HNSCC, it seems unlikely it is responsible for the increased Treg recruitment observed in the TME.

CCR4 was lower in the population of $CD4^+CD25^-CD39^+$ cells in TIL than in PBMC Although, this phenotype represents a heterogeneous cell population, $CD4^+CD25^-CD39^+$ is a phenotype of Tr1 cells and of precursors to $FoxP3^+$ iTreg (Bergmann *et al.*, 2007;

Moncrieffe *et al.*, 2010). Three of the patients had a slight increased proportion of CCR4 expressing $CD4^+CD25^-CD39^+$ in TIL compared to PBMC, compared to the much lower level observed in the other six patients. However, there was no obvious common factor between these three patients; one with a T4 LSCC, one a T1 OSCC and one a T4 OSCC. This could be indicative of a decrease in the accumulation of either Tr1 or iTreg precursors in the TIL, favouring the hypothesis that the accumulation of Treg is due to recruitment of nTreg rather than iTreg induction. However, due to the heterogeneity within this population it would require further investigation to confirm this.

#### 6.4.3.3 *CCR5 on circulating T cells and TIL from HNSCC patients*

The percentage of cells expressing CCR5 was increased on all the T cell subsets in the TIL compared to PBMC, this is in contrast to the previously described study by Liu *et al*. (2015), where the proportion of $CCR5^+$ expressing cells was only increased on $CD8^+$ CTL in the TIL, and not on $CD4^+FoxP3^+$ Treg of ESCC (Section 6.1.2). Similarly, CCR5 was also found in increased proportions of CTL and non-regulatory Th cells in NPC TIL compared to PBMC by Parsonage *et al.* (2012), while the proportion of CCR5 in Treg was the same. The difference between the expression of CCR5 on Treg in this study compared to the other two studies may simply reflect differences between cancer types. However, it may also be due to differences in the markers used to define Treg ($CD4^+FoxP3^+$ and $CD4^+CD45RA^-FoxP3^+$by Liu and Parsonage respectively, compared with $CD4^+CD25^{hi}FoxP3^+$ in the current study). Furthermore, in the study by Parsonage *et al.*, the expression of CCR5 on Treg was only analysed on a small number of patients (n=6), however the percentage of $CCR5^+$ cells was higher in the Treg in TIL compared with PBMC in 5/6 paired samples, and the overall median percentage of CCR5 was markedly higher in Treg in TIL (~75%) compared to PBMC (~45%). Liu *et al*., observed much fewer $CCR5^+$ Treg (11.6±14.3% in PBMC and 19.3±17.4% in TIL) and $CCR5^+$ CTL (21.6±15.8% in PBMC and 45.9.6±25.3% % in TIL) compared with either the current study or the Parsonage study. The marked increase in CCR5 expression on TIL, suggests that CCR5 may be important for the recruitment of infiltrating T cells. However as it is increased on all T cell subsets there is no evidence to suggest it may influence the T cell balance in the TME by selective recruitment. In addition to migration it has also been shown to have a role in the retention of CTL in CRC (Francisco *et al.*, 2009).

#### 6.4.3.4 *CCR6 on circulating T cells and TIL from HNSCC patients*

There were no differences were observed in the proportion of cells which were positive for CCR6 in any of the T cell populations between TIL and PBMC in the current study. Decreased CCR6 mRNA has been noted previously in LSCC compared with adjacent tissue, however this was extracted from whole tissue and would therefore include all cell types in the TME and not just immune cells (Chen *et al.*, 2013). Other cancer studies that have used flow cytometry with multiple T cell markers to determine CCR6 expression on cells have given mixed results. For example increased CCR6 expression has been observed on Treg from ESCC TIL compared with PBMC, while contrastingly, CCR6 was lower on mTreg in TIL than PBMC (Redjimi *et al.*, 2012; Liu *et al.*, 2015). Other studies have also supported a role for CCR6 in Treg recruitment in cancer: $CCR6^+$ Treg were recruited to CRC by macrophages in mice (Liu *et al.*, 2011) and in a mouse model of breast cancer, $CCR6^+$ $FoxP3^+$ Treg were found to be enriched in TIL from late stage tumours compared to $CCR6^-$ $FoxP3^+$ Treg. However, this enrichment was determined to be primarily due to the induction of $CCR6^+$ Treg proliferation, rather than their selective recruitment (Xu *et al.*, 2011). This supports the hypothesis that tumours influence the proportions of cells in the TIL directly rather than actively causing their selective recruitment.

### 6.4.4 **Chemokine receptors on circulating T cells from HNSCC patients and healthy controls**

#### 6.4.4.1 *CXCR3 and CCR5 on circulating T cells from HNSCC patients and healthy controls*

In the HNSCC patient periphery, there was a moderate decrease in the percentage of $CD3^+$ lymphocytes expressing CXCR3 compared to those in healthy controls, however no difference was observed between the expression on the individual T cell subsets. This could indicate that the differential CXCR3 expression is due to altered CXCR3 expression on another T cell population that has not been investigated in the present study. The percentage of $CCR5^+$ cells was no different between healthy control and patient PBMC on any of the T cells. That $CXCR3^+$ and $CCR5^+$ T cells are increased in the TIL, but are not increased in patient peripheral blood compared to healthy controls, may be indicative that they have a role in T cell migration to the tumour site. However, it is also possible the increased proportion of T cells expressing these markers is due to the preferential expansion of CXCR3 and CCR5 expressing T cell populations *in situ*.

#### 6.4.4.2 *CCR4 and CCR6 on circulating T cells from HNSCC patients and healthy controls*

The proportion of $CCR4^+$ cells was higher in Treg from patient PBMC compared to those from healthy donor PBMC, this is in agreement with Strauss *et al*. (2007) who observed more than double the percentage of circulating $CD4^+CD25^{hi}$ Treg in HNSCC patients expressing CCR4 compared with healthy controls (nearly 90% *vs.* approx. 40%). Although the percentage of $CCR4^+$ Treg in the HNSCC cohort was comparable to that observed in the current study, the healthy cohort had a much lower percentage of $CCR4^+$ Treg. The results of Strauss *et al*. (2007) and the current study are in contrast to those of Schott *et al*. (2010), who observed no significant difference in the percentage of $CD4^+CD25^{hi}CD127^{low}$ expressing CCR4 in PBMC from HNSCC patients compared with healthy controls. This could be because Schott *et al*. (2010), used $CD4^+CD25^{hi}CD127^{low}$ expression to define Treg compared to $CD4^+CD25^{hi}FoxP3^+$ used in the current study. Although CD127 is generally considered to be a negative Treg marker with expression reciprocal to that of FoxP3, $CD4^+CD25^{hi}CD127^{low}$ and CD4+$CD25^{hi}FoxP3^+$ populations will not be identical. That being said the mean percentage of $CCR4^+$ Treg in HNSCC from the Schott study was very close to the value observed in the current results (86.9% *vs.* 89.3±1.7%). It is the percentage found in the healthy controls that differs between the studies. The same study did however see an increase in the mean fluorescence intensity of CCR4 on $CD4^+CD25^{hi}CD127^{low}$ of patients with active disease (n=16), compared to patients that had undergone surgery and had no evidence of any active disease (n=14), whereas in the current study only patients with no previous cancer were included. An increased percentage of CCR4 expressing cells has also been observed in peripheral Treg from patients with glioblastoma compared to healthy controls (74±4% *vs.* 43±3%; Jordan *et al.*, 2008). The current study also noted an increase in the proportion of $CCR4^+CD4^+$ T cells in HNSCC patient PBMC compared to healthy controls, but not on the $CD4^+CD25^-CD39^+$ cells, suggesting the increased CCR4 on The cells may be due to the increase in the Treg subset. Overall, an increase in $CCR4^+$ on patient peripheral Treg compared to healthy controls, lends support to the hypothesis that the tumour is having a wider systemic effect on chemokine receptor expression. Rather than releasing chemokines that recruit $CCR4^+$ Treg, it may be inducing the expression of CCR4 on these cells, which is in turn causing an accumulation of Treg.

CCR6 was expressed on a greater proportion of circulating Treg from patients compared with healthy controls. This is supported by previous observations that CCR6 expression on peripheral blood $CD4^+CD25^+FoxP3^+$ Treg was higher in LSCC patients (82.70±15.08%)

compared to healthy controls (65.43±22.71%; Chen *et al.*, 2013). CCR6 expression was also more prevalent on Treg compared to other Th cells and CTL, as is the case with CCR4, which may suggest a role in the selective migration of Treg to HNSCC.

Chemokine receptor expression is dynamic, and can be effected by T cell activation (Campbell *et al.*, 2001). It maybe that the receptors responsible for the recruitment of T cells to the tumour are down regulated on arrival and others are upregulated. This would be representative of other immunological scenarios, such as migration to lymph node, in which case the expression of CCR7 mediates the homing of naïve T cells to secondary lymphoid tissue, where it is then down-regulated to allow the cells to pass back out into the periphery (Zlotnik & Yoshie, 2012). Although receptors that are increased in the TIL may have been the receptors mediating their migration, it is also possible that they have additional roles other than chemotaxis.

Overall, the increased CXCR3 and CCR5 in the TIL but not in the periphery of HNSCC patients could reflect their role in the general migration of T cells to the TME. It could also be an effect of the tumour on the cells once in the TME, so might be more important for retention or have a functional relevance. However, in both cases there is no strong evidence of selective recruitment caused by these chemokine receptors.

The increased proportion of CCR4 and CCR6 on circulating patient Treg, but not on CTL, may be leading to their preferential migration to the HNSCC tissue. However, expression of both receptors is not increased on Treg fraction in TIL. This finding may seem to be in opposition to the hypothesis that these cells may be being selectively recruited, however, it could be that the tumour influences chemokine receptor expression on Treg in the periphery, rather than that the tumour is releasing chemokines that cause the recruitment of cells expressing appropriate receptors. Further investigation is required in order to determine whether the chemokines released by the tumour are actively recruiting T cells, and whether this recruitment is causing the preferential recruitment of different T cell sub sets.

### 6.4.5 **Migration assays**

Migration assays were performed to further elucidate whether the differences observed in chemokine receptor expression could be due to the selective migration of cells toward chemokines in the TME. For a positive control, a number of wells were supplemented with

CXCL12 (CXCL12), a ligand of the receptor CXCR4. CXCR4 is constitutively expressed on both activated and resting T cells and has been reported to be involved in T cell co-stimulation as well as their migration toward CXCL12 (Yonezawa *et al.*, 2000). As expected, there was a strong chemotactic effect of CXCL12 in transwell migration assays, with considerably more $CD3^+$ lymphocytes from all healthy controls and patients migrating toward the CXCL12 supplemented GM compared to GM only. Overall, there was a tendency toward an increased proportion of $CD3^+CD4^+$ cells and decreased proportion of $CD3^+CD8^+$ cells migrating toward GM supplemented with CXCL12 compared to the migration towards GM alone, indicating that CXCL12 may favour the migration of Th cells over CTL in these donors. However, due to the small sample size, no statistical analysis was carried out and firm conclusions cannot be drawn.

If HNSCC release chemokines that preferentially recruit Treg it would be expected that a higher proportion of Treg would be observed to migrate toward CM compared to GM regardless of the source of the cells. However, if the increased migration is due to the induced expression of chemokine receptors on Treg, it would be expected that HNSCC patient Treg migrate more toward CM than those of healthy donors.

CM derived from dissociated tumour biopsies were not able to induce the migration of $CD3^+$ T cells in Transwell migration assays. It could be that chemokines were present in the CM, but were not at sufficiently high concentrations to induce T cell migration. Interestingly, CM from the hypopharyngeal tumour, that released the least detectable levels of any chemokines in the proteome profiler, was also the CM that was the most similar to the GM control. It is also of note, that often T cells are activated *in vitro*, prior to use in Transwell assays. In this study, T cells were used directly following isolation, without activation, to limit the effects from external manipulation of the cells. Although, the level of activated T cells in fresh PBMC would be a lot lower than with activated PBMC, it was hoped that there would still be enough active cells to see an effect of the various conditioned media, and that this would be more representative of the *in vivo* HNSCC patient periphery.

In addition to the lack of chemotactic effect of the CM, there was no obvious difference in the proportion of different cell types that had migrated. In some cases there was a slightly higher proportion of $CD4^+$ cells and lower proportion of $CD8^+$ cells in the migrated lymphocytes, however overall the actual number of migrated cells showed no evidence that

CM was inducing selective recruitment of T cells. This was the case for T cells from both HNSCC patients and healthy controls. To test the effect of a chemokine receptor of interest on T cell migration it may be necessary to supplement GM with the appropriate chemokines. However, due to the redundancy between the chemokine-receptor interactions, results may not always be easy to interpret. Moreover, looking at chemokines individually this way is not representative of the effect of the combination of chemokines present in the tumour milieu. Another option could be to try CM from different sources, for example, HNSCC cell line and tumour-derived CAF. In addition to soluble forms, chemokines can be presented as membrane bound ligands. This form of chemokine presentation is important for the trans-endothelial migration of T cells out of the circulation (Section 1.3.). In this study only soluble forms of chemokines were investigated. It may be that membrane bound ligands on the tumour cells are predominantly responsible for recruitment into the tumour. To investigate this, co-culture experiments could be carried out with tumour cells seeded into the bottom of wells and lymphocytes placed in transwells above.

It may also be of interest to investigate whether the tumour influences chemokine receptor expression directly. T cells could be cultured in CM and the expression of receptors analysed on the different cell types. This would be of interest for CCR4 and CCR6 in particular, as these receptors are both increased on Treg in cancer patients compared to controls. An up- or downregulation of chemokine receptors mediated by soluble factors released by the tumour may be a mechanism used by tumours to influence retention of T cells. How the immune cells are dispersed throughout the tumour may also be important to the role they play. Further investigation into the relation of chemokine receptor location in the tumour and the localisation of T cells using IHC could help to elucidate thier role in the TME. Overall, although further work is required the current chapter has highlighted some chemokine receptors that may be worth further investigation. It also favours the hypothesis that rather than preferential recruitment of particular T cell subsets, effects once in the tumour, such as increased proliferation, or *in situ* generation may be what causes the accumulation of Treg.

### 6.4.6 **Conclusion**

A range of chemokines were found to be released by HNSCC tumour cells. Furthermore, the chemokine receptors CXCR3 and CCR5 were expressed on high proportions of T cells in HNSCC TIL compared to PBMC, and CCR4 and CCR6 were expressed on high

proportions of Treg from HNSCC patient PBMC compared to healthy controls. Despite these observation, CM did not induce T cell migration or influence the selective recruitment of $CD4^+$ Th cells, $CD8^+$ CTL or Treg. Further investigation is required in order to clarify the role of these receptors in migration to the HNSCC microenvironment. However, the findings of this chapter provide a foundation for future work.

# Chapter 7 Final Discussion

The prognosis for HNSCC patients is poor. In many cases, patients present with advanced disease and the three year survival is low (~32%; Hauswald *et al.*, 2011). Developing novel ways to combat the disease is imperative and will require an increased understanding of the HNSCC tumour biology. One of the more recently proposed hallmarks of cancer, which has been at the forefront of modern day cancer research and drug development is immunotherapy (Hanahan & Weinberg, 2011). In the early 20$^{th}$ century, Paul Erhlich originally hypothesised that the immune system was continuously recognising and mediating the removal of malignant cells, thereby preventing tumour formation (Klein, 2012). In the decades since, interest into the involvement of the immune system in cancer has grown, revealing an increasingly complex relationship between the immune system and tumour cells. The appreciation of the importance of this interaction is perhaps now stronger than ever and harnessing the immune system to eradicate established tumours *in vivo* is an active area in cancer research.

Some of the earlier immunotherapies to be investigated for cancer treatment, such as cytokine therapies, were aimed more broadly at "kick-starting" the immune system (Rosenberg, 2014). Administration of IL2, causes the stimulation and expansion of T cells, which mediate tumour regression in mice (Jackaman *et al.*, 2003). IL2 was approved for the treatment of melanoma and advanced renal cancer more than 25 years ago, after it was found to be effective in a subset of patients (Atkins *et al.*, 1999; Dutcher, 2002). However due to its broad-acting effects it was associated with significant multi-systemic toxicity. In HNSCC studies, results from clinical trials with cytokine therapies, such as IL2 and IFN-α, were disappointing, with variable results between studies (Hoesli & Moyer, 2016). Although treatment regimens have been refined, reducing the cytotoxicity associated with cytokine therapies, a move has been made toward more targeted immunotherapies, aimed at reversing the immune dysregulation in the tumour.

The progression of HNSCC is highly dependent on immune evasion, and in support of this HNSCC patients are often immunosuppressed. Inhibiting the mechanisms employed by tumours to induce this immunosuppression, thus freeing the immune system to mount an active anti-tumour response, is therefore an appealing prospect for treatment in these patients. Drugs that target immune checkpoints, releasing the cytotoxic effects of T cells, have shown success in treatments of advanced metastatic tumours, renal cell carcinoma

(RCC) and non-small cell lung carcinoma (NSCLC; Brahmer *et al.*, 2015; Motzer *et al.*, 2015; Weber *et al.*, 2015). In a randomised phase III trial in 361 patients with recurrent HNSCC, who had previously undergone platinum-based therapy, treatment with the PD-1 inhibitor Nivolumab resulted in an increased median survival (7.5 months) and estimated increased 1-year survival rate (36.0%) compared to treatment with single agent chemotherapy (5.1 months and 16.6%; Ferris *et al.*, 2016). Following this study, in 2016 Nivolumab was approved for use in HNSCC patients who have previously undergone platinum-based therapy, in the UK. In addition Nivolumab is approved for the treatment of relapsed or refractory Hodgkin Lymphoma and metastatic melanoma, renal cell carcinoma RCC and NSCLC. CTLA-4 blockade (using Ipilimumab) has also shown promising results in phase III clinical trials of melanoma, RCC and NSCLC, while investigations into its efficacy in HNSCC are currently on going (Bauman *et al.*, 2017). The use of concurrent treatment with Nivolumab and Ipilimumab has been approved in metastatic melanoma, where the combined treatment increased 3-year survival (58%) compared to treatment with either Nivolumab (52%) or Ipilimumab (34%) alone (Wolchok *et al.*, 2017). Given the number of clinical studies currently underway into the efficacy of various immune blockade drugs and combinatorial treatments in HNSCC (Economopoulou *et al.*, 2016), it is likely other treatments are set to follow.

Other therapies that have aimed at inducing an immune response, for example through delivery of active tumour targeting immune cells, and tumour vaccines have been less effective (Rosenberg *et al.*, 2004; June, 2007). This may be in part due to the immunosuppressive factors still present in the TME. In particular this has been shown to be true in HNSCC, where increased levels of Treg are present in the TME. Therefore, inhibiting immunosuppression in tandem with targeted activation of the cytotoxic immune cells may lead to better treatment outcomes. The aim of this thesis was to increase the understanding of the roles of soluble factors in shaping the immunosuppressive TME, specifically focussing on the accumulation of Treg. Elucidating the pathways involved would hopefully lead to novel targets for future cancer therapy.

## 7.1 Summary of Findings

How Treg become enriched in the TME is unclear, although various mechanisms have been implicated, including the induction of Treg *de novo* at the tumour site and the induced migration of nTreg from the periphery. In the current study soluble factors within the TME

were not observed to induce functional Treg, however, an increase in the ectonucleotidase CD39 was observed in cells cultured with CM derived from dispersed tumour samples. In addition to Treg, expression of this enzyme has been found on exhausted T cells that are particularly susceptible to apoptosis following TCR stimulation (Fang *et al.*, 2016). Furthermore, the overall induction of CD26 expression and lack of induced FoxP3 expression, suggests the $CD39^+$ cells observed in this study are more similar to the exhausted T cells than iTreg. Despite the increase in CD39 expression, the current study did not find a significant induction of apoptosis following the culture of lymphocytes in CM. This might not be surprising given that membrane bound ligands are thought to have a stronger effect on apoptosis then their soluble forms.

The lack of any effect from the HNSCC cell lines and CAF CM on the expression of Treg markers, may suggest that the tumour infiltrating immune cells are the cells causing the greatest regulatory effects in the HNSCC microenvironment. Activated leucocytes release high levels of cytokines that in turn induce the activation and migration of other immune cells. For example, tumour activated M2 macrophages release factors that can cause the induction of Treg, which in turn drive the differentiation of macrophages toward an M2 phenotype, in a positive feedback loop (Sun *et al.*, 2017). The increased levels of Treg-attracting CCL2 in melanoma has been attributed to CTL in the tumour milieu, rather than by the tumour cells themselves (Spranger *et al.*, 2013); a negative feedback mechanism that probably evolved to restore homeostasis following a normal immune reaction. It is not known if a similar mechanism occurs in HNSCC.

An alternative hypothesis to iTreg induction at the tumour site is the recruitment and expansion of existing, thymically-derived, nTreg. Some studies in mice support the theory that tumour infiltrating Treg are primarily nTreg (Hindley *et al.*, 2011; Savage *et al.*, 2014). Savage *et al*. (2014) noted that the antigen specificity of infiltrating Treg in a mouse model of prostate cancer were distinct from those of $CD4^+FoxP3^-$ 'non-Tregs'. This would suggest that iTreg are not being induced from the same pool of infiltrating $CD4^+FoxP3^-$ precursors as conventional T cells. Furthermore, following transfer of naïve $CD4^+FoxP3^-$ T cells specific for an antigen frequently found on the Treg infiltrating the tumours of these mice, little iTreg induction was observed. Other studies that have used mouse tumour models and transfer of antigen specific T cells have noted that both nTreg expansion and iTreg induction can contribute toward tumour immune escape (Zhou & Levitsky, 2007; Getnet *et al.*, 2009).

Although measuring the contribution of the two populations separately is difficult due to the absence of any distinguishing markers, some results from antigen specific T cell adoptive transfer experiments in mice have suggested that nTreg expansion is more efficient than iTreg induction and may contribute more towards the immunosuppressive environment observed (Zhou & Levitsky, 2007).

The current study observed differences in the expression of chemokine receptors on TIL compared to circulating T cells. These differences could be responsible for their recruitment and retention, however could also reflect their activation status. The results suggest a role for CXCR3 and CCR5 in the accumulation of T lymphocytes, however whether this is due to a chemotactic effect or proliferation is uncertain without further investigation. Furthermore, the percentage expression of both receptors is increased on all Treg, CTL and Th cells, indicating any role is apparently general to T cells and is unlikely to influence the balance of these individual T cell populations in the tumour. On the other hand, the differences in CCR4 and CCR6 between HNSCC patients and controls appears to be restricted to Treg. Although no enrichment of $CCR4^+$ and $CCR6^+$ Treg was observed in HNSCC tumours compared to in the periphery, the increased percentage on Treg in the patient periphery compared to that of healthy controls may suggest that the migratory capacity of patient Treg is higher. The therapeutic targeting of chemokine/receptor interactions is appealing as drugs already exist for many and in some cases, have been approved for use in other diseases, therefore, their toxicity and side effects are well documented. For example, the CCR5 inhibitor maraviroc, has been used in the treatment of HIV for over ten years, with relatively few adverse effects (Lieberman-Blum *et al.*, 2008). Testing the efficacy of drug targeting chemokines and their receptors remains a challenge as the chemokine network is complex, with redundancy between chemokines and their promiscuous binding to receptors. There are a multitude of studies looking at the effect of modulating chemokine/receptor interactions in immunological diseases, as well as in cancer (Scholten *et al.*, 2012). It will be important to consider the effects of blocking or promoting chemokine/receptor interactions, not just on the different leucocyte populations but also on cancer cells themselves, as the upregulation of many chemokine receptors on cancer cells has been linked with metastasis (Chow & Luster, 2014). It may not be possible to effect one without also effecting the other, and what may be beneficial for T cell migration to the tumour, may promote metastasis. CCR5 blockade with maraviroc is currently under investigation in advanced refractory CRC. A small phase I clinical trial looking at the effect

of maraviroc in eleven patients with CRC liver metastases observed a reduction in tumour cell proliferation and induction of cell death in biopsies taken from patients after two months, measured by Ki67 staining and cell morphological changes respectively (Halama *et al.*, 2016).

Overall, the lack of iTreg induction and the differences in chemokine receptor expression favours the hypothesis that soluble factors are primarily involved in nTreg recruitment to the TME, rather than iTreg induction. The increased proliferation by soluble factors in the TME was not investigated in this study, however recruitment alone does not explain the changes in the HNSCC patient periphery, such as the increase in the proportion of Treg compared to healthy controls. This could be caused by increased Treg proliferation or may suggest that there are still other, as yet undiscovered, factors that cause iTreg induction *in vivo*.

## 7.2 Limitations of Study

Some studies have noted differences between the immune infiltrate of HNSCC subtypes and between primary tumours and metastases (Pretscher *et al.*, 2009; Green *et al.*, 2013), however due to the limited number of samples collected it was not possible to compare between different cancer types in the current study. Moreover, the HPV status of HNSCC tumour is known to reflect two distinctly different tumour types, with $HPV^+$ tumours inducing a much a stronger immune response, and being associated with a significantly better prognosis (Dok & Nuyts, 2016). Unfortunately, information as to the HPV status of patients was not available to the author but this is an important aspect for future research. The current study was also limited by the amount of tumour CM that could be collected. Due to the small size of the tumour specimens, not enough CM was collected to use in multiple Treg induction experiments, or chemokine migration assays, which limited the subsequent statistical analysis that could be performed.

Although, soluble factors that have been implicated in the induction of iTreg have been observed to be released by cells of the HNSCC microenvironment, additional factors may be required that are absent from *in vitro* models. For example, there could be a requirement for cell-cell contact or the presence of surface bound molecules. TGF-β is known to play a role in iTreg induction however requires other factors, such as the transmembrane proteins, integrins, for its activation. Some malignant cells overexpress integrins, which can activate

TGF-β directly as well as aid in MMP-mediated activation (Bates *et al.*, 2005), and generate reactive oxygen species (Wu, 2006). The integrins involved in the activation of TGF-β1 (αvβ6 and αvβ8) are present on epithelial cells, $CD4^+$ T cells and dendritic cells (DC) (Worthington *et al.*, 2012). Conditional knockout experiments in mice have shown that the immune population responsible for the inflammatory disorder observed in intergrin αvβ8 knockout mice, were DC, while knockout of the receptor on Th cells only, had no effect on the phenotype of these mice (Travis *et al.*, 2007). Neither epithelial cells nor DC, were present in the cultures used for iTreg induction in the current study, so TGF-β in the CM is likely to remain in its latent form. DC have also been implicated directly in the induction of iTreg (Kushwah & Hu, 2011). The cytokine milieu in the local tissue microenvironment can promote a state of tolerance in DC (Torres-Aguilar *et al.*, 2010). These tolerogenic DC express reduced levels of co-stimulatory molecules that are insufficient for conventional effector T cell activation; however the sub optimal level of activation promotes iTreg induction (Raker *et al.*, 2015). In the TME, DC with a tolerogenic phenotype are prevalent and are another factor that may contribute to iTreg induction (Han *et al.*, 2014). It would be interesting to carry out experiments using co-cultures of T cells with tumour cells, or tumour-derived stromal cells to see if there are effects on Treg induction or lymphocyte apoptosis.

A limiting factor when studying Treg remains the lack of a definitive phenotype and it is still unclear as to the prognostic relevance of Treg. Although, generally immunosuppression is considered to promote tumour progression this might not always be the case, and studies in HNSCC have led to conflicting reports as to the prognostic relevance of increased Treg levels. Further hindrance to the study of Treg is the different sub-populations that have now been identified. Whether these sub-groups have different roles (or even opposing roles) or differ in terms of prognosis has not been investigated, making interpreting results from the Treg population as a whole difficult.

## 7.3 Future Work

It is becoming increasingly clear that Treg represent a heterogeneous cell population, and in future work it will be essential to look at the expression of additional markers when investigating the role of Treg in HNSCC. For example $CD4^+FoxP3^{hi}CD45RA^-$ are an activated Treg population, high levels of which are associated with a negative prognosis in

HNSCC (Ihara *et al.*, 2017). In future studies it will be important to incorporate CD45RA into antibody panels when looking at Treg in PBMC or TIL, and analysing Treg recruitment.

To investigate whether cell contact dependent mechanisms are necessary for iTreg induction, or the presence of additional cells are required in order to enhance the effects of soluble factors in CM, co-culture experiments with $CD4^+CD25^-$ and tumour derived cell types could be used. It would also be interesting to carry out further analysis of the $CD39^+$ cells upregulated following the culture of $CD4^+CD25^-$ T cells in CM, to determine whether they are exhausted T cells. The expression of other markers of exhaustion, such as PD-1 could be analysed following culture and apoptosis could be measured in these cells following their re-stimulation, to determine whether they are more prone to apoptosis.

Although overall, CM did not induce apoptosis in T cells following culture in CM, whether the levels of apoptosis differ between T cell populations could be investigated by sorting CTL, Treg and convention Th cells, and carrying out apoptosis assays on the separate T cell populations. The induction of apoptosis of different T cell populations, and compensation by other subgroups, could be another contributing factor to the alterations in the proportions of cell types in the TME.

Building on the findings of the current study and looking at the expression of chemokine receptors in more patient samples, it would be possible to investigate the involvement of chemokine receptors in different HNSCC sub types, as well as between primary tumours and metastatic nodes and $HPV^+$ and $HPV^-$ tumours. In order to determine whether the increase in the expression of the chemokine receptors CXCR3, CCR4, CCR5 and CCR6 is causing their active recruitment to HNSCC tumours, migration assays using UMSCC cell line CM or tumour-derived CAF CM could be carried out. The expression of chemokine receptors on the migrated cells could be analysed in addition to T cell markers to determine which chemokine receptors are causing recruitment. To determine whether tumours can influence the expression of chemokine receptors on T cells and cause recruitment this way, rather than by releasing more chemokines, or whether it increases expression of markers associated with an activated phenotype (CXCR3 and CCR5), chemokine receptor expression could be assessed on T cells following culture in CM. Additionally, further characterisation of the soluble factors released by the tumour by mass spectrometry could lead to the identification of additional factors of interest.

## 7.4 Concluding Statement

Overall, results from the current study have highlighted areas that may be of interest for further research. Although, soluble factors may have a role in establishing the immunosuppression in tumours, it is likely that cell-cell interactions also have an important part to play in this process. Potential mechanisms for the accumulation of Treg in the HNSCC microenvironment have been identified, in particular recruitment by CCR4 and CCR6 ligands, however require further investigation. Furthermore, an increased understanding is required into the roles the repertoire of Treg play in cancer, and in which cases they may be beneficial and detrimental to tumour progression. Inhibiting immune suppression by preventing the accumulation of Treg in the TME may not be beneficial to all patients, however understanding the pathways involved could lead to possible therapeutic targets in some, which can be utilised when the role of Treg is better understood.

# References


Accomando, W. P*., et al* (2012) Decreased NK Cells in Patients with Head and Neck Cancer Determined in Archival DNA. *Clinical Cancer Research*, 18(22), 6147-6154.

Akimova, T*., et al* (2011) Helios Expression Is a Marker of T Cell Activation and Proliferation. *Plos One*, 6(8).

Alam, M. S*., et al* (2008) Gastric Th Cells Express CD39 and CD73 Leading to Adenosine Accumulation that Suppresses Helicobacter-induced Gastritis by Modulating Th Cell Function. *Faseb Journal*, 22.

Albert, S*., et al* (2013) Focus on the role of the CXCL12/CXCR4 chemokine axis in head and neck squamous cell carcinoma. *Head and Neck-Journal for the Sciences and Specialties of the Head and Neck*, 35(12), 1819-1828.

Allan, S. E*., et al* (2007) Activation-induced FOXP3 in human T effector cells does not suppress proliferation or cytokine production. *International Immunology*, 19(4), 345-354.

Allard, B*., et al* (2012) CD73-Generated Adenosine: Orchestrating the Tumor-Stroma Interplay to Promote Cancer Growth. *Journal of Biomedicine and Biotechnology*.

Alon, R*., et al* (1996) Interactions through L-selectin between leukocytes and adherent leukocytes nucleate rolling adhesions on selectins and VCAM-1 in shear flow. *Journal of Cell Biology*, 135(3), 849-865.

Alves, N. L*., et al* (2008) Differential regulation of human IL-7 receptor alpha expression by IL-7 and TCR signaling. *Journal of Immunology*, 180(8), 5201-5210.

Alvi, A. J*., et al* (2002) Mutation screening analysis of the retinoblastoma related gene RB2/p130 in sporadic ovarian cancer and head and neck squamous cell cancer. *Journal of Clinical Pathology-Molecular Pathology*, 55(3), 153-155.

Andersen, M. H*., et al* (2006) Cytotoxic T cells. *Journal of Investigative Dermatology*, 126(1), 32-41.

Andree, H. A. M*., et al* (1990) Binding of vascular anticoagulant-alpha (VAC-α) to planar phospholipid-bilayers. *Journal of Biological Chemistry*, 265(9), 4923-4928.

Andrews, L. P*., et al* (2017) LAG3 (CD223) as a cancer immunotherapy target. *Immunological Reviews*, 276(1), 80-96.

Ansel, K. M*., et al* (2000) A chemokine-driven positive feedback loop organizes lymphoid follicles. *Nature*, 406(6793), 309-314.

Antonioli, L*., et al* (2013) CD39 and CD73 in immunity and inflammation. *Trends in Molecular Medicine*, 19(6), 355-367.

Ara, T*., et al* (2003) A role of CXC chemokine ligand 12/stromal cell-derived factor-1/pre-B cell growth stimulating factor and its receptor CXCR4 in fetal and adult T cell development in vivo. *Journal of Immunology*, 170(9), 4649-4655.

Argiris, A*., et al* (2008) Head and neck cancer. *Lancet*, 371(9625), 1695-1709.

Asano, M*., et al* (1996) Autoimmune disease as a consequence of developmental abnormality of a T cell subpopulation. *The Journal of Experimental Medicine*, 184(2), 387-396.

Asseman, C*., et al* (1999) An essential role for interleukin 10 in the function of regulatory T cells that inhibit intestinal inflammation. *Journal of Experimental Medicine*, 190(7), 995-1003.

Atkins, M. B*., et al* (1999) High-dose recombinant interleukin 2 therapy for patients with metastatic melanoma: Analysis of 270 patients treated between 1985 and 1993. *Journal of Clinical Oncology*, 17(7), 2105-2116.

Ayyoub, M*., et al* (2013) Comment on "Helios(-) and Helios(-) Cells Coexist within the Natural FOXP3(+) T Regulatory Cell Subset in Humans". *Journal of Immunology*, 190(9), 4439-4440.

Bacchetta, R*., et al* (2002) Growth and expansion of human T regulatory type 1 cells are independent from TCR activation but require exogenous cytokines. *European Journal of Immunology*, 32(8), 2237-2245.

Badoual, C*., et al* (2013) PD-1-Expressing Tumor-Infiltrating T Cells Are a Favorable Prognostic Biomarker in HPV-Associated Head and Neck Cancer. *Cancer Research*, 73(1), 128-138.

Badoual, C*., et al* (2006) Prognostic value of tumor-infiltrating CD4(+) T-cell subpopulations in head and neck cancers. *Clinical Cancer Research*, 12(2), 465-472.

Baecher-Allan, C*., et al* (2001) CD4+CD25(high) regulatory cells in human peripheral blood. *Journal of Immunology*, 167(3), 1245-1253.

Baeyens, A*., et al* (2015) Exit Strategies: S1P Signaling and T Cell Migration. *Trends in Immunology*, 36(12), 778-787.

Baine, I*., et al* (2013) Helios Induces Epigenetic Silencing of Il2 Gene Expression in Regulatory T Cells. *Journal of Immunology*, 190(3), 1008-1016.

Balermpas, P*., et al* (2014a) Tumour-infiltrating lymphocytes predict response to definitive chemoradiotherapy in head and neck cancer. *Br J Cancer*, 110(2), 501-509.

Balermpas, P*., et al* (2014b) Head and neck cancer relapse after chemoradiotherapy correlates with CD163+macrophages in primary tumour and CD11b+myeloid cells in recurrences. *British Journal of Cancer*, 111(8), 1509-1518.

Balkwill, F. (2004) Cancer and the chemokine network. *Nature Reviews Cancer*, 4(7), 540-550.

Bao, X. F*., et al* (2010) Endothelial Heparan Sulfate Controls Chemokine Presentation in Recruitment of Lymphocytes and Dendritic Cells to Lymph Nodes. *Immunity*, 33(5), 817-829.

Bardel, E*., et al* (2008) Human CD4(+)CD25(+)Foxp3(+) Regulatory T Cells Do Not Constitutively Express IL-35. *Journal of Immunology*, 181(10), 6898-6905.

Baron, U., *et al* (2007) DNA demethylation in the human FOXP3 locus discriminates regulatory T cells from activated FOXP3+ conventional T cells. *European journal of immunology*, 37(9), 2378-2389.

Barreiro, O., *et al* (2002) Dynamic interaction of VCAM-1 and ICAM-1 with moesin and ezrin in a novel endothelial docking structure for adherent leukocytes. *Journal of Cell Biology*, 157(7), 1233-1245.

Barrientos, S., *et al* (2008) Growth factors and cytokines in wound healing. *Wound Repair and Regeneration*, 16(5), 585-601.

Bates, R. C., *et al* (2005) Transcriptional activation of integrin beta 6 during the epithelial-mesenchymal transition defines a novel prognostic indicator of aggressive colon carcinoma. *Journal of Clinical Investigation*, 115(2), 339-347.

Battaglia, A., *et al* (2008) Neuropilin-1 expression identifies a subset of regulatory T cells in human lymph nodes that is modulated by preoperative chemoradiation therapy in cervical cancer. *Immunology*, 123(1), 129-138.

Battaglia, M. & Roncarolo, M. G. (2009) The Tregs' world according to GARP. *European Journal of Immunology*, 39(12), 3296-3300.

Bauman, J. E., *et al* (2017) Immunotherapy of Head and Neck Cancer: Emerging Clinical Trials From a National Cancer Institute Head and Neck Cancer Steering Committee Planning Meeting. *Cancer*, 123(7), 1259-1271.

Bayer, A. L., *et al* (2005) Essential role for interleukin-2 for CD4(+)CD25(+) T regulatory cell development during the neonatal period. *Journal of Experimental Medicine*, 201(5), 769-777.

Belloc, F., *et al* (2000) *CaspACE™ FITC-VAD-FMK In Situ Marker as a Probe for Flow Cytometry Detection of Apoptotic Cells.* Available online: http://www.promega.co.uk/resources/pubhub/enotes/caspace-fitcvadfmk-in-situ-marker-a-probe-for-flow-cytometry-detection-of-apoptotic-cells/ [Accessed 01.06.2017].

Benechet, A. P., *et al* (2016) T cell-intrinsic S1PR1 regulates endogenous effector T-cell egress dynamics from lymph nodes during infection. *Proceedings of the National Academy of Sciences of the United States of America*, 113(8), 2182-2187.

Bennett, C. L., *et al* (2001) The immune dysregulation, polyendocrinopathy, enteropathy, X-linked syndrome (IPEX) is caused by mutations of FOXP3. *Nature Genetics*, 27(1), 20-21.

Berard, M. & Tough, D. F. (2002) Qualitative differences between naive and memory T cells. *Immunology*, 106(2), 127-138.

Bergmann, C., *et al* (2007) Expansion and characteristics of human T regulatory type 1 cells in co-cultures simulating tumor microenvironment. *Cancer Immunology, Immunotherapy*, 56(9), 1429-1442.

Berhanu, D., *et al* (2003) Optimized lymphocyte isolation methods for analysis of chemokine receptor expression. *Journal of Immunological Methods*, 279(1-2), 199-207.

Bernier, J. & Bentzen, S. M. (2003) Altered fractionation and combined radio-chemotherapy approaches: pioneering new opportunities in head and neck oncology. *European Journal of Cancer*, 39(5), 560-571.

Bettelli, E*., et al* (2006) Reciprocal developmental pathways for the generation of pathogenic effector T(H)17 and regulatory T cells. *Nature*, 441(7090), 235-238.

Bhowmick, N. A*., et al* (2004) Stromal fibroblasts in cancer initiation and progression. *Nature*, 432(7015), 332-337.

Bierie, B. & Moses, H. L. (2010) Transforming growth factor beta (TGF-beta) and inflammation in cancer. *Cytokine Growth Factor Rev*, 21(1), 49-59.

Blot, W. J*., et al* (1988) Smoking and drinking in relation to oral and pharyngeal cancer. *Cancer Research*, 48(11), 3282-3287.

Boeing, H*., et al* (2006) Intake of fruits and vegetables and risk of cancer of the upper aero-digestive tract: the prospective EPIC-study. *Cancer Causes & Control*, 17(7), 957-969.

Borghaei, H*., et al* (2015) Nivolumab versus Docetaxel in Advanced Nonsquamous Non-Small-Cell Lung Cancer. *New England Journal of Medicine*, 373(17), 1627-1639.

Born, W. K*., et al* (2013) Diversity of gamma delta T-cell antigens. *Cellular & Molecular Immunology*, 10(1), 13-20.

Borsellino, G*., et al* (2007) Expression of ectonucleotidase CD39 by Foxp3(+) Treg cells: hydrolysis of extracellular ATP and immune suppression. *Blood*, 110(4), 1225-1232.

Bosch, F. X*., et al* (2002) The causal relation between human papillomavirus and cervical cancer. *Journal of Clinical Pathology*, 55(4), 244-265.

Bottcher, A*., et al* (2013) Gene Expression Profiling of Circulating Natural Killer Cells in Head and Neck Squamous Cell Carcinoma. *Cancer Genomics & Proteomics*, 10(5), 197-207.

Brahmer, J*., et al* (2015) Nivolumab versus Docetaxel in Advanced Squamous-Cell Non-Small-Cell Lung Cancer. *New England Journal of Medicine*, 373(2), 123-135.

Bravi, F*., et al* (2012) Dietary patterns and upper aerodigestive tract cancers: an overview and review. *Annals of Oncology*, 23(12), 3024-3039.

Bray, F*., et al* (2005) Trends in cervical squamous cell carcinoma incidence in 13 European countries: Changing risk and the effects of screening. *Cancer Epidemiology Biomarkers & Prevention*, 14(3), 677-686.

Breitfeld, D*., et al* (2000) Follicular B helper T cells express CXC chemokine receptor 5, localize to B cell follicles, and support immunoglobulin production. *Journal of Experimental Medicine*, 192(11), 1545-1551.

Brenner, J. C*., et al* (2010) GENOTYPING OF 73 UM-SCC HEAD AND NECK SQUAMOUS CELL CARCINOMA CELL LINES. *Head and Neck-Journal for the Sciences and Specialties of the Head and Neck*, 32(4), 417-426.

Bron, L.*, et al* (2013) Prognostic value of arginase-II expression and regulatory T-cell infiltration in head and neck squamous cell carcinoma. *International Journal of Cancer*, 132(3), E85-E93.

Browman, G. P.*, et al* (1993) Influence of cigarette-smoking on the
efficacy of radiation-therapy in head and neck-cancer. *New England Journal of Medicine*, 328(3), 159-163.

Bruder, D.*, et al* (2004) Neuropilin-1: a surface marker of regulatory T cells. *European Journal of Immunology*, 34(3), 623-630.

Brunkow, M. E.*, et al* (2001) Disruption of a new forkhead/winged-helix protein, scurfin, results in the fatal lymphoproliferative disorder of the scurfy mouse. *Nature Genetics*, 27(1), 68-73.

Burnet, M. (1957) Cancer; a biological approach. I. The processes of control. *British medical journal*, 1(5022), 779-86.

Campbell, D. J. & Butcher, E. C. (2002) Intestinal attraction: CCL25 functions in effector lymphocyte recruitment to the small intestine. *Journal of Clinical Investigation*, 110(8), 1079-1081.

Campbell, J. J.*, et al* (2001) CCR7 expression and memory T cell diversity in humans. *Journal of Immunology*, 166(2), 877-884.

Candia, E.*, et al* (2017) Single and combined effect of retinoic acid and rapamycin modulate the generation, activity and homing potential of induced human regulatory T cells. *Plos One*, 12(7).

Cao, X. F.*, et al* (2007) Granzyme B and perforin are important for regulatory T cell-mediated suppression of tumor clearance. *Immunity*, 27(4), 635-646.

Catakovic, K.*, et al* (2017) T cell exhaustion: from pathophysiological basics to tumor immunotherapy. *Cell Communication and Signaling*, 15.

Chang, J. E. & Turley, S. J. (2015) Stromal infrastructure of the lymph node and coordination of immunity. *Trends in Immunology*, 36(1), 30-39.

Chang, K. C.*, et al* (2000) The state diagram for cell adhesion under flow: Leukocyte rolling and firm adhesion. *Proceedings of the National Academy of Sciences of the United States of America*, 97(21), 11262-11267.

Chang, K. P.*, et al* (2008) Macrophage Inflammatory Protein-3 alpha Is a Novel Serum Marker for Nasopharyngeal Carcinoma Detection and Prediction of Treatment Outcomes. *Clinical Cancer Research*, 14(21), 6979-6987.

Chang, K. P.*, et al* (2011) Overexpression of macrophage inflammatory protein-3alpha in oral cavity squamous cell carcinoma is associated with nodal metastasis. *Oral Oncology*, 47, S47-S47.

Chang, K. P.*, et al* (2013) Serum levels of chemokine (C-X-C motif) ligand 9 (CXCL9) are associated with tumor progression and treatment outcome in patients with oral cavity squamous cell carcinoma. *Oral Oncology*, 49(8), 802-807.

Charo, I. F. & Ransohoff, R. M. (2006) Mechanisms of disease - The many roles of chemokines and chemokine receptors in inflammation. *New England Journal of Medicine*, 354(6), 610-621.

Chaudhary, B*., et al* (2014) Neuropilin 1: function and therapeutic potential in cancer. *Cancer Immunology Immunotherapy*, 63(2), 81-99.

Chen, B*., et al* (2013) High CCR6/CCR7 expression and Foxp3(+) Treg cell number are positively related to the progression of laryngeal squamous cell carcinoma. *Oncology Reports*, 30(3), 1380-1390.

Chen, L. P. & Flies, D. B. (2013) Molecular mechanisms of T cell co-stimulation and co-inhibition. *Nature Reviews Immunology*, 13(4), 227-242.

Chen, S. C*., et al* (2010) Expression of chemokine receptor CXCR3 by lymphocytes and plasmacytoid dendritic cells in human psoriatic lesions. *Archives of Dermatological Research*, 302(2), 113-123.

Chen, W. J*., et al* (2003) Conversion of peripheral CD4(+)CD25(-) naive T cells to CD4(+)CD25(+) regulatory T cells by TGF-beta induction of transcription factor Foxp3. *Journal of Experimental Medicine*, 198(12), 1875-1886.

Chen, Z*., et al* (1999) Expression of proinflammatory and proangiogenic cytokines in patients with head and neck cancer. *Clinical Cancer Research*, 5(6), 1369-1379.

Chi, L. J*., et al* (2010) Involvement of T helper type 17 and regulatory T cell activity in tumour immunology of bladder carcinoma. *Clinical and Experimental Immunology*, 161(3), 480-489.

Chong, C. R. & Janne, P. A. (2013) The quest to overcome resistance to EGFR-targeted therapies in cancer. *Nature Medicine*, 19(11), 1389-1400.

Chow, M. T. & Luster, A. D. (2014) Chemokines in Cancer. *Cancer Immunology Research*, 2(12), 1125-1131.

Christofakis, E. P*., et al* (2008) Roles of CXCL8 in squamous cell carcinoma proliferation and migration. *Oral Oncology*, 44(10), 920-926.

Chuang, J. Y*., et al* (2009) CCL5/CCR5 Axis Promotes the Motility of Human Oral Cancer Cells. *Journal of Cellular Physiology*, 220(2), 418-426.

Chuang, S. C*., et al* (2012) Diet and the risk of head and neck cancer: a pooled analysis in the INHANCE consortium. *Cancer Causes & Control*, 23(1), 69-88.

Collison, L. W*., et al* (2010) IL-35-mediated induction of a potent regulatory T cell population. *Nature Immunology*, 11(12), 1093-U97.

Cosmi, L*., et al* (2003) Human CD8(+)CD25(+) thymocytes share phenotypic and functional features with CD4(+)CD25(+) re latory thyrnocytes. *Blood*, 102(12), 4107-4114.

Costa, D. L*., et al* (2015) Tr-1-Like CD4(+)CD25(-)CD127(-/low)FOXP3(-) Cells Are the Main Source of Interleukin 10 in Patients With Cutaneous Leishmaniasis Due to Leishmania braziliensis. *Journal of Infectious Diseases*, 211(5), 708-718.

Coulie, P. G.*, et al* (2014) Tumour antigens recognized by T lymphocytes: at the core of cancer immunotherapy. *Nature Reviews Cancer*, 14(2), 135-146.

Couper, K. N.*, et al* (2008) IL-10: The master regulator of immunity to infection. *Journal of Immunology*, 180(9), 5771-5777.

Cousins, D. J. (2017) Pinning allergies on pathogenic T(H)2 cells. *Science Translational Medicine*, 9(401).

Coussens, L. M. & Werb, Z. (2002) Inflammation and cancer. *Nature*, 420(6917), 860-867.

Csoka, B.*, et al* (2008) Adenosine A(2A) receptor activation inhibits T helper 1 and T helper 2 cell development and effector function. *Faseb Journal*, 22(10), 3491-3499.

Cullen, S. P.*, et al* (2010) Granzymes in cancer and immunity. *Cell Death and Differentiation*, 17(4), 616-623.

Curiel, T. J. (2007) Tregs and rethinking cancer immunotherapy. *Journal of Clinical Investigation*, 117(5), 1167-1174.

Curiel, T. J.*, et al* (2004) Specific recruitment of regulatory T cells in ovarian carcinoma fosters immune privilege and predicts reduced survival. *Nature Medicine*, 10(9), 942-949.

Curry, J. M.*, et al* (2014) Tumor Microenvironment in Head and Neck Squamous Cell Carcinoma. *Seminars in Oncology*, 41(2), 217-234.

Cyster, J. G. & Schwab, S. R. (2012) Sphingosine-1-Phosphate and Lymphocyte Egress from Lymphoid Organs. *Annual Review of Immunology, Vol 30*, 30, 69-94.

Czystowska, M.*, et al* (2009) IRX-2, a novel immunotherapeutic, protects human T cells from tumor-induced cell death. *Cell Death and Differentiation*, 16(5), 708-718.

D'Souza, G.*, et al* (2007) Case-control study of human papillomavirus and oropharyngeal cancer. *New England Journal of Medicine*, 356(19), 1944-1956.

da Silva, J. M.*, et al* (2016) Significance of chemokine and chemokine receptors in head and neck squamous cell carcinoma: A critical review. *Oral Oncology*, 56, 8-16.

Danaei, G.*, et al* (2005) Causes of cancer in the world: comparative risk assessment of nine behavioural and environmental risk factors. *Lancet*, 366(9499), 1784-1793.

Darzynkiewicz, Z.*, et al* (2001) Difficulties and pitfalls in analysis of apoptosis. *Methods Cell Biol*, 63, 527-46.

Davies, E. G.*, et al* (2017) Thymus transplantation for complete DiGeorge syndrome: European experience. *Journal of Allergy and Clinical Immunology*, 140(6), 1660-+.

de Medeiros, M. C.*, et al* (2017) HNSCC subverts PBMCs to secrete soluble products that promote tumor cell proliferation. *Oncotarget*, 8(37), 60860-60874.

Deaglio, S.*, et al* (2007) Adenosine generation catalyzed by CD39 and CD73 expressed on regulatory T cells mediates immune suppression. *Journal of Experimental Medicine*, 204(6), 1257-1265.

Della Chiesa, M.*, et al* (2016) Features of Memory-Like and PD-1(+) Human nK Cell Subsets. *Frontiers in Immunology*, 7.

Desgrosellier, J. S. & Cheresh, D. A. (2010) Integrins in cancer: biological implications and therapeutic opportunities. *Nature Reviews Cancer*, 10(1), 9-22.

Dok, R. & Nuyts, S. (2016) HPV Positive Head and Neck Cancers: Molecular Pathogenesis and Evolving Treatment Strategies. *Cancers*, 8(4).

Dong, H. D.*, et al* (2002) Tumor-associated B7-H1 promotes T-cell apoptosis: A potential mechanism of immune evasion. *Nature Medicine*, 8(8), 793-800.

Dong, R. P.*, et al* (1996) Characterization of adenosine deaminase binding to human CD26 on T cells and its biologic role in immune response. *Journal of Immunology*, 156(4), 1349-1355.

Doorbar, J. (2006) Molecular biology of human papillomavirus infection and cervical cancer. *Clinical Science*, 110(5), 525-541.

Drabsch, Y. & ten Dijke, P. (2012) TGF-beta signalling and its role in cancer progression and metastasis. *Cancer and Metastasis Reviews*, 31(3-4), 553-568.

Drennan, S.*, et al* (2013) Increased frequency and suppressive activity of CD127(low/-) regulatory T cells in the peripheral circulation of patients with head and neck squamous cell carcinoma are associated with advanced stage and nodal involvement. *Immunology*, 140(3), 335-343.

Drennan, S.*, et al* (2014) Frequency Over Function: Raised Levels of $CD127^{low/-}$ Regulatory T cells in the Tumour Microenvironment Compared with the Periphery of Head and Neck Cancer Patients Journal of Clinical and Cellular Immunology.

Duray, A.*, et al* (2010) Immune Suppression in Head and Neck Cancers: A Review. *Clinical & Developmental Immunology*.

Durham, N. M.*, et al* (2014) Lymphocyte Activation Gene 3 (LAG-3) Modulates the Ability of CD4 T-cells to Be Suppressed In Vivo. *Plos One*, 9(11).

Dutcher, J. (2002) Current status of interleukin-2 therapy for metastatic renal cell carcinoma and metastatic melanoma. *Oncology-New York*, 16(11), 4-10.

Dwyer, K. M.*, et al* (2010) Expression of CD39 by Human Peripheral Blood CD4(+)CD25(+) T Cells Denotes a Regulatory Memory Phenotype. *American Journal of Transplantation*, 10(11), 2410-2420.

Dyer, A. R.*, et al* (2003) Dietary intake in male and female smokers, ex-smokers, and never smokers: The INTERMAP Study. *Journal of Human Hypertension*, 17(9), 641-654.

Dyson, N. (1998) The regulation of E2F by pRB-family proteins. *Genes & Development*, 12(15), 2245-2262.

Economopoulou, P.*, et al* (2016) The promise of immunotherapy in head and neck squamous cell carcinoma: combinatorial immunotherapy approaches. *Esmo Open*, 1(6).

Elkord, E. (2009) Frequency of human T regulatory cells in peripheral blood is significantly reduced by cryopreservation. *Journal of Immunological Methods*, 347(1-2), 87-90.

Ellyard, J. I.*, et al* (2007) Th2-mediated anti-tumour immunity: friend or foe? *Tissue Antigens*, 70(1), 1-11.

Elmore, S. (2007) Apoptosis: A review of programmed cell death. *Toxicologic Pathology*, 35(4), 495-516.

Erdman, S. E. & Poutahidis, T. (2010) Cancer inflammation and regulatory T cells. *International Journal of Cancer*, 127(4), 768-779.

Erdman, S. E.*, et al* (2003) CD4(+) CD25(+) regulatory T lymphocytes inhibit microbially induced colon cancer in Rag2-deficient mice. *American Journal of Pathology*, 162(2), 691-702.

Evans, R.*, et al* (2009) Integrins in immunity. *Journal of Cell Science*, 122(2), 215-225.

Fadok, V. A.*, et al* (1992) Exposure of phosphatidylserine on the surface of apoptotic lymphocytes triggers specific recognition and removal by macrophages. *Journal of Immunology*, 148(7), 2207-2216.

Fakhry, C.*, et al* (2008) Improved survival of patients with human papillomavirus-positive head and neck squamous cell carcinoma in a prospective clinical trial. *Journal of the National Cancer Institute*, 100(4), 261-269.

Fang, F. Q.*, et al* (2016) Expression of CD39 on Activated T Cells Impairs their Survival in Older Individuals. *Cell Reports*, 14(5), 1218-1231.

Feldman, R.*, et al* (2016) Molecular profiling of head and neck squamous cell carcinoma. *Head and Neck-Journal for the Sciences and Specialties of the Head and Neck*, 38, E1625-E1638.

Ferreira, F. O.*, et al* (2008) Association of CCL2 with lymph node metastasis and macrophage infiltration in oral cavity and lip squamous cell carcinoma. *Tumor Biology*, 29(2), 114-121.

Ferris, R. L.*, et al* (2016) Nivolumab for Recurrent Squamous-Cell Carcinoma of the Head and Neck. *New England Journal of Medicine*, 375(19), 1856-1867.

Filipazzi, P.*, et al* (2012) Phenotype, function and clinical implications of myeloid-derived suppressor cells in cancer patients. *Cancer Immunology Immunotherapy*, 61(2), 255-263.

Finney, O. C.*, et al* (2010) Phenotypic analysis of human peripheral blood regulatory T cells (CD4(+)FOXP3(+)CD127(lo/-)) ex vivo and after in vitro restimulation with malaria antigens. *European Journal of Immunology*, 40(1), 47-60.

Flavell, R. A.*, et al* (2010) The polarization of immune cells in the tumour environment by TGF beta. *Nature Reviews Immunology*, 10(8), 554-567.

Fontenot, J. D*., et al* (2003) Foxp3 programs the development and function of CD4(+)CD25(+) regulatory T cells. *Nature Immunology*, 4(4), 330-336.

Forster, R*., et al* (2008) CCR7 and its ligands: balancing immunity and tolerance. *Nature Reviews Immunology*, 8(5), 362-371.

Forster, R*., et al* (1999) CCR7 coordinates the primary immune response by establishing functional microenvironments in secondary lymphoid organs. *Cell*, 99(1), 23-33.

Francisco, L. M*., et al* (2009) PD-L1 regulates the development, maintenance, and function of induced regulatory T cells. *Journal of Experimental Medicine*, 206(13), 3015-3029.

Franciszkiewicz, K*., et al* (2012) Role of Chemokines and Chemokine Receptors in Shaping the Effector Phase of the Antitumor Immune Response. *Cancer Research*, 72(24), 6325-6332.

Fredholm, B. B*., et al* (1994) NOMENCLATURE AND CLASSIFICATION OF PURINOCEPTORS. *Pharmacological Reviews*, 46(2), 143-156.

Fujii, N*., et al* (2012) Cancer-associated fibroblasts and CD163-positive macrophages in oral squamous cell carcinoma: their clinicopathological and prognostic significance. *Journal of Oral Pathology & Medicine*, 41(6), 444-451.

Gagliani, N*., et al* (2015) TH17 cells transdifferentiate into regulatory T cells during resolution of inflammation. *Nature*, 523(7559), 221-U225.

Galkina, E*., et al* (2007) T lymphocyte rolling and recruitment into peripheral lymph nodes is regulated by a saturable density of L-selectin (CD62L). *European Journal of Immunology*, 37(5), 1243-1253.

Garrido, F*., et al* (1997) Implications for immunosurveillance of altered HLA class I phenotypes in human tumours. *Immunology Today*, 18(2), 89-95.

Garris, C. S*., et al* (2014) Sphingosine-1-phosphate receptor 1 signalling in T cells: trafficking and beyond. *Immunology*, 142(3), 347-353.

Gastman, B. R*., et al* (1999) Fas ligand is expressed on human squamous cell carcinomas of the head and neck, and it promotes apoptosis of T lymphocytes. *Cancer Research*, 59(20), 5356-5364.

Gavin, M. A*., et al* (2006) Single-cell analysis of normal and FOXP3-mutant human T cells: FOXP3 expression without regulatory T cell development. *Proceedings of the National Academy of Sciences of the United States of America*, 103(17), 6659-6664.

Geginat, J*., et al* (2016) Reverse plasticity: TGF-beta and IL-6 induce Th1-to-Th17-cell transdifferentiation in the gut. *Eur J Immunol*, 46(10), 2306-2310.

Germain, R. N. (2002) T-cell development and the CD4-CD8 lineage decision. *Nature Reviews Immunology*, 2(5), 309-322.

Getnet, D*., et al* (2009) Tumor Recognition and Self-Recognition Induce Distinct Transcriptional Profiles in Antigen-Specific CD4 T Cells. *Journal of Immunology*, 182(8), 4675-4685.

Ghiringhelli, F.*, et al* (2005) CD4(+) CD25(+) regulatory T cells inhibit natural killer cell functions in a transforming growth factor-beta-dependent manner. *Journal of Experimental Medicine*, 202(8), 1075-1085.

Ghoreschi, K.*, et al* (2010) Generation of pathogenic T(H)17 cells in the absence of TGF-beta signalling. *Nature*, 467(7318), 967-U144.

Giovannetti, A.*, et al* (2008) Apoptosis in the homeostasis of the immune system and in human immune mediated diseases. *Current Pharmaceutical Design*, 14(3), 253-268.

Gleeson, M. J., and Ray C. Clarke, eds. (2008) *Scott-Brown's Otorhinolaryngology: Head and Neck Surgery*, *3 volume set* vols, *7Ed* edition.CRC Press.

Gondek, D. C.*, et al* (2005) Cutting edge: Contact-mediated suppression by CD4(+)-CD25(+) regulatory cells involves a granzyme B-dependent, perforin-independent mechanism. *Journal of Immunology*, 174(4), 1783-1786.

Goodman, A. M.*, et al* (2017) Tumor Mutational Burden as an Independent Predictor of Response to Immunotherapy in Diverse Cancers. *Molecular Cancer Therapeutics*, 16(11), 2598-2608.

Gordon, S. (2003) Alternative activation of macrophages. *Nature Reviews Immunology*, 3(1), 23-35.

Gorrell, M. D.*, et al* (2001) CD26: A multifunctional integral membrane and secreted protein of activated lymphocytes. *Scandinavian Journal of Immunology*, 54(3), 249-264.

Grandis, J. R. & Tweardy, D. J. (1993) Elevated levels of transforming growth-factor-alpha and epidermal growth-factor receptor messenger-RNA are early markers of carcinogenesis in head and neck-cancer. *Cancer Research*, 53(15), 3579-3584.

Green, V. L.*, et al* (2013) Increased prevalence of tumour infiltrating immune cells in oropharyngeal tumours in comparison to other subsites: relationship to peripheral immunity. *Cancer Immunology Immunotherapy*, 62(5), 863-873.

Griffith, J. W.*, et al* (2014) Chemokines and Chemokine Receptors: Positioning Cells for Host Defense and Immunity. *Annual Review of Immunology, Vol 32*, 32, 659-702.

Grohmann, U.*, et al* (2002) CTLA-4-Ig regulates tryptophan catabolism in vivo. *Nature Immunology*, 3(11), 1097-1101.

Groom, J. R. & Luster, A. D. (2011) CXCR3 in T cell function. *Experimental Cell Research*, 317(5), 620-631.

Grossman, W. J.*, et al* (2004) Human T regulatory cells can use the perforin pathway to cause autologous target cell death. *Immunity*, 21(4), 589-601.

Grosso, J. F.*, et al* (2007) LAG-3 regulates CD8+T cell accumulation and effector function in murine self- and tumor-tolerance systems. *Journal of Clinical Investigation*, 117(11), 3383-3392.

Groux, H.*, et al* (1997) A CD4+T-cell subset inhibits antigen-specific T-cell responses and prevents colitis. *Nature*, 389(6652), 737-742.

Gunaydin, R. O*., et al* (2012) Identification of the peripheral blood levels of interleukin-12, interleukin-10, and transforming growth factor-beta in patients with laryngeal squamous cell carcinoma. *Head and Neck-Journal for the Sciences and Specialties of the Head and Neck*, 34(3), 393-397.

Gupta, P. K*., et al* (2015) CD39 Expression Identifies Terminally Exhausted CD8(+) T Cells. *PLoS Pathogens*, 11(10), 21.

Ha, H*., et al* (2017) Role of the CXCL8-CXCR1/2 Axis in Cancer and Inflammatory Diseases. *Theranostics*, 7(6), 1543-1588.

Haghshenas, M. R*., et al* (2015) Immune regulatory cells and IL17-producing lymphocytes in patients with benign and malignant salivary gland tumors. *Immunology Letters*, 164(2), 109-116.

Halama, N*., et al* (2016) Tumoral Immune Cell Exploitation in Colorectal Cancer Metastases Can Be Targeted Effectively by Anti-CCR5 Therapy in Cancer Patients. *Cancer Cell*, 29(4), 587-601.

Halpern, A. C. & Schuchter, L. M. (1997) Prognostic models in melanoma. *Seminars in Oncology*, 24(1), S2-S7.

Han, Y. M*., et al* (2014) Human CD14(+)CTLA-4(+) Regulatory Dendritic Cells Suppress T-Cell Response by Cytotoxic T-Lymphocyte Antigen-4-Dependent IL-10 and Indoleamine-2,3-Dioxygenase Production in Hepatocellular Carcinoma. *Hepatology*, 59(2), 567-579.

Hanahan, D. & Weinberg, R. A. (2000) The hallmarks of cancer. *Cell*, 100(1), 57-70.

Hanahan, D. & Weinberg, R. A. (2011) Hallmarks of Cancer: The Next Generation. *Cell*, 144(5), 646-674.

Hanke, T*., et al* (2015) High intratumoral FOXP3(+) T regulatory cell (Tregs) density is an independent good prognosticator in nodal negative colorectal cancer. *International Journal of Clinical and Experimental Pathology*, 8(7), 8227-8235.

Hankins, H. M*., et al* (2015) Role of Flippases, Scramblases and Transfer Proteins in Phosphatidylserine Subcellular Distribution. *Traffic*, 16(1), 35-47.

Hansen, W*., et al* (2012) Neuropilin 1 deficiency on CD4(+)Foxp3(+) regulatory T cells impairs mouse melanoma growth. *Journal of Experimental Medicine*, 209(11), 2001-2016.

Haringer, B*., et al* (2009) Identification and characterization of IL-10/IFN-gamma-producing effector-like T cells with regulatory function in human blood. *Journal of Experimental Medicine*, 206(5), 1009-1017.

Hashibe, M*., et al* (2007) Alcohol drinking in never users of tobacco, cigarette smoking in never drinkers, and the risk of head and neck cancer: Pooled analysis in the international head and neck cancer epidemiology consortium. *Journal of the National Cancer Institute*, 99(10), 777-789.

Hashibe, M*., et al* (2009) Interaction between Tobacco and Alcohol Use and the Risk of Head and Neck Cancer: Pooled Analysis in the International Head and Neck Cancer Epidemiology Consortium. *Cancer Epidemiology Biomarkers & Prevention*, 18(2), 541-550.

Hasina, R.*, et al* (2008) Angiogenic heterogeneity in head and neck squamous cell carcinoma: biological and therapeutic implications. *Laboratory Investigation*, 88(4), 342-353.

Hathaway, B.*, et al* (2005) Multiplexed analysis of serum cytokines as biomarkers in squamous cell carcinoma of the head and neck patients. *Laryngoscope*, 115(3), 522-527.

Hauswald, H.*, et al* (2011) Long-term outcome and patterns of failure in patients with advanced head and neck cancer. *Radiation Oncology*, 6.

Hehlmann, R.*, et al* (2005) Chronic myeloid leukemia: a model for oncology. *Annals of Hematology*, 84(8), 487-497.

Henry, C. M.*, et al* (2013) Measuring apoptosis by microscopy and flow cytometry. *Methods*, 61(2), 90-97.

Herrero, R.*, et al* (2003) Human papillomavirus and oral cancer: The international agency for research on cancer multicenter study. *Journal of the National Cancer Institute*, 95(23), 1772-1783.

Himmel, M. E.*, et al* (2013) Helios(+) and Helios(-) Cells Coexist within the Natural FOXP3(+) T Regulatory Cell Subset in Humans. *Journal of Immunology*, 190(5), 2001-2008.

Hindley, J. P.*, et al* (2011) Analysis of the T-Cell Receptor Repertoires of Tumor-Infiltrating Conventional and Regulatory T Cells Reveals No Evidence for Conversion in Carcinogen-Induced Tumors. *Cancer Research*, 71(3), 736-746.

Hippen, K. L.*, et al* (2011) Generation and Large-Scale Expansion of Human Inducible Regulatory T Cells That Suppress Graft-Versus-Host Disease. *American Journal of Transplantation*, 11(6), 1148-1157.

Ho, T.*, et al* (2007) Epidemiology of carcinogen metabolism genes and risk of squamous cell carcinoma of the head and neck. *Head and Neck-Journal for the Sciences and Specialties of the Head and Neck*, 29(7), 682-699.

Hodi, F. S.*, et al* (2010) Improved Survival with Ipilimumab in Patients with Metastatic Melanoma. *New England Journal of Medicine*, 363(8), 711-723.

Hoerning, A.*, et al* (2011) Subsets of human CD4(+) regulatory T cells express the peripheral homing receptor CXCR3. *European Journal of Immunology*, 41(8), 2291-2302.

Hoesli, R. C. & Moyer, J. S. (2016) Immunotherapy for Head and Neck Squamous Cell Carcinoma. *Current oral health reports* 3(2), 74–81.

Hoff, C. M.*, et al* (2012) Effect of smoking on oxygen delivery and outcome in patients treated with radiotherapy for head and neck squamous cell carcinoma - A prospective study. *Radiotherapy and Oncology*, 103(1), 38-44.

Hoffmann, D.*, et al* (2001) The less harmful cigarette: A controversial issue. A tribute to Ernst L. Wynder. *Chemical Research in Toxicology*, 14(7), 767-790.

Hoffmann, P.*, et al* (2004) Large-scale in vitro expansion of polyclonal human CD4(+)CD25(high) regulatory T cells. *Blood*, 104(3), 895-903.

Hoffmann, T. K.*, et al* (2002) Spontaneous apoptosis of circulating T lymphocytes in patients with head and neck cancer and its clinical importance. *Clinical Cancer Research*, 8(8), 2553-2562.

Hohlbaum, A. M.*, et al* (2000) Opposing effects of transmembrane and soluble Fas ligand expression on inflammation and tumor cell survival. *Journal of Experimental Medicine*, 191(7), 1209-1219.

Holcik, M. & Korneluk, R. G. (2001) XIAP, the guardian angel. *Nature Reviews Molecular Cell Biology*, 2(7), 550-556.

Hopkins, J.*, et al* (2008) Genetic Polymorphisms and head and neck cancer outcomes: A review. *Cancer Epidemiology Biomarkers & Prevention*, 17(3), 490-499.

Hori, S.*, et al* (2003) Control of regulatory T cell development by the transcription factor Foxp3. *Science*, 299(5609), 1057-1061.

Hsieh, C. S.*, et al* (2006) An intersection between the self-reactive regulatory and nonregulatory T cell receptor repertoires. *Nature Immunology*, 7(4), 401-410.

Hsu, P.*, et al* (2015) IL-10 Potentiates Differentiation of Human Induced Regulatory T Cells via STAT3 and Foxo1. *Journal of Immunology*, 195(8), 3665-3674.

Huang, C. B.*, et al* (2017) Tumour-derived Interleukin 35 promotes pancreatic ductal adenocarcinoma cell extravasation and metastasis by inducing ICAM1 expression. *Nature Communications*, 8.

Huang, C. T.*, et al* (2004) Role of LAG-3 in regulatory T cells. *Immunity*, 21(4), 503-513.

Ichihara, F.*, et al* (2003) Increased populations of regulatory T cells in peripheral blood and tumor-infiltrating lymphocytes in patients with gastric and esophageal cancers. *Clinical Cancer Research*, 9(12), 4404-4408.

Ihara, F.*, et al* (2017) CD45RA−Foxp3high regulatory T cells have a negative impact on the clinical outcome of head and neck squamous cell carcinoma. *Cancer Immunology, Immunotherapy*, 1-11.

Inobe, J.*, et al* (1998) IL-4 is a differentiation factor for transforming growth factor-beta secreting Th3 cells and oral administration of IL-4 enhances oral tolerance in experimental allergic encephalomyelitis. *European Journal of Immunology*, 28(9), 2780-2790.

Itoh, M.*, et al* (1999) Thymus and autoimmunity: Production of CD25(+)CD4(+) naturally anergic and suppressive T cells as a key function of the thymus in maintaining immunologic self-tolerance. *Journal of Immunology*, 162(9), 5317-5326.

Iwamoto, T.*, et al* (2008) Molecular aspects of rheumatoid arthritis: chemokines in the joints of patients. *Febs Journal*, 275(18), 4448-4455.

Jackaman, C.*, et al* (2003) IL-2 intratumoral immunotherapy enhances CD8(+) T cells that mediate destruction of tumor cells and tumor-associated vasculature: A novel mechanism for IL-2(1). *Journal of Immunology*, 171(10), 5051-5063.

Janssen, E. M*., et al* (2005) CD4(+) T-cell help controls CD8(+) T-cell memory via TRAIL-mediated activation-induced cell death. *Nature*, 434(7029), 88-93.

Jemal, A. (2011) Global Cancer Statistics (vol 61, pg 69, 2011). *Ca-a Cancer Journal for Clinicians*, 61(2), 134-134.

Jie, H. B*., et al* (2013) Intratumoral regulatory T cells upregulate immunosuppressive molecules in head and neck cancer patients. *British Journal of Cancer*, 109(10), 2629-2635.

Johansson-Lindbom, B. & Agace, W. W. (2007) Generation of gut-homing T cells and their localization to the small intestinal mucosa. *Immunological Reviews*, 215, 226-242.

Johansson, A. C*., et al* (2012) Cancer-Associated Fibroblasts Induce Matrix Metalloproteinase-Mediated Cetuximab Resistance in Head and Neck Squamous Cell Carcinoma Cells. *Molecular Cancer Research*, 10(9), 1158-1168.

John, A. E*., et al* (2003) Respiratory syncytial virus-induced CCL5/RANTES contributes to exacerbation of allergic airway inflammation. *European Journal of Immunology*, 33(6), 1677-1685.

Johnsen, A*., et al* (1998) Down-regulation of the transporter for antigen presentation, proteasome subunits, and class I major histocompatibility complex in tumor cell lines. *Cancer Research*, 58(16), 3660-3667.

Jordan, J. T*., et al* (2008) Preferential migration of regulatory T cells mediated by glioma-secreted chemokines can be blocked with chemotherapy. *Cancer Immunology Immunotherapy*, 57(1), 123-131.

Ju, S. T*., et al* (1995) FAS(CD95) FASL INTERACTIONS REQUIRED FOR PROGRAMMED CELL-DEATH AFTER T-CELL ACTIVATION. *Nature*, 373(6513), 444-448.

June, C. H. (2007) Adoptive T cell therapy for cancer in the clinic. *Journal of Clinical Investigation*, 117(6), 1466-1476.

Kabelitz, D*., et al* (2007) Perspectives of gamma delta T cells in tumor immunology. *Cancer Research*, 67(1), 5-8.

Kaiser, A*., et al* (2005) CC chemokine ligand 19 secreted by mature dendritic cells increases naive T cell scanning behavior and their response to rare cognate antigen. *Journal of Immunology*, 175(4), 2349-2356.

Kalluri, R. (2016) The biology and function of fibroblasts in cancer. *Nature Reviews Cancer*, 16(9), 582-598.

Kang, H*., et al* (2015) Emerging biomarkers in head and neck cancer in the era of genomics. *Nature Reviews Clinical Oncology*, 12(1), 11-26.

Karpinich, N. O*., et al* (2006) The course of etoposide-induced apoptosis in Jurkat cells lacking p53 and Bax. *Journal of Cellular Physiology*, 208(1), 55-63.

Kassouf, N. & Thornhill, M. H. (2008) Oral cancer cell lines can use multiple ligands, including Fas-L, TRAIL and TNF-alpha, to induce apoptosis in Jurkat T cells: Possible mechanisms for immune escape by head and neck cancers. *Oral Oncology*, 44(7), 672-682.

Kato, J.*, et al* (1993) DIRECT BINDING OF CYCLIN-D TO THE RETINOBLASTOMA GENE-PRODUCT (PRB) AND PRB PHOSPHORYLATION BY THE CYCLIN D-DEPENDENT KINASE CDK4. *Genes & Development*, 7(3), 331-342.

Kavathia, N.*, et al* (2009) Serum markers of apoptosis decrease with age and cancer stage. *Aging-Us*, 1(7), 652-663.

Kawamoto, K.*, et al* (2010) Transforming growth factor beta 1 (TGF-beta 1) and rapamycin synergize to effectively suppress human T cell responses via upregulation of FoxP3(+) Tregs. *Transplant Immunology*, 23(1-2), 28-33.

Kazerounian, S.*, et al* (2008) Thrombospondins in cancer. *Cellular and Molecular Life Sciences*, 65(5), 700-712.

Keir, M. E.*, et al* (2008) PD-1 and its ligands in tolerance and immunity, *Annual Review of Immunology*. Translated from English by. Annual Review of Immunology. Palo Alto: Annual Reviews, 677-704.

Kerr, J. F. R.*, et al* (1972) Apoptosis - Basic biological phenomenon with wide-ranging implications in tissue kinetics. *British Journal of Cancer*, 26(4), 239-&.

Kesselring, R.*, et al* (2010) Human Th17 cells can be induced through head and neck cancer and have a functional impact on HNSCC development. *British Journal of Cancer*, 103(8), 1245-1254.

Kessenbrock, K.*, et al* (2010) Matrix Metalloproteinases: Regulators of the Tumor Microenvironment. *Cell*, 141(1), 52-67.

Khattri, R.*, et al* (2003) An essential role for Scurfin in CD4(+)CD25(+) T regulatory cells. *Nature Immunology*, 4(4), 337-342.

Kidd, P. (2003) Th1/Th2 balance: the hypothesis, its limitations, and implications for health and disease. *Alternative medicine review : a journal of clinical therapeutic*, 8(3), 223-46.

Kim, J. M.*, et al* (2007) Regulatory T cells prevent catastrophic autoimmunity throughout the lifespan of mice. *Nature Immunology*, 8(2), 191-197.

Kim, Y. C.*, et al* (2012) Oligodeoxynucleotides stabilize Helios-expressing Foxp3(+) human T regulatory cells during in vitro expansion. *Blood*, 119(12), 2810-2818.

Kimpfler, S.*, et al* (2009) Skin Melanoma Development in ret Transgenic Mice Despite the Depletion of CD25(+)Foxp3(+) Regulatory T Cells in Lymphoid Organs. *Journal of Immunology*, 183(10), 6330-6337.

Kimura, A. & Kishimoto, T. (2010) IL-6: Regulator of Treg/Th17 balance. *European Journal of Immunology*, 40(7), 1830-1835.

Kinoshita, T.*, et al* (2013) Forkhead box P3 regulatory T cells coexisting with cancer associated fibroblasts are correlated with a poor outcome in lung adenocarcinoma. *Cancer Science*, 104(4), 409-415.

Klein, G. (2012) Tumor resistance. *Oncoimmunology*, 1(8), 1355-1359.

Kleinewietfeld, M. & Hafler, D. A. (2013) The plasticity of human Treg and Th17 cells and its role in autoimmunity. *Seminars in Immunology*, 25(4), 305-312.

Klinger, A.*, et al* (2009) Cyclical expression of L-selectin (CD62L) by recirculating T cells. *International Immunology*, 21(4), 443-455.

Koch, M.*, et al* (2006) Tumor infiltrating T lymphocytes in colorectal cancer - Tumor-selective activation and cytotoxic activity in situ. *Annals of Surgery*, 244(6), 986-993.

Koch, M. A.*, et al* (2009) The transcription factor T-bet controls regulatory T cell homeostasis and function during type 1 inflammation. *Nature Immunology*, 10(6), 595-U57.

Kojima, A. & Prehn, R. T. (1981) Genetic susceptibility to post-thymectomy autoimmune-diseases in mice. *Immunogenetics*, 14(1-2), 15-27.

Kojima, A.*, et al* (1976) Spontaneous development of autoimmune thyroiditis in neonatally thymectomized mice. *Laboratory Investigation*, 34(6), 550-557.

Koopman, G.*, et al* (1994) Annexin-v for flow cytometric detection of phosphatidylserine expression on b-cells undergoing apoptosis. *Blood*, 84(5), 1415-1420.

Koreck, A.*, et al* (2002) CD3(+) CD56(+) NK T cells are significantly decreased in the peripheral blood of patients with psoriasis. *Clinical and Experimental Immunology*, 127(1), 176-182.

Krakauer, M.*, et al* (2006) Dynamic T-lymphocyte chemokine receptor expression induced by interferon-beta therapy in multiple sclerosis. *Scandinavian Journal of Immunology*, 64(2), 155-163.

Kushwah, R. & Hu, J. (2011) Role of dendritic cells in the induction of regulatory T cells. *Cell and Bioscience*, 1.

La Vecchia, C.*, et al* (1999) Vegetables and fruit and human cancer: Update of an Italian study. *International Journal of Cancer*, 82(1), 151-152.

Lacotte, S.*, et al* (2009) CXCR3, Inflammation, and Autoimmune Diseases. *Contemporary Challenges in Autoimmunity*, 1173, 310-317.

Lang, M. L. (2009) How do natural killer T cells help B cells? *Expert Review of Vaccines*, 8(8), 1109-1121.

Lathers, D. M. R. & Young, M. R. I. (2004) Increased aberrance of cytokine expression in plasma of patients with more advanced squamous cell carcinoma of the head and neck. *Cytokine*, 25(5), 220-228.

Lathrop, S. K.*, et al* (2008) Antigen-specific peripheral shaping of the natural regulatory T cell population. *Journal of Experimental Medicine*, 205(13), 3105-3117.

Lawrence, M. S*., et al* (2013) Mutational heterogeneity in cancer and the search for new cancer-associated genes. *Nature*, 499(7457), 214-218.

Lawson, C. & Wolf, S. (2009) ICAM-1 signaling in endothelial cells. *Pharmacological Reports*, 61(1), 22-32.

Leach, D. R*., et al* (1996) Enhancement of antitumor immunity by CTLA-4 blockade. *Science*, 271(5256), 1734-1736.

Leemans, C. R*., et al* (2011) The molecular biology of head and neck cancer. *Nature Reviews Cancer*, 11(1), 9-22.

Lehnert, C*., et al* (2014) TRAIL-Receptor Costimulation Inhibits Proximal TCR Signaling and Suppresses Human T Cell Activation and Proliferation. *Journal of Immunology*, 193(8), 4021-4031.

Leone, P*., et al* (2013) MHC Class I Antigen Processing and Presenting Machinery: Organization, Function, and Defects in Tumor Cells. *Jnci-Journal of the National Cancer Institute*, 105(16), 1172-1187.

Levi, F*., et al* (1998) Food groups and risk of oral and pharyngeal cancer. *International Journal of Cancer*, 77(5), 705-709.

Levine, A. J. (1997) p53, the cellular gatekeeper for growth and division. *Cell*, 88(3), 323-331.

Levings, M. K*., et al* (2005) Differentiation of Tr1 cells by immature dendritic cells requires IL-10 but not CD25(+)CD4(+) Tr cells. *Blood*, 105(3), 1162-1169.

Levy, L. & Hill, C. S. (2006) Alterations in components of the TGF-beta superfamily signaling pathways in human cancer. *Cytokine & Growth Factor Reviews*, 17(1-2), 41-58.

Li, K*., et al* (2015a) Impact of chemokine receptor CXCR3 on tumor-infiltrating lymphocyte recruitment associated with favorable prognosis in advanced gastric cancer. *International Journal of Clinical and Experimental Pathology*, 8(11), 14725-14732.

Li, P*., et al* (1997) Cytochrome c and dATP-dependent formation of Apaf-1/caspase-9 complex initiates an apoptotic protease cascade. *Cell*, 91(4), 479-489.

Li, R. X*., et al* (2007) Targeting antiapoptotic Bcl-2 family members with cell-permeable BH3 peptides induces apoptosis signaling and death in head and neck squamous cell carcinoma cells. *Neoplasia*, 9(10), 801-U17.

Li, X. W*., et al* (2013a) Human Papillomavirus Infection and Laryngeal Cancer Risk: A Systematic Review and Meta-Analysis. *Journal of Infectious Diseases*, 207(3), 479-488.

Li, X. Y*., et al* (2015b) The cancer-associated fibroblasts and drug resistance. *European Review for Medical and Pharmacological Sciences*, 19(11), 2112-2119.

Li, Y. Q*., et al* (2013b) Tumor Secretion of CCL22 Activates Intratumoral Treg Infiltration and Is Independent Prognostic Predictor of Breast Cancer. *Plos One*, 8(10).

Liang, B. T.*, et al* (2008) Regulatory T cells inhibit dendritic cells by lymphocyte activation gene-3 engagement of MHC class II. *Journal of Immunology*, 180(9), 5916-5926.

Liang, Y.*, et al* (2001) Apoptosis in the absence of caspase 3. *Oncogene*, 20(45), 6570-6578.

Lieberman-Blum, S. S.*, et al* (2008) Maraviroc: A CCR5-receptor antagonist for the treatment of HIV-1 infection. *Clinical Therapeutics*, 30(7), 1228-1250.

Lieberman, J. (2010) Granzyme A activates another way to die. *Immunological Reviews*, 235, 93-104.

Lievre, A.*, et al* (2006) KRAS mutation status is predictive of response to cetuximab therapy in colorectal cancer. *Cancer Research*, 66(8), 3992-3995.

Lin, J. W.*, et al* (2011) Carcinoma-associated fibroblasts promotes the proliferation of a lingual carcinoma cell line by secreting keratinocyte growth factor. *Tumor Biology*, 32(3), 597-602.

Lin, X.*, et al* (2013) Advances in distinguishing natural from induced Foxp3(+) regulatory T cells. *International Journal of Clinical and Experimental Pathology*, 6(2), 116-123.

Liu, J.*, et al* (2011) Tumor-Associated Macrophages Recruit CCR6(+) Regulatory T Cells and Promote the Development of Colorectal Cancer via Enhancing CCL20 Production in Mice. *Plos One*, 6(4).

Liu, J. Y.*, et al* (2015) CTL- vs T-reg lymphocyte-attracting chemokines, CCL4 and CCL20, are strong reciprocal predictive markers for survival of patients with oesophageal squamous cell carcinoma. *British Journal of Cancer*, 113(5), 747-755.

Liu, J. Y.*, et al* (2016) Metabolic rewiring in cancer-associated fibroblasts provides a niche for oncogenesis and metastatic dissemination. *Molecular & Cellular Oncology*, 3(1).

Liu, W.*, et al* (2006) CD127 expression inversely correlates with FoxP3 and suppressive function of human CD4(+) T reg cells. *Journal of Experimental Medicine*, 203(7), 1701-1711.

Liu, W. Y.*, et al* (1998) Fas ligand is constitutively secreted by prostate cancer cells in vitro. *Clinical Cancer Research*, 4(7), 1803-1811.

Liu, Z. Z.*, et al* (2017) The transdifferentiation of regulatory T and Th17 cells in autoimmune/inflammatory diseases and its potential implications in pregnancy complications. *American Journal of Reproductive Immunology*, 78(2).

Liyanage, U. K.*, et al* (2002) Prevalence of regulatory T cells is increased in peripheral blood and tumor microenvironment of patients with pancreas or breast adenocarcinoma. *Journal of Immunology*, 169(5), 2756-2761.

Lo, M. C.*, et al* (2013) Role of MIF/CXCL8/CXCR2 signaling in the growth of nasopharyngeal carcinoma tumor spheres. *Cancer Letters*, 335(1), 81-92.

Locksley, R. M.*, et al* (2001) The TNF and TNF receptor superfamilies: Integrating mammalian biology. *Cell*, 104(4), 487-501.

Logue, S. E. & Martin, S. J. (2008) Caspase activation cascades in apoptosis. *Biochemical Society Transactions*, 36, 1-9.

Long, S. A. & Buckner, J. H. (2008) Combination of rapamycin and IL-2 increases de novo induction of human CD4(+)CD25(+)FOXP3(+) T cells. *Journal of Autoimmunity*, 30(4), 293-302.

Louie, K. S*., et al* (2015) Trends in head and neck cancers in England from 1995 to 2011 and projections up to 2025. *Oral oncology*, 51(4), 341-8.

Lowe, S. W. & Lin, A. W. (2000) Apoptosis in cancer. *Carcinogenesis*, 21(3), 485-495.

Lowenstein, C. J*., et al* (2005) Regulation of Weibel-Palade body exocytosis. *Trends in Cardiovascular Medicine*, 15(8), 302-308.

Lu, B. F*., et al* (2004a) Kinetic analysis of genomewide gene expression reveals molecule circuitries that control T cell activation and Th1/2 differentiation. *Proceedings of the National Academy of Sciences of the United States of America*, 101(9), 3023-3028.

Lu, L*., et al* (2010a) Characterization of Protective Human CD4(+)CD25(+) FOXP3(+) Regulatory T Cells Generated with IL-2, TGF-beta and Retinoic Acid. *Plos One*, 5(12), 12.

Lu, L*., et al* (2010b) Characterization of Protective Human CD4(+)CD25(+) FOXP3(+) Regulatory T Cells Generated with IL-2, TGF-β and Retinoic Acid. *Plos One*, 5(12), 12.

Lu, S. L*., et al* (2004b) Overexpression of transforming growth factor beta 1 in head and neck epithelia results in inflammation, angiogenesis, and epithelial hyperproliferation. *Cancer Research*, 64(13), 4405-4410.

Luckheeram, R. V*., et al* (2012) CD4(+)T Cells: Differentiation and Functions. *Clinical & Developmental Immunology*.

Lukas, J*., et al* (2004) Mammalian cell cycle checkpoints: signalling pathways and their organization in space and time. *DNA Repair*, 3(8-9), 997-1007.

Lukesova, E*., et al* (2014) High level of Tregs is a positive prognostic marker in patients with HPV-positive oral and oropharyngeal squamous cell carcinomas. *BioMed research international*, 2014, 303929-303929.

Lundgren, A*., et al* (2005) Mucosal FOXP3-expressing CD4(+) CD25(high) regulatory T cells in Helicobacter pylori-infected patients. *Infection and Immunity*, 73(1), 523-531.

Lydiatt, W. M*., et al* (2017) Head and Neck Cancers-Major Changes in the American Joint Committee on Cancer Eighth Edition Cancer Staging Manual. *Ca-a Cancer Journal for Clinicians*, 67(2), 122-137.

MacDonald, K. G*., et al* (2013) Response to Comment on "Helios(+) and Helios(-) Cells Coexist within the Natural FOXP3(+) T Regulatory Cell Subset in Humans". *Journal of Immunology*, 190(9), 4440-4441.

Maggi, E. (2010) T cell responses induced by allergen-specific immunotherapy. *Clinical and Experimental Immunology*, 161(1), 10-18.

Makita, N.*, et al* (2015) IL-10 enhances the phenotype of M2 macrophages induced by IL-4 and confers the ability to increase eosinophil migration. *International Immunology*, 27(3), 131-141.

Maloy, K. J.*, et al* (2003) CD4(+)CD25(+) T-R cells suppress innate immune pathology through cytokine-dependent mechanisms. *Journal of Experimental Medicine*, 197(1), 111-119.

Mamdouh, Z.*, et al* (2003) Targeted recycling of PECAM from endothelial surface-connected compartments during diapedesis. *Nature*, 421(6924), 748-753.

Mamdouh, Z.*, et al* (2009) Transcellular migration of leukocytes is mediated by the endothelial lateral border recycling compartment. *Journal of Experimental Medicine*, 206(12), 2795-2808.

Mandal, R.*, et al* (2016) The head and neck cancer immune landscape and its immunotherapeutic implications. *Jci Insight*, 1(17).

Mandapathil, M.*, et al* (2010a) Generation and Accumulation of Immunosuppressive Adenosine by Human CD4(+)CD25(high)FOXP3(+) Regulatory T Cells. *Journal of Biological Chemistry*, 285(10), 7176-7186.

Mandapathil, M.*, et al* (2009) Isolation of functional human regulatory T cells (Treg) from the peripheral blood based on the CD39 expression. *Journal of Immunological Methods*, 346(1-2), 55-63.

Mandapathil, M.*, et al* (2012) CD26 expression and adenosine deaminase activity in regulatory T cells (Treg) and CD4(+) T effector cells in patients with head and neck squamous cell carcinoma. *Oncoimmunology*, 1(5), 659-669.

Mandapathil, M.*, et al* (2010b) Adenosine and Prostaglandin E-2 Cooperate in the Suppression of Immune Responses Mediated by Adaptive Regulatory T Cells. *Journal of Biological Chemistry*, 285(36), 27571-27580.

Mannino, M. H.*, et al* (2015) The paradoxical role of IL-10 in immunity and cancer. *Cancer Letters*, 367(2), 103-107.

Mao, F. Y.*, et al* (2017) Increased tumor-infiltrating CD45RA(-)CCR7(-) regulatory T-cell subset with immunosuppressive properties foster gastric cancer progress. *Cell Death & Disease*, 8.

Marino, G. & Kroemer, G. (2013) Mechanisms of apoptotic phosphatidylserine exposure. *Cell Research*, 23(11), 1247-1248.

Marmot, M.*, et al* (2007) Food, nutrition, physical activity, and the prevention of cancer: a global perspective.

Marrogi, A. J.*, et al* (1997) Study of tumor infiltrating lymphocytes and transforming growth factor-beta as prognostic factors in breast carcinoma. *International Journal of Cancer*, 74(5), 492-501.

Marsh, D.*, et al* (2011) Stromal features are predictive of disease mortality in oral cancer patients. *Journal of Pathology*, 223(4), 470-481.

Martin, S. J.*, et al* (1995) Early redistribution of plasma-membrane phosphatidylserine is a general feature of apoptosis regardless of the initiating stimulus - inhibition by overexpression of Bcl-2 and Abl. *Journal of Experimental Medicine*, 182(5), 1545-1556.

Martinez-Forero, I.*, et al* (2008) IL-10 suppressor activity and ex vivo Tr1 cell function are impaired in multiple sclerosis. *European Journal of Immunology*, 38(2), 576-586.

Martinez-Outschoorn, U. E.*, et al* (2011) Stromal-epithelial metabolic coupling in cancer: Integrating autophagy and metabolism in the tumor microenvironment. *International Journal of Biochemistry & Cell Biology*, 43(7), 1045-1051.

Maruyama, T.*, et al* (2010) CCL17 and CCL22 chemokines within tumor microenvironment are related to infiltration of regulatory T cells in esophageal squamous cell carcinoma. *Diseases of the Esophagus*, 23(5), 422-429.

Mascanfroni, I. D.*, et al* (2015) Metabolic control of type 1 regulatory T cell differentiation by AHR and HIF1-alpha. *Nature Medicine*, 21(6), 638-646.

Masopust, D. & Schenkel, J. M. (2013) The integration of T cell migration, differentiation and function. *Nature Reviews Immunology*, 13(5), 309-320.

Massague, J.*, et al* (2000) TGF beta signaling in growth control, cancer, and heritable disorders. *Cell*, 103(2), 295-309.

Maurya, S. S.*, et al* (2014) Polymorphisms in Drug-Metabolizing Enzymes and Risk to Head and Neck Cancer: Evidence for Gene-Gene and Gene-Environment Interaction. *Environmental and Molecular Mutagenesis*, 55(2), 134-144.

McHugh, R. S.*, et al* (2002) CD4(+)CD25(+) immunoregulatory T cells: Gene expression analysis reveals a functional role for the glucocorticoid-induced TNF receptor. *Immunity*, 16(2), 311-323.

McStay, G. P. & Green, D. R. (2014) Measuring apoptosis: caspase inhibitors and activity assays. *Cold Spring Harb Protoc*, 2014(8), 799-806.

Mehra, R.*, et al* (2008) The role of cetuximab for the treatment of squamous cell carcinoma of the head and neck. *Clinical advances in hematology & oncology : H&O*, 6(10), 742-50.

Melief, S. M.*, et al* (2013) Multipotent Stromal Cells Induce Human Regulatory T Cells Through a Novel Pathway Involving Skewing of Monocytes Toward Anti-inflammatory Macrophages. *Stem Cells*, 31(9), 1980-1991.

Messina, J. L.*, et al* (2012) 12-Chemokine Gene Signature Identifies Lymph Node-like Structures in Melanoma: Potential for Patient Selection for Immunotherapy? *Scientific Reports*, 2.

Meyer, M. S.*, et al* (2008) Human Papillomavirus-16 Modifies the Association between Fruit Consumption and Head and Neck Squam aas Cell Carcinoma. *Cancer Epidemiology Biomarkers & Prevention*, 17(12), 3419-3426.

Mikhak, Z.*, et al* (2006) STAT1 in peripheral tissue differentially regulates homing of antigen-specific Th1 and Th2 cells. *Journal of Immunology*, 176(8), 4959-4967.

Miller, A. M.*, et al* (2006) CD4(+)CD25(high) T cells are enriched in the tumor and peripheral blood of prostate cancer patients. *Journal of Immunology*, 177(10), 7398-7405.

Milpied, P.*, et al* (2009) Neuropilin-1 is not a marker of human Foxp3(+) Treg. *European Journal of Immunology*, 39(6), 1466-1471.

Miyazaki, H.*, et al* (2006) Down-regulation of CXCL5 inhibits squamous carcinogenesis. *Cancer Research*, 66(8), 4279-4284.

Mizukami, Y.*, et al* (2008a) CCL17 and CCL22 chemokines within tumor microenvironment are related to accumulation of Foxp3(+) regulatory T cells in gastric cancer. *International Journal of Cancer*, 122(10), 2286-2293.

Mizukami, Y.*, et al* (2008b) Localisation pattern of Foxp3(+) regulatory T cells is associated with clinical behaviour in gastric cancer. *British Journal of Cancer*, 98(1), 148-153.

Moncrieffe, H.*, et al* (2010) High Expression of the Ectonucleotidase CD39 on T Cells from the Inflamed Site Identifies Two Distinct Populations, One Regulatory and One Memory T Cell Population. *Journal of Immunology*, 185(1), 134-143.

Montecucco, A.*, et al* (2015) MOLECULAR MECHANISMS OF ETOPOSIDE. *Excli Journal*, 14, 95-108.

Moore, K. L. (1998) Structure and function of P-selectin Glycoprotein ligand-1. *Leukemia & Lymphoma*, 29(1-2), 1-15.

Morbini, P. & Benazzo, M. (2016) Human papillomavirus and head and neck carcinomas: focus on evidence in the babel of published data. *Acta Otorhinolaryngologica Italica*, 36(4), 249-258.

Mori, K.*, et al* (2011) Infiltration of m2 tumor-associated macrophages in oral squamous cell carcinoma correlates with tumor malignancy. *Cancers*, 3(4), 3726-39.

Moser, B. & Willimann, K. (2004) Chemokines: role in inflammation and immune surveillance. *Annals of the Rheumatic Diseases*, 63, 84-89.

Motz, K.*, et al* (2016) Changes in Unknown Primary Squamous Cell Carcinoma of the Head and Neck at Initial Presentation in the Era of Human Papillomavirus. *Jama Otolaryngology-Head & Neck Surgery*, 142(3), 223-228.

Motzer, R. J.*, et al* (2015) Nivolumab versus Everolimus in Advanced Renal-Cell Carcinoma. *New England Journal of Medicine*, 373(19), 1803-1813.

Muller, T.*, et al* (2017) PD-L1: a novel prognostic biomarker in head and neck squamous cell carcinoma. *Oncotarget*, 8(32), 52889-52900.

Muller, W. A. (2011) Mechanisms of Leukocyte Transendothelial Migration. *Annual Review of Pathology: Mechanisms of Disease, Vol 6*, 6, 323-344.

Muller, W. A. (2016) Transendothelial migration: unifying principles from the endothelial perspective. *Immunological Reviews*, 273(1), 61-75.

Munger, K.*, et al* (1989) THE E6-GENE AND E7-GENE OF THE HUMAN PAPILLOMAVIRUS TYPE-16 TOGETHER ARE NECESSARY AND SUFFICIENT FOR TRANSFORMATION OF PRIMARY HUMAN KERATINOCYTES. *Journal of Virology*, 63(10), 4417-4421.

Muranski, P. & Restifo, N. P. (2013) Essentials of Th17 cell commitment and plasticity. *Blood*, 121(13), 2402-2414.

Murphy, K. (2017) Janeway's Immunobiology. *In:* Weaver, C. (ed.) 9th ed. New York, USA: Garland Science.

Naito, Y.*, et al* (1998) CD8(+) T cells infiltrated within cancer cell nests as a prognostic factor in human colorectal cancer. *Cancer Research*, 58(16), 3491-3494.

Nakano, O.*, et al* (2001) Proliferative activity of intratumoral CD8(+) T-lymphocytes as a prognostic factor in human renal cell carcinoma: Clinicopathologic demonstration of antitumor immunity. *Cancer Research*, 61(13), 5132-5136.

Namazie, A.*, et al* (2002) Cyclin D1 amplification and p16(MTS1/CDK4I) deletion correlate with poor prognosis in head and neck tumors. *Laryngoscope*, 112(3), 472-481.

Narisawa-Saito, M. & Kiyono, T. (2007) Basic mechanisms of high-risk human papillomavirus-induced carcinogenesis: Roles of E6 and E7 proteins. *Cancer Science*, 98(10), 1505-1511.

Nasman, A.*, et al* (2012) Tumor Infiltrating CD8(+) and Foxp3(+) Lymphocytes Correlate to Clinical Outcome and Human Papillomavirus (HPV) Status in Tonsillar Cancer. *Plos One*, 7(6).

Nassari, S.*, et al* (2017) The chemokines CXCL12 and CXCL14 differentially regulate connective tissue markers during limb development. *Scientific Reports*, 7.

Negri, E.*, et al* (2009) Family history of cancer: Pooled analysis in the International Head and Neck Cancer Epidemiology consortium. *International Journal of Cancer*, 124(2), 394-401.

Nevins, J. R. (2001) The Rb/E2F pathway and cancer. *Human Molecular Genetics*, 10(7), 699-703.

NICE (2016) Cancer of the upper aerodigestive tract: act: assessment and management in people assessment and management in people aged 16 and o aged 16 and ov ver *NICE guideline*.

Nieto, J. C.*, et al* (2012) Selective Loss of Chemokine Receptor Expression on Leukocytes after Cell Isolation. *Plos One*, 7(3).

Nizzoli, G.*, et al* (2016) IL-10 promotes homeostatic proliferation of human CD8(+) memory T cells and, when produced by CD1c(+) DCs, shapes naive CD8(+) T-cell priming. *Eur J Immunol*, 46(7), 1622-32.

Nordfors, C.*, et al* (2013) CD8(+) and CD4(+) tumour infiltrating lymphocytes in relation to human papillomavirus status and clinical outcome in tonsillar and base of tongue squamous cell carcinoma. *European Journal of Cancer*, 49(11), 2522-2530.

O'Garra, A.*, et al* (1998) T-cell subsets: Chemokine receptors guide the way. *Current Biology*, 8(18), R646-R649.

Oliveira-Neto, H. H.*, et al* (2013) The expression of chemokines CCL19, CCL21 and their receptor CCR7 in oral squamous cell carcinoma and its relevance to cervical lymph node metastasis. *Tumor Biology*, 34(1), 65-70.

Ondondo, B.*, et al* (2015) A distinct chemokine axis does not account for enrichment of Foxp3(+) CD4(+) T cells in carcinogen-induced fibrosarcomas. *Immunology*, 145(1), 94-104.

Onizuka, S.*, et al* (1999) Tumor rejection by in vivo administration of anti-CD25 (interleukin-2 receptor alpha) monoclonal antibody. *Cancer Research*, 59(13), 3128-3133.

Orimo, A. & Weinberg, R. A. (2007) Heterogeneity of stromal fibroblasts in tumors. *Cancer Biology & Therapy*, 6(4), 618-619.

Otranto, M.*, et al* (2012) The role of the myofibroblast in tumor stroma remodeling. *Cell Adhesion & Migration*, 6(3), 203-219.

Owonikoko, T. K.*, et al* (2013) Soluble FAS ligand as a biomarker of disease recurrence in differentiated thyroid cancer. *Cancer*, 119(8), 1503-1511.

Pacholczyk, R. & Kern, J. (2008) The T-cell receptor repertoire of regulatory T cells. *Immunology*, 125(4), 450-458.

Pai, S. I.*, et al* (2017) A retrospective cohort study of PD-L1 expression in recurrent and/or metastatic squamous cell carcinoma of the head and neck (SUPREME-HN). *Journal of Clinical Oncology*, 35.

Pandiyan, P.*, et al* (2007) CD4(+) CD25(+) Foxp3(+) regulatory T cells induce cytokine deprivation - mediated apoptosis of effector CD4(+) T cells. *Nature Immunology*, 8(12), 1353-1362.

Panther, E.*, et al* (2003) Adenosine affects expression of membrane molecules, cytokine and chemokine release, and the T-cell stimulatory capacity of human dendritic cells. *Blood*, 101(10), 3985-3990.

Parish, C. R. (1999) Fluorescent dyes for lymphocyte migration and proliferation studies. *Immunology and Cell Biology*, 77(6), 499-508.

Parsonage, G.*, et al* (2012) CXCR6 and CCR5 Localize T Lymphocyte Subsets in Nasopharyngeal Carcinoma. *American Journal of Pathology*, 180(3), 1215-1222.

Partlova, S.*, et al* (2015) Distinct patterns of intratumoral immune cell infiltrates in patients with HPV-associated compared to non-virally induced head and neck squamous cell carcinoma. *Oncoimmunology*, 4(1).

Passerini, L.*, et al* (2011) Functional type 1 regulatory T cells develop regardless of FOXP3 mutations in patients with IPEX syndrome. *European Journal of Immunology*, 41(4), 1120-1131.

Pease, J. E. & Williams, T. J. (2006) The attraction of chemokines as a target for specific anti-inflammatory therapy. *British Journal of Pharmacology*, 147, S212-S221.

Peggs, K. S., *et al* (2009) Blockade of CTLA-4 on both effector and regulatory T cell compartments contributes to the antitumor activity of anti-CTLA-4 antibodies. *Journal of Experimental Medicine*, 206(8), 1717-1725.

Pelucchi, C., *et al* (2006) Cancer risk associated with alcohol and tobacco use: Focus on upper aero-digestive tract and liver. *Alcohol Research & Health*, 29(3), 193-198.

Peters, E. S., *et al* (2008) Dairy products, leanness, and head and neck squamous cell carcinoma. *Head and Neck-Journal for the Sciences and Specialties of the Head and Neck*, 30(9), 1193-1205.

Peto, J., *et al* (2004) The cervical cancer epidemic that screening has prevented in the UK. *Lancet*, 364(9430), 249-256.

Pickup, M., *et al* (2013) The roles of TGF beta in the tumour microenvironment. *Nature Reviews Cancer*, 13(11), 788-799.

Piek, E., *et al* (1999) Specificity, diversity, and regulation in TGF-beta superfamily signaling. *Faseb Journal*, 13(15), 2105-2124.

Pignon, J. P., *et al* (2009) Meta-analysis of chemotherapy in head and neck cancer (MACH-NC): An update on 93 randomised trials and 17,346 patients. *Radiotherapy and Oncology*, 92(1), 4-14.

Pillai, V., *et al* (2007) Transient regulatory T-cells: A state attained by all activated human T-cells. *Clinical Immunology*, 123(1), 18-29.

Pinna, A. (2014) Adenosine A(2A) Receptor Antagonists in Parkinson's Disease: Progress in Clinical Trials from the Newly Approved Istradefylline to Drugs in Early Development and Those Already Discontinued. *Cns Drugs*, 28(5), 455-474.

Poeta, M. L., *et al* (2007) TP53 mutations and survival in squamous-cell carcinoma of the head and neck. *New England Journal of Medicine*, 357(25), 2552-2561.

Postow, M. A., *et al* (2015) Immune Checkpoint Blockade in Cancer Therapy. *Journal of Clinical Oncology*, 33(17), 1974-U161.

Pot, C., *et al* (2009) Cutting Edge: IL-27 Induces the Transcription Factor c-Maf, Cytokine IL-21, and the Costimulatory Receptor ICOS that Coordinately Act Together to Promote Differentiation of IL-10-Producing Tr1 Cells. *Journal of Immunology*, 183(2), 797-801.

Powrie, F. & Mason, D. (1990) OX-22HIGH CD4+ T-CELLS INDUCE WASTING DISEASE WITH MULTIPLE ORGAN PATHOLOGY - PREVENTION BY THE OX-22LOW SUBSET. *Journal of Experimental Medicine*, 172(6), 1701-1708.

Pretscher, D., *et al* (2009) Distribution of immune cells in head and neck cancer: CD8(+) T-cells and CD20(+) B-cells in metastatic lymph nodes are associated with favourable outcome in patients with oro- and hypopharyngeal carcinoma. *Bmc Cancer*, 9.

Protti, M. P., *et al* (2014) Tumor antigen-specific CD4(+) T cells in cancer immunity: from antigen identification to tumor prognosis and development of therapeutic strategies. *Tissue Antigens*, 83(4), 237-246.

Qureshi, O. S*., et al* (2011) Trans-Endocytosis of CD80 and CD86: A Molecular Basis for the Cell-Extrinsic Function of CTLA-4. *Science*, 332(6029), 600-603.

Raker, V. K*., et al* (2015) Tolerogenic Dendritic Cells for Regulatory T Cell Induction in Man. *Frontiers in Immunology*, 6.

Rave-Frank, M*., et al* (2016) Prognostic value of CXCL12 and CXCR4 in inoperable head and neck squamous cell carcinoma. *Strahlentherapie Und Onkologie*, 192(1), 47-54.

Read, S*., et al* (2000) Cytotoxic T lymphocyte-associated antigen 4 plays an essential role in the function of CD25(+)CD4(+) regulatory cells that control intestinal inflammation. *Journal of Experimental Medicine*, 192(2), 295-302.

Redjimi, N*., et al* (2012) CXCR3(+) T Regulatory Cells Selectively Accumulate in Human Ovarian Carcinomas to Limit Type I Immunity. *Cancer Research*, 72(17), 4351-4360.

Refaeli, Y*., et al* (1998) Biochemical mechanisms of IL-2-regulated Fas-mediated T cell apoptosis. *Immunity*, 8(5), 615-623.

Reichert, T. E*., et al* (1998) Mechanisms responsible for signaling and functional defects. *Journal of Immunotherapy*, 21(4), 295-306.

Rentoft, M*., et al* (2014) Expression of CXCL10 is associated with response to radiotherapy and overall survival in squamous cell carcinoma of the tongue. *Tumor Biology*, 35(5), 4191-4198.

Revzina, N. V. & DiClemente, R. J. (2005) Prevalence and incidence of human papillomavirus infection in women in the USA: a systematic review. *International Journal of Std & Aids*, 16(8), 528-537.

Riis, J. L*., et al* (2011) Kinetics and differential expression of the skin-related chemokines CCL27 and CCL17 in psoriasis, atopic dermatitis and allergic contact dermatitis. *Experimental Dermatology*, 20(10), 789-794.

Ring, S*., et al* (2015) Regulatory T Cell-Derived Adenosine Induces Dendritic Cell Migration through the Epac-Rap1 Pathway. *Journal of Immunology*, 194(8), 3735-3744.

Rizvi, N. A*., et al* (2015) Mutational landscape determines sensitivity to PD-1 blockade in non-small cell lung cancer. *Science*, 348(6230), 124-128.

Robert, C*., et al* (2015) Nivolumab in Previously Untreated Melanoma without BRAF Mutation. *New England Journal of Medicine*, 372(4), 320-330.

Roberts, A. B*., et al* (1986) TRANSFORMING GROWTH-FACTOR TYPE-BETA - RAPID INDUCTION OF FIBROSIS AND ANGIOGENESIS INVIVO AND STIMULATION OF COLLAGEN FORMATION INVITRO. *Proceedings of the National Academy of Sciences of the United States of America*, 83(12), 4167-4171.

Roberts, A. D*., et al* (2005) Differential contributions of central and effector memory T cells to recall responses. *Journal of Experimental Medicine*, 202(1), 123-133.

Rock, K. L. & Shen, L. (2005) Cross-presentation: underlying mechanisms and role in immune surveillance. *Immunological Reviews*, 207, 166-183.

Roncarolo, M. G., *et al* (2006) Interleukin-10-secreting type 1 regulatory T cells in rodents and humans. *Immunological Reviews*, 212, 28-50.

Ronchetti, S., *et al* (2015) Glucocorticoid-Induced Tumour Necrosis Factor Receptor-Related Protein: A Key Marker of Functional Regulatory T Cells. *Journal of Immunology Research*.

Rosenberg, S. A. (2014) IL-2: The First Effective Immunotherapy for Human Cancer. *Journal of Immunology*, 192(12), 5451-5458.

Rosenberg, S. A., *et al* (2004) Cancer immunotherapy: moving beyond current vaccines. *Nature Medicine*, 10(9), 909-915.

Rosenthal, E., *et al* (2004) Elevated expression of TGF-beta 1 in head and neck cancer - Associated fibroblasts. *Molecular Carcinogenesis*, 40(2), 116-121.

Rothenberg, S. M. & Ellisen, L. W. (2012) The molecular pathogenesis of head and neck squamous cell carcinoma. *Journal of Clinical Investigation*, 122(6), 1951-1957.

Rouvier, E., *et al* (1993) FAS INVOLVEMENT IN CA2+-INDEPENDENT T-CELL-MEDIATED CYTOTOXICITY. *Journal of Experimental Medicine*, 177(1), 195-200.

Russell, S., *et al* (2013) Immune cell infiltration patterns and survival in head and neck squamous cell carcinoma. *Head & neck oncology*, 5(3), 24.

Russo, R. C., *et al* (2014) The CXCL8/IL-8 chemokine family and its receptors in inflammatory diseases. *Expert Review of Clinical Immunology*, 10(5), 593-619.

Ruwali, M., *et al* (2009) Cytochrome P450 2E1 and Head and Neck Cancer: Interaction With Genetic and Environmental Risk Factors. *Environmental and Molecular Mutagenesis*, 50(6), 473-482.

Saito, T., *et al* (1999) Spontaneous ex vivo apoptosis of peripheral blood mononuclear cells in patients with head and neck cancer. *Clinical Cancer Research*, 5(6), 1263-1273.

Sakaguchi, K., *et al* (1998) DNA damage activates p53 through a phosphorylation-acetylation cascade. *Genes & Development*, 12(18), 2831-2841.

Sakaguchi, S., *et al* (1985) ORGAN-SPECIFIC AUTOIMMUNE-DISEASES INDUCED IN MICE BY ELIMINATION OF T-CELL SUBSET .1. EVIDENCE FOR THE ACTIVE PARTICIPATION OF T-CELLS IN NATURAL SELF-TOLERANCE - DEFICIT OF A T-CELL SUBSET AS A POSSIBLE CAUSE OF AUTOIMMUNE-DISEASE. *Journal of Experimental Medicine*, 161(1), 72-87.

Sakaguchi, S., *et al* (1995) IMMUNOLOGICAL SELF-TOLERANCE MAINTAINED BY ACTIVATED T-CELLS EXPRESSING IL-2 RECEPTOR ALPHA-CHAINS (CD25) - BREAKDOWN OF A SINGLE MECHANISM OF SELF-TOLERANCE CAUSES VARIOUS AUTOIMMUNE-DISEASES. *Journal of Immunology*, 155(3), 1151-1164.

Salama, P., *et al* (2009) Tumor-Infiltrating FOXP3(+) T Regulatory Cells Show Strong Prognostic Significance in Colorectal Cancer. *Journal of Clinical Oncology*, 27(2), 186-+.

Salgado, F. J*., et al* (2012) CD26: A negative selection marker for human Treg cells. *Cytometry Part A*, 81A(10), 843-855.

Sallusto, F*., et al* (1999) Two subsets of memory T lymphocytes with distinct homing potentials and effector functions. *Nature*, 401(6754), 708-712.

Saloura, V*., et al* (2014) Correlation of T-cell inflamed phenotype with mesenchymal subtype, expression of PD-L1, and other immune checkpoints in head and neck cancer. *Journal of Clinical Oncology*, 32(15).

Sanderson, R. J. & Ironside, J. A. D. (2002) Squamous cell carcinomas of the head and neck. *British Medical Journal*, 325(7368), 822-827.

Sanjabi, S*., et al* (2009) Anti-inflammatory and pro-inflammatory roles of TGF-beta, IL-10, and IL-22 in immunity and autoimmunity. *Current Opinion in Pharmacology*, 9(4), 447-453.

Saraste, A. & Pulkki, K. (2000) Morphologic and biochemical hallmarks of apoptosis. *Cardiovascular Research*, 45(3), 528-537.

Sato, H*., et al* (2009) Altered expression of glycoproteins on the cell surface of Jurkat cells during etoposide-induced apoptosis: Shedding and intracellular translocation of glycoproteins. *Biochimica Et Biophysica Acta-General Subjects*, 1790(10), 1198-1205.

Sato, M*., et al* (2000) Genetically high susceptibility to oral squamous cell carcinoma in terms of combined genotyping of CYP1A1 and GSTM1 genes. *Oral Oncology*, 36(3), 267-271.

Sattui, S*., et al* (2012) Cryopreservation modulates the detection of regulatory T cell markers. *Cytometry Part B-Clinical Cytometry*, 82B(1), 54-58.

Savage, P. A*., et al* (2014) Shaping the repertoire of tumor-infiltrating effector and regulatory T cells. *Immunological Reviews*, 259(1), 245-258.

Schleimer, R. P*., et al* (1992) IL-4 induces adherence of human eosinophils and basophils but not neutrophils to endothelium. Association with expression of VCAM-1. *The Journal of Immunology*, 148(4), 1086-1092.

Schmidt, A*., et al* (2016a) Comparative Analysis of Protocols to Induce Human CD4+Foxp3+ Regulatory T Cells by Combinations of IL-2, TGF-beta, Retinoic Acid, Rapamycin and Butyrate. *PLoS One*, 11(2), e0148474.

Schmidt, A*., et al* (2016b) Human macrophages induce CD4(+)Foxp3(+) regulatory T cells via binding and re-release of TGF-beta. *Immunology and Cell Biology*, 94(8), 747-762.

Schmitt, C. A. & Lowe, S. W. (1999) Apoptosis and therapy. *Journal of Pathology*, 187(1), 127-137.

Scholten, D. J*., et al* (2012) Pharmacological modulation of chemokine receptor function. *British Journal of Pharmacology*, 165(6), 1617-1643.

Schott, A. K*., et al* (2010) Permanent up-regulation of regulatory T-lymphocytes in patients with head and neck cancer. *International Journal of Molecular Medicine*, 26(1), 67-75.

Schuler, P. J., *et al* (2013) Effects of Adjuvant Chemoradiotherapy on the Frequency and Function of Regulatory T Cells in Patients with Head and Neck Cancer. *Clinical Cancer Research*, 19(23), 6585-6596.

Schuler, P. J., *et al* (2014) Human CD4(+)CD39(+) regulatory T cells produce adenosine upon co-expression of surface CD73 or contact with CD73(+) exosomes or CD73(+) cells. *Clinical and Experimental Immunology*, 177(2), 531-543.

Schuler, P. J., *et al* (2012) Phenotypic and functional characteristics of CD4(+)CD39(+)FOXP3(+) and CD4(+)CD39(+)FOXP3(neg) T-cell subsets in cancer patients. *European Journal of Immunology*, 42(7), 1876-1885.

Schumacher, K., *et al* (2001) Prognostic significance of activated CD8(+) T cell infiltrations within esophageal carcinomas. *Cancer Research*, 61(10), 3932-3936.

Sedger, L. M., *et al* (2010) Extreme lymphoproliferative disease and fatal autoimmune thrombocytopenia in FasL and TRAIL double-deficient mice. *Blood*, 115(16), 3258-3268.

Seitz, H. K. & Stickel, F. (2007) Molecular mechanisms of alcohol-mediated carcinogenesis. *Nature Reviews Cancer*, 7(8), 599-612.

Seiwert, T. Y., *et al* (2007a) The chemoradiation paradigm in head and neck cancer. *Nature Clinical Practice Oncology*, 4(3), 156-171.

Seiwert, T. Y., *et al* (2007b) The concurrent chemoradiation paradigm - general principles. *Nature Clinical Practice Oncology*, 4(2), 86-100.

Shang, B., *et al* (2015) Prognostic value of tumor-infiltrating FoxP3(+) regulatory T cells in cancers: a systematic review and meta-analysis. *Scientific Reports*, 5.

Sharma, H., *et al* (2005) Antisense-mediated downregulation of anti-apoptotic proteins induces apoptosis and sensitizes head and neck squamous cell carcinoma cells to chemotherapy. *Cancer Biology & Therapy*, 4(7), 720-727.

Shevach, E. M. & Thornton, A. M. (2014) tTregs, pTregs, and iTregs: similarities and differences. *Immunological Reviews*, 259(1), 88-102.

Shiboski, C. H., *et al* (2005) Tongue and tonsil carcinoma - Increasing trends in the US population ages 20-44 years. *Cancer*, 103(9), 1843-1849.

Shields, J. D., *et al* (2010) Induction of Lymphoidlike Stroma and Immune Escape by Tumors That Express the Chemokine CCL21. *Science*, 328(5979), 749-752.

Shiga, K., *et al* (2015) Cancer-Associated Fibroblasts: Their Characteristics and Their ole in Tumor Growth. Cancers.

Shimizu, J., *et al* (1999) Induction of tumor immunity by removing CD25(+)CD4(+) T cells: A common basis between tumor immunity and autoimmunity. *Journal of Immunology*, 163(10), 5211-5218.

Shintani, S., *et al* (2001) Inactivation of the p14(ARF), p15(INK4B) and p16(INK4A) genes is a frequent event in human oral squamous cell carcinomas. *Oral Oncology*, 37(6), 498-504.

Shiow, L. R., *et al* (2006) CD69 acts downstream of interferon-alpha/beta to inhibit S1P(1) and lymphocyte egress from lymphoid organs. *Nature*, 440(7083), 540-544.

Silva, T. A., *et al* (2007) Dual role of CCL3/CCR1 in oral squamous cell carcinoma: Implications in tumor metastasis and local host defense. *Oncology Reports*, 18(5), 1107-1113.

Smeets, S. J., *et al* (2006) Genome-wide DNA copy number alterations in head and neck squamous cell carcinomas with or without oncogene-expressing human papillomavirus. *Oncogene*, 25(17), 2558-2564.

Smith, H., *et al* (1991) EFFECTOR AND REGULATORY CELLS IN AUTOIMMUNE OOPHORITIS ELICITED BY NEONATAL THYMECTOMY. *Journal of Immunology*, 147(9), 2928-2933.

Smith, J. D. (2016) *The effect of HNSCC-derived soluble factors on the proliferation and function of immune cells*. PhD 312. The University of Hull, February 2016.

Smyth, M. J., *et al* (2006) CD4(+)-CD25(+) T regulatory cells suppress NK cell-mediated immunotherapy of cancer. *Journal of Immunology*, 176(3), 1582-1587.

Snijders, P. J. F., *et al* (2006) HPV-mediated cervical carcinogenesis: concepts and clinical implications. *Journal of Pathology*, 208(2), 152-164.

Somers, W. S., *et al* (2000) Insights into the molecular basis of leukocyte tethering and rolling revealed by structures of P- and E-selectin bound to SLe(X) and PSGL-1. *Cell*, 103(3), 467-479.

Song, E., *et al* (2001) Soluble Fas ligand released by colon adenocarcinoma cells induces host lymphocyte apoptosis: an active mode of immune evasion in colon cancer. *British Journal of Cancer*, 85(7), 1047-1054.

Sparano, A., *et al* (2004) Modulation of Th1 and Th2 cytokine profiles and their association with advanced head and neck squamous cell carcinoma. *Otolaryngology-Head and Neck Surgery*, 131(5), 573-576.

Spertini, O., *et al* (1996) P-selectin glycoprotein ligand 1 is a ligand for L-selectin on neutrophils, monocytes, and CD34(+) hematopoietic progenitor cells. *Journal of Cell Biology*, 135(2), 523-531.

Spranger, S., *et al* (2013) Up-Regulation of PD-L1, IDO, and T-regs in the Melanoma Tumor Microenvironment Is Driven by CD8(+) T Cells. *Science Translational Medicine*, 5(200).

Srinivasula, S. M., *et al* (1998) Autoactivation of procaspase-9 by Apaf-1-mediated oligomerization. *Molecular Cell*, 1(7), 949-957.

Stover, D. G., *et al* (2007) A delicate balance: TGF-beta and the tumor microenvironment. *Journal of Cellular Biochemistry*, 101(4), 851-861.

Strauss, L., *et al* (2007a) The frequency and suppressor function of CD4(+)CD25(high) Foxp3(+) T cells in the circulation of patients with squamous cell carcinoma of the head and neck. *Clinical Cancer Research*, 13(21), 6301-6311.

Strauss, L.*, et al* (2007b) A unique subset of CD4(+)CD25(high) Foxp3(+) T cells secreting interleukin-10 and transforming growth factor-beta 1 mediates suppression in the tumor microenvironment. *Clinical Cancer Research*, 13(15), 4345-4354.

Strauss, L.*, et al* (2009) Human Circulating CD4(+)CD25(high)Foxp3(+) Regulatory T Cells Kill Autologous CD8(+) but Not CD4(+) Responder Cells by Fas-Mediated Apoptosis. *Journal of Immunology*, 182(3), 1469-1480.

Sturgis, E. M. & Cinciripini, P. M. (2007) Trends in head and neck cancer incidence in relation to smoking prevalence - An emerging epidemic of human papillomavirus-associated cancers? *Cancer*, 110(7), 1429-1435.

Sun, D. S.*, et al* (2012) The correlation between tumor-infiltrating Foxp3+regulatory T cells and cyclooxygenase-2 expression and their association with recurrence in resected head and neck cancers. *Medical Oncology*, 29(2), 707-713.

Sun, W.*, et al* (2014) CD45RA(-)Foxp3(high) but not CD45RA(+) Foxp3(low) suppressive T regulatory cells increased in the peripheral circulation of patients with head and neck squamous cell carcinoma and correlated with tumor progression. *Journal of Experimental & Clinical Cancer Research*, 33.

Sun, W.*, et al* (2015) Functionally distinct subsets of CD4(+) regulatory T cells in patients with laryngeal squamous cell carcinoma are indicative of immune deregulation and disease progression. *Oncology Reports*, 33(1), 354-362.

Sun, W.*, et al* (2017) A positive-feedback loop between tumour infiltrating activated Treg cells and type 2-skewed macrophages is essential for progression of laryngeal squamous cell carcinoma. *British Journal of Cancer*, 117(11), 1631-1643.

Szajnik, M.*, et al* (2010) Tumor-Derived Microvesicles Induce, Expand and Up-Regulate Biological Activities of Human Regulatory T Cells (Treg). *Plos One*, 5(7).

Tabarkiewicz, J.*, et al* (2015) The Role of IL-17 and Th17 Lymphocytes in Autoimmune Diseases. *Archivum Immunologiae Et Therapiae Experimentalis*, 63(6), 435-449.

Taguchi, O.*, et al* (1980) AUTOIMMUNE OOPHORITIS IN THYMECTOMIZED MICE - DETECTION OF CIRCULATING ANTIBODIES AGAINST OOCYTES. *Clinical and Experimental Immunology*, 40(3), 540-553.

Takaba, H. & Takayanagi, H. (2017) The Mechanisms of T Cell Selection in the Thymus. *Trends Immunol*, 38(11), 805-816.

Takahashi, H.*, et al* (2015) Immunosuppressive activity of cancer-associated fibroblasts in head and neck squamous cell carcinoma. *Cancer Immunology Immunotherapy*, 64(11), 1407-1417.

Takahashi, T.*, et al* (1998) Immunologic self-tolerance maintained by CD25(+)CD4(+) naturally anergic and suppressive T cells: induction of autoimmune disease by breaking their anergic/suppressive state. *International Immunology*, 10(12), 1969-1980.

Takahashi, T.*, et al* (2000) Immunologic self-tolerance maintained by CD25(+)CD4(+) regulatory T cells constitutively expressing cytotoxic T lymphocyte-associated antigen 4. *Journal of Experimental Medicine*, 192(2), 303-309.

Takata, H.*, et al* (2004) Cutting edge: Expression of chemokine receptor CXCR1 on human effector CD8(+) T cells. *Journal of Immunology*, 173(4), 2231-2235.

Talhout, R.*, et al* (2011) Hazardous Compounds in Tobacco Smoke. *International Journal of Environmental Research and Public Health*, 8(2), 613-628.

Tan, M. C. B.*, et al* (2009) Disruption of CCR5-Dependent Homing of Regulatory T Cells Inhibits Tumor Growth in a Murine Model of Pancreatic Cancer. *Journal of Immunology*, 182(3), 1746-1755.

Tanaka, M.*, et al* (1998) Downregulation of Fas ligand by shedding. *Nature Medicine*, 4(1), 31-36.

Tanaka, M.*, et al* (1996) Fas ligand in human serum. *Nature Medicine*, 2(3), 317-322.

Tanaka, Y. (2000) Integrin activation by chemokines: Relevance to inflammatory adhesion cascade during T cell migration. *Histology and Histopathology*, 15(4), 1169-1176.

Tanaka, Y. (2001) The role of chemokines and adhesion molecules in the pathogenesis of rheumatoid arthritis. *Drugs of Today*, 37(7), 477-484.

Tang, Q. Z.*, et al* (2004) In vitro-expanded antigen-specific regulatory T cells suppress autoimmune diabetes. *Journal of Experimental Medicine*, 199(11), 1455-1465.

Thibult, M. L.*, et al* (2013) PD-1 is a novel regulator of human B-cell activation. *International Immunology*, 25(2), 129-+.

Thompson, E. D.*, et al* (2010) Tumor masses support naive T cell infiltration, activation, and differentiation into effectors. *Journal of Experimental Medicine*, 207(8), 1791-1804.

Thornton, A. M.*, et al* (2010) Expression of Helios, an Ikaros transcription factor family member, differentiates thymic-derived from peripherally induced Foxp3+ T regulatory cells. *The Journal of Immunology*, 184(7), 3433-3441.

Thornton, A. M. & Shevach, E. M. (1998) CD4(+)CD25(+) immunoregulatory T cells suppress polyclonal T cell activation in vitro by inhibiting interleukin 2 production. *Journal of Experimental Medicine*, 188(2), 287-296.

Torre, L. A.*, et al* (2015) Global Cancer Statistics, 2012. *Ca-a Cancer Journal for Clinicians*, 65(2), 87-108.

Torres-Aguilar, H.*, et al* (2010) Tolerogenic Dendritic Cells Generated With Different Immunosuppressive Cytokines Induce Antigen-Specific Anergy and Regulatory Properties in Memory CD4(+) T Cells. *Journal of Immunology*, 184(4), 1765-1775.

Tran, D. Q.*, et al* (2009) Selective expression of latency-associated peptide (LAP) and IL-1 receptor type I/II (CD121a/CD121b) on activated human FOXP3(+) regulatory T cells allows for their purification from expansion cultures. *Blood*, 113(21), 5125-5133.

Tran, D. Q*., et al* (2007) Induction of FOXP3 expression in naive human CD4(+)FOXP3(-) T cells by T-cell receptor stimulation is transforming growth factor-beta-dependent but does not confer a regulatory phenotype. *Blood*, 110(8), 2983-2990.

Trask, D. K*., et al* (2002) Expression of Bcl-2 family proteins in advanced laryngeal squamous cell carcinoma: Correlation with response to chemotherapy and organ preservation. *Laryngoscope*, 112(4), 638-644.

Travis, M. A*., et al* (2007) Loss of integrin alpha(v)beta(8) on dendritic cells causes autoimmunity and colitis in mice. *Nature*, 449(7160), 361-+.

Trellakis, S*., et al* (2011) Polymorphonuclear granulocytes in human head and neck cancer: enhanced inflammatory activity, modulation by cancer cells and expansion in advanced disease. *International Journal of Cancer*, 129(9), 2183-2193.

Trimble, C. L*., et al* (2005) Spontaneous regression of high-grade cervical dysplasia: Effects of human papillomavirus type and HLA phenotype. *Clinical Cancer Research*, 11(13), 4717-4723.

Tung, K. S. K*., et al* (1987) MURINE AUTOIMMUNE OOPHORITIS, EPIDIDYMOORCHITIS, AND GASTRITIS INDUCED BY DAY-3 THYMECTOMY - IMMUNOPATHOLOGY. *American Journal of Pathology*, 126(2), 293-302.

Turner, M. D*., et al* (2014) Cytokines and chemokines: At the crossroads of cell signalling and inflammatory disease. *Biochimica Et Biophysica Acta-Molecular Cell Research*, 1843(11), 2563-2582.

Turowski, P*., et al* (2008) Phosphorylation of vascular endothelial cadherin controls lymphocyte emigration. *Journal of Cell Science*, 121(1), 29-37.

Ueda, M*., et al* (2010) Expression of CC-chemokine receptor 7 (CCR7) and CXC-chemokine receptor 4 (CXCR4) in head and neck squamous cell carcinoma. *Auris Nasus Larynx*, 37(4), 488-495.

Valmori, D*., et al* (2006) Rapamycin-mediated enrichment of T cells with regulatory activity in stimulated CD4(+) T cell cultures is not due to the selective expansion of naturally occurring regulatory T cells but to the induction of regulatory functions in conventional CD4(+) T cells. *Journal of Immunology*, 177(2), 944-949.

Van Allen, E. M*., et al* (2015) Genomic correlates of response to CTLA-4 blockade in metastatic melanoma. *Science*, 350(6257), 207-211.

van der Burg, S. H*., et al* (2016) Vaccines for established cancer: overcoming the challenges posed by immune evasion. *Nature Reviews Cancer*, 16(4), 219-233.

van Elsas, A*., et al* (1999) Combination immunotherapy of B16 melanoma using anti-cytotoxic T lymphocyte-associated antigen 4 (CTLA-4) and granulocyte/macrophage colony-stimulating factor (GM-CSF)-producing vaccines induces rejection of subcutaneous and metastatic tumors accompanied by autoimmune depigmentation. *Journal of Experimental Medicine*, 190(3), 355-366.

Van Hemelen, D*., et al* (2010) Cryopreservation does not alter the frequency of regulatory T cells in peripheral blood mononuclear cells. *Journal of Immunological Methods*, 353(1-2), 138-140.

Vela, M.*, et al* (2015) Chemokine receptor-specific antibodies in cancer immunotherapy: achievements and challenges. *Frontiers in Immunology*, 6.

Venet, F.*, et al* (2010) Percentage of regulatory T cells CD4(+)CD25(+)CD127(-) in HIV-infected patients is not reduced after cryopreservation. *Journal of Immunological Methods*, 357(1-2), 55-58.

Vercoulen, Y.*, et al* (2009) Human Regulatory T Cell Suppressive Function Is Independent of Apoptosis Induction in Activated Effector T Cells. *Plos One*, 4(9).

Vesalainen, S.*, et al* (1994) HISTOLOGICAL GRADE, PERINEURAL INFILTRATION, TUMOR-INFILTRATING LYMPHOCYTES AND APOPTOSIS AS DETERMINANTS OF LONG-TERM PROGNOSIS IN PROSTATIC ADENOCARCINOMA. *European Journal of Cancer*, 30A(12), 1797-1803.

Vieira, P. L.*, et al* (2004) IL-10-secreting regulatory T cells do not express Foxp3 but have comparable regulatory function to naturally occurring CD4(+)CD25(+) regulatory T cells. *Journal of Immunology*, 172(10), 5986-5993.

Vignali, D. A. A. & Kuchroo, V. K. (2012) IL-12 family cytokines: immunological playmakers. *Nature Immunology*, 13(8), 722-728.

Vijayan, D.*, et al* (2017) Targeting immunosuppressive adenosine in cancer. *Nature Reviews Cancer*, 17(12), 709-+.

Vitale, M.*, et al* (2014) Effect of tumor cells and tumor microenvironment on NK-cell function. *European Journal of Immunology*, 44(6), 1582-1592.

von Bernstorff, W.*, et al* (2001) Systemic and local immunosuppression in pancreatic cancer patients. *Clinical Cancer Research*, 7(3), 925S-932S.

Vos, S. M.*, et al* (2011) All tangled up: how cells direct, manage and exploit topoisomerase function. *Nature Reviews Molecular Cell Biology*, 12(12), 827-841.

Waickman, A. T.*, et al* (2012) Enhancement of tumor immunotherapy by deletion of the A(2A) adenosine receptor. *Cancer Immunology Immunotherapy*, 61(6), 917-926.

Walczak, H. & Sprick, M. R. (2001) Biochemistry and function of the DISC. *Trends in Biochemical Sciences*, 26(7), 452-453.

Wan, Y. Y. & Flavell, R. A. (2006) The roles for cytokines in the generation and maintenance of regulatory T cells. *Immunological reviews*, 212(1), 114-130.

Wan, Y. Y. & Flavell, R. A. (2008) TGF-beta and Regulatory T Cell in Immunity and Autoimmunity. *Journal of Clinical Immunology*, 28(6), 647-659.

Wang, D. Z. & DuBois, R. N. (2015) Immunosuppression associated with chronic inflammation in the tumor microenvironment. *Carcinogenesis*, 36(10), 1085-1093.

Wang, J.*, et al* (1998) Dynamic regulation of gastric autoimmunity by thyroid hormone. *International Immunology*, 10(2), 231-236.

Wang, J.*, et al* (2009a) De Novo Generation and Enhanced Suppression of Human CD4(+)CD25(+) Regulatory T Cells by Retinoic Acid. *Journal of Immunology*, 183(6), 4119-4126.

Wang, R.*, et al* (2009b) Expression of GARP selectively identifies activated human FOXP3+regulatory T cells. *Proceedings of the National Academy of Sciences of the United States of America*, 106(32), 13439-13444.

Ward, S. T.*, et al* (2015) The effects of CCR5 inhibition on regulatory T-cell recruitment to colorectal cancer. *Br J Cancer*, 112(2), 319-328.

Weber, J. S.*, et al* (2015) Nivolumab versus chemotherapy in patients with advanced melanoma who progressed after anti-CTLA-4 treatment (CheckMate 037): a randomised, controlled, open-label, phase 3 trial. *Lancet Oncology*, 16(4), 375-384.

Wei, S.*, et al* (2005) Plasmacytoid dendritic cells induce CD8(+) regulatory T cells in human ovarian carcinoma. *Cancer Research*, 65(12), 5020-5026.

Wei, X. D.*, et al* (2017) Reciprocal Expression of IL-35 and IL-10 Defines Two Distinct Effector Treg Subsets that Are Required for Maintenance of Immune Tolerance. *Cell Reports*, 21(7), 1853-1869.

Weinberger, P. M.*, et al* (2004) Prognostic significance of p16 protein levels in oropharyngeal squamous cell cancer. *Clinical Cancer Research*, 10(17), 5684-5691.

Weiner, H. L. (1997) Oral tolerance: immune mechanisms and treatment of autoimmune diseases. *Immunology Today*, 18(7), 335-343.

Weiss, J. M.*, et al* (2012) Neuropilin 1 is expressed on thymus-derived natural regulatory T cells, but not mucosa-generated induced Foxp3+ T reg cells. *The Journal of experimental medicine*, 209(10), 1723-1742.

Westra, W. H. (2009) The changing face of head and neck cancer in the 21st century: the impact of HPV on the epidemiology and pathology of oral cancer. *Head and neck pathology*, 3(1), 78-81.

Wherry, E. J. (2011) T cell exhaustion. *Nature Immunology*, 12(6), 492-499.

Whiteside, T. L.*, et al* (2012) Induced and natural regulatory T cells in human cancer. *Expert Opinion on Biological Therapy*, 12(10), 1383-1397.

Wildin, R. S.*, et al* (2002) Clinical and molecular features of the immunodysregulation, polyendocrinopathy, enteropathy, X linked (IPEX) syndrome. *Journal of Medical Genetics*, 39(8), 537-545.

Williams, O.*, et al* (1998) The action of bax and bcl-2 on T cell selection. *Journal of Experimental Medicine*, 188(6), 1125-1133.

Wilson, D. I.*, et al* (1993) DIGEORGE-SYNDROME - PART OF CATCH-22. *Journal of Medical Genetics*, 30(10), 852-856.

Wing, K.*, et al* (2008) CTLA-4 control over Foxp3(+) regulatory T cell function. *Science*, 322(5899), 271-275.

Wing, K. & Sakaguchi, S. (2010) Regulatory T cells exert checks and balances on self tolerance and autoimmunity. *Nature Immunology*, 11(1), 7-13.

Wolchok, J. D.*, et al* (2017) Overall Survival with Combined Nivolumab and Ipilimumab in Advanced Melanoma. *New England Journal of Medicine*, 377(14), 1345-1356.

Wolff, H. A.*, et al* (2011) Analysis of chemokine and chemokine receptor expression in squamous cell carcinoma of the head and neck (SCCHN) cell lines. *Radiation and Environmental Biophysics*, 50(1), 145-154.

Woo, E. Y.*, et al* (2001) Regulatory CD4(+)CD25(+) T cells in tumors from patients with early-stage non-small cell lung cancer and late-stage ovarian cancer. *Cancer Research*, 61(12), 4766-4772.

Woo, S. R.*, et al* (2012) Immune Inhibitory Molecules LAG-3 and PD-1 Synergistically Regulate T-cell Function to Promote Tumoral Immune Escape. *Cancer Research*, 72(4), 917-927.

Worthington, J. J.*, et al* (2012) Regulation of TGF beta in the immune system: An emerging role for integrins and dendritic cells. *Immunobiology*, 217(12), 1259-1265.

Wu, L. C.*, et al* (2002) Two-step binding mechanism for T-cell receptor recognition of peptide-MHC. *Nature*, 418(6897), 552-556.

Wu, M. H.*, et al* (2011) Targeting Galectin-1 in Carcinoma-Associated Fibroblasts Inhibits Oral Squamous Cell Carcinoma Metastasis by Downregulating MCP-1/CCL2 Expression. *Clinical Cancer Research*, 17(6), 1306-1316.

Wu, R. Q.*, et al* (2014) The mucosal immune system in the oral cavity-an orchestra of T cell diversity. *International Journal of Oral Science*, 6(3), 125-132.

Wu, W.*, et al* (2017) IL-35 expression is increased in laryngeal squamous cell carcinoma and in the peripheral blood of patients. *Oncology Letters*, 13(5), 3303-3308.

Wu, Y.*, et al* (2009) Human gamma delta T Cells: A Lymphoid Lineage Cell Capable of Professional Phagocytosis. *Journal of Immunology*, 183(9), 5622-5629.

Wu, W. S. (2006) The signaling mechanism of ROS in tumor progression. *Cancer and Metastasis Reviews*, 25(4), 695-705.

Wyble, C. W.*, et al* (1997) TNF-alpha and IL-1 upregulate membrane-bound and soluble E-selectin through a common pathway. *Journal of Surgical Research*, 73(2), 107-112.

Xu, L.*, et al* (2011) In Situ Prior Proliferation of CD4(+) CCR6(+) Regulatory T Cells Facilitated by TGF-beta Secreting DCs Is Crucial for Their Enrichment and Suppression in Tumor Immunity. *Plos One*, 6(5).

Xu, L. L.*, et al* (2007) Cutting edge: Regulatory T cells induce CD4(+)CD25(-)Foxp3(-) T cells or are self-induced to become Th17 cells in the absence of exogenous TGF-beta. *Journal of Immunology*, 178(11), 6725-6729.

Xu, S.*, et al* (2013) Synergy between the ectoenzymes CD39 and CD73 contributes to adenosinergic immunosuppression in human malignant gliomas. *Neuro-Oncology*, 15(9), 1160-1172.

Xue, J.*, et al* (2014) Transcriptome-Based Network Analysis Reveals a Spectrum Model of Human Macrophage Activation. *Immunity*, 40(2), 274-288.

Yadav, M.*, et al* (2012) Neuropilin-1 distinguishes natural and inducible regulatory T cells among regulatory T cell subsets in vivo. *Journal of Experimental Medicine*, 209(10), 1713-1722.

Yaguchi, T. & Kawakami, Y. (2016) Cancer-induced heterogeneous immunosuppressive tumor microenvironments and their personalized modulation. *International Immunology*, 28(8), 393-399.

Yamagiwa, S.*, et al* (2001) A role for TGF-beta in the generation and expansion of CD4(+)CD25(+) regulatory T cells from human peripheral blood. *Journal of Immunology*, 166(12), 7282-7289.

Yamazaki, T.*, et al* (2008) CCR6 Regulates the Migration of Inflammatory and Regulatory T Cells. *Journal of Immunology*, 181(12), 8391-8401.

Yang, L. & Zhang, Y. (2017) Tumor-associated macrophages: from basic research to clinical application. *Journal of Hematology & Oncology*, 10.

Ye, J.*, et al* (2013) The Role and Regulation of Human Th17 Cells in Tumor Immunity. *American Journal of Pathology*, 182(1), 10-20.

Yokoyama, A.*, et al* (1998) Alcohol-related cancers and aldehyde dehydrogenase-2 in Japanese alcoholics. *Carcinogenesis*, 19(8), 1383-1387.

Yonezawa, A.*, et al* (2000) SDF-1 has costimulatory effects on human T cells: Possible involvement of MAPK (ERK2) activation. *Microbiology and Immunology*, 44(2), 135-141.

Yoshimura, A. (2006) Signal transduction of inflammatory cytokines and tumor development. *Cancer Science*, 97(6), 439-447.

Yoshimura, T. & Oppenheim, J. J. (2011) Chemokine-like receptor 1 (CMKLR1) and chemokine (C-C motif) receptor-like 2 (CCRL2); Two multifunctional receptors with unusual properties. *Experimental Cell Research*, 317(5), 674-684.

Yu, G. T.*, et al* (2015) PD-1 blockade attenuates immunosuppressive myeloid cells due to inhibition of CD47/SIRPa axis in HPV negative head and neck squamous cell carcinoma. *Oncotarget*, 6(39), 42067-42080.

Zarek, P. E.*, et al* (2008) A(2A) receptor signaling promotes peripheral tolerance by inducing T-cell anergy and the generation of adaptive regulatory T cells. *Blood*, 111(1), 251-259.

Zarour, H. M. (2016) Reversing T-cell Dysfunction and Exhaustion in Cancer. *Clinical Cancer Research*, 22(8), 1856-1864.

Zeng, H. Y.*, et al* (2015) Type 1 regulatory T cells: a new mechanism of peripheral immune tolerance. *Cellular & Molecular Immunology*, 12(5), 566-571.

Zeng, J. C.*, et al* (2013) Assessing the role of IL-35 in colorectal cancer progression and prognosis. *International Journal of Clinical and Experimental Pathology*, 6(9), 1806-1816.

Zhang, C.-y., *et al* (2015) The role of CCL20/CCR6 axis in recruiting Treg cells to tumor sites of NSCLC patients. *Biomedicine & Pharmacotherapy*, 69, 242-248.

Zhang, L., *et al* (2003) Intratumoral T cells, recurrence, and survival in epithelial ovarian cancer. *New England Journal of Medicine*, 348(3), 203-213.

Zhang, T. Q., *et al* (2006) Migration of cytotoxic T lymphocytes toward melanoma cells in three-dimensional organotypic culture is dependent on CCL2 and CCR4. *European Journal of Immunology*, 36(2), 457-467.

Zhao, C., *et al* (2014) Induced regulatory T-cells (iTregs) generated by activation with anti-CD3/CD28 antibodies differ from those generated by the physiological-like activation with antigen/APC. *Cellular Immunology*, 290(2), 179-184.

Zhao, D. M., *et al* (2006) Activated CD4(+)CD25(+) T cells selectively kill B lymphocytes. *Blood*, 107(10), 3925-3932.

Zheng, S. G., *et al* (2002) Generation ex vivo of TGF-beta-producing regulatory T cells from CD4(+)CD25(-) precursors. *Journal of Immunology*, 169(8), 4183-4189.

Zheng, Y., *et al* (2010) Role of conserved non-coding DNA elements in the Foxp3 gene in regulatory T-cell fate. *Nature*, 463(7282), 808-U120.

Zhou, G. & Levitsky, H. I. (2007) Natural regulatory T cells and de novo-induced regulatory T cells contribute independently to tumor-specific tolerance. *Journal of Immunology*, 178(4), 2155-2162.

Zhou, L., *et al* (2009) Plasticity of CD4(+) T Cell Lineage Differentiation. *Immunity*, 30(5), 646-655.

Zlotnik, A. & Yoshie, O. (2000) Chemokines: A new classification system and their role in immunity. *Immunity*, 12(2), 121-127.

Zlotnik, A. & Yoshie, O. (2012) The Chemokine Superfamily Revisited. *Immunity*, 36(5), 705-716.

Zou, W. P. (2005) Immunosuppressive networks in the tumour environment and their therapeutic relevance. *Nature Reviews Cancer*, 5(4), 263-274.

Zou, W. P. & Chen, L. P. (2008) Inhibitory B7-family molecules in the tumour microenvironment. *Nature Reviews Immunology*, 8(6), 467-477.

Zou, W. P., *et al* (2016) PD-L1 (B7-H1) and PD-1 pathway blockade for cancer therapy: Mechanisms, response biomarkers, and combinations. *Science Translational Medicine*, 8(328).

# Appendix A.

## Reagents

*PBS*

1 phosphate buffered saline tablet (Oxoid) was dissolved per 100 ml distilled water (was this autoclaved)

*PBS/BSA/Azide*

2.5 g BSA and 6.24 ml 10mM sodium azide was added to 1.0 L PBS

*IL10 ELISA coating buffer*

8.4 g $NaHCO_3$ and 3.56 g $Na_2CO_3$ was dissolved in 1.0 L deionized water, pH 9.5

*UMSCC cell line growth medium*

DMEM was supplemented with 10% FBS, 0.1 U/ml penicillin/ 0.1 mg/ml streptomycin, 0.1 mM, non-essential amino acids and 2mM L-glutamine

*Fibroblast/dissociated tumour growth medium*

DMEM was supplemented with 10% FBS, 0.1 U/ml penicillin/ 0.1 mg/ml streptomycin, 0.1 mM, 2.5 μg/ml Amphotericin B and 2mM L-glutamine

*Jurkat Growth medium*

X-Vivo 20 Medium supplemented with 10% FBS and 0.1 U/ml penicillin/ 0.1 mg/ml streptomycin

*Lymphocyte growth medium (LGM)*

X-Vivo 20 medium supplemented with 5% human AB serum and 0.1 U/ml penicillin/ 0.1 mg/ml streptomycin

*Low serum lymphocyte growth medium*

X-Vivo 20 medium supplemented with 0.5% human AB serum and 0.1 U/ml penicillin/ 0.1 mg/ml streptomycin

# Appendix B.

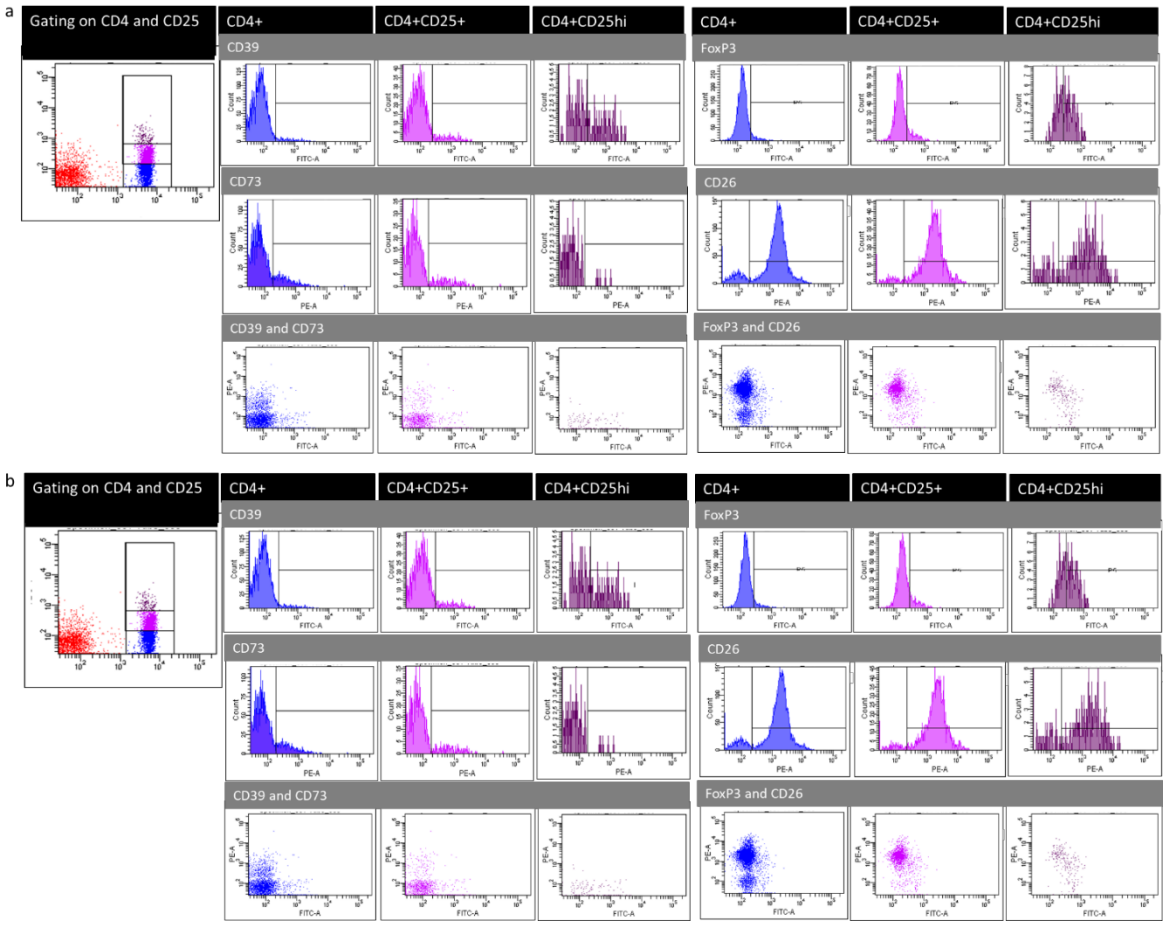


**Figure B.1:** Representative scatter plots of CD4/CD25 expression in PBMC (a) and TIL (b) of HNSCC patients and gating of $CD4^+$, $CD4^+CD25^+$ and $CD4^+CD25^{hi}$ lymphocyte populations. Representative histograms and scatter plots showing the expression of Treg markers and dual expression of CD39/CD73 and FoxP3/CD26 on the $CD4^+$, $CD4^+CD25^+$ and $CD4^+CD25^{hi}$ lymphocytes of PBMC (a) and TIL (b).

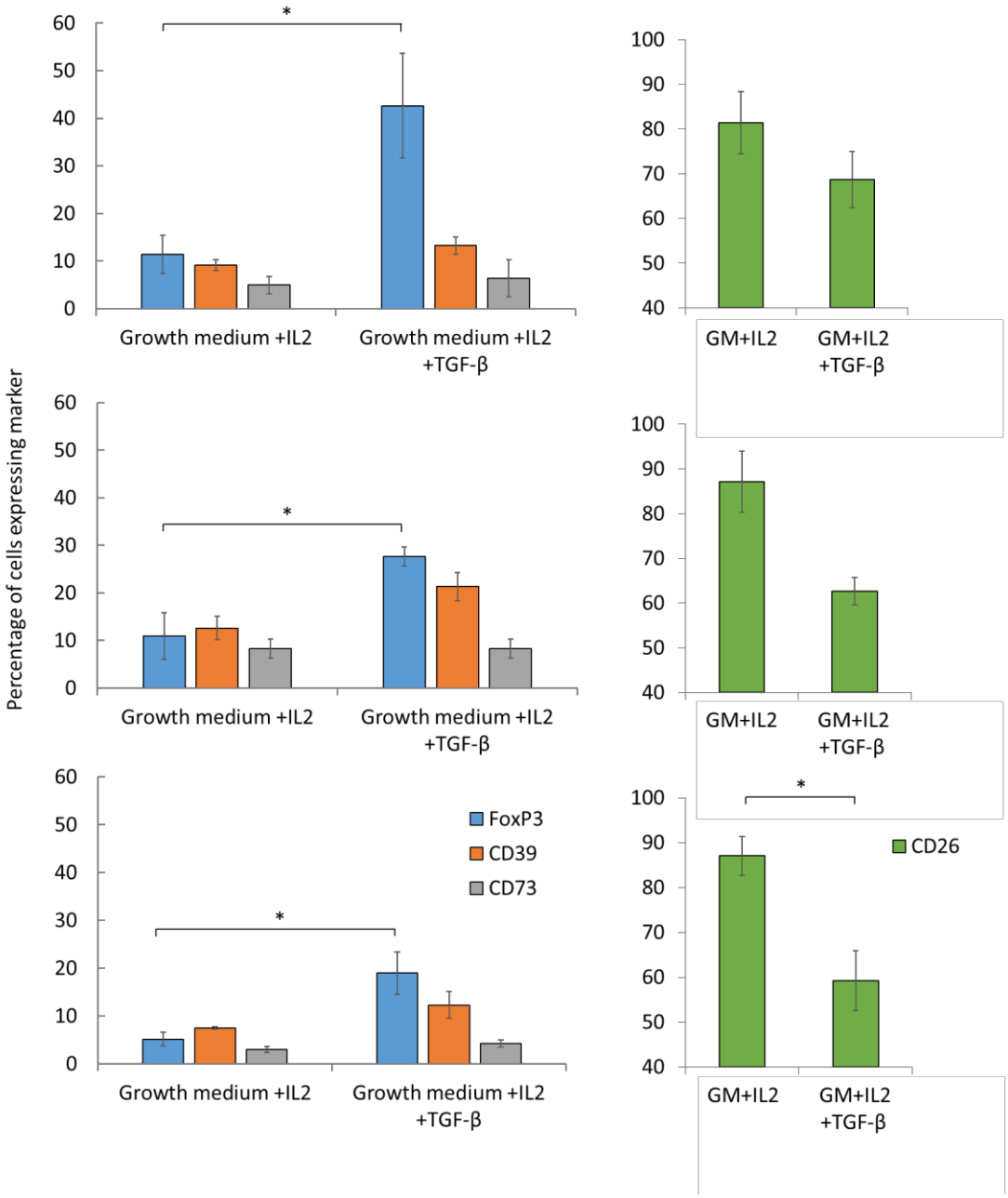


**Figure B.2: Treg marker expression on $CD4^+CD25^-$ lymphocytes from three separate lymphocyte cones cultured with TGF-β**

Mean percentage of $CD4^+CD25^-$ lymphocytes sorted from the PBMC of three healthy controls (n=3,4,3) expressing Treg markers (FoxP3, CD39 and CD73) and the negative marker CD26 following 5 days of culture in medium containing anti-CD3/28 DynaBeads and IL2 (100 U/ml), with or without TGF-β (5 ng/ml). Bars represent mean ±SEM, and statistically significant differences (*$p$<0.05) were determined using independent T tests.

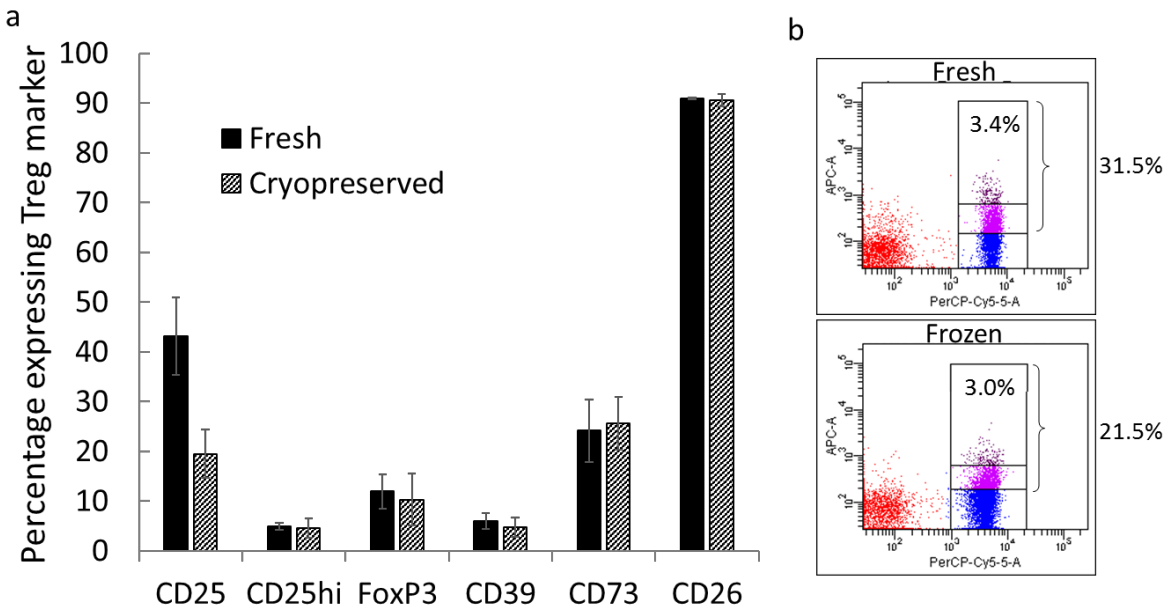


**Figure B.3: The effect of cryopreservation on the expression of Treg markers**
PBMC were isolated from three HNSCC patients and stained immediately for CD25 ($p$=0.062), FoxP3, CD39, CD73 and CD26, or were cryopreserved before staining. Bars represent mean (±SEM) percentage of $CD4^+$ lymphocytes that express each marker (a) and scatter plots show representative CD25 expression on fresh (top) and frozen (bottom) PBMC from a single donor (b).

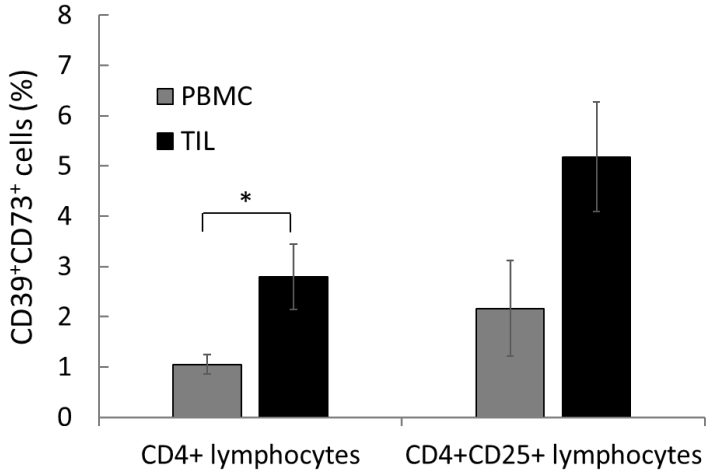


**Figure B.4: Dual CD39 and CD73 expression on $CD4^+$ and $CD4^+CD25^+$ lymphocytes of HNSCC patient PBMC and TIL**
PBMC and TIL from eight HNSCC patients were labelled with fluorescent CD4, CD25, CD39 and CD73 antibodies, and the expression of CD39 and CD73 was assessed on cells within the $CD4^+$ and $CD4^+CD25^+$ lymphocyte gates. Bars represent mean percentage of cells ±SEM, *$p$=0.23 using an independent T test.

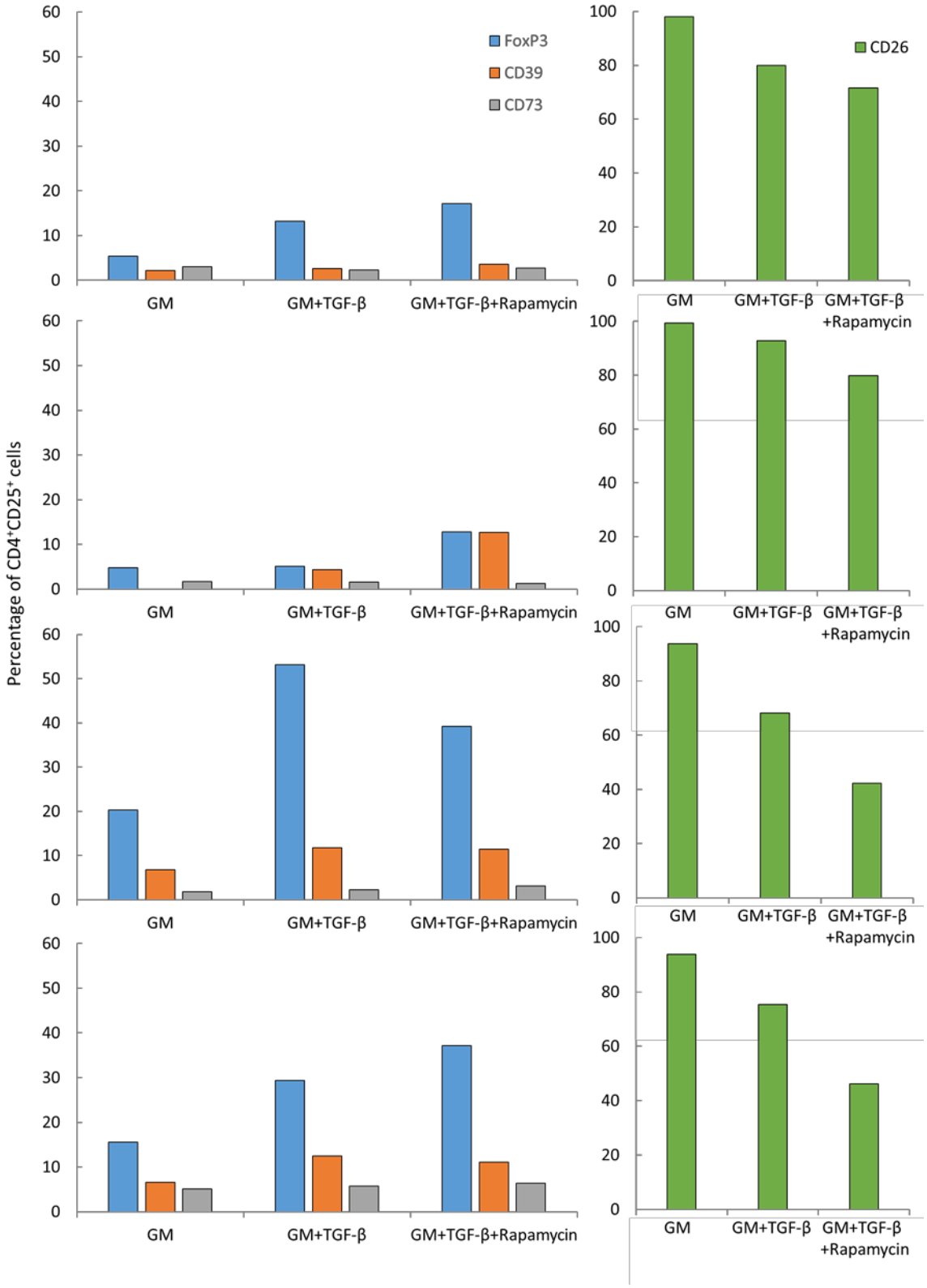


**Figure B.5: Induction of Treg makers on $CD4^+CD25^+$ lymphocytes from four individual donors by TGF-β and TGF-β and rapamycin**

Percentage of $CD4^+CD25^+$ lymphocytes expressing Treg markers (FoxP3, CD39 and CD73) and the negative marker CD26, following the 5-day culture of $CD4^+CD25^-$ from the PBMC of four healthy controls (n=1) in growth medium containing anti-CD3/CD28 DynaBeads and IL2 (100 U/ml), with or without TGF-β (5 ng/ml) and rapamycin (100 ng/ml).

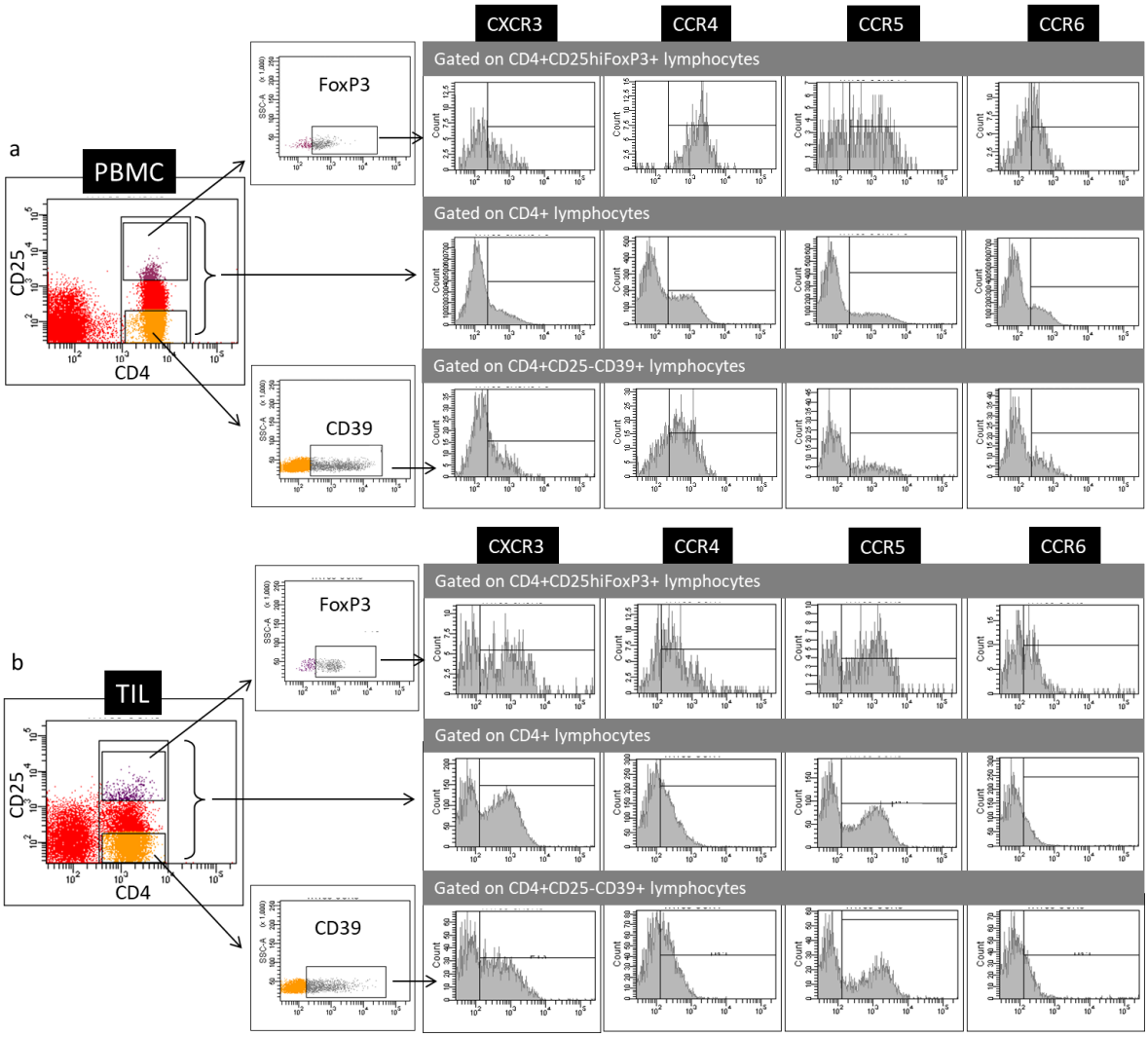


**Figure B.8: Gating strategy for the analysis of chemokine receptor expression on $CD4^+$, $CD4^+CD25^{hi}FoxP3^+$ and $CD4^+CD25^-CD39^+$ lymphocytes on PBMC (a) and TIL (b).**